



HAL
open science

Mechanics of intermediate filaments and microtubules in living cells

Nathan Lardier

► **To cite this version:**

Nathan Lardier. Mechanics of intermediate filaments and microtubules in living cells. Cellular Biology. Université Paris sciences et lettres, 2021. English. NNT : 2021UPSLS058 . tel-03402660

HAL Id: tel-03402660

<https://pastel.hal.science/tel-03402660>

Submitted on 25 Oct 2021

HAL is a multi-disciplinary open access archive for the deposit and dissemination of scientific research documents, whether they are published or not. The documents may come from teaching and research institutions in France or abroad, or from public or private research centers.

L'archive ouverte pluridisciplinaire **HAL**, est destinée au dépôt et à la diffusion de documents scientifiques de niveau recherche, publiés ou non, émanant des établissements d'enseignement et de recherche français ou étrangers, des laboratoires publics ou privés.

THÈSE DE DOCTORAT
DE L'UNIVERSITÉ PSL

Préparée à l'Institut Curie

**Propriétés mécaniques des filaments intermédiaires et des
microtubules dans les cellules vivantes**

Mechanics of intermediate filaments and microtubules in living
cells

Soutenue par

Nathan LARDIER

Le 1 juillet 2021

École doctorale n°515

Complexité du Vivant

Spécialité

Biologie cellulaire

Composition du jury :

Olivia DU ROURE
Directrice de recherche, ESPCI Paris *Présidente du jury*

Sylvie HÉNON
Professeur des universités, Université de Paris *Rapporteuse*

Manuel THÉRY
Directeur de recherche, Institut de recherche Saint-Louis *Rapporteur*

Jean-Baptiste MANNEVILLE
Directeur de recherche, Institut Curie *Directeur de thèse*

Carsten JANKE
Directeur de recherche, Institut Curie *Invité*

Remerciements

Quarante-deux.

Comme le nombre de kilomètres que composent un marathon.

Comme la *réponse à la grande question sur la vie, l'univers et le reste*.

Quarante-deux, c'est aussi le nombre de mois que j'aurai passé à l'Institut Curie.

Depuis mon arrivée dans l'équipe en janvier 2018, bien des choses ont changé.

Certains portent fièrement sur leur maillot une deuxième étoile en guise de flocage.

D'autres portent, plus par obligation que par fierté, un masque sur leur visage.

Quant à moi, je porte une nouvelle histoire : celle du doctorat. Et comme toute histoire, celle-ci a ses personnages.

Laissez-moi vous les raconter ; je leur dois bien un hommage !

Sylvie et Manuel : je commence par vous. La recherche est un travail qui demande beaucoup de temps, et le nombre de tâches que vous devez chaque jour accomplir ne va pas en diminuant. Aussi, en ayant accepté d'être rapporteurs de ce manuscrit de thèse, vous avez fait preuve de disponibilité et d'intérêt pour mon sujet de recherche et pour l'approche novatrice que nous avons utilisée. Je vous suis reconnaissant pour le temps que vous avez mis à disposition pour analyser, critiquer et discuter les résultats de ce long travail. Bien que je quitte la recherche, j'aurai toujours un œil sur l'évolution de vos passionnants travaux et garderai en mémoire nos sympathiques échanges.

Carsten: the fact that you accept to be part of my PhD jury did not seem obvious to me! As a biochemist (at least by training), you could have easily argued that this work had too little biochemistry for you! Instead, you have been very interested about the project and your questions have brought a different point of view and new perspectives. Thank you very much for this!

Olivia, je suis honoré que tu aies accepté de présider ce jury de thèse. Après tout, pour moi qui quitte la recherche, c'est une belle façon de *boucler la boucle*, moi qui suis *rentré* dans la recherche en mai 2013 dans ton équipe. Depuis lors, nous ne nous sommes jamais réellement quittés. Tes nombreux retours lors des comités de thèse ont permis d'augmenter en substance la qualité du présent manuscrit et des résultats obtenus. Je tiens également à te remercier pour la bienveillance et le soutien dont tu as fait preuve. Je vais bientôt démarrer une nouvelle histoire, mais tu auras eu un rôle important dans celle-ci. Merci pour tout et je ne doute pas que nous nous reverrons bientôt.

Lorsque j'étais encore en Master, des doctorants étaient venus échanger avec nous. Un de leurs messages, qui m'a autant surpris que marqué, était qu'il valait mieux choisir un directeur de thèse qu'un sujet de thèse (le mieux étant - bien sûr - de choisir les deux). Si mon intérêt pour le sujet a crû au cours de ces trois ans et demi, je n'ai jamais cessé de penser que choisir Jean-Baptiste fut une décision

extrêmement bénéfique. Ton caractère, tes qualités humaines et scientifiques, ton enthousiasme, ta naïveté parfois, ta gentillesse, ta pédagogie, ton goût pour le dialogue, *etc.* ont permis que cette thèse se passe d'une manière très agréable - bien qu'il y eût des moments plus difficiles -, et provoquent chez moi admiration et respect. Nous n'avons pas totalement fini de travailler ensemble, et j'espère avoir l'occasion, avec des étudiants ou sans d'ailleurs, de revenir te voir pour parler science !

Fort heureusement la recherche ne se fait pas seul, et je garde de très beaux souvenirs de l'équipe *Mécanismes moléculaires du transport intracellulaire*.

Bruno : mon sujet n'était sans doute pas au centre de tes intérêts scientifiques. Ainsi, je te remercie d'autant plus pour la hauteur de vue que tu lui as apportée durant les deux dernières années. Stéphanie, ton expertise en microscopie fut précieuse, moi qui ne connaissais absolument pas les microscopes utilisés par les biologistes. Ta bonne humeur et ta spontanéité résonnent encore dans ma tête, et ce fut un plaisir de partager ce bureau avec toi. Kristine: finally we have not done any *in vitro* experiment, sorry about this! I remind numerous discussions (and debates) about culture, Germany, politics, vegetarian diet, your kids, and so on. I have really appreciated talking to you and wish you the best in your new team! Sabine, tu auras été sans doute la permanente du laboratoire avec qui j'aurai le plus échangé. Les nombreux repas à la cantine nous ont vu partager nos joies, nos coups de moins bien, nos ras-le-bol, mais aussi de nombreux rires sur bien des sujets que je n'écrirai pas ici ! J'aurai toujours plaisir à aller déjeuner avec toi pour que tu changes d'air !

La recherche se base aussi beaucoup sur des femmes et des hommes de passage. J'en ai vu partir, d'autres arriver. Tous les citer serait difficile ; qu'ils me pardonnent si je les ai oubliés.

David : merci pour ta mauvaise foi, tes qualités intrinsèques pour résoudre les contrepèteries du *Canard*, ta mémoire toujours très précise des discussions, tes goûts footballistiques douteux. Plus sérieusement, merci pour les nombreuses contributions sur les parties d'analyse d'images de ce manuscrit : sans toi, je n'aurai pas pu en faire autant ! Que serait David sans son *partner in crime*? Hugo, tu es le seul survivant de notre association de malfaiteurs. J'imagine que, même dans des années, tu auras encore des *questions de physique* à me poser. Outre tous les bons moments qu'on aura passés, je reste impressionné par ta curiosité et ta culture scientifique. J'ai beaucoup appris, mais surtout j'ai beaucoup réfléchi à tes côtés. Et bien que l'envie de t'insulter n'est jamais totalement absente, il me tarde de voir la brillante carrière qui t'attend !

Senior PhD fellow, this is for you! My dear Yamini, thank you for your support and for guiding me toward the light! Your good mood was essential to the lab, and it was really nice to share all those little breaks. Sharing this desk (and my charger!) led to funny moments. All the best for the future, you will be a brilliant scientist! I spent the whole PhD with another brilliant girl: Pallavi! It took us a while to interact and really get to know each other but I am grateful for your smile, your

kindness, your support and all the drinks we have shared. Best of luck for the end of your PhD!

Ahora te toca a ti, Silvia. Nos hemos conocido paso a paso, en Curie, pero también en Portugal o durante el *retreat* en la región de Angers. Gracias por tu buen humor: eres el remedio contra el malestar. Aunque nuestra colaboración no ha dado los resultados que ambos esperábamos, estos últimos experimentos fueron divertidos. Gracias por las propuestas musicales, los lugares que me enseñaste para cenar y tomar un vaso, y otras muchas charlas. Me impresionan todas tus competencias cada vez que presentas tus resultados. ¡Tu defensa va a ser un éxito!

Je pourrais continuer ainsi et écrire un paragraphe pour chaque personne croisée au laboratoire, mais ces remerciements commençant à être sacrément longs, je me contenterai de remercier Tanguy pour son travail précieux et sa bonne humeur, Surya pour sa gentillesse et le soleil dans sa voix, Samuel pour m'avoir fait découvrir l'équipe et pour ses talents musicaux, Anaïs pour avoir été la preuve qu'on peut faire une thèse avant un stage de Master, Kotryna for your enthusiastic project and for being such an easy-going person, Katka for the good moments we had playing board games, Charlotte pour sa bonne humeur constante face aux ressources humaines de PSL ... Merci aussi à Edwige, Slimane, Aurélie, Maïté, Frédérique, Manuel, Lara, Ana, Pauline, Benjamin, Amal, Pierre, Marusa, Pascal, Inés, Juanma, Lucie ...

La recherche, c'est très prenant. Mais, je le confesse aisément, je ne suis pas toujours resté au labo ! J'allais parfois retrouver d'autres personnages tout aussi principaux de mon histoire.

Et puisque la meilleure façon de couper avec la recherche c'est de se retrouver avec des enseignants, il est temps de dire : *Vive les mariés !* Clara et Pierre-Simon, merci pour votre amitié fidèle et durable. Tous les moments passés à République, à Nation ou ailleurs me font mesurer à quel point j'ai de la chance de vous avoir. Merci de m'avoir invité à connaître vos élèves le temps d'une journée ou d'une demi-journée. Mickaël, tu as de la chance que ces remerciements soient écrits et non oraux ! J'aurais sans doute loué ta sincère sympathie, ton sens systématique de l'organisation d'événements sociaux, ta spontanéité singulière, *etc.* Merci pour les nombreuses invitations en Haute-Savoie, ça a vraiment permis de régulièrement se ressourcer¹. Petit clin d'œil à Maëva aussi que je ne connaissais pas avant cette thèse, et qui a le mérite de te supporter quotidiennement². Christian, mon cœur restera toujours rouge et blanc, mais à ton contact il a maintenant de belles nuances jaunes et vertes. T'es le vieux de la bande, ça va bientôt faire dix ans ! Merci à toi d'avoir toujours été là, d'emporter toujours avec toi ton sens de l'humour décalé et ta profonde gentillesse. T'as un petit souci avec les deadlines, mais t'es quelqu'un de bien quand même. Manon, tu es désormais partie vers de nouvelles aventures (après en avoir testé pas mal quand même, entre les stations haut-savoyardes, les

¹Désolé, mais c'était vraiment trop tentant !

²Y'en a qui ont essayé ...

restaurants, les associations andalouses, *etc.*), et je sais que nous nous verrons moins (snif). Merci pour toutes les petites virées à Melun, à Annecy ou dans Paris. T'es vraiment une chouette meuf.

Julien et Laura, votre déménagement à Nancy, le COVID et la fin de thèse auront bien diminué la fréquence de nos retrouvailles. Je sais néanmoins que vous serez toujours là et j'espère bientôt passer de froides soirées d'hiver ou de longues soirées d'été avec vous, à Chamonix, à Stockholm ou ailleurs. Basile, j'ai pas voulu te mettre trop près de Christian de peur que ça fasse des étincelles à l'évocation du jaune et du vert ! Merci pour les footings, les repas et les petites virées rennaises. On remet ça quand tu veux. J'aurais presque envie de dire : *Rebelote !* Lucas, tu es devenu un grand garçon maintenant. Tu cours même plus vite que moi ! Qui l'aurait cru ? Plus que te remercier, je voudrais surtout te dire que je crois que la troisième fois sera la bonne³. Tu feras un super prof. Romain, tu es sans doute la personne de ce paragraphe qui m'a le plus entendu parler de ce manuscrit. C'est sympa d'avoir un compagnon de course aussi régulier et qui me suit toujours à peu près dans mes folies. Émilie et Gaëtan, votre mariage fut l'un des plus beaux moments de ce printemps 2021. Je sais que nous nous retrouverons bientôt autour d'un verre de vin, d'un jeu de société et de succulents accras de morue. Chloé, depuis la Nouvelle-Zélande nous ne nous sommes jamais vraiment quittés. J'ai hâte de refaire des concerts avec toi quand ça reprendra vraiment. D'ici là, bonne chance pour la fin de thèse et tu viens manger à République quand tu veux !

Merci aussi à tous mes amis rencontrés à Paris qui sont encore dans la recherche : Louis, Barbara, Guilhem, Manon. Bon courage à vous pour la suite ! Merci à tous mes amis arbitres avec qui j'ai beaucoup partagé pendant ces trois années, entre discussions et entraînements : Édouard, Loïc, Damien, Adrien, Clément.

Enfin, il est temps de rendre hommage à ceux qui m'entourent depuis très longtemps. La liste est longue, mais je commencerai par mes grands-parents. Bien que vous ne soyez plus que trois, je suis touché par votre présence à la soutenance, vous qui m'avez tant apporté les mercredis et pendant les vacances. J'espère que vous avez pu mesurer le chemin parcouru depuis l'époque où je comptais les châteaux d'eau et qu'inlassablement je vous sollicitais pour jouer comme les grands. Je remercie également mes nombreux cousins qui ont tous eu des parcours variés et sources de belles discussions lors des réunions de famille. Merci à ma marraine avec qui j'ai passé beaucoup de temps étant jeune, et qui a toujours su assouvir ma curiosité. Fabrice, bien que ce soit impossible pour toi de te rendre à la soutenance, je suis très heureux du lien très nourri que nous maintenons encore aujourd'hui. J'ai plein de merveilleux souvenirs en tête, depuis le moustique de Rayman, en passant par le manoir anglais et les excursions à Mons, jusqu'aux matches au Grand Stade tout gris. Avec Christelle, Maria et Raphaëlle, nous avons eu de beaux moments d'échange, de joie et de rire.

³C'est surtout que j'ai envie de gagner un escape game !

Papa et Maman, je ne souhaite pas, moi, vous séparer. Vous êtes des parents comme beaucoup rêveraient en avoir. Élever un enfant qui a toujours une question à la bouche, ça n'a pas dû être une mince affaire. Vous avez su installer un cocon protecteur mais pas trop, chaleureux, vivant et bienveillant. Je ne pense pas pouvoir un jour vous rendre tout ce que vous m'avez donné, mais je vous dois clairement une partie de ma réussite actuelle. Je vous souhaite à tous les deux le bonheur dans votre vie actuelle et future. Le soleil finit toujours par revenir.

Elsa, te voilà à l'aube d'un nouveau départ. Je suis très fier de tout ce que tu as accompli. Tu vas pouvoir réaliser un rêve d'enfant en devenant artiste de cirque. Je n'ai aucun doute sur le fait que ta vie suédoise va te ravir et que tu t'y sentiras bien, à défaut de t'y sentir chez toi. Je ne saurais lister toutes tes qualités et tous les souvenirs que j'ai avec toi, mais tu es - modestement - une des personnes les plus importantes de ma vie. Depuis cinq ans, Baptiste partage ta vie, et je dois dire que c'est là une chouette trouvaille ! Merci Baptiste pour ta bonne humeur et les souvenirs sous la couette à Uzès, et belle vie dans ta caravane !

Oscar, siempre recordaré aquel uno de abril. Cerca al lago Reuilly, nos vimos por primera vez y nunca nos separamos después. Eres el mayor cambio en mi vida durante estos tres años. Nos fuimos conociendo el uno al otro poco a poco, y la verdad es que no podría prescindir de ti ahora. Gracias por tu ayuda, sobre todo durante la fase de redacción del presente manuscrito. Gracias por todo lo que me das de manera cotidiana, por lo que me enseñas de historia o de América del Sur, por todos los momentos que paso contigo. Al acabar estos largos agradecimientos, te quiero desear lo mejor con tu doctorado : pronto estaré leyendo los agradecimientos tuyos. Junto a ti.

Contents

List of Acronyms	xvii
1 The cytoskeleton	1
1.1 A network of crosslinked filamentous biopolymers	1
1.2 Functions of the cytoskeleton in eukaryotic cells	5
1.2.1 Actin filaments regulate cell shape and movement	5
1.2.2 Intermediate filaments maintain cellular integrity	6
1.2.3 Microtubules provide a structural framework and orchestrate intracellular trafficking	9
1.3 Intermediate filaments	10
1.3.1 Diversity of intermediate filaments in eukaryotic cells	10
1.3.2 Structure and assembly of intermediate filaments	11
1.3.3 Vimentin, an intermediate filament protein present in many cells	13
1.4 Microtubules	17
1.4.1 Dynamics of microtubules	17
1.4.2 Microtubules and post-translational modifications	19
2 Mechanical properties of the cytoskeleton	23
2.1 Measuring mechanical properties in cell biology	24
2.1.1 Cytoskeletal mechanics measurements <i>in vitro</i>	24
2.1.2 Whole-cell-scale, cortical and intracellular force measurements	30
2.1.3 Our approach: combining optical tweezers-based intracellular rheology with live cell imaging	32
2.2 Mechanics of microtubules <i>in vitro</i>	32
2.2.1 Anisotropic stiffness of microtubules	32
2.2.2 Variability in the measurements of microtubule flexural rigidity	33
2.2.3 Microtubule response to repeated mechanical stress	34
2.3 Mechanics of intermediate filaments <i>in vitro</i>	36
2.3.1 Networks of intermediate filaments: highly deformable and almost unbreakable	36
2.3.2 Individual intermediate filaments exhibit nonlinear strain-stif- fening	37
2.4 Microtubules and intermediate filaments <i>in cellulo</i>	41
2.4.1 Measuring mechanics of cytoskeletal filaments <i>in cellulo</i>	41
2.4.2 Mechanical contribution of microtubules in cells	43
2.4.3 Mechanical contribution of intermediate filaments in cells	44

3	Mechanical coupling within the cytoskeleton	49
3.1	Cytoskeletal crosstalk involving vimentin intermediate filaments and microtubules	49
3.1.1	Crosstalk through molecular motors	50
3.1.2	Crosstalk through crosslinking proteins	51
3.2	Impact of cytoskeletal crosstalk on network organization and cell mechanics	54
3.2.1	Synergistic organization of cytoskeletal networks	54
3.2.2	Mechanical reinforcement mediated by cytoskeletal interactions	57
4	Aims of the PhD project	63
5	Materials and Methods	67
5.1	Cell culture	67
5.2	Immunofluorescence staining and fixed cell imaging	68
5.3	Live cell imaging of vimentin and tubulin <i>in cellulo</i>	68
5.4	Drugs targeting microtubules	68
5.5	ATP depletion	69
5.6	Optical tweezer-based microrheology	69
5.7	Data analysis: from the movies to the effective stiffness	72
5.8	Statistical tests	74
6	Results and Discussion	77
6.1	Mechanics of vimentin bundles and microtubules	77
6.1.1	<i>In cellulo</i> , vimentin bundles are stiffer than microtubules	77
6.1.2	Sequential deflections make vimentin bundles more rigid	83
6.2	Mechanical coupling between microtubules and vimentin intermediate filaments	87
6.2.1	The vimentin network does not play a key role in the mechanical properties of microtubules	88
6.2.2	Modifying microtubule stability affects vimentin mechanical behaviour	90
6.3	Study of a post-translational modification: acetylation	94
6.3.1	Acetylation leads to microtubule softening	96
6.3.2	Acetylated microtubules impact vimentin bundle mechanics	99
6.4	Preliminary results: role of ATP in cytoskeletal mechanics	101
7	Conclusion and Perspectives	103
	Appendices	109
A	Protocols	111
A.1	Cell culture	111
A.2	Immunofluorescence staining	112

Contents	ix
<hr/>	
A.3 Live cell imaging of vimentin and tubulin <i>in cellulo</i>	113
A.4 Post-treatment of images before creating kymographs	114
B MATLAB codes	115
C Power law analysis	127
Bibliography	129

List of Figures

1.1	Fluorescence micrograph of a cultured fibroblast showing the cytoskeleton	2
1.2	Structure of the three major cell cytoskeletal filaments	4
1.3	Actin-based movements in animal cells	6
1.4	Intermediate filaments: role in cellular responses to extracellular stimuli	8
1.5	Detailed structure of cytoplasmic and nuclear intermediate filament proteins	12
1.6	Schematic representation of the assembly of intermediate filaments .	14
1.7	Selected functions of vimentin	15
1.8	Imaging of intermediate filaments in astrocytes	16
1.9	Microtubule assembly and dynamic instability	18
1.10	Modes of K40 acetylation by ATAT1	21
2.1	Persistence length of polymers	25
2.2	<i>In vitro</i> measurements of flexural rigidity	27
2.3	Deflection of an individual filament using atomic force microscopy .	28
2.4	Fluid particle under a shear stress	29
2.5	Microtubule response to repeated mechanical stress	35
2.6	Shear stress/strain behaviour of microtubules, actin and vimentin filaments	37
2.7	Molecular dynamics simulation of vimentin intermediate filament dimer under tensile deformation	39
2.8	Role of the loading rate in the mechanics of individual vimentin filaments.	40
2.9	Cyclic stretching softens vimentin intermediate filaments	41
2.10	Role of the surrounding cytoskeleton on microtubule buckling	42
2.11	Impact of K40 acetylation on long-lived microtubules	44
2.12	Role of vimentin filaments in cytoplasmic mechanics	46
2.13	Role of the vimentin network in cells undergoing cyclic loadings . . .	48
3.1	Role of microtubules in vimentin filament assembly and motility . .	51
3.2	Influence of plectin on vimentin network organization in fibroblasts .	52
3.3	Plectin crosslinks vimentin, microtubule and actomyosin networks .	53
3.4	Physical interactions between the three cytoskeletal subsystems . . .	54
3.5	The absence of vimentin intermediate filaments disturbs the organization of the microtubule network	56
3.6	Heterogeneous reconstituted networks exhibit peculiar mechanical behaviours	58
3.7	Vimentin-dependent cell deformability is compensated by actin filaments but not by microtubules.	59

3.8	Effect of network disruptions on the persistence lengths of vimentin intermediate filaments and microtubules	60
5.1	Schematic representation of the optical tweezers	70
5.2	Optical tweezers: analogy with a hookean spring	71
5.3	Calibration of the optical trap	72
5.4	Scheme and images of an optical tweezer-based intracellular microrheology experiment.	73
5.5	The effective stiffness is calculated from linear fits of force-deflection curves at small deformations	75
6.1	The force-deflection curves exhibit an important variability	78
6.2	The effective stiffness of vimentin bundles is higher than that of microtubules	79
6.3	Cytoskeletal fibers are not deformed in the same way if they are fixed to one or to both ends	80
6.4	Beads can localize next to single cytoskeletal subcomponents or next to composite structures made of vimentin bundles and microtubules.	81
6.5	Simultaneous labelling of vimentin and microtubules shows that they can deform in a different way in composite structures	82
6.6	Microtubule effective stiffness does not change upon repeated mechanical stress	84
6.7	The effective stiffness of vimentin bundles increases upon repeated mechanical stress	85
6.8	Increase in vimentin effective stiffness upon a sequence of three intracellular microrheology experiments	86
6.9	The expression of intermediate filament proteins is greatly reduced in vimentin-KO cells	89
6.10	Immunofluorescence images of control and vimentin-KO U373 cells	90
6.11	Knock-out of vimentin has no effect on microtubule mechanics	91
6.12	Immunofluorescence images of U373 cells treated with microtubule-targeting drugs	92
6.13	Microtubule-stabilizing drugs have no major effects on vimentin bundle effective stiffness	93
6.14	Destabilizing microtubules reduces vimentin bundle stiffening upon sequential deflections	95
6.15	Immunofluorescence images of U373 cells treated with tubacin	96
6.16	SiR-tubulin has a much weaker effect than tubacin on K40 acetylation	97
6.17	K40 acetylation reduces microtubule effective stiffness but does not affect that of vimentin bundles	98
6.18	Microtubule acetylation reduces the stiffening of vimentin bundles upon sequential deflections	100
6.19	Inhibiting active cellular processes by ATP depletion increases the effective stiffness of vimentin bundles	102

C.1 Power law analysis of the force-deflection curves of vimentin bundles
in DMSO-, nocodazole- and taxol-treated cells. 128

List of Tables

1.1	Temporal and spatial features of the cytoskeletal filaments.	4
1.2	Classification of intermediate filament proteins by type	11
5.1	List of used antibodies.	68
5.2	Drugs targeting microtubules: experimental procedures	68
5.3	ATP depletion protocol	69
6.1	Nature of the bead micro-environment: quantification.	82
C.1	List of p -values that are below the level of significance for the pref-actor F_0	127

List of Acronyms

+TIPs Plus-end tracking proteins	52
AFM Atomic Force Microscopy	27
APC Adenomatous Polyposis Coli	52
ATAT1 α -Tubulin N-Acetyltransferase 1	20
ATP Adenosine Triphosphate	5
CHO Chinese Hamster Ovary	50
CRISPR Clustered Regularly Interspaced Short Palindromic Repeats	67
DMSO Dimethyl Sulfoxide	92
eGFP enhanced Green Fluorescent Protein	60
EMT Epithelial-Mesenchymal Transition	14
FCS Fetal Calf Serum	67
FRET Förster Resonance Energy Transfer	107
GAPDH Glyceraldehyde-3-phosphate dehydrogenase	89
GFAP Glial Fibrillary Acidic Protein	10
GFP Green Fluorescent Protein	68
GTP Guanosine Triphosphate	13
HDAC6 Histone Deacetylase 6	20
IF Intermediate Filament	37
K40 Lysine 40	20
KO Knocked-Out	44
LINC Linker of Nucleoskeleton and Cytoskeleton	7
MAPs Microtubule-Associated Proteins	33
MEFs Mouse Embryonic Fibroblasts	45

MFs Actin Filaments	56
MTs Microtubules	55
MTC Magnetic Twisting Cytometry	32
MTOCs Microtubule-Organizing Centers	17
NLS Nuclear Localization Signal	11
PTM Post-Translational Modifications	19
RNA Ribonucleic Acid	11
shRNA Short Hairpin Ribonucleic Acids	51
siRNA Small Interfering Ribonucleic Acid	43
SIRT2 Sirtuin Type 2	20
TFM Traction Force Microscopy	31
WT Wild-Type	45

The cytoskeleton

Contents

1.1	A network of crosslinked filamentous biopolymers	1
1.2	Functions of the cytoskeleton in eukaryotic cells	5
1.2.1	Actin filaments regulate cell shape and movement	5
1.2.2	Intermediate filaments maintain cellular integrity	6
1.2.3	Microtubules provide a structural framework and orchestrate intracellular trafficking	9
1.3	Intermediate filaments	10
1.3.1	Diversity of intermediate filaments in eukaryotic cells	10
1.3.2	Structure and assembly of intermediate filaments	11
1.3.3	Vimentin, an intermediate filament protein present in many cells	13
1.4	Microtubules	17
1.4.1	Dynamics of microtubules	17
1.4.2	Microtubules and post-translational modifications	19

In this first chapter, we introduce the object of our research, the cytoskeleton. After reviewing its biological functions, some key aspects of the two networks of interest for this work - *intermediate filaments* and *microtubules* - will be enhanced. Mechanical features of the cytoskeleton will not be discussed in this chapter and will be the focus of chapter 2.

1.1 A network of crosslinked filamentous biopolymers

Eukaryotic cells - which have their genetic material packed into a specific compartment called *nucleus* - are able to divide, migrate, resist deformations, adapt their size and shape to their environment, exchange materials with the outside, *etc.* Nonetheless, neither the cytosol that contains the cellular organelles - being purely liquid - nor the plasma membrane - which is rather soft - are able to achieve these functions: the cytoskeleton, a network of filamentous structures, provides both strength and elasticity to the cell, and supports the functions mentioned above.

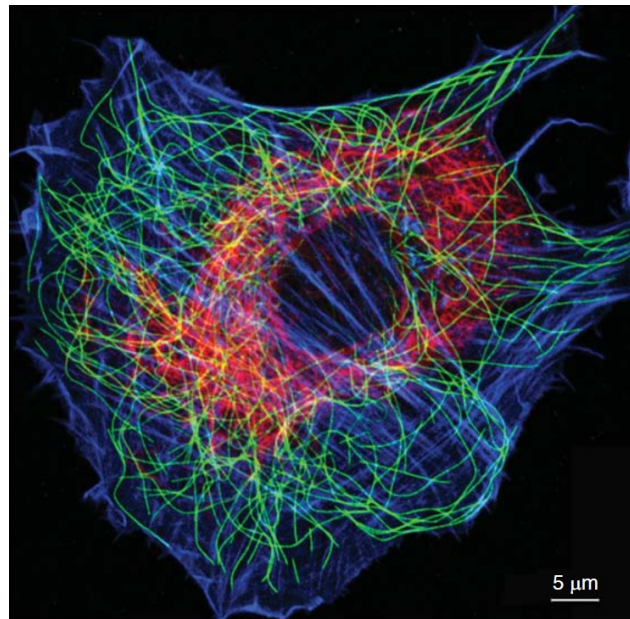


Figure 1.1: Fluorescence micrograph of a cultured fibroblast showing actin (blue, stained with phalloidin), microtubules (green) and intermediate filaments (red). Taken from [Pollard & Goldman 2018].

The cytoskeleton is mainly composed of three types of filaments: microtubules, actin filaments (also known as *microfilaments*) and intermediate filaments¹. A fluorescence microscopy image of a cell stained with fluorescent markers targeting the three cytoskeletal subcomponents is shown in figure 1.1. These three components share the common property of being a repetition of small units of typically 10 nm length called *monomers* that assemble² in order to give rise to *polymer* networks that spread on much larger distances, typically up to 10 μm which is the usual order of magnitude for the size of a cell. However, microtubules, actin filaments and intermediate filaments differ in their size, structure, roles, stability and localization inside the cell. While the role of each cytoskeleton will be detailed in section 1.2, here we describe their structural features:

- **Actin filaments** are the thinnest filaments of the cytoskeleton: their diameter is between 7 nm and 8 nm. Actin filaments - *F-actin* - are composed of actin monomers - *G-actin* - which have a globular structure. G-actin is soluble in the cytoplasm and the amino acid sequence of cytoplasmic G-actin is extremely conserved among all eukaryotic organisms, including humans, actin being one of the most highly conserved proteins [Hanukogge *et al.* 1983]. A G-actin protein contains 374 amino acids: its molecular weight is 42 kDa for a diameter of 5.5 nm. In cells, G-actin polymerizes into two parallel F-actin

¹Functions, roles and mechanics of septins, the fourth cytoskeletal subcomponent which can form hetero-oligomeric complexes as well as filaments and rings, will not be discussed in this manuscript.

²The way filaments assemble can be more or less complex and depends on their nature.

strands lying on top of each other, creating a double-strand helix repeating every 370 Å. G-actin monomers are composed of four different domains, making them asymmetric. Therefore, G-actin is a polar protein: the (-) end is called *pointed end* and the (+) end is called *barbed end*. This implies that association constants are different according to the end. During polymerization, barbed ends bind pointed ends: an actin filament is thus a polar structure with a barbed end and a pointed end (see figure 1.2.A).

- **Intermediate filaments** are the most complex structures of the cytoskeleton.

First, there is a high variety of intermediate filament proteins: in human, there are more than seventy different types. Intermediate filaments measure between 8 nm and 12 nm in diameter: they are mid-sized between actin filaments and microtubules, as their name suggests. Depending on their amino acid sequences, human intermediate filament proteins can be subcategorized into six types [Szeverenyi *et al.* 2008]. Unlike actin filaments, intermediate filaments are made of fibrous proteins, such as keratins, desmin or vimentin. We will describe the different types of intermediate filament proteins in 1.3.1. Second, intermediate filament assembly occurs in several steps: for most intermediate filaments, the basic element is a tetramer. Eight tetramers are required to associate laterally and form a structure called *unit-length filament* (see figure 1.2.B). Unit-length filaments assemble into protofilaments, then into filaments. This unique way of polymerizing makes intermediate filaments the most stable and the least dynamic structures of the cytoskeleton. Intermediate filaments are the only structures of the cytoskeleton which are not polar, due to the symmetry of tetramers. A more precise description of intermediate filament assembly will be given in 1.3.2

- **Microtubules** - contrary to actin filaments and intermediate filaments - are hollow tubes. Their outer diameter ranges from 23 nm to 27 nm and their inner diameter is between 11 nm and 15 nm. Microtubules are formed by two different globular proteins: α -tubulin and β -tubulin. Tubulin consists of 450 amino acids and it has a molecular weight similar to actin: 50 kDa. Heterodimers of α - and β -tubulin polymerise into thirteen protofilaments arranged in a ring shape (see figure 1.2.C). As for actin, due to the asymmetry of heterodimers, microtubules are polar: the (-) end is where α -tubulin is exposed and the (+) end corresponds to the extremity with β -tubulin exposed. Microtubules are highly dynamic structures that switch between polymerization phases at their (+) ends and depolymerization phases at their (-) ends [Desai & Mitchison 1997]. Dynamic instability of microtubules and its implications will be described in 1.4.1. Microtubules can reach important lengths, typically 10 μ m, which is still much smaller than their persistence length (see table 1.1).

Table 1.1 gives an overview of the structural characteristics of the cytoskeletal subcomponents.

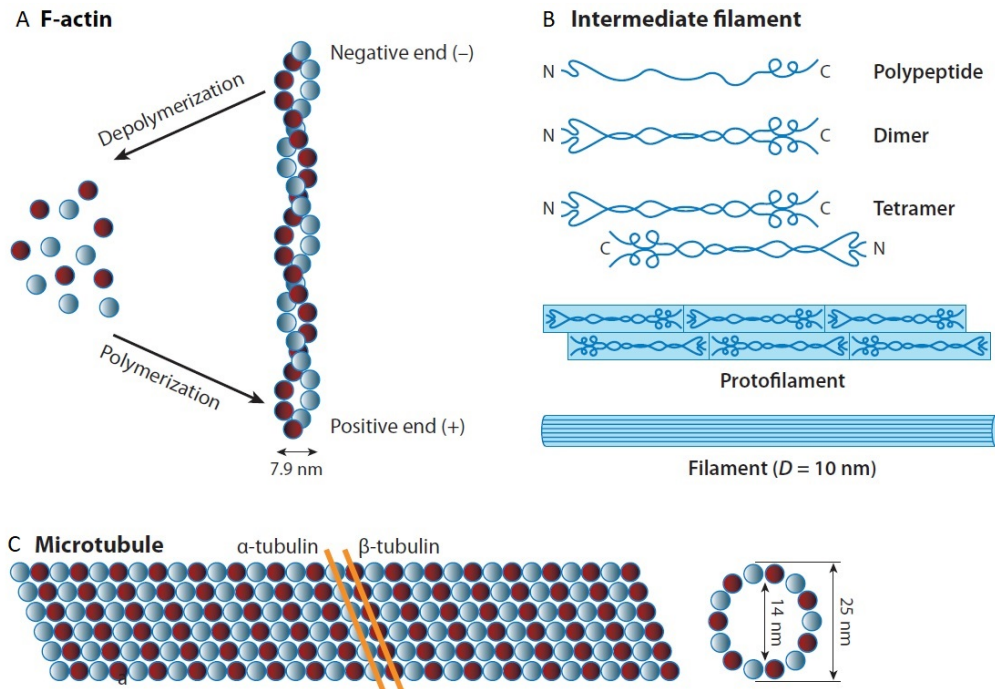


Figure 1.2: Structure of the three major cell cytoskeletal filaments. From [Mofrad 2009].

	Outer diameter	Turnover	Persistence length	Polarity
Actin filament	6 nm	< 1 min	10 μm	Yes
Intermediate filament	10 nm	1 h	$\leq 1 \mu\text{m}$	No
Microtubule	25 nm	10 min	> 1 mm	Yes

Table 1.1: Temporal and spatial features of the cytoskeletal filaments.

The three cytoskeletal filaments do not act separately: for most cell functions, more than one cytoskeletal component is required. Filaments can be connected to the plasma membrane, to the nucleus or to specific intracellular organelles, and to other filaments: the cytoskeleton is a highly crosslinked network. Many experimental studies have characterized a given cytoskeletal component, especially with *in vitro* assays of polymerized filaments or reconstituted gels of cytoskeletal polymers. This approach greatly improved our understanding of each cytoskeleton, from structural, functional or mechanical points of view. However, to take into account the high level of crosslinking within the cytoskeleton, *in vitro* reconstitution of more than one cytoskeleton and/or experiments in living cells have to be performed in order to describe the functional and mechanical interactions between actin filaments, microtubules and intermediate filaments.

1.2 Functions of the cytoskeleton in eukaryotic cells

1.2.1 Actin filaments regulate cell shape and movement

Discovered in the 1940s in muscle cells [Straub 1942], actin is the most studied subcomponent of the cytoskeleton so far. Actin forms filaments that are key players in mechanical support and in cell movement and that are implicated in a number of biological processes in eukaryotic cells. Providing an exhaustive list is not the aim here and we will only mention three of the most crucial biological processes involving actin in eukaryotic cells:

- **Myosin motors bind actin and transport organelles along actin filaments.** Myosin proteins - a superfamily of actin motor proteins - use cycles of Adenosine Triphosphate (ATP) hydrolysis to walk along actin filaments. In other words, myosins convert chemical energy (taken from ATP) into mechanical energy to generate forces and movements. In many eukaryotic cells, the actin network is referred to as the *actomyosin network*. Cells use myosin motors to transport organelles along actin filaments (see figure 1.3.C). For instance, myosin V walks from the pointed end to the barbed end, transporting vesicles and intracellular organelles.
- **Contractile rings of actin filaments allow animal cells to perform cytokinesis.** Other myosins, such as myosin II, are associated with contractile activity. During the last step of the cell cycle, the two daughter cells get separated in a process called *cytokinesis*. Several organisms, such as fungi, animals and amoebas, pinch their cells in two by using a contractile ring of actin filaments and myosin II. The process relies on myosin II polymerization into bipolar filaments able to produce a contraction by pulling actin filaments together (see figure 1.3.D). In animal cells, this contractile ring machinery is found in muscle cells, in which the actomyosin complex is very abundant.
- **Cellular motility is achieved by actin filaments acting as a treadmill.** The ability to migrate is a key feature of eukaryotic cells: embryonic morphogenesis mostly relies on cell migration; tissue integrity and regeneration is ensured by migrating cells; the motility of immune cells allows them to search and destroy pathogens; and many diseases - like cancer - take advantage of this cellular ability in order to move inside the organism. Cell polarization is essential to migration: the molecular processes at the front and at the back of a moving cell are different [Ridley 2003]. Actin plays a key part in the migration process which occurs in several steps. First, a complex linked to actin (called Arp2/3, see figure 1.3.A) initiates a protrusion at the front of the cell by growing branches of actin, making structures called *lamellipodia* and *filopodia*. These structures push the plasma membrane forward. During the extension of actin protrusions, the cell forms focal adhesions at the front of the cell to provide adhesion to the extra-cellular environment. Next,

a forward force is generated by contractions of the actomyosin network. Finally, retraction fibres pull the rear of the cell in the direction of the leading edge [Mattila & Lappalainen 2008] (see figure 1.3.B). The *treadmilling effect* of actin is a meaningful description of this cycle of localized polymerizations and depolymerizations of actin which allows cells to move.

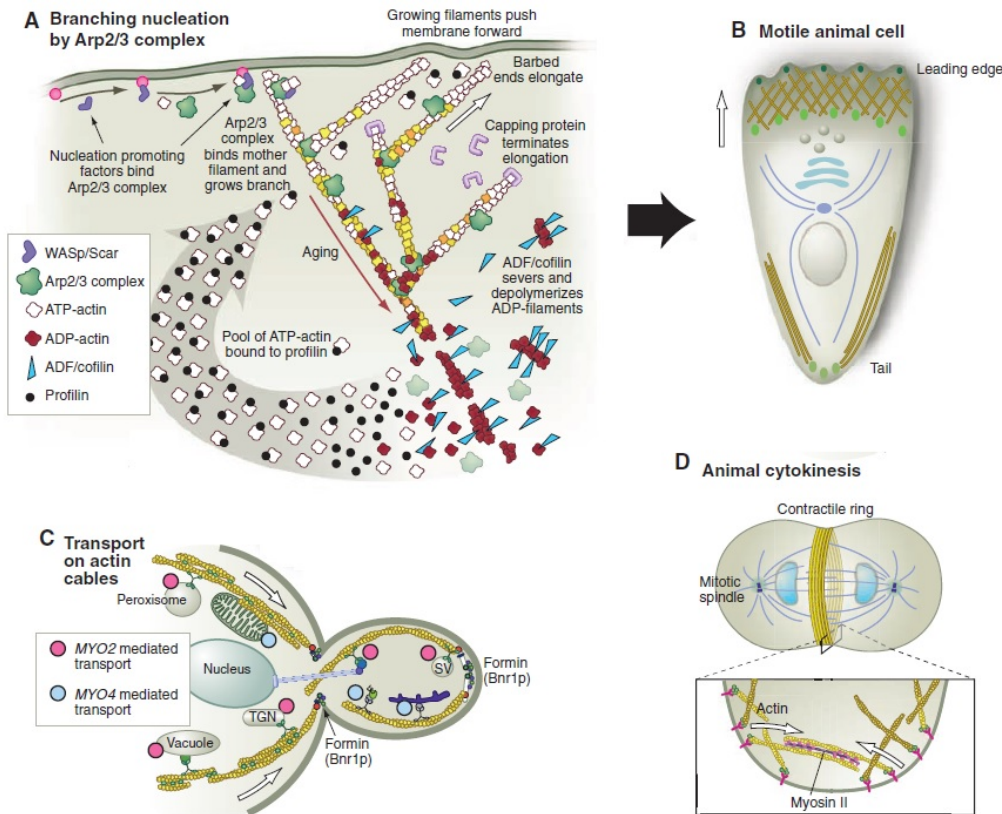


Figure 1.3: Actin-based movements in animal cells. Adapted from [Pollard & Cooper 2009].

1.2.2 Intermediate filaments maintain cellular integrity

Despite the great diversity of intermediate filament proteins, our knowledge of intermediate filament functions is still very young and fragmented. Unlike microtubules and actin filaments, the expression of intermediate filament proteins is extremely dependent on the cell type. Also, intermediate filaments can be found in the cytoplasm or in the nucleus (the nuclear intermediate filaments are called *lamins*). In this section, we will only mention cytoplasmic intermediate filaments:

- **Because of their unique physical properties, intermediate filaments control cell shape and prevent cells from irreversible mechanical damage.** Intermediate filaments are the only cytoskeletal subcomponent

which is not polar: they are symmetric and no molecular motor associated with any intermediate filament type is known so far. Also, as indicated in table 1.1, typical persistence lengths of intermediate filaments range from 100 nm to 1 μ m. Their persistence length being much smaller than microtubule and actin persistence lengths, they are the most flexible cytoskeletal subcomponent. As a consequence, intermediate filaments play a peculiar role in cell mechanics by providing strength and resistance to cells. For instance, in keratinocytes, keratin loss leads to significant cell softening [Ramms *et al.* 2013]. Intermediate filaments also seem to exhibit an adapted response to the applied forces. Strain-stiffening of individual vimentin filaments has been measured *in vitro*: at low forces, intermediate filaments are fully elastic whereas at high forces, they stiffen and deform in a plastic manner [Block *et al.* 2015]. Intermediate filaments can be seen as a guardian of cellular integrity, providing mechanical resistance to avoid large and fast cellular deformations.

- **Intermediate filaments are associated to several linkers and membrane-associated proteins and play a crucial role in intracellular organization.** Along with microtubules and actin filaments, cytoplasmic intermediate filaments are connected to the nucleus by the Linker of Nucleoskeleton and Cytoskeleton (LINC) complex, an assembly of proteins connected to the nuclear envelope [Dupin & Etienne-Manneville 2011]. It has been shown that intermediate filaments regulate the size, shape and rigidity of the nucleus, but also chromatin organization [Keeling *et al.* 2017]. As previously stated, intermediate filaments are not associated to any molecular motor. Unlike microtubules, they are not major players in vesicular transport. However, intermediate filaments interact with virtually all intracellular organelles, among which mitochondria or the Golgi apparatus, through linking proteins. Keratins, desmin and neurofilaments control mitochondrial location and function, and Golgi positioning is regulated by keratins, vimentin and neurofilaments, and endosomal/lysosomal protein distribution by vimentin [Toivola *et al.* 2005].
- **Intermediate filaments are involved in many dynamic cellular processes.** Most of our knowledge related to intermediate filaments comes from diseases in which cells have major dysregulations of some intermediate filament proteins. Not only are intermediate filament proteins drastically different from one cell type to another, but they also evolve during the cell cycle and dynamic processes within a given cell type. Intermediate filaments has been found to play a crucial role in the regulation of apoptotic events by protecting cells from apoptosis [Omary *et al.* 2004]. Mutations on some keratins correlate with increased cell apoptosis and liver injury [Omary *et al.* 2009]. Intermediate filaments are also critical in cell migration: in astrocytes, intermediate filaments depletion slows cell migration [Dupin & Etienne-Manneville 2011]. In many cell types, intermediate filaments facilitate cell motility and migration, so that increased intermediate filament protein expression can be associated with can-

cer progression and metastasis in some cases [Etienne-Manneville 2018]. Finally, intermediate filaments impact cell size, cell growth and proliferation. Figure 1.4 depicts the role of intermediate filaments in cellular responses to extracellular stimuli.

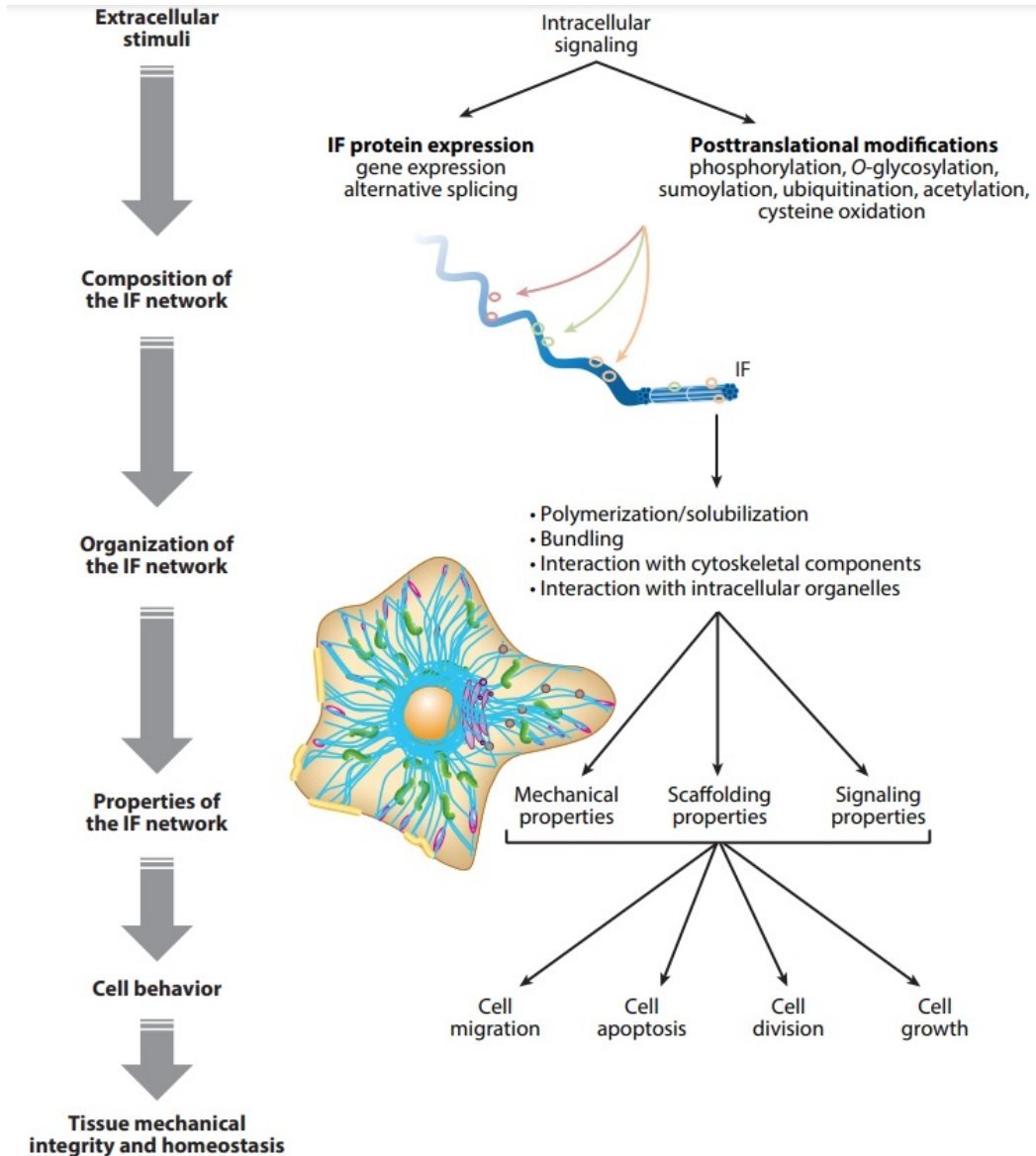


Figure 1.4: Intermediate filaments: role in cellular responses to extracellular stimuli. From [Etienne-Manneville 2018].

1.2.3 Microtubules provide a structural framework and orchestrate intracellular trafficking

Microtubules have become a research topic *per se* during the 1960s. Their association with several molecular motors and their dynamics make microtubules a key player in cell polarity, cell organization and intracellular transport. Here, we give three of the main functions of microtubules:

- **Microtubules establish the global polarity of the cell.** One of the most important properties of the microtubule network is that they are highly dynamic, constantly polymerizing and depolymerizing, as we will describe in 1.4.1. Microtubule half-time vary during the cell cycle, but it ranges from 10 s to 10 min. Interestingly, cells lacking a proper dynamic microtubule network - *e.g.* after using drugs affecting its dynamics - are often much less motile and poorly polarized. While actin structures are crucial in cell motility, it has been shown that microtubules induce cortical polarity and regulate actin dynamics [Siegrist & Doe 2007]. Microtubules, rather than establishing cell polarity, ensure its maintenance by mediating the distribution of inhibitory signals [Zhang *et al.* 2014]. Microtubules also impact the organization of the nucleus and of other organelles. For instance, in *Xenopus*, microtubule dynamics is balanced spatially and temporally for nuclear formation and its perturbation changes nuclear morphology [Xue *et al.* 2013].
- **Molecular motors associate with microtubules to perform intracellular trafficking.** As myosins bind actin filaments to transport vesicles along them, two types of molecular motors bind microtubules : *kinesins* and *dynein*. Discovered in 1985, kinesins are *anterograde* transport motors, which means that they transport vesicles, organelles and other cargoes towards the (+) ends of microtubules from the center of a cell to its periphery [Vale *et al.* 1985]. Fourteen families of human kinesins exist and all share a common amino acid sequence of the motor domain. Conversely, cytoplasmic dynein moves on microtubules towards their (-) ends: it is a *retrograde* transport motor. Dynein-induced retrograde transport is important to send endocytosis products to the center of the cell. As myosins, both kinesins and dynein convert the chemical energy stored in **ATP** into mechanical work.
- **Microtubules spatially regulate mitosis and cytokinesis.** We already mentioned the crucial role of actin, making contractile rings, to perform cytokinesis. This contraction occurs at the end of mitosis, whereas the first steps of mitosis (and also cytokinesis) are regulated by microtubules. First, microtubules determine the cleavage plane and position the site of division. Second, they transport vesicles to the cleavage plane. Microtubules form the mitotic apparatus (composed of the mitotic spindle and of the aster) which pulls the sister chromatides in opposite directions. The construction of this machinery is spatially regulated by microtubules but also requires the coordinated activities of many proteins [Straight & Field 2000].

1.3 Intermediate filaments

1.3.1 Diversity of intermediate filaments in eukaryotic cells

With more than seventy different proteins, intermediate filaments show a high variability. They are subcategorized in six different types that we will briefly describe below and which are recapitulated in table 1.2.

Keratins are part of type I (acidic keratins) and type II (neutral or basic keratins). There are more than fifty different keratins in animal cells. They are among the smallest intermediate filament proteins with a molecular weight between 40 kDa and 70 kDa. Keratins are mostly expressed in epithelial cells, in which one type I keratin copolymerizes with one type II keratin to give rise to a keratin filament. Keratins are widespread in the cytoplasm of epithelial cells, but also form specific structures like hair, nails and horns.

Type III intermediate filament proteins include vimentin, which can be found in a lot of cell types, from fibroblasts to endothelial cells. Another well-characterized type III protein is desmin, which can be found in muscle cells. Glial Fibrillary Acidic Protein (GFAP) is specifically expressed in glial cells. All type III intermediate filament proteins have molecular weights around 55 kDa.

Neurofilaments constitute the type IV intermediate filament proteins. As their name suggests, they are found in neurons, specially in the axons of motor neurons. They are thought to be crucial for these long and thin processes than can reach 1 m to join neurons between them. Type IV intermediate filament proteins are the largest ones with molecular weights up to 240 kDa³.

Notably, type V intermediate filament proteins are not part of the cytoskeleton: they are part of the nuclear envelope and are called *lamins*. Lamins have a molecular weight around 70 kDa

Finally, type VI⁴ intermediate filament proteins are structurally quite different from the other types, being characterized by a long C-terminal tail. Among them, some proteins are specifically found in lens.

Most of our knowledge regarding intermediate filaments comes from studies of intermediate filament-associated diseases. For instance, early-onset megalencephaly, progressive spasticity and dementia characterize Alexander disease, which is caused by a mutation on the gene coding for GFAP [Omary *et al.* 2004]. Mutated desmin cause myopathies, and Charcot-Marie-Tooth disease (characterized by symmetrical muscle weakness, wasting, foot deformities, difficulty walking, reduced tendon reflexes) is due to mutations in lamins [Omary *et al.* 2004]. The research carried out on these diseases have led to greatly improve our understanding of the functions and the diversity of intermediate filament proteins.

³Some type VI intermediate filament proteins - like nestin and synemin - are considered by some papers to be part of type IV because their genomic structure is similar to the neurofilament family and α -internexin [Liem 2013].

⁴They are historically referred to as "orphans".

Type	Name	Size (kDa)	Genes	Tissue distribution
I	Acidic keratins	44 – 66	> 25	Soft epithelia (skin, liver, <i>etc.</i>) Hard epithelia (hair, nail, <i>etc.</i>)
II	Neutral-Basic keratins	52 – 68	> 25	
III	Vimentin	57	1	Mesenchyme
	Desmin	54	1	Muscle
	GFAP	50	1	Glial cells
	Peripherin	57	1	Neurons
	Syncoilin	64	1	Muscle
IV	Neurofilaments	68 – 240	3	Neurons
	α -internexin	66	1	Neurons
V	Lamins	62 – 78	3	Ubiquitous (nuclear)
VI	Synemin	41 – 180	1	Neural stem cells, muscle, endothelium
	Nestin	240	1	Neurons, astrocytes, muscle
	Filensin	94	1	Lens
	Phakinin	49	1	Lens

Table 1.2: Classification of intermediate filament proteins by type. Adapted from [Cooper 2000], [Chung *et al.* 2013] and [Leduc & Etienne-Manneville 2015]

1.3.2 Structure and assembly of intermediate filaments

- The tripartite monomer structure of intermediate filament proteins.**
 Like all proteins, intermediate filament proteins have two ends: an amine group, called the *N-terminus* and a carboxylic group, called the *C-terminus*. As they are translated from messenger Ribonucleic Acid (RNA), they are created from N-terminus to C-terminus. The domain next to the N-terminus of intermediate filament proteins is called the *head* and the one next to the C-terminus is called the *tail*. Between these two domains, we can find several α -helical structures: they form the *rod* (see figure 1.5.A). All intermediate filaments share this tripartite monomer structure. Under stress, the rod domain can stretch and some parts of the α -helical domain can be uncoiled and form β sheets instead [Qin *et al.* 2009]. Nuclear intermediate filaments - lamins - also have this structure. Their structural singularity relies on the much longer C-terminal domain in which can be found a Nuclear Localization Signal (NLS), required for transport into the nucleus (see figure 1.5.B-C that compares human lamin and human vimentin structures).
- Assembly of intermediate filament proteins depends on their type.**
 All intermediate filaments are assembled from fibrous proteins that exhibit a central α -helical rod domain which facilitates the formation of dimeric coiled-coil complexes. However, their assembly vary a lot depending on the type of intermediate filament protein involved. The first step common to all interme-

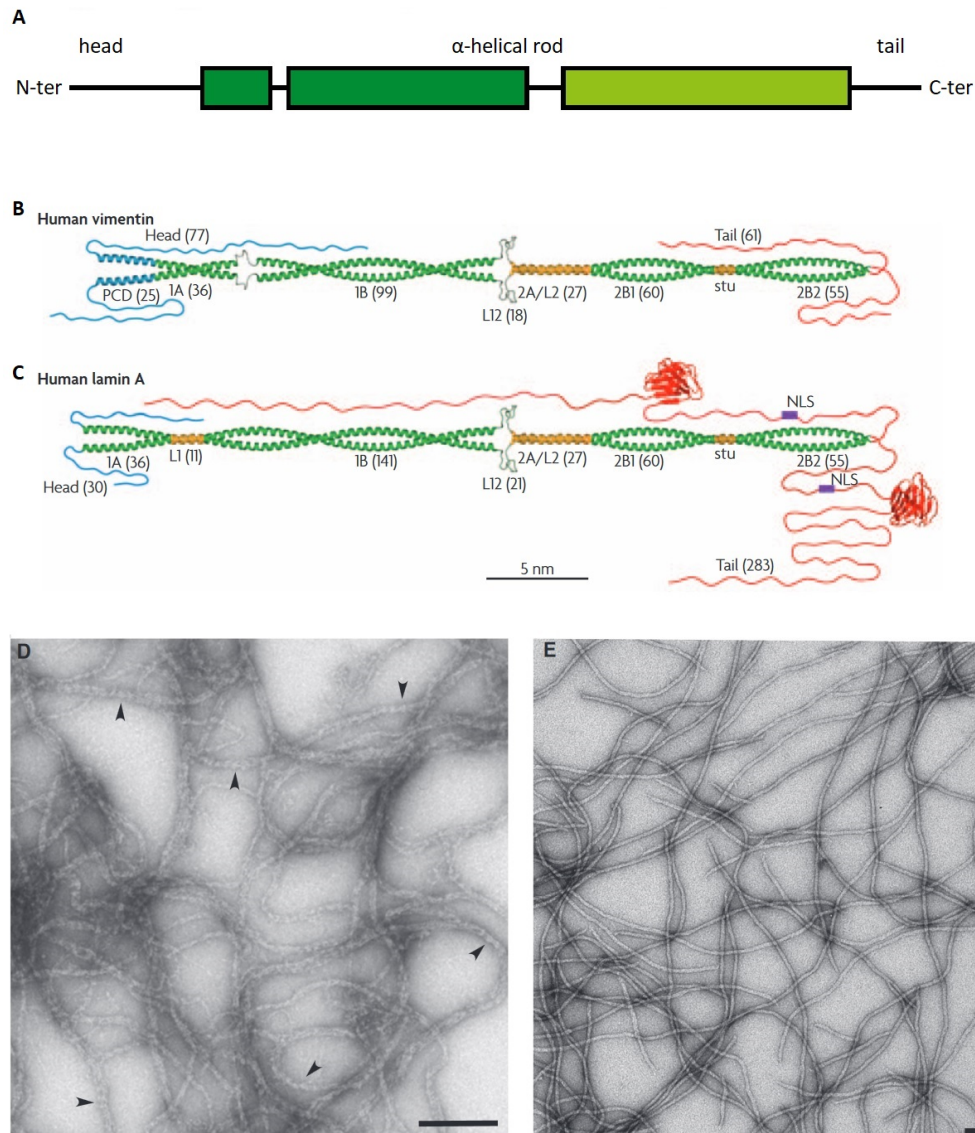


Figure 1.5: Detailed structure of cytoplasmic and nuclear intermediate filament proteins. *A*. Intermediate filaments are composed of head, rod and tail domains. Adapted from [Lopez et al. 2016] *B* & *C*. Structural models of human vimentin, a cytoplasmic intermediate filament protein (*B*) and human lamin A, a nuclear intermediate filament protein (*C*). Scale bar: 5 nm. From [Herrmann et al. 2007] *D* & *E*. Electron microscopy of recombinant human lamin A (*D*) and recombinant vimentin (*E*). Scale bar: 200 nm. Arrow heads indicate prominent "beadings" of the filaments, which are typical structures found when lamins are reconstituted in vitro. From [Herrmann & Aebi 2016].

Intermediate filament proteins is the formation of a dimer after two monomers bind to each other by their rod domain. The two monomers involved can be identical and form homodimers or they can be different and form heterodimers. Keratins, for instance, always form heterodimers by associating a type I keratin protein (acidic) with a type II keratin protein (neutral-basic). The next step varies:

- for **cytoplasmic** intermediate filament proteins, two dimers form a tetramer in a half-staggered manner through the rod domains aligned in an antiparallel orientation. This tetramer is non polar and is called *protofilament*. Then, eight tetramers are aligned laterally to form a unit-length filament. Several unit-length filaments will finally anneal end-to-end to form a non-polar and mature intermediate filament. This process is depicted in figure 1.6.A.
- regarding **lamins**, dimers bind their N-terminus to the C-terminus of another dimer by a peptide bond, forming a long polar structure. Two of these structures will then align laterally in an anti-parallel orientation to form a protofilament. Protofilaments then assemble to create a symmetric filament, which now is also non-polar, like cytoplasmic intermediate filaments (see figure 1.6.B.)

Figure 1.5.D-E shows electron microscopy images of these intermediate filaments.

Unlike microtubules and actin filaments, **ATP** and Guanosine Triphosphate (**GTP**) are not directly required in the assembly of intermediate filaments because the different steps (monomer to dimer, dimer to tetramer, *etc.*) do not rely on **ATP**-bound or **GTP**-bound monomers. However, immature intermediate filaments are transported along microtubules, or actin filaments for most keratins, and therefore require chemical energy for their transport.

1.3.3 Vimentin, an intermediate filament protein present in many cells

With keratins, vimentin is among the most studied intermediate filament proteins. It can be found in many different cell types, specially in mesenchymal cells. Human vimentin is a 57 kDa protein the structure of which appears in figure 1.5.A-B,E. Here, we review some of the key aspects of vimentin⁵.

- **Vimentin is crucial in the epithelial-mesenchymal transition.** Animal tissues can be divided into four different families. Among them, epithelium corresponds to the cells lining the outer surfaces of organs and blood vessels. *Epithelial cells* are highly polarized and are strongly connected by several junctions between them. Epithelial cells can leave their original tissue and,

⁵Mechanical aspects of vimentin filaments will be detailed in chapter 2.

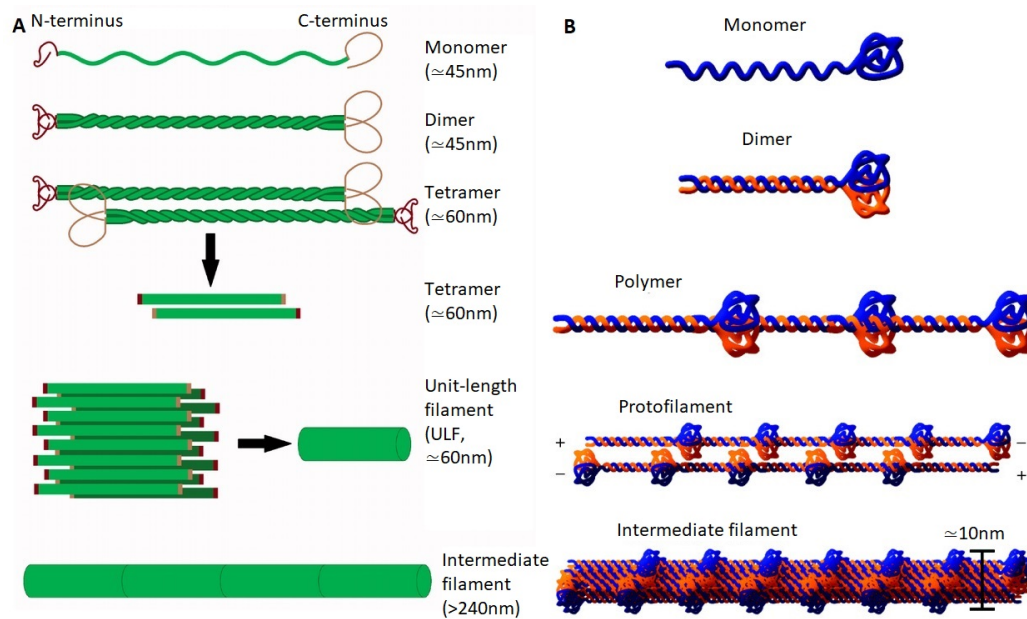


Figure 1.6: Schematic representation of the assembly of intermediate filaments.

A : Assembly of cytoplasmic intermediate filaments. Adapted from [Hohmann & Dehghani 2019]. *B* : Assembly of nuclear intermediate filaments (lamins). Adapted from [Dittmer & Misteli 2011].

after losing their polarity and breaking cell-cell adhesions, become multipotent cells called *mesenchymal cells*. This process is called the Epithelial-Mesenchymal Transition (EMT) and is required for numerous developmental processes, wound healing but also to initiate metastasis during cancer. Gene expression is modified during EMT and, while vimentin expression is quite low in epithelium, it is upregulated in mesenchymal cells. For instance, it has been shown that vimentin promotes EMT phenotypes in breast cancer cells by mediating the expression of slug, an EMT protein [Liu *et al.* 2015]. Vimentin is not only involved in signalling pathways, but also in migration. Non-metastatic breast cancer cells MCF-7 - an epithelial cell line than normally does not express vimentin - rapidly adopt mesenchymal shapes after vimentin transfection. Conversely, silencing vimentin causes mesenchymal cells to adopt epithelial shapes [Mendez *et al.* 2010]. Along with these shape transitions, increase in cell motility and in focal adhesions dynamics were measured to be coincident with vimentin filament assembly [Mendez *et al.* 2010]. In the context of the EMT, vimentin appears to play a major role in the gain of migratory properties, as shown in figure 1.7.A.

- **Vimentin in organelle positioning.** In addition to increasing migration properties, vimentin filaments also regulate the positioning of several organelles in eukaryotic cells. For instance, vimentin interacts a lot with

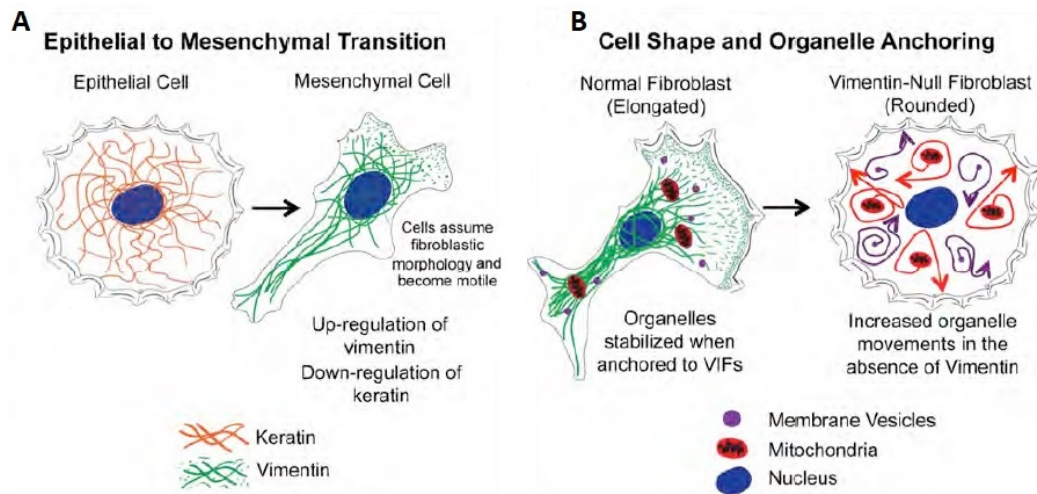


Figure 1.7: Selected functions of vimentin. Adapted from [Lowery *et al.* 2015].

mitochondria. Cells lacking an intact vimentin filament network exhibit an increased level in the motility of mitochondria [Nekrasova *et al.* 2011]. The authors suggest that vimentin intermediate filaments bind to mitochondria and anchor them within the cytoplasm. Vimentin has also been shown to interact with the Golgi apparatus [Gao & Sztul 2001] and with melanosomes, forming an intricate cage around them [Chang *et al.* 2009]. Finally, vimentin has been recently described to form ball-like structures and rings around the nucleus during the first step of adhesion that are able to strongly deform the cell nucleus [Terriac *et al.* 2019]. These features are schematically recapitulated in figure 1.7.B.

- **Vimentin in astrocytes and glioma cells.** As my PhD resorts to a cell line derived from a human malignant astrocytoma⁶, we focus here on vimentin - as well as its links to other intermediate filament proteins - in astrocytes and glioma cells. Like in other cancers [Satelli & Li 2011], vimentin is upregulated in glioma and *glioblastoma*, a grade IV glioma. Interestingly, using withaferin-A (a chemical inhibitor of vimentin) in glioblastoma induces glioblastoma cell morphology changes, inhibits the motility of glioblastoma cells and leads to a reduction of glioblastoma cell growth *in vitro* [Zhao *et al.* 2018]. More than being a marker of tumour in glial cells, vimentin is a marker of a poor outcome in glioblastoma patients [Zhao *et al.* 2018].

Another type III intermediate filament protein is expressed in astrocytes (and is even specific for glial cells): the Glial Fibrillary Acidic Protein (GFAP). Even though studies on the link between GFAP expression and malignant phenotypes or tumour growth are controversial, it has been shown long ago that

⁶The brain is mainly made of two cell types - *neuronal cells* and *glial cells*. Among glial cells, we can find several subtypes, such as *astrocytes*, *oligodendrocytes*, *etc.*. Tumours derived from these cells are called *glioma*, *astrocytoma*, *oligodendrocytoma*, *etc.*

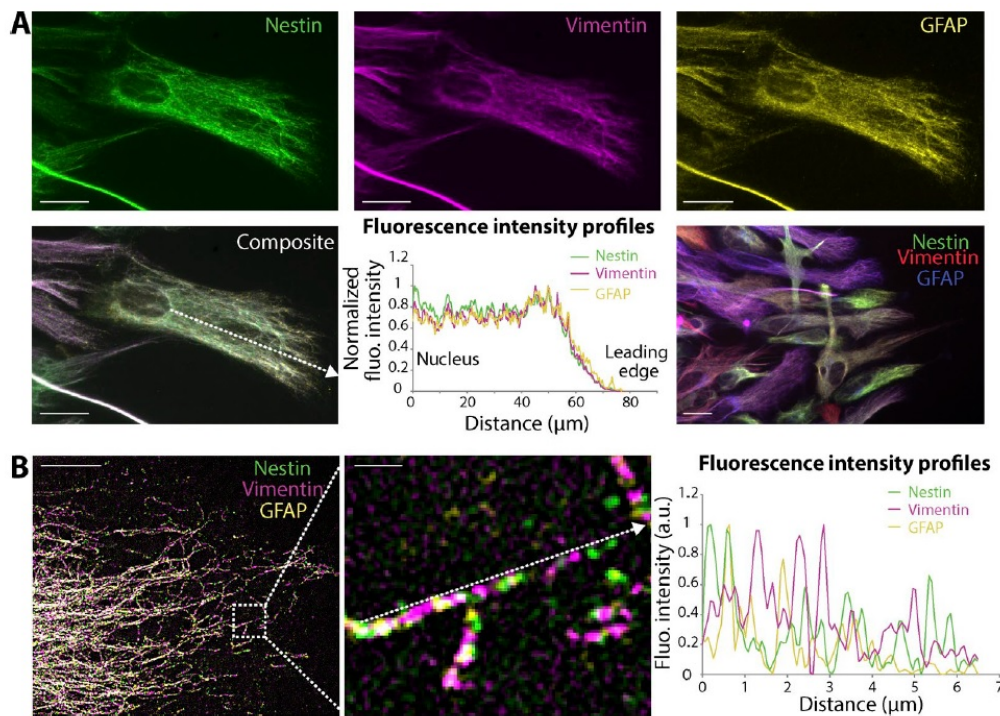


Figure 1.8: Imaging of intermediate filaments in astrocytes.

A: Epifluorescence image of nestin, GFAP and vimentin. Scale bars: 20 μm . *B*: 3D structured illumination microscopy picture. Scale bars: 10 μm (main image) and 1 μm (inset). Both fluorescence intensity profiles were obtained along the corresponding dotted arrow. From [Leduc & Etienne-Manneville 2017].

human gliomas co-express GFAP and vimentin [Herpers *et al.* 1986] and that both proteins copolymerize in the same intermediate filament system [Wang *et al.* 1984]. More recently, epifluorescence microscopy and 3D structured illumination microscopy images have shed light on the distribution of cytoplasmic intermediate filaments in astrocytes [Leduc & Etienne-Manneville 2017]. In addition to GFAP and vimentin, the authors studied another intermediate filament protein: nestin. Figure 1.8.A shows that astrocytes have a heterogeneous expression of intermediate filament proteins but their distributions are similar. Besides, they strongly colocalize in cells expressing several intermediate filament proteins. Figure 1.8.B uses a superresolution imaging technique to show that single filaments are composed of several intermediate filament proteins.

1.4 Microtubules

1.4.1 Dynamics of microtubules

Unlike intermediate filaments, microtubules are extremely dynamic: they exhibit a fast turnover in living cells. In 1986, *in vitro* experiments showed that 80% of the microtubules in interphase cells turn over in 15 min [Schulze & Kirschner 1986]. Microtubules exhibit a cyclic behaviour, oscillating between long and progressive phases of polymerization and short and brutal depolymerization events. This process has been named *dynamic instability* and will be defined below.

- **Microtubule polymerization is initiated by nucleation on pre-existing seeds⁷.** If recruiting heterodimers of $\alpha\beta$ -tubulin to elongate an already formed microtubule is an energetically favourable process which explains why microtubules polymerize fast, initiating microtubule polymerization is a highly unfavourable process. Hence, initiation is the rate-limiting step in microtubule polymerization. *In vitro*, microtubule initial growth progresses slowly, as it proceeds from small entities for which disassembly is energetically favoured over assembly (see figure 1.9.A). In cells, some preformed nuclei are found at Microtubule-Organizing Centers (MTOCs). For instance, γ -tubulin ring complexes (γ -TuRC) are made of γ -tubulin, another member of the tubulin family. These complexes are the structural basis of the thirteen protofilament structure of microtubules (see figure 1.9.B). In bulk assembly assays, the presence of preformed nuclei increases the fraction of polymerized microtubules with time (see figure 1.9.C) [Kollman *et al.* 2011].
- **Growing and shrinking, the dynamic instability of microtubules.** The complexity of microtubule dynamics goes further than nucleation-elongation processes. While microtubules elongate, their polymerization is regularly and abruptly stopped by depolymerization phases. The transition point between polymerization and depolymerization is called *catastrophe*. Conversely, when a microtubule is (quickly) depolymerizing, it can switch back to a polymerization phase by an event called *rescue* (see figure 1.9.D-E). Microtubules are therefore constantly growing and shrinking [Mitchison & Kirschner 1984], and what governs the transitions between these phases - especially rescues - is still not totally established.

Catastrophes have long been viewed as the result of the loss of a protective end structure [Mitchison & Kirschner 1984] [Desai & Mitchison 1997]. Under this hypothesis, the probability of a catastrophe event has to be constant over time. However, this does not match the measurements. It is now accepted that catastrophes are not a single step process but a multiple step process, which implies that the probability of undergoing a catastrophe in-

⁷In many studies, this *nucleation seed* is simply called nucleus. We have used here the word seed - as in thermodynamics - to introduce the concept and avoid any confusion with the cell nucleus. In the following, we use the word nucleus to better match the literature.

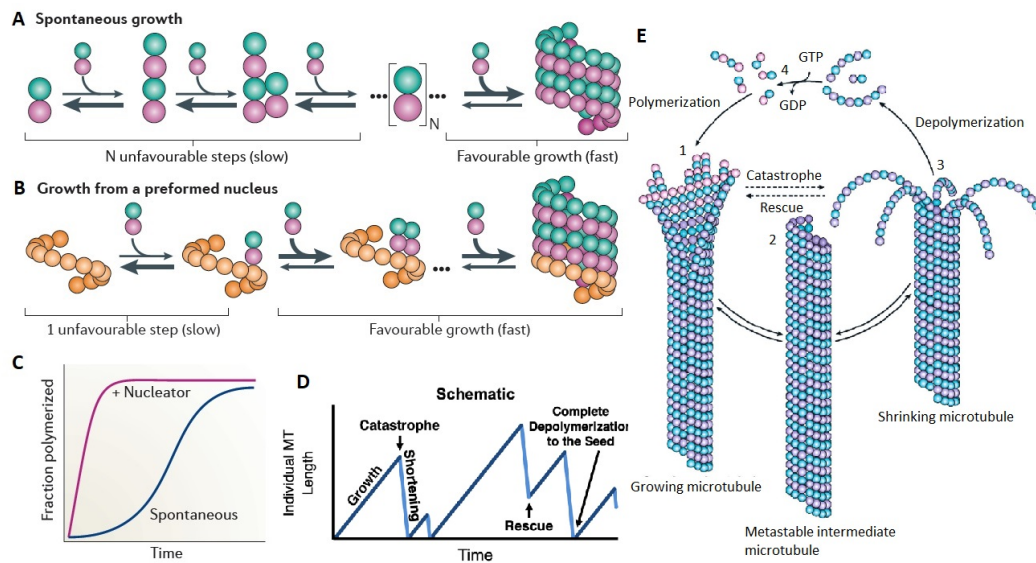


Figure 1.9: Microtubule assembly and dynamic instability.

A: De novo formation of microtubules from heterodimers of $\alpha\beta$ -tubulin is energetically unfavourable until a sufficiently large oligomer is formed (after N steps). **B:** Preformed nuclei (such as the γ -TuRC complex) allow microtubule to bypass the slow phase in vivo. **C:** Influence of the presence of a preformed nucleus on the polymerization kinetics. Adapted from [Kollman et al. 2011]. **D:** Microtubule length against time depicting dynamic instability and showing catastrophes and rescues. Adapted from [Mauro et al. 2019]. **E:** Schematic representation of dynamic instability of microtubules. (1) Closure of the terminal sheet structure generates a metastable, blunt-ended microtubule (2) which may pause, undergo further growth or switch to the depolymerization phase. A shrinking microtubule is characterized by fountain-like arrays of ring and spiral protofilament structures (3). This cycle is completed by exchanging GDP of the disassembly products with GTP (4). Adapted from [Dráber et al. 2012].

increases with time: microtubule catastrophe can be viewed as an aging process [Gardner et al. 2013]. The rescue process remains much more debated. It was shown *in vitro* that rescue events increase with free tubulin concentration [Walker et al. 1988]. More recently, after observing with a specific antibody that microtubules host some GTP-tubulin islands (or *remnants*) within their lattice, it has been hypothesized that rescue events initiate from these remnants [Dimitrov et al. 2008]. Molecular dynamics simulations and *in vitro* experiments show that GTP-tubulin remnants regulate the kinetics of depolymerization [Bollinger et al. 2020]. But how these remnants appear in the lattice is still an open question.

- **Microtubule dynamics and drugs targeting tubulin.** Regulating microtubule dynamics in cells can be of interest, as microtubules are implicated in many cellular functions (see 1.2.3). For example, *paclitaxel* - also known as *taxol* - is used for the treatment of many cancers. Its action is well known: while it poorly binds to soluble tubulin, it has a high affinity for the β -

tubulin subunit along the length of the microtubule. By doing so, it stabilizes the microtubule and increases microtubule polymerization, which drastically reduces microtubule dynamic instability. From a therapeutic point of view, suppression of microtubule dynamics by paclitaxel leads to a mitotic block and prevents the dividing cancer cells from proliferating and eventually leads to apoptosis [Jordan & Wilson 2004]. Another key drug for my PhD is *nocodazole*. Nocodazole binds to an arginine residue on β -tubulin and has an action that depends on its concentration. At high concentrations - typically $10\ \mu\text{M}$ -, nocodazole rapidly depolymerizes microtubules [De Brabander *et al.* 1976]. At low concentrations - typically $0.1 - 1\ \mu\text{M}$ -, nocodazole inhibits microtubule dynamic instability [Vasquez *et al.* 1997]. Because microtubules are not able to properly polymerize when they are in presence of nocodazole, the mitotic spindle is not formed when cells enter metaphase. Hence, nocodazole is also frequently used to synchronize cells in mitosis.

1.4.2 Microtubules and post-translational modifications

Even if they are composed of a single heterodimer motif of $\alpha\beta$ -tubulin, microtubules can show some diversity in cells. First, α -tubulin and β -tubulin consist of isotypes encoded by different genes in amino acid sequence. In human, there are seven isotypes of α -tubulin and eight isotypes of β -tubulin [Ludueña & Banerjee 2008]. This point will not be discussed further in the present manuscript. Second, microtubules can undergo a variety of Post-Translational Modifications (PTM) that decorate both α -tubulin and β -tubulin. Together, these modifications form the so called *tubulin code*.

- **Tubulin PTM: nature, localization, mechanism, functions.** Several PTM can decorate microtubules. Some of them were already known in other contexts, such as *phosphorylation*, *acetylation*, *methylation*, *palmitoylation*, *etc.*, whereas others were discovered in the specific context of microtubule studies: *tyrosination*, *glycylation*, *glutamylolation*, *etc.* [Janke & Bulinski 2011]. These modifications can take place on the tubulin body, either on the β -tubulin subunit - like phosphorylation or polyamination -, or on the α -tubulin - like methylation or palmitoylation. Some of them can occur on both: for instance, there are five different known sites for phosphorylation and there are also two different sites for acetylation. Other modifications are seen on the C-terminal tails of the tubulin subunit, such as tyrosination, polyglycylation, polyglutamylolation. Most of these PTM are catalyzed by enzymes that in general preferentially bind tubulin assembled within microtubules over soluble tubulin. Some modifications are reversible (acetylation, detyrosination) but for many of them no reverse reaction or enzymes is known. Microtubule PTM can modify microtubule properties and, by doing so, favour or impair some of their cellular functions. How PTM impact cell mechanics will be discussed in detail in chapter 2. They also have consequences on cellular and physiological processes [Janke & Magiera 2020] which are out of the scope of this work.

- **Acetylation, the most studied microtubule post-translational modification.** The cell line used for my PhD work - derived from an astrocytoma - shows a very low basal level of acetylated microtubules. Hence, studying the effect of acetylation on the cytoskeleton mechanics can be of interest. As acetylation can occur at different sites, it is important to mention at this stage that we will deal with Lysine 40 (K40) acetylation in which lysine 40 on α -tubulin gets acetylated. This post-translational modification is the only one known to date which takes place inside the microtubule, in the intraluminal region (see figure 1.10.A). It is also known to occur only on microtubules as it is not found on soluble tubulin [L'Hernault & Rosenbaum 1985]. How this acetylation is catalyzed remained unknown for a long time but in 2010 α -Tubulin N-Acetyltransferase 1 (ATAT1) (also known as aTAT1, α TAT1 or simply TAT1) was discovered as an acetyltransferase facilitating K40 acetylation [Shida *et al.* 2010]. The way ATAT1 precisely accesses the lumen is still controversial but the current hypothesis is that it uses defects in the microtubule lattice (cracks) and, once in the lumen, it modifies available K40 sites (see figure 1.10.B-C) [Janke & Montagnac 2017]. ATAT1 is also thought to be able to enter from the open ends of microtubules (see figure 1.10.B). Conversely, two deacetylases have been identified so far: Histone Deacetylase 6 (HDAC6) [Hubbert *et al.* 2002] and Sirtuin Type 2 (SIRT2) [North *et al.* 2003]. Like ATAT1, HDAC6 is thought to be able to enter the microtubule lumen from the open ends, but recent evidence indicates that HDAC6 can also enter through the lattice as deacetylation was observed all along microtubules *in vitro* [Miyake *et al.* 2016]. The main difference with ATAT1 is that HDAC6 preferentially binds soluble tubulin. Acetylated microtubules are also known to be more stable and long-lived structures. The causal link between stability and acetylation has been debated [Janke & Montagnac 2017] and we will come back to this point in chapter 2. However, it is important to mention at this stage that acetylation efficiently protects microtubules from mechanical stress *in vitro* [Xu *et al.* 2017].

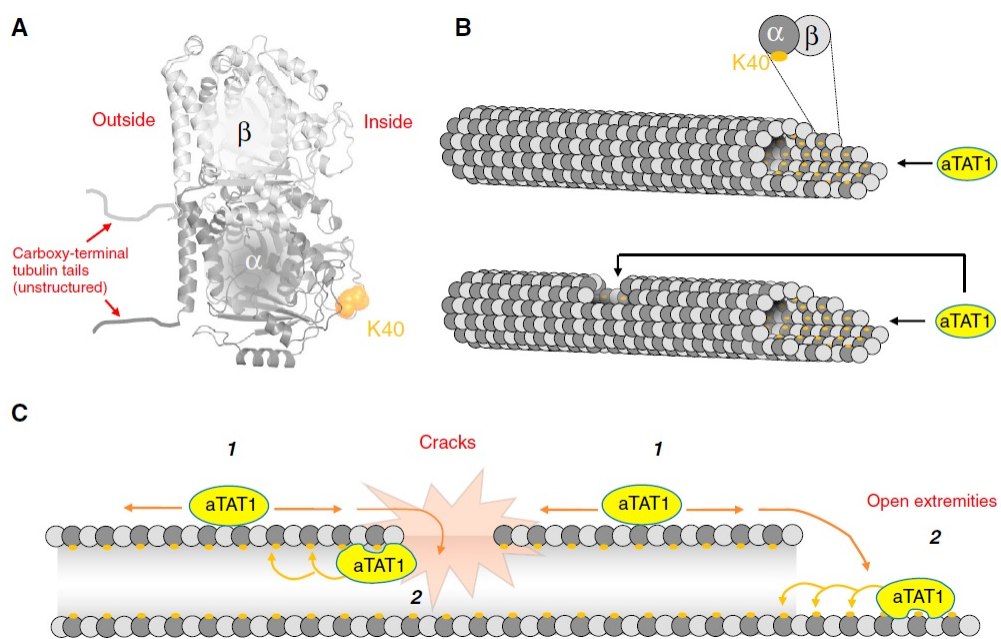


Figure 1.10: Modes of K40 acetylation by ATAT1. A: Structure of the tubulin heterodimer. The position of lysine 40 (K40) is shown in orange. B: Different entry sites of ATAT1. C: Hypothetical mechanistic model for ATAT1 access to the lumen. ATAT1 scans the outer surface of microtubules (1) in order to find accessible K40 modification sites at microtubules ends or at cracks in the microtubule lattice (2). From [Janke & Montagnac 2017].

Mechanical properties of the cytoskeleton

Contents

2.1	Measuring mechanical properties in cell biology	24
2.1.1	Cytoskeletal mechanics measurements <i>in vitro</i>	24
2.1.2	Whole-cell-scale, cortical and intracellular force measurements	30
2.1.3	Our approach: combining optical tweezers-based intracellular rheology with live cell imaging	32
2.2	Mechanics of microtubules <i>in vitro</i>	32
2.2.1	Anisotropic stiffness of microtubules	32
2.2.2	Variability in the measurements of microtubule flexural rigidity	33
2.2.3	Microtubule response to repeated mechanical stress	34
2.3	Mechanics of intermediate filaments <i>in vitro</i>	36
2.3.1	Networks of intermediate filaments: highly deformable and almost unbreakable	36
2.3.2	Individual intermediate filaments exhibit nonlinear strain-stiffening	37
2.4	Microtubules and intermediate filaments <i>in cellulo</i>	41
2.4.1	Measuring mechanics of cytoskeletal filaments <i>in cellulo</i> . . .	41
2.4.2	Mechanical contribution of microtubules in cells	43
2.4.3	Mechanical contribution of intermediate filaments in cells . .	44

Cells are complex biological objects composed of several organelles. Attempting to specifically measure the mechanical properties of the cytoskeleton is an exciting challenge considering that the mechanical properties of a cell can also be influenced by its environment, in particular by the presence of neighboring cells. Hence, many studies on the cytoskeleton have been carried out *in vitro* - using minimal systems and following bottom-up approaches - with a reduced number of control parameters. Mechanical constants of a given cytoskeletal subcomponent can be measured at different time scales, and compared to other conditions. The complementary approach is to work *in cellulo* and to modify some features of the cytoskeleton (*e.g.* composition, dynamics, PTM, *etc.*), and compare them to control cells: this is a top-down approach. In this case, the mechanics of the whole cytoskeleton, or even of the cell, is probed. Both the theoretical models and the experimental aspects

differ considerably depending on the chosen approach. In this chapter, after reviewing past and current methods to measure mechanical properties which are relevant in cell biology, we will summarize the known (to date) mechanical properties of the microtubule and the intermediate filament networks, both *in vitro* and in living cells. The mechanical interactions between these networks will be developed in chapter 3.

2.1 Measuring mechanical properties in cell biology

2.1.1 Cytoskeletal mechanics measurements *in vitro*

The cytoskeletal subcomponents come in many forms. They can be soluble proteins in the cytoplasm, form individual filaments, *bundles*¹ or networks. Studies carried out *in vitro* reflect and explore all this hierarchical organization, from individual filaments to crosslinked networks. Experimental techniques are accordingly selected for each biological object which is being probed, and we will detail here the main methods that have been developed to study the mechanics of the cytoskeleton *in vitro*. We can distinguish between two different types of measurements of mechanical properties: *active* measurements, where a force is applied on the cytoskeletal filament and *passive* measurements, where spontaneous fluctuations give access to the mechanical properties.

- **Probing the mechanics of individual filaments and bundles.**

- *Imaging fluctuations to measure mechanical properties.*

Cytoskeletal filaments are biopolymers. Hence, many studies resort to tools standardly used by polymer physics whose theoretical framework needs to be developed here. In particular, the stiffness of biopolymers is related to its persistence length. The persistence length l_p is defined as the length over which correlations in the direction tangent to the polymer are lost. To provide an expression of the persistence length, let us consider a cytoskeletal filamentous polymer of total length L . The parameter defining the position along this filament is the curvilinear abscissa s . The shape of this filament is given by the tangent vector $\vec{t}(s) = \frac{d\vec{r}(s)}{ds}$ tangent to the polymer at position s where $\vec{r}(s)$ is the distance to the (arbitrary) origin (see figure 2.1).

Due to thermal fluctuations, this filament bends over a typical length - the persistence length l_p - given by [Brochard-Wyart *et al.* 2019]:

$$\langle \vec{t}(s) \cdot \vec{t}(0) \rangle = \exp\left(-\frac{s}{l_p}\right) \quad (2.1)$$

¹A bundle, also called *fiber* is a structure composed of a lot of very close individual filaments which acts as a single entity. This structure is mostly observed for actin and intermediate filaments.

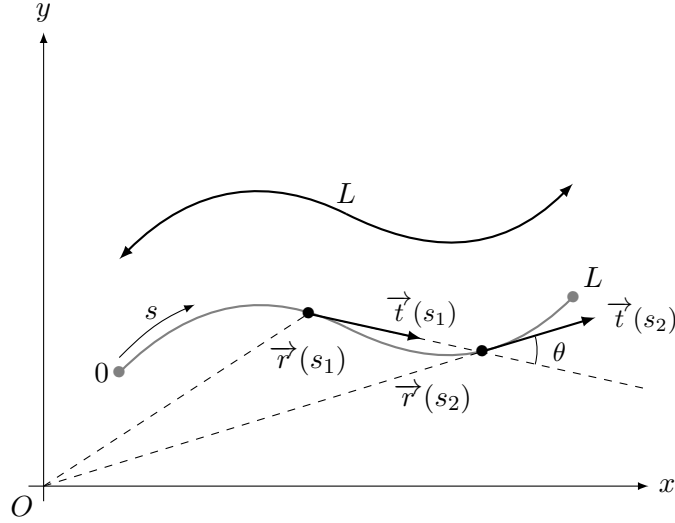


Figure 2.1: Persistence length of polymers.

All introduced parameters appear in this scheme, along with another representation of $\vec{t}(s) \cdot \vec{t}(0)$ by introducing θ such as $\cos \theta = \vec{t}(s_2) \cdot \vec{t}(s_1)$. Adapted from [Brochard-Wyart et al. 2019].

where $\langle \rangle$ is the temporal mean. In particular, we can check that for $s \ll l_p$, $\langle \vec{t}(s) \cdot \vec{t}(0) \rangle \rightarrow 1$. In this case, both tangent vectors have the same direction: at this length scale, the filament appears to be straight. Also, for $s \gg l_p$, we have $\langle \vec{t}(s) \cdot \vec{t}(0) \rangle \rightarrow 0$. The spatial correlations are lost as the two tangent vectors have independent orientations. Given the persistence lengths appearing in table 1.1, it is interesting to notice that intermediate filaments, actin filaments and microtubules are in three different regimes. To illustrate this, we can give an order of magnitude of the length of cytoskeletal fibers in living cells: typically $L \approx 10 \mu\text{m}$. For microtubules, the persistence length is larger than the typical microtubule length in cells ($L \ll l_p < 1 \text{ mm}$), which makes them appear often as straight structures² when imaged: microtubules are *rigid biopolymers*. In sharp contrast, mature intermediate filaments are *flexible biopolymers*: their lengths exceed by far their persistence length: $L \gg l_p > 1 \mu\text{m}$. This explains why intermediate filaments looks curly in cells. Actin filaments are in the intermediate regime, where $L \approx l_p \approx 10 \mu\text{m}$: actin filaments are *semiflexible biopolymers*.

Next, it is important to link these different behaviours to the mechanical properties of cytoskeletal subcomponents. The flexural rigidity κ of the filament (in Nm^2) - the resistance of the polymer to bending perpendicular to its long axis - is related to its persistence length l_p

²Microtubules can also be bent due to buckling: this point will be discussed later in this chapter.

by [Brochard-Wyart *et al.* 2019]:

$$l_p = \frac{\kappa}{k_B T} \quad (2.2)$$

where k_B is the Boltzmann constant and T the temperature. This mechanical parameter is directly related to the elastic modulus E of the polymer (in N m^{-2}) by $\kappa = EI$ with I the second moment of area of the cross section (in m^4) which takes into account the geometric properties of the polymer. By combining equations 2.1 and 2.2, we have a direct relationship between the fluctuations of the filament and its mechanical properties.

Imaging the shape fluctuations of filaments can thus provide measurements of l_p and hence κ and E . The easiest way to use the theory mentioned above is to label a cytoskeletal filament with a fluorescent tag and then mount it between a microscope slide and a coverslip. In 1993, the persistence length of single actin filaments and microtubules were measured for the first time with this method [Gittes *et al.* 1993] [Ott *et al.* 1993]. More recent studies adapted this method and used spectral analysis methods to determine the flexural rigidity of cytoskeletal filaments [Valdman *et al.* 2012]. However, for some cytoskeletal subcomponents like microtubules, due to sliding between protofilaments while bending, persistence lengths can depend on the total length of the filament [Pampaloni *et al.* 2006]. However, in cells, spatial dynamics of a given cytoskeletal filament (or bundle) is strongly influenced by interactions with the nucleus, organelles and other cytoskeletal subcomponents: this will be the focus of section 2.4 and chapter 3. It is thus a very precise method to study the mechanics *in vitro* - where interactions can be monitored accordingly - whereas in cells other methods are preferred.

– *Bending filaments.*

Beside this passive method, active methods have been developed to measure flexural rigidities in the cytoskeleton *in vitro* by using optical traps³ or hydrodynamic flows [Kikumoto *et al.* 2006]. By using beads attached to both ends of a filament (one fixed bead and one bead trapped with optical tweezers), it is possible to measure the rigidity of buckling filaments [Kurachi *et al.* 1995]. Several parameters can lead to independent estimations of the flexural rigidity, such as the critical load of buckling, the deflected length and the angles of bending to show the self-consistency of the method depicted in figure 2.2.A. This method was later improved with a double optical tweezers where both beads could be displaced [Kikumoto *et al.* 2006]. By docking one end of a microtubule to an axoneme⁴ and putting it into an hydrodynamic flow (see figure 2.2.C), it is possible to derive from the shape of the filament at equilibrium its

³More details about optical trapping will be provided at the end of this section.

⁴An axoneme is a long microtubule-based cytoskeletal structure that forms the core of a cilium

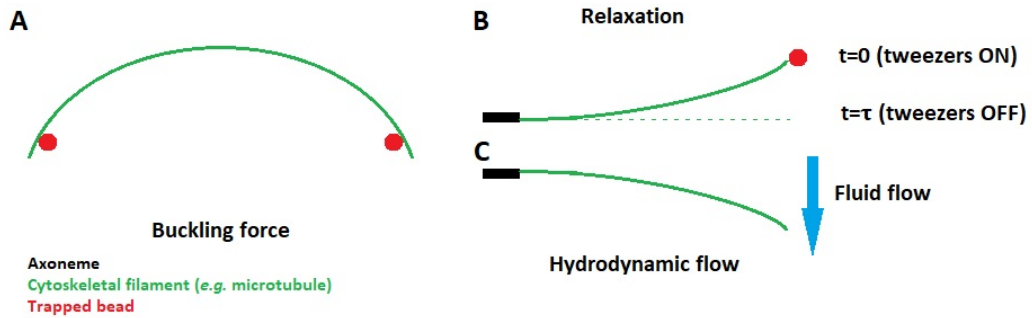


Figure 2.2: *In vitro* measurements of flexural rigidity.

A: The distance between two trapped beads attached to the ends of a cytoskeletal filament is decreased to measure the flexural rigidity of the corresponding filament. B: A cantilevered cytoskeletal filament is deformed by an optically trapped bead that exerts a force on the filament. At $t = 0$, the tweezers - which was on - is set off. The filament reaches the equilibrium at $t = \tau$. C: A cantilevered cytoskeletal filament is subject to a hydrodynamic flow. The flow being precisely known, the flexural rigidity of the filament is deduced from its shape.

mechanical properties [Venier *et al.* 1994]. The authors compared it to a thermal fluctuation method and showed both methods led to similar results. Finally, this system can be used with an optical trap: after docking one end of a filament, it is possible to impose a displacement to the other end trapped with an optical tweezers and, by imaging the dynamics of the relaxation process and knowing the expression of the hydrodynamics drag force, to determine the flexural rigidity [Felgner *et al.* 1996] [Felgner *et al.* 1997]. A scheme of this method can be found in figure 2.2.B.

– *Elongating filaments.*

As previously stated, the flexural rigidity is related to the elastic modulus E . Indeed, for a filament with an original length L_0 undergoing a longitudinal deformation that increases its length by ΔL on which a force F is applied on a surface area A , the elastic modulus E gives the relation between the stress $\sigma = F/A$ and the strain $\varepsilon = \Delta L/L_0$ in the elastic linear region:

$$\sigma = E\varepsilon \quad (2.3)$$

Thus, by exerting an orthogonal force or performing traction force assays on a specific cytoskeletal filament *in vitro*, it is possible to change the filament length and determine the elastic modulus E of this filament. Atomic Force Microscopy (AFM) can be used to deform individual filaments by applying a force along a line perpendicular to the filament [Guzmán *et al.* 2006] [Kreplak *et al.* 2008]. Two situations occur: sometimes the filament breaks to the applied force, sometimes it elon-

or flagellum. In this experimental setup, it is an efficient way of anchoring the microtubule to the microscope stage.

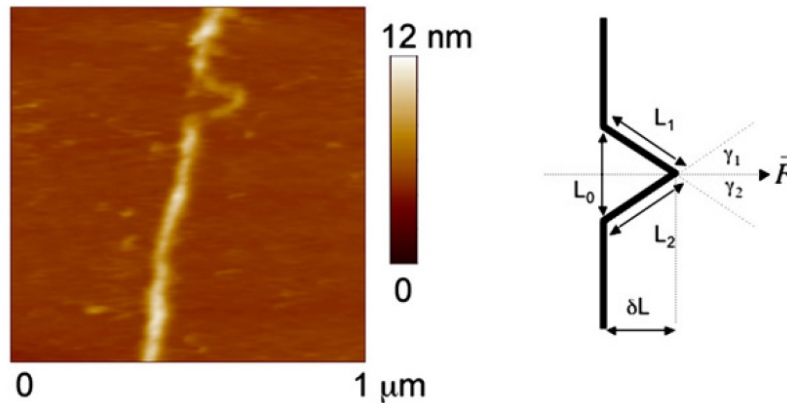


Figure 2.3: Deflection of an individual filament using AFM.

Left: AFM image after the application of the force perpendicularly to the filament. Right: Schematic representation of the force and the shape of the filament. From [Kreplak *et al.* 2008].

gates in a typical V-shape (see figure 2.3). By combining a microfluidic device and a double optical trap, individual filaments trapped between two beads have also been stretched longitudinally [Block *et al.* 2017]. The results of this experiment will be detailed in section 2.3 and the experimental setup appears in figure 2.8.

In summary, by applying forces on cytoskeletal subcomponents and imaging their deformations or looking at their fluctuations, the mechanical properties of (individual) filaments have been measured. The viscoelastic properties of reconstituted networks *in vitro* have also been measured by many different rheologic methods to decipher how this higher level of organization impacts mechanics.

- **Measuring forces in gels or networks.**

To reconstitute networks *in vitro*, cytoskeletal subcomponents are purified and crosslinked at a concentration high enough to form a gel. Whilst the mechanical properties of individual filaments have been mostly described using elastic constants, gels - by their semi-solid nature - have interesting viscoelastic properties. Their study is therefore performed with experimental setups called viscometers or rheometers, which are standard techniques in fluid mechanics to characterize complex fluids.

One of the most classical viscosimeter is the falling-sphere viscometer which allows to measure the viscosity of a transparent Newtonian fluid. A falling-sphere viscometer is composed of a vertical tube filled with the fluid of interest in which a sphere of known size and density is allowed to fall through the fluid. Stokes law establishes a linear relationship between the viscosity of the gel and the terminal velocity of the falling sphere (or ball). Historically, the first measurements of the viscosity of gels of different types of intermediate filaments

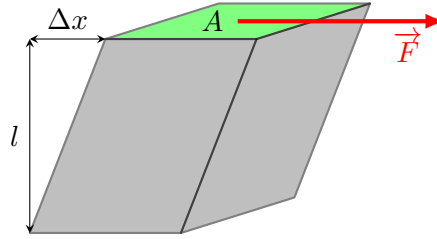


Figure 2.4: Fluid particle under a shear stress

were carried out with this method [Letierrier & Eyer 1987]. In reconstituted gels of cytoskeletal filaments, most studies rely on methods in which networks undergo shear stresses. The mechanical parameter obtained in this case is the *shear* modulus G that links the shear stress $\tau = F/A$ and the shear strain $\gamma = \Delta x/l$ (see figure 2.4) by:

$$\tau = G\gamma \quad (2.4)$$

It is important to mention that this relation is only valid if we consider purely elastic materials (hookean solids), *i.e.* if viscous effects are neglected compared to elastic effects. In general, we consider gels in which the viscosity has to be taken into account. Conversely, in purely viscous materials, the *dynamic viscosity* η is related to the time derivative of the shear strain $\dot{\gamma} = \frac{d\gamma}{dt}$ and the shear stress τ by:

$$\tau = \eta\dot{\gamma} \quad (2.5)$$

In continuum mechanics, both elasticity and viscosity often have to be considered, leading to more complex relations. In many studies on viscoelastic materials, oscillatory shear stresses are applied and the oscillatory⁵ shear strain is measured. Complex representations can be used to define the shear strain:

$$\begin{cases} \underline{\gamma} = \gamma_0 e^{i\omega t} \\ \underline{\tau} = \tau_0 e^{i(\omega t + \delta)} \end{cases} \quad (2.6)$$

where $\omega = 2\pi f$ with f the frequency of the oscillatory strain, t is time and δ the phase lag between stress and strain. The *complex shear modulus* G^* links these two mechanical parameters:

$$G^* = \frac{\underline{\tau}}{\underline{\gamma}} = \frac{\tau_0}{\gamma_0} e^{i\delta} = G' + iG'' \quad (2.7)$$

where $G' = \mathcal{R}e(G^*)$ is the shear storage modulus (which corresponds to the elastic response) and $G'' = \mathcal{I}m(G^*)$ the shear loss modulus (which corresponds to the viscous response).

Shear rheometers can be used to obtain the complex shear modulus of gels of reconstituted cytoskeletal networks. In 1991, Janmey *et al.* compared

⁵The resulting strain is oscillatory provided that shear stresses are not too high.

the viscoelastic properties of gels made of the three major cytoskeletal sub-components by using a torsion pendulum [Janmey *et al.* 1991]. More recent studies have used oscillatory [Leterrier *et al.* 1996], [Wagner *et al.* 2007], parallel plate [Janmey *et al.* 2006] [Lin *et al.* 2010a], cone-plate [Yamada *et al.* 2003], [Lin *et al.* 2010b], [Schopferer *et al.* 2009], [Esue *et al.* 2006], [Bousquet *et al.* 2001] shear rheometry, *etc.* In order to improve the number of gels probed, high-throughput strategies have been recently developed [Pujol *et al.* 2012] [Osada *et al.* 2016]. As values of complex shear moduli strongly depend on several control parameters - such as the filament concentration or the crosslinking level - comparisons of complex shear moduli between several conditions (type and concentration of cytoskeletal subcomponent, effect of crosslinkers) have provided more insights on the viscoelastic properties of the cytoskeleton *in vitro*. Besides, the variety of experimental setups allows to probe viscoelastic properties at different time scales. We will detail below the results obtained for microtubules (see section 2.2) and intermediate filaments (see section 2.3).

2.1.2 Whole-cell-scale, cortical and intracellular force measurements

In living cells, performing direct measurements of mechanical properties of cytoskeletal subcomponents is difficult, as they are surrounded by the cytosol, organelles, linkers, membranes, vesicles, *etc.* In particular, the techniques mentioned above do not apply in cells: measuring the persistence length or moduli of a single filament (or even of a bundle of filaments) remains technically extremely challenging. Other biological elements interfere, contribute to and have to be taken into account to infer the mechanical properties of a cytoskeletal subcomponent. Hence, very few studies claim to precisely measure the mechanics of a given cytoskeleton in cells. Yet, several studies have investigated the influence of the cytoskeleton on cellular mechanics at different scales.

- **Measuring the contribution of the cytoskeleton to cell mechanics.**

A large number of studies analyzing the role of the cytoskeleton in cellular mechanical properties have used the deflection of a cantilever whose indenter tip is in contact with the top of a cell. In most cases, the tip of an AFM is used to indent the cell. Optical measurement of the cell indentation allows the experimenter to determine the Young's modulus E of the cell - the deflection of the cantilever being known [Kuznetsova *et al.* 2007] and using the Hertz model. By disrupting, stabilizing or modifying the expression of cytoskeletal proteins, it is possible to study their contribution to the elastic modulus of the cell. Using AFM raises the question of which part of the cell is mechanically probed. The shape of the tip seems to be crucial: while sharp tips emphasize properties of the actin-rich shell of the cell, round tips emphasize those of the noncortical intracellular network [Vahabikashi *et al.* 2019]. Other techniques based on deflections of cantilevers have been set up. For instance, single cell rheometers are made of two parallel microplates (one rigid, one flexible) to

which a cell can adhere [Desprat *et al.* 2006]. In this case, whole-cell-scale mechanics (and not local mechanics) is measured. Interestingly, we have shown using this technique that the scale at which cell mechanics is probed is crucial, as intracellular techniques applied on the same cell line can exhibit opposite mechanical features [Alibert *et al.* 2021] (see below).

Rather than applying forces, other methods to quantify cytoskeletal mechanics focus on detecting forces developed by the cell. For instance, Traction Force Microscopy (TFM) is based on analyzing the deformation of the substrate on which a cell is plated thanks to the movement of fluorescent markers incorporated into this substrate. This tracking allows to calculate the cell-induced traction stresses [Tseng *et al.* 2011]. Such a method is very useful to probe the mechanics of the cell cortex, and modifications on *e.g.* the actin network can be made to assess how they impact mechanics [Ehrlicher *et al.* 2015].

- **Intracellular measurements.**

The order of magnitude of the size of a cell being around 10 μm , using objects of smaller sizes - typically around 1 μm - provides access to mechanical properties at smaller length scales. Micrometric objects (*e.g.* beads) controlled with different methods are powerful tools to sense intracellular mechanics.

First, optical trapping is largely used, both *in vitro* and *in cellulo*. The experimental setup which is used is called *optical tweezers* and relies on a laser beam highly focused on micrometric objects which can therefore be held or moved appropriately [Ashkin 1970]. The physics of optical tweezers will be described in more details in 5.6. We simply draw here an analogy between an elastic spring and optical tweezers: the trapped microscopic object behaves as if it were elastically linked to the trap center - its position at rest. Hence, the force applied by the optical tweezers on the object (in the range of 1 – 1000 pN) is proportional to the distance between the object and the trap center. As there is no physical contact between the cell and the experimental setup which generates the force, intracellular measurements can be performed without interfering with the membrane or the cortex mechanics [Zhang & Liu 2008]. Many studies have carried out rheology experiments in the cytoplasm with optical tweezers and have investigated the role of cytoskeletal filaments in its rigidity [Guo *et al.* 2013] [Mandal *et al.* 2016] [Charrier *et al.* 2018].

Other researches resort to magnetic micromanipulation techniques to look at intracellular mechanics [Robert *et al.* 2012]. As in optical trapping, magnetic tweezers use (superparamagnetic) microscopic objects that can be trapped and used to measure forces. Even though the physics of magnetic tweezers differ from that of optical trapping, the applied forces (in the range of 1 – 100 nN) allow to perform local measurements without probing the mechanics of the whole cell. The force on the bead is proportional to the gradient of the potential $U = -\frac{1}{2}\vec{m} \cdot \vec{B}$ (where \vec{m} is the magnetic moment of the bead immersed in the magnetic field \vec{B}), which gives a force proportional to ∇B^2

if the magnetic field is not too strong⁶ [Neuman *et al.* 2007]. Compared to optical tweezers, magnetic tweezers do not heat the bead microenvironment and appear to be less phototoxic. Along with optical trapping, they constitute complementary approaches, and studies can use both techniques to perform intracellular mechanical measurements [Charrier *et al.* 2018]. Even if not central for the present work, the role of magnetic and optical tweezers to probe membrane mechanics (*e.g.* membrane tension) has to be mentioned here [Nussenzveig 2017] [Hosu *et al.* 2007]. Another technique relies on applying a magnetic field: Magnetic Twisting Cytometry (MTC). MTC uses ferromagnetic beads in a homogeneous magnetic field on which are applied forces and torques [Wu *et al.* 2018]. MTC has been mostly used to measure shear moduli, especially at the plasma membrane and at the cell cortex [Guo *et al.* 2013].

2.1.3 Our approach: combining optical tweezers-based intracellular rheology with live cell imaging

To probe the mechanics of the cytoskeleton in living cells, we chose a novel approach based on a micromanipulation technique that combines optical trapping microrheology and fast confocal in living cells. The principle is to 1) trap endocytosed beads which are close to a cytoskeletal fiber, 2) deflect the fiber by applying a force perpendicular to its axis, 3) image the displacements of the fluorescent bead and the deflection of the fluorescent cytoskeletal fiber using confocal microscopy. The physics of optical tweezers and our experimental approach will be detailed in chapter 5.

Optical tweezers have been used previously by us and others to carry out mechanical measurements in living cells [Guo *et al.* 2013] [Guet *et al.* 2014] [Mandal *et al.* 2016] [Hu *et al.* 2019]. The originality of our approach is that our aim is to perform rheology experiments directly on cytoskeletal elements and inferring their viscoelastic constants in different conditions. The experimental setup that we use allows us to image the deformations of the cytoskeleton in order to locally probe the mechanics of a given cytoskeletal subcomponent (see chapter 5).

2.2 Mechanics of microtubules *in vitro*

2.2.1 Anisotropic stiffness of microtubules

As stated above, microtubules exhibit the highest persistence length among the cytoskeletal subcomponents. In one of the first flexural rigidity measurement [Gittes *et al.* 1993], the authors wrote in the abstract: "If tubulin were homogeneous and isotropic, then the microtubule's Young's modulus would be ~ 1.2 GPa, similar to Plexiglas and rigid plastics." More than measuring for the first time the flexural

⁶The magnetic field has to remain below the material-dependent saturation magnetic field \vec{B}_{sat} to have this simple relation.

rigidity of microtubules *in vitro*, they raised a very important question: can microtubules be considered homogeneous and isotropic? Based on their structure, polarity and dynamics, this assumption seems rather mistaken. Yet, it is interesting to wonder whether these properties are reflected on the mechanics of microtubules. The first key feature of microtubules *in vitro* is that their flexural rigidity is length-dependent, whether measurements were carried out using passive [Pampaloni *et al.* 2006] or active [Kurachi *et al.* 1995] techniques. In the latter, the difference in flexural rigidity, using the exact same protocol, can reach two order of magnitudes: from $\kappa = 1.3 \times 10^{-24} \text{ N m}^2$ to $\kappa = 1.2 \times 10^{-22} \text{ N m}^2$, evaluated from critical load measurements. Using AFM, Schaap *et al.* studied the effects of radial indentations at different locations of microtubules. With stiffness maps, they showed that: 1) protofilaments appeared 10% softer than the gaps between them and 2) the stiffness in the center and up to a few nm to each side was constant and then decreased slightly toward its sides [Schaap *et al.* 2006]. Taken together, these results suggest that microtubules have an anisotropic stiffness due to their inhomogeneous and anisotropic structure. A more recent study showed that the longitudinal bonds between tubulin dimers within protofilaments are stronger than lateral interprotofilament bonds [Sui & Downing 2010]. This property makes microtubules similar to other biological materials - such as wood or bamboo - which are also stiffer longitudinally [Hawkins *et al.* 2010]. High lateral deformability associated with high longitudinal stiffness have been reported as inherent properties of assembled microtubules and appear to be crucial for their structural stability in living cells [Huber *et al.* 2013].

2.2.2 Variability in the measurements of microtubule flexural rigidity

Many studies have measured the flexural rigidity κ of single microtubules *in vitro*, using a wide range of techniques, and obtained values ranging from $1.3 \times 10^{-25} \text{ N m}^2$ to $2.0 \times 10^{-22} \text{ N m}^2$ [Hawkins *et al.* 2010]. This variability of about three orders of magnitude seems to partially rely on specific experimental conditions that led to under-estimate the persistence length, such as microtubules attachment by one end which can lead to atypical positions [Mizushi-Masugano *et al.* 1983] [Hawkins *et al.* 2010]. Also, microtubule polymerization speed is determinant for measurements of flexural rigidity: fast-growing microtubules have been shown to be less stiff than slow-growing microtubules [Janson & Dogterom 2004]. One explanation is that structural defects in the microtubule lattice - associated with a higher flexibility of microtubules as they affect bonds between dimers - are more likely to occur during fast polymerization events [Huber *et al.* 2013].

The presence of Microtubule-Associated Proteins (MAPs), which decorate microtubules in cells and bind to the tubulin subunits, can also affect measurements of flexural rigidity. It has long been established that MAPs increase microtubule stiffness [Mickey & Howard 1995] [Felgner *et al.* 1997]. These authors studied neuronal MAPs - Tau and MAP2 - which stabilize long neuronal structures like dendrites

and axons by increasing microtubule stiffness. More recent studies have shown that other MAPs either have no effect on microtubule flexural rigidity [Cassimeris *et al.* 2001] or decrease it [Portran *et al.* 2013].

Finally, the effect of taxol on microtubule mechanics is - to some extent - controversial. Most of the studies show that taxol decreases microtubule flexural rigidity [Dye *et al.* 1993] [Venier *et al.* 1994] [Kurachi *et al.* 1995] [Felgner *et al.* 1996] [Kikumoto *et al.* 2006] and this observation is confirmed by theoretical models which establish that stabilizing microtubules with taxol should decrease their stiffness [VanBuren *et al.* 2005]. In contrast, other publications reported that treating microtubules with taxol had no effect on their mechanics [Vale *et al.* 1994] or increased their stiffness [Mickey & Howard 1995]. Even though the debate "*more rigid or more compliant?*" is still not totally closed, one hypothesis in the field is that taxol stabilizes microtubules by enhancing the flexibility of the bonds between tubulin dimers [Sept & MacKintosh 2010] [Hawkins *et al.* 2013].

2.2.3 Microtubule response to repeated mechanical stress

Most of the studies mentioned above have measured mechanical properties of microtubules with a large variety of active techniques. Yet, these techniques share the common property of applying a single stress on a given microtubule. In cells, microtubules undergo repeated stresses whilst being described as the cytoskeletal subcomponent with the highest persistence length. Surprisingly, microtubule breakage is not frequently observed in cells. It is interesting to investigate how microtubules react to repeated stress *in vitro*. Using a microfluidic device, Schaedel *et al.* performed cycles of bending of 10s with a hydrodynamic flow, separated by pauses of 10s without any flow [Schaedel *et al.* 2015]. They showed that a majority of microtubules soften under mechanical stress, being twice as soft as their initial state after six bending cycles (see figure 2.5.A-B). Interestingly, they showed that when they increased the rest period from 10s to 100s, microtubule stiffness was unchanged from one cycle to another (see figure 2.5.C). Their data suggested that softened microtubules are able to self-repair over longer time scales. In agreement, a protocol of five rapid bending cycles followed by a 100s rest showed that most of the microtubules which softened during the five bending cycles exhibited significant recovery after the rest period (see figure 2.5.D). They proposed a model to interpret their data composed of five main steps: 1) before any stress, defects in the microtubule lattice can pre-exist; 2) while being mechanically stressed, protofilaments close to the defects are deformed as they have fewer lateral interactions; 3) the pre-existing lattice defects enlarge due to dimer loss and crack propagation contributing to global and local microtubule softening; 4) after the stress, the microtubule goes back to its original shape and protofilaments progressively re-establish lateral interactions by dimer incorporation; 5) after self-healing, the microtubule has recovered its original stiffness.

A later study by the same group questioned the role of K40 acetylation in microtubule mechanics and breakage, both *in vitro* and in living cells [Xu *et al.* 2017].

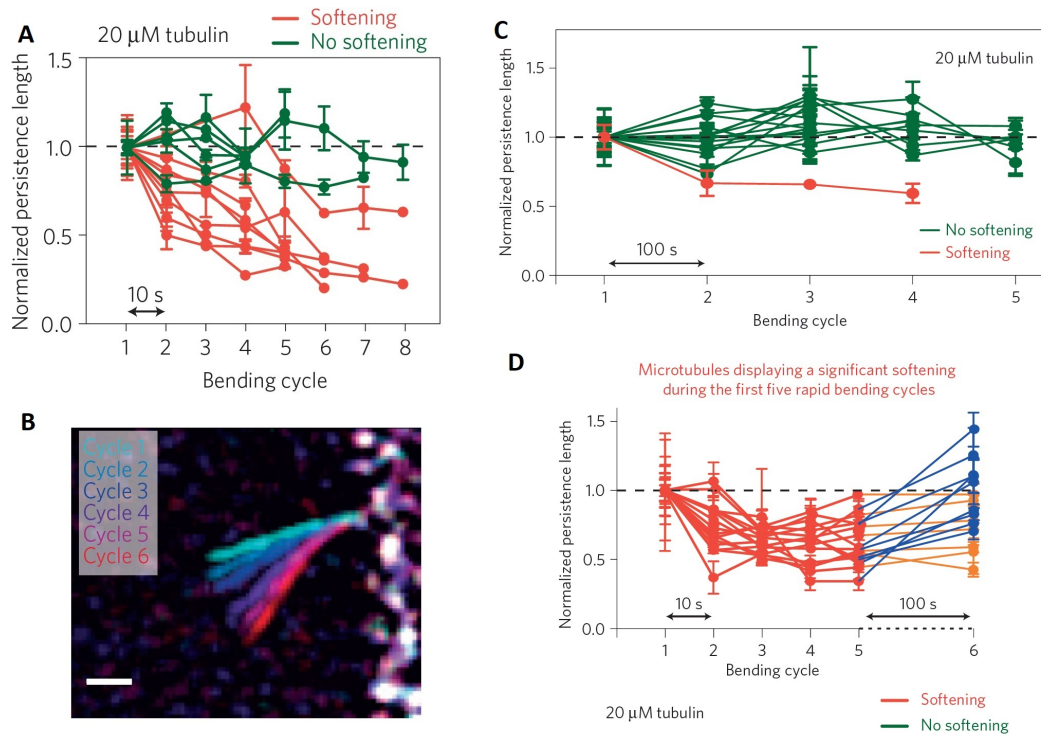


Figure 2.5: Microtubule response to repeated mechanical stress.

A&C: Evolution of microtubule persistence length over successive bending cycles separated by a 10 s rest period (A) or a 100 s rest period (C). Microtubules that soften appear in red, microtubules that do not soften appear in green. The persistence length is normalized by setting the persistence length in the first bending cycle at 1 for each microtubule. B: Overlay of microtubule maximal deformation during each bending cycle corresponding to A. Scale bar: 3 μm . D: Evolution of microtubule persistence length following five rapid bending cycles. Data shown correspond to softening microtubules. The delay between the first five bending cycles was 10 s, while the delay between the fifth and the sixth bending cycle was 100 s. Microtubules exhibiting significant recovery are shown in blue, the others in orange. Adapted from [Schaedel et al. 2015].

The experiments carried out in cells will be presented in section 2.4. As far as *in vitro* experiments are concerned, the authors compared two populations of microtubules made from enzymatically acetylated and deacetylated tubulin: one with very high level of K40 acetylation (97.2%) and another one with almost no K40 acetylation (0.8%). They showed that microtubule flexural rigidity is decreased by acetylation: highly-acetylated microtubules had an average persistence length $l_p = 2$ mm compared to $l_p = 5$ mm for deacetylated microtubules. The authors then slightly adapted their protocol by adding to the microfluidic device large beads close to the microtubules to serve as fixed obstacles to be able to study the effect of acetylation on microtubule breakage. They showed that the time to breakage, as well as the proportion of microtubules that did not break at a given mechanical stress, was significantly increased when microtubule were acetylated. They concluded that

intraluminal acetylation directly protects microtubules from mechanical breakage. This was confirmed in another study showing that acetylated microtubules do not soften under repeated mechanical stress, as opposed to deacetylated microtubules for which the flexural rigidity incrementally decreased with each bending cycle [Portran *et al.* 2017]. Acetylation thus suppresses microtubule fatigue and limits the ageing of long-lived microtubules. A more recent publication has given insight into the structure of microtubule and suggests that K40 acetylation, which occurs in an unstructured loop of α -tubulin, reduces interprotofilament interactions [Eshun-Wilson *et al.* 2019]. This finding implies that protofilament sliding is facilitated in acetylated microtubules, which could explain their higher flexibility.

2.3 Mechanics of intermediate filaments *in vitro*

Because of their short persistence length compared to actin filaments and microtubules, intermediate filaments are considered as flexible biopolymers. In 1991, the mechanics of individual intermediate filaments has recently gained increasing interest, especially *in vitro*.

2.3.1 Networks of intermediate filaments: highly deformable and almost unbreakable

The first studies on intermediate filament mechanics were performed using reconstituted gels or networks. Janmey *et al.* compared the viscoelastic properties of vimentin gels with microtubule and actin gels *in vitro* [Janmey *et al.* 1991]. In this paper, the authors evidence the unique properties of vimentin networks compared to other cytoskeletal subcomponents. Using a torsion pendulum, they measure that microtubule can deform a lot (up to 60%) before breaking (and beginning to flow, like a viscous liquid) under low stress and that actin filaments can not be deformed more than 20% and then break and flow. On the contrary, vimentin filaments can reach high deformations and undergo high levels of stress without breaking (see figure 2.6). Also, the slope of the vimentin stress/strain curve shows that vimentin gels exhibit a strain-stiffening behaviour, unlike actin filaments and microtubules. The mechanics of neurofilaments and vimentin have later been compared [Leterrier *et al.* 1996] [Lin *et al.* 2010b]. Both networks exhibit predominantly elastic behaviour with strong nonlinear strain stiffening. Interestingly, neurofilament gels have a shear modulus G one order of magnitude higher than vimentin gels. Consistent with one of the earliest mechanical studies on intermediate filament gels [Leterrier & Eyer 1987], Lin *et al.* also demonstrated that divalent ions - such as Mg^{2+} - play a crucial role in crosslinking both networks, as they do for actin gels [Tang *et al.* 2001]. The behaviour of vimentin and neurofilaments at high strain is one of the major differences: unlike vimentin gels, neurofilament gels have been described to rupture (typically at a 100%-strain) and rapidly recover afterwards [Wagner *et al.* 2007]. The authors conclude that intermediate filaments self-repair when they withstand important deformations. Other intermediate filament proteins have been compared

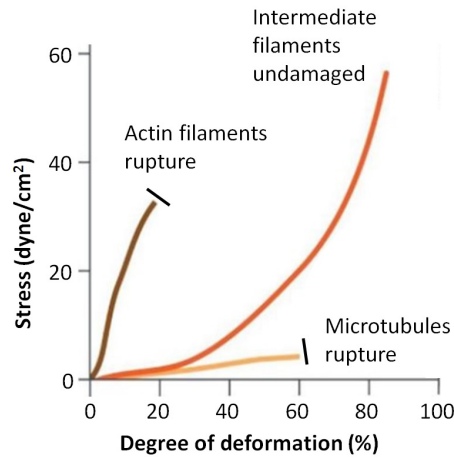


Figure 2.6: Shear stress/strain behaviour of microtubules, actin and vimentin filaments. Adapted from [Janmey *et al.* 1991]

to vimentin. Desmin filaments ($l_p \approx 900$ nm) have been measured to be twice as stiff as vimentin filaments ($l_p \approx 400$ nm), but remain much more flexible than actin filaments [Schopferer *et al.* 2009]. In both gels, electrostatic repulsion between divalent ions affects the network stiffness but the ratio of repulsive to attractive electrostatic interactions which induce the formation of junctions within the network is significantly weaker for desmin than for vimentin. The origin of attractive interactions within intermediate filament gels have been investigated in keratin and vimentin gels [Pawelzyk *et al.* 2014]. The authors demonstrate that electrostatic attraction originates from hydrophobic and hydrogen bonds - mostly located in the tail domain -, show that these properties determine the strain-stiffening behaviour of intermediate filament networks, and conclude: "Strain stiffening is another characteristic and physiologically relevant feature of Intermediate Filament (IF) networks. This requires stronger attractive forces at filament contact points." It is interesting to mention at this point that strain-stiffening is also measured for individual intermediate filaments as we will see in 2.3.2. In gels, many studies mentioned earlier reported that intermediate filament networks exhibit shear moduli ten times higher at high strain (typically 100%) than in the regime of low strain [Charrier & Janmey 2016].

2.3.2 Individual intermediate filaments exhibit nonlinear strain-stiffening

The mechanics of single intermediate filaments has been investigated more than a decade after the first experiments on viscoelasticity of intermediate filament gels. The mechanical properties of single desmin filaments, keratin filaments and neurofilaments were first probed by using AFM (see figure 2.3) [Kreplak *et al.* 2005]. By performing lateral displacement and stretching of single filaments, they measured an average 2.6-fold extension (ranging from 1.4 to 3.6) associated with a significant reduction in filament diameter, which suggests a structural change in the fil-

aments. They also made the hypothesis that intermediate filaments could serve as a protecting structure from the destructive effects of a repetitive mechanical stress, comparing them to a *security belt*. Other publications by the same group used the same experimental set-up (and electron microscopy) to specifically measure the mechanical properties of vimentin individual filaments *in vitro*. They found that the persistence length of vimentin filaments is $1\ \mu\text{m}$ [Mücke *et al.* 2004] and that the bending modulus of non-stabilized vimentin filaments ranges from 300 MPa to 400 MPa [Guzmán *et al.* 2006]. In the latter publication, the bending modulus of stabilized intermediate filaments is also found to be twice or three times higher than that of non-stabilized intermediate filaments.

- **The α -helix to β -sheet transition.**

Molecular dynamics simulations investigated the structural mechanism which can explain the high extensions which have been measured [Qin *et al.* 2009]. The rod domain of vimentin filaments α helices can unfold and be replaced by β sheets instead. These $\alpha - \beta$ transition processes can explain the diameter reduction measured by Kreplak *et al.* With these molecular dynamics simulations, Qin *et al.* find that force-strain curves of single intermediate filaments should have three regimes (see figure 2.7):

1. the pulling force increases linearly with strain until it reaches an angular point, where a dramatic change in the slope occurs (the angular point corresponds to the point where the first unfolding in the protein occurs);
2. the force-strain curve reaches a plateau, where the pulling force remains almost constant with a slight increase of force at increasing deformation. Unfolding of all α -helical domains occurs in this regime;
3. the stretching force increases rapidly as the strain increases, indicating a significant stiffening of the local (tangent) elastic properties. This is caused by pulling the unfolded polypeptide backbone of the protein, where the stretching of covalent bonds leads to a much higher stiffness.

- **Subunit gliding.**

The numerical results are in agreement with many experimental studies [Ackbarow *et al.* 2007] [Ackbarow & Buehler 2007] [Kreplak *et al.* 2001]. In addition, another important mechanism involved in the high stretchability of intermediate filaments has been established: *subunit gliding*. Using confocal microscopy, longitudinal movements of dimeric or tetrameric subunits along the intermediate filament axis have been observed thanks to a microfluidic device that allows to mix fluorescent subunits and mature filaments [Nöding *et al.* 2014]. When they associate laterally, intermediate filament tetramers undergo molecular interactions (ionic and hydrophobic). This complex system of binding activities enables intermediate filaments to tolerate high mechanical: subunit gliding - *i.e.* disassociations and reassociations within a given intermediate filament - allows structural modifications in intermediate filaments upon longitudinal stretching [Köster *et al.* 2015]

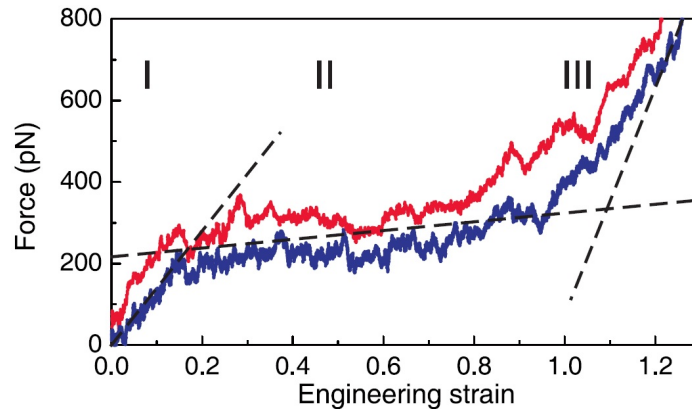


Figure 2.7: Molecular dynamics simulation of vimentin intermediate filament dimer under tensile deformation.

Force-strain relations for tensile deformation of the vimentin dimer (pulling speeds: 0.01 \AA ps^{-1} in blue and 0.1 \AA ps^{-1} in red). From [Qin *et al.* 2009].

- **Loading-rate-dependent responses of intermediate filaments.**

The mechanical properties of individual intermediate filaments have been further investigated experimentally. The role of the loading rate, *i.e.* the speed at which filaments are stretched (corresponding to the pulling speed in figure 2.7), has been assessed using AFM and optical tweezers [Block *et al.* 2017]. In this study, the authors resorted to a microfluidic device coupled to a double optical trapping system (see figure 2.8.A). First, this study is consistent with the simulations done by Qin *et al.*⁷: whatever the value of the loading rate, the force-strain curves can be split into three regimes: a first linear increase at low strain (elastic stretching of α -helical domains) followed by a plateaulike regime that corresponds to uncoiling of α helices into β sheets. In the third regime, the filaments stiffen with the strain, corresponding to increased pulling on the β sheets (see figure 2.8.B). Second, it shows that the loading rate has a clear effect on the evolution of the force with the applied strain. Even though it does not change the strain at which the plateaulike regime begins (about $\varepsilon = 0.1$), the loading rate has a dramatic effect on the length of this regime: the higher the loading rate, the shortest the plateau. When the loading rate increases, the filaments begin to stiffen at a lower strain and are much less extended at a given force value, again similar to a safety belt. AFM data gave consistent data with these measurements performed by fluorescence microscopy. By making the "safety belt" image their own, the authors have added a relevant element: at slow deformation, intermediate filaments are easily deformable and highly extensible whereas at fast deformation, they become much stiffer. At slow deformation, the filaments can reach a 2-fold extension without needing a high force ($F = 200 \text{ pN}$ for $\varepsilon = 1$). At fast deformation, overcoming

⁷However, it is worth mentioning that the order of magnitudes for the loading rate are totally different: $1 \mu\text{m s}^{-1}$ [Block *et al.* 2017] compared to $10^6 \mu\text{m s}^{-1}$ [Qin *et al.* 2009].

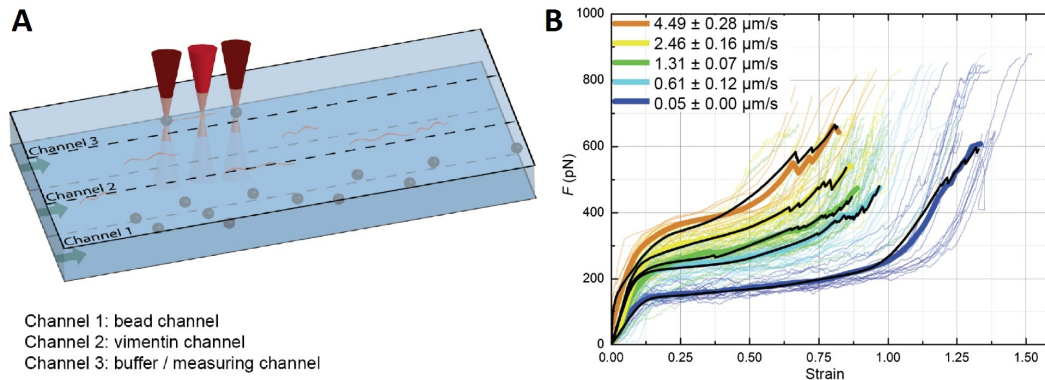


Figure 2.8: Role of the loading rate in the mechanics of individual vimentin filaments.

A: Schematic representation of the microfluidic device. Two beads are first captured in channel 1 with the optical tweezers, then by moving the microfluidic device with respect to the optical traps, filaments are attached to the beads in channel 2. Experiments are carried out in channel 3. *B*: Force-strain curves at different loading rates. Thin lines: single experiments, thick lines: average for each loading rate, black lines: averaged fits for each loading rate. From [Block *et al.* 2017]

a 1.5-fold extension requires higher forces ($F = 400$ pN) increasing rapidly as this point correspond to the third regime. These mechanical features of vimentin filaments observed *in vitro* could play a role in cell mechanics by providing strength to cells under large deformations and by absorbing large amounts of energy through unfolding mechanisms, as already hypothesized in earlier publications [Ackbarow & Buehler 2007] [Fudge *et al.* 2003].

- **Repeated mechanical stress soften vimentin filaments.**

By performing stretching cycles on vimentin intermediate filaments with a double optical trap, a recent study highlighted a softening of vimentin intermediate filaments (figure 2.9.A-B), whatever the waiting time (figure 2.9.C-E) [Forsting *et al.* 2019]. The authors hypothesized that, along with the two conformational states mentioned above (α helices and β sheets), vimentin intermediate filaments can be found under a third conformational state, less well defined: the *unfolded* conformation. After the first stretching, vimentin intermediate filaments go from the α -helical to the unfolded state, and this transition is assumed to be irreversible. This explains both the hysteresis observed when vimentin intermediate filaments return to equilibrium during the first stretching cycle and the softening of vimentin intermediate filaments.

- **Post-translational modifications**

Like for microtubules, PTM seem to significantly contribute to intermediate filament mechanics. A recent publication by the same group reports that phosphorylation softens vimentin filaments [Kraxner *et al.* 2021]. In this study, they more generally show that additional negatively charged amino acids soften vimentin filaments. How phosphorylation precisely soften vimentin

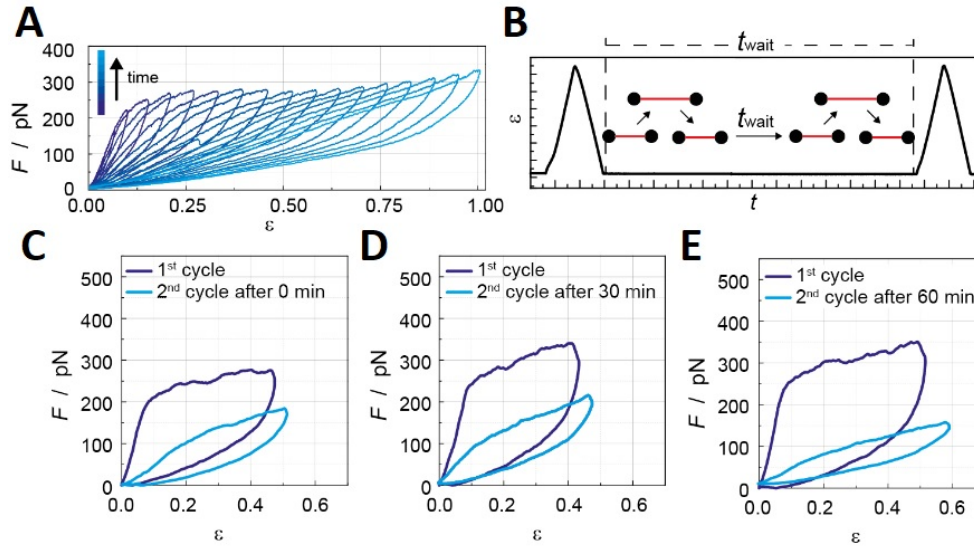


Figure 2.9: Cyclic stretching softens vimentin intermediate filaments.

A: Force is plotted as a function of strain. Vimentin intermediate filaments are stretched to increasing distances with each cycle. B: Experimental protocol: two stretching cycles are separated by a waiting time t_{wait} . C, D and E: Examples of force-strain curves with different waiting times: $t_{\text{wait}} = 0$ min (C), $t_{\text{wait}} = 20$ min (D) and $t_{\text{wait}} = 60$ min (E). Adapted from [Forsting *et al.* 2019].

filaments is not clear, but mass spectrometry analysis indicate that phosphorylation decreases the number of cross-links between vimentin tetramers. The authors thus hypothesize that decreased interactions within the individual vimentin filament leads to its softening.

2.4 Microtubules and intermediate filaments *in cellulo*

2.4.1 Measuring mechanics of cytoskeletal filaments *in cellulo*

Living cells are systems which are not at thermodynamic equilibrium. Many internal and external forces act on them. Therefore, measuring the mechanics of organelles, nucleus or cytoskeleton subcomponents separately is highly challenging as many unknown forces coming from active processes and external cues interfere with the measurements. For instance, microtubule buckling requires active forces that can be generated by or transmitted through MAPs [Pallavicini *et al.* 2017]. In an earlier study of microtubule buckling [Brangwynne *et al.* 2006], the authors showed how the presence of the surrounding elastic cytoskeleton reinforces microtubules in living cells: free microtubules *in vitro* typically buckle on a length scale $L \approx 10 \mu\text{m}$ of the filament, at a small critical buckling force f_c . Microtubules in living cells are surrounded by a reinforcing cytoskeleton: the critical force is increased and microtubules typically buckle on a shorter wavelength $\lambda \approx 1 \mu\text{m}$ (figure 2.10).

For instance, an analysis based on lateral motion of microtubules and on Fourier decomposition of microtubule shape consistently measured persistence lengths around $20\ \mu\text{m}$, much lower than the values measured *in vitro* ($l_p \approx 1\ \text{mm}$) [Pallavicini *et al.* 2014].

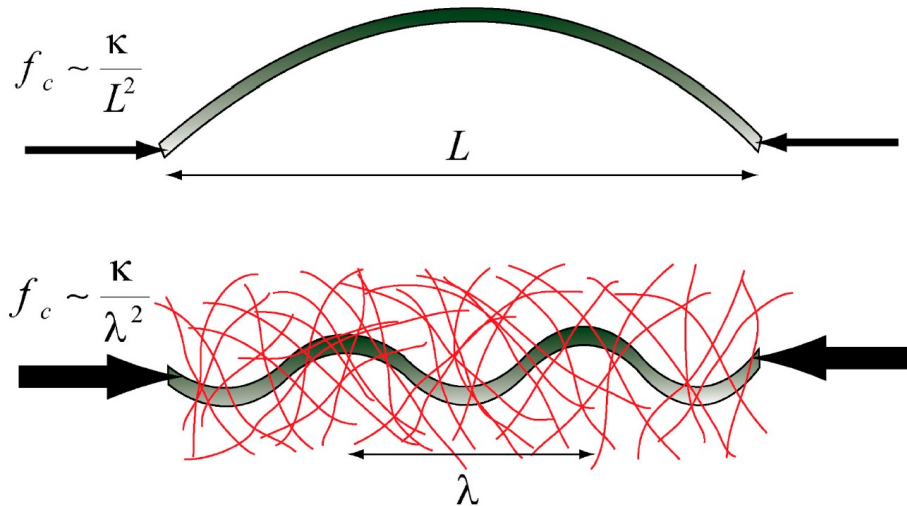


Figure 2.10: Role of the surrounding cytoskeleton on microtubule buckling.

Top: *in vitro*, microtubules buckle on the large length scale on the filament L . *Bottom:* *in living cells*, microtubules buckle on a shorter length λ , due to their interactions with the reinforcing cytoskeleton. *In living cells*, a given microtubule of flexural rigidity κ can bear higher forces before reaching the critical buckling force f_c than *in vitro*. From [Brangwynne *et al.* 2006].

Cilia and flagella are long structures extending from the surface of some eukaryotic cells containing bundles of doublet microtubules [Snell *et al.* 2004]. As they are spatially enclosed in a structure which can be seen as a cellular extension, microtubule mechanics can be probed in a more direct way in cilia and flagella than when they are surrounded by organelles, other cytoskeletal subcomponents, *etc.* Two studies calculated the flexural rigidity and persistence lengths of microtubules in such conditions [Baba 1972] [Battle *et al.* 2015]. In [Baba 1972], the author writes: "The Young's modulus of the microtubule is estimated to be $5 - 9 \times 10^{10}$ dyne/cm² on the basis that the outer doublet microtubules are tightly connected with one another." The Young's modulus is therefore estimated to be $5 - 9$ GPa, and the flexural rigidity around 10^{-18} N m² which is higher than the values measured *in vitro* that range from 10^{-25} N m² to 10^{-22} N m² (see 2.2.2). Battle *et al.* make the opposite hypothesis, by assuming that the crosslinking within the bundle is weak, so that the bundle rigidity can be expressed as the sum of the flexural rigidities of individual microtubules. They found that the flexural rigidity of a single microtubule is $3 - 4 \times 10^{-24}$ N m², which is in the range of values measured *in vitro*. Due to the low number of studies in living cells, it is difficult to assess the validity of the hypothesis on the strength of the crosslinking within the microtubule bundle made by these two papers. The key importance of this hypothesis illustrates

how challenging measuring mechanical properties of cytoskeletal subcomponents *in cellulo* can be. Passive methods have also been used in living cells to measure the mechanical properties of microtubules *in cellulo*.

As far as intermediate filaments are concerned, to our knowledge, there are only few studies which have measured their flexural rigidity (or persistence length) in living cells. Most of the time, experiments aimed at measuring the viscoelastic properties of the whole cell or of the cytoplasm and quantifying the role of a given cytoskeletal fiber/network. However, we can mention a recent work based on Fourier analysis of the shape of vimentin bundles [Smoler *et al.* 2020]. In this publication, the authors show that the apparent persistence length of vimentin bundles typically is $l_p \approx 2\mu\text{m}$. This mechanical parameter also appears to be modified by some cytoskeleton perturbations: this part of the results will be discussed in chapter 3.

2.4.2 Mechanical contribution of microtubules in cells

- **Microtubule stability and cell mechanics.**

In order to better understand the role of microtubules in the mechanical properties of eukaryotic cells, a large number of studies have used drugs targeting tubulin. We cite below only a few of these studies, to highlight that contradictory results exist in the literature. By using an optical trap and endogenous vesicles embedded in the cytoplasm of mouse oocytes, Ahmed *et al.* applied an oscillatory force while measuring its displacement, and calculated the local shear modulus G . They showed that neither the storage nor the loss modulus was significantly different under nocodazole treatment that induces microtubule depolymerization [Ahmed *et al.* 2018]. However, it was reported earlier that the same treatment in retinal pigmented epithelial cells (RPE1) plated on micropatterns decreased both G' and G'' [Mandal *et al.* 2016]. The same study shows that stabilizing microtubules with taxol induces an important increase of G' and G'' , which can be surprising given the results *in vitro* that do not report such a dramatic increase. The hypothesis here is that taxol, by decreasing microtubule dynamics, also decreases active forces acting on the cytoplasm. This leads to increasing the rigidity of the cytoplasm⁸. Some publications may thus appear contradictory and the complexity of a living cell, its compensating mechanisms - added to the fact that studies often carry out all their measurements in a specific cell line - make it even more challenging to formulate general and reliable results in cells.

- **Acetylated microtubules in living cells.**

Microtubules have been shown to be protected from mechanical ageing *in vitro* [Xu *et al.* 2017] (see 2.2.3). Using a Small Interfering Ribonucleic Acid (siRNA) strategy in RPE cells, the same publication studied the impact of the absence of K40 acetylation on microtubule mechanics. They treated cells with nocodazole to depolymerize microtubules and noticed that the re-

⁸Depleting ATP leads to a similar result

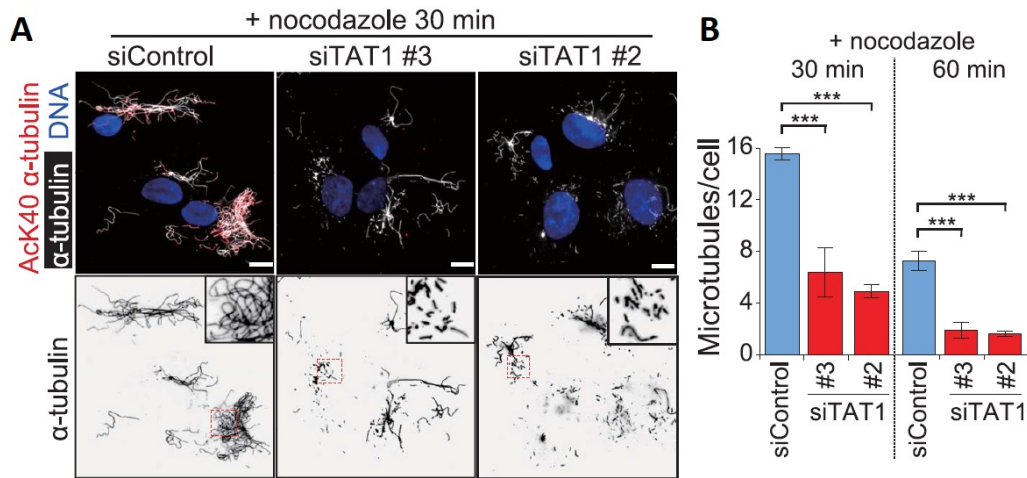


Figure 2.11: Impact of K40 acetylation on long-lived microtubules.

*A: Immunofluorescence images of siRNA-treated RPE1 cells treated with 2 μ M nocodazole and stained for α -tubulin (white), acetylated α -tubulin (red) and DNA (blue). (Bottom) The α -tubulin channel alone. (Insets) Highly curved microtubules are present in control cells while very short microtubules are observed in *ATAT1*-depleted cells. Scale bar: 10 μ m (main panels). Insets are 10 μ m by 10 μ m. *B: Number of microtubules remaining after nocodazole treatment. Adapted from [Xu et al. 2017].**

remaining microtubules were long and highly curved in control cells - which is a typical phenotype of long-lived microtubules - whereas they were very short in *ATAT1*-depleted cells. Microtubules were also less numerous in *ATAT1*-depleted cells (see figure 2.11). By highlighting that microtubules are highly acetylated in curved regions, this study suggests that the activity of *ATAT1* is enhanced in these regions that had been previously described to be sites where cracks and lattice defects are mostly found [Schaap et al. 2006]. They could be entry points for the enzyme to repair the lattice defects and make microtubules more resistant to mechanical stress. This finding challenges the idea that K40 acetylation is a consequence of microtubule stabilization, as it was shown that increased tubulin acetylation levels do not stabilize microtubules [Palazzo et al. 2003].

2.4.3 Mechanical contribution of intermediate filaments in cells

- **Intermediate filaments in cortical and whole-cell-scale mechanics.**

Many publications studied the role of intermediate filament proteins in cell mechanics for at least two decades [Charrier & Janmey 2016]. Among these proteins, vimentin has been (one of) the most studied. The mechanical properties of primary fibroblasts from vimentin Knocked-Out (KO) rats were probed using rotational force magnetic twisting cytometry by two different groups [Eckes et al. 1998] [Wang & Stamenović 2000]. Both studies reported cortical softening in vimentin KO-cells; Eckes et al. quantified that the rigid-

ity of the cortex was reduced by 40% compared to Wild-Type (WT) rats. Hence, the vimentin network may contribute to the cortex stiffness by reinforcing it. However, this is still debated as a more recent publication using magnetic twisting cytometry in primary fibroblasts from vimentin KO mice reports no significant difference in the rigidity of the cortex [Guo *et al.* 2013]. As far as cortical mechanics is concerned, the role of desmin - another type III intermediate filament protein which is specifically expressed in muscle cells - is also quite controversial. In primary human fibroblasts from patients carrying a desmin mutation (R350P) which disrupts the desmin network, the rigidity of the cortex has been measured to be twice that of cells from control patients without this mutation [Bonakdar *et al.* 2012]. Yet, by using three types of cell rheometers, a recent study in mouse myoblasts (C2C12) in which desmin was mutated shows that the mechanical properties of the cell cortex are not correlated with the quantity, nor the quality of the expressed desmin [Charrier *et al.* 2018].

At the whole cell scale, the effect of desmin and vimentin is much clearer. The overexpression of wild-type-desmin increases the overall rigidity of C2C12 myoblasts [Charrier *et al.* 2016]. Similarly, cells treated with drugs targeting vimentin - such as withaferin A and calyculin A - exhibit a higher deformability [Brown *et al.* 2001] and a lower stiffness [Gladilin *et al.* 2014]. Another study in primary human articular chondrocytes reported a global 3-fold softening of cells in which the vimentin network had been disrupted with acrylamide [Haudenschild *et al.* 2011]. Locally, vimentin overexpression has been recently found to stiffen the perinuclear region [Patteson *et al.* 2019]. The loss of other intermediate filament proteins - mostly keratins and neurofilaments - has also been described to decrease the elastic moduli of the cell and increase its deformability: this might be a common feature for most of intermediate filament proteins [Charrier & Janmey 2016].

- **Intermediate filaments form crucial networks for cytoplasm stiffness.**

Several groups have performed intracellular mechanical measurements with a special focus on intermediate filaments. While they do not claim to measure mechanical properties of these filaments, they studied the importance of intermediate filament networks on intracellular mechanics. Because this PhD work mainly focuses on a type III intermediate filament protein, we highlight here some of the key results for vimentin and desmin. In Mouse Embryonic Fibroblasts (MEFs), Guo *et al.* used endocytosed beads optically trapped in WT and deficient vimentin mice [Guo *et al.* 2013]. They found that the storage modulus G' is decreased in cells without vimentin whereas the loss modulus G'' is not significantly different (see figure 2.12.A-B). The physical origin of these moduli (elasticity for G' , viscosity for G'') indicates that vimentin plays an essential role in the elasticity of the cytoplasm by increasing it. In other words, vimentin filaments stiffen the cytoplasm. In the same paper, they also

observed the movement of endogenous vesicles. If the trajectories in both conditions are random, the vesicles in vimentin deficient MEFs move further over the same timescale (see figure 2.12.C): in WT MEFs, the vimentin network constrains the diffusive-like movement of organelles (see figure 2.12.D). Similarly, in mouse myoblasts, the cytoplasmic stiffness has been shown to be correlated to the amount of functional desmin [Charrier *et al.* 2018]. Conversely, the same study shows that the cytoplasmic stiffness is decreased when a desmin mutant induces the formation of desmin aggregates in the (partially depleted) desmin network. Taken together, these results suggest that both vimentin and desmin filaments are determinants of the cell cytoplasmic mechanics.

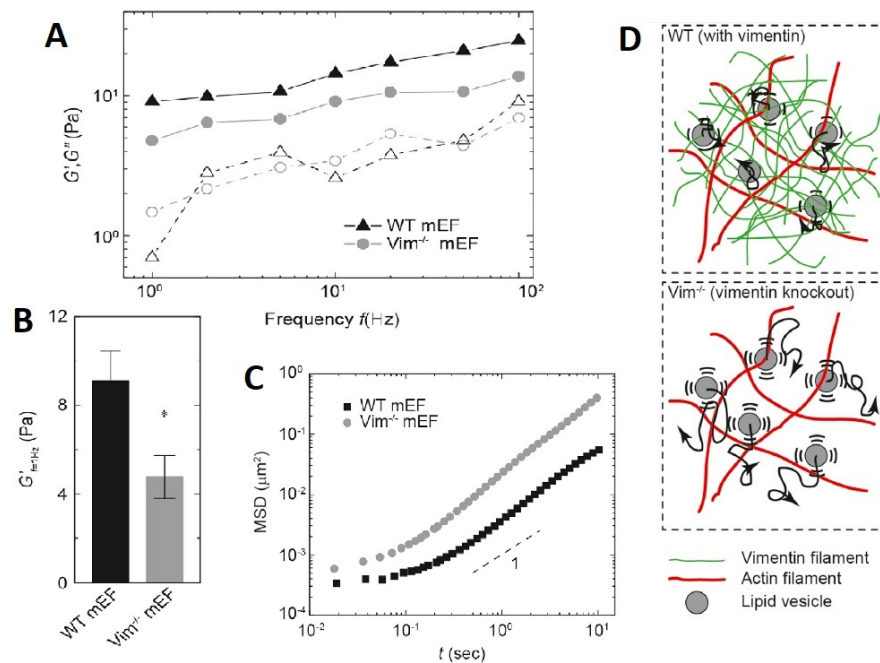


Figure 2.12: Role of vimentin filaments in cytoplasmic mechanics.

A: Frequency-dependent cytoplasmic storage moduli G' (solid symbols) and loss moduli G'' (open symbols) of the WT and $Vim^{-/-}$ MEFs. *B*: Storage moduli at 1 Hz. Error bars: SEM. *C*: Time evolution of mean square displacement in both conditions. *D*: Schematic representation of random vesicle movements in networks with and without vimentin. Adapted from [Guo *et al.* 2013].

A more recent publication focuses on the role of vimentin filaments when MEFs undergo large deformations [Hu *et al.* 2019]. The authors show how the vimentin network is a key regulator of intracellular mechanics and how it provides resistance to large deformations and thus maintains cell viability. The vimentin network is hyperelastic and highly stretchable, and increases three parameters related to cytoplasmic mechanics: the force relaxation, the relaxation time and the resilience of the cytoplasm. They also study the link

with the other cytoskeletal subcomponents by using *ghost cells* that do not contain microtubules nor actin filaments. Interestingly, they find that the mechanical parameters are independent of the loading rate in ghost cells, whereas they increase with the loading rate in both **WT** and vimentin deficient cells. This finding is very interesting as it suggests that the dependence on the loading rate - here: the speed at which stage is displaced relatively to the optical trap - in cells comes from interaction between cytoskeletal subcomponents. Yet, *in vitro*, it has been shown that individual vimentin filaments show a highly loading-rate-dependent behaviour [Block *et al.* 2017] (see 2.3.2). The last important result of this publication for our work is the impact of repeated mechanical stress - cyclic loadings - on cytoplasmic mechanics. By doing cycles of loading and unloading in the cytoplasm (see figure 2.13.A), they quantify the elastic and dissipated mechanical energy upon repeated stress. In ghost cells, the loading and unloading curves collapse and remain unchanged over more than 100 cycles. This confirms that energy dissipation is negligible in the vimentin network (see figure 2.13.A). In both **WT** and vimentin deficient **MEFs**, the loading and unloading cycle exhibit a hysteresis behaviour, typical of dissipated energy (see figure 2.13.B-C). Interestingly, in both conditions, when the cell is not mechanically stressed for 10 min, the loading curve after this rest time is identical to the first loading curve. This result reflects the self-reorganizing ability of other cytoskeletal subcomponents. In **WT MEFs**, the cytoplasm softens during the first three cycles and becomes similar to that measured in the ghost cell after 10 cycles (see figure 2.13.B). In vimentin deficient **MEFs**, the resistant force is very weak from the first cycle (see figure 2.13.C). This suggests that cyclic loadings induce major cytoskeletal rearrangements and/or damage without vimentin. Finally, by integrating the area looped by the first loading and unloading curves, they quantify the dissipated and elastic energies. They find that both energies are decreased in vimentin deficient cells compared to **WT** cells (see figure 2.13.D). However, measurements in ghost cells show that the contribution of the vimentin network *per se* in energy dissipation is negligible. The observed enhancement in energy dissipation in wild-type cells is thus likely due to the interactions between the vimentin network and other cellular components (actin filaments, microtubules, cytosol). This highlights the dramatic role of cytoskeletal crosstalk in cell mechanics that will be the focus of the next chapter.

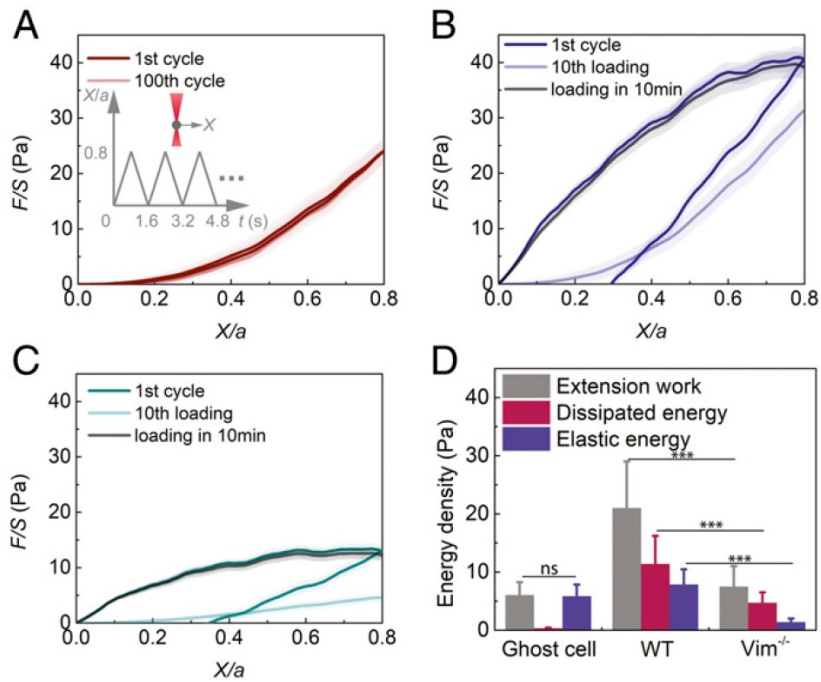


Figure 2.13: Role of the vimentin network in cells undergoing cyclic loadings.

A: Cyclic loading in ghost cells containing only intermediate filaments and no actin or microtubule networks (inset). The first and 100th loading and unloading curves in ghost cells overlap. *B-C:* First and 10th cyclic loading curves in WT MEFs (*B*) and $Vim^{-/-}$ MEFs (*C*). After being damaged by repeated loadings, both cells recover to original levels in 10 min (curves labeled as "loading in 10 min" in panels *B* and *C*). *D:* Extension work, dissipated and elastic energies in ghost, WT and $Vim^{-/-}$ cells. From [Hu et al. 2019].

Mechanical coupling within the cytoskeleton

Contents

3.1 Cytoskeletal crosstalk involving vimentin intermediate filaments and microtubules	49
3.1.1 Crosstalk through molecular motors	50
3.1.2 Crosstalk through crosslinking proteins	51
3.2 Impact of cytoskeletal crosstalk on network organization and cell mechanics	54
3.2.1 Synergistic organization of cytoskeletal networks	54
3.2.2 Mechanical reinforcement mediated by cytoskeletal interactions	57

Dividing the cytoskeleton into different subsystems has long been the most widespread approach to study its functions, structure or mechanics in eukaryotic cells. Although they exhibit quite different structural and physical properties, these subsystems are not independent and many cellular functions are achieved by more than one cytoskeletal subcomponent. Most cell functions require a strong cytoskeletal crosstalk and microtubule, actin and intermediate filament networks are highly connected and interacting. Here, although the coupling between actin and the other cytoskeleton has been widely studied, we will mostly focus on the interactions involving microtubules and vimentin intermediate filaments¹, and how these interactions influence cell mechanics, especially intracellular mechanics.

3.1 Cytoskeletal crosstalk involving vimentin intermediate filaments and microtubules

Direct binding between two cytoskeletal subcomponents is the more intuitive physical link that can be imagined. For instance, it was shown *in vitro* that actin and vimentin intermediate filaments interact together in the absence of other proteins [Esue *et al.* 2006]. This interaction has been established to occur through the binding of actin filaments to the tail domain of vimentin intermediate filaments: this

¹Many other intermediate filaments interact with microtubules, but in this chapter we focus on vimentin as it is the intermediate filament protein of interest in our research.

domain mediates inter-filament interactions. In cells, the crucial role of vimentin in mitosis through its interplay with the actin cortex has been highlighted [Duarte *et al.* 2019]. More precisely, the authors show that the vimentin tail was required to observe a correct vimentin network distribution. Conversely, tailless vimentin leads to aberrant mitosis. Nonetheless, it is difficult to determine whether these interactions take only place through direct binding between actin and vimentin, or if they also arise from the presence of actin-associated proteins, molecular motors or crosslinking proteins like plectin. Broadly speaking, only few direct bindings within the cytoskeleton have been demonstrated². Most interactions forming cytoskeletal crosstalk are mediated by active (molecular motors) and passive crosslinking protein complexes.

3.1.1 Crosstalk through molecular motors

- **Myosins link actin filaments to microtubules.**

By far, actin and microtubules have been the most studied elements of the cytoskeleton. In the early 1990s, the common conception in the field was that microtubules formed a network used for long-range transport whereas the actin network was thought to achieve short-range transport [Langford 1995]. Yet, direct interactions between a myosin (Va) and a kinesin (KhcU) were shown to happen both *in vitro* and in a yeast two-hybrid screen [Huang *et al.* 1999]. The authors hypothesized that this crosstalk through an actin and a microtubule molecular motor should play a functional role in coordinating organelle transport along these networks. Later studies have shown that myosin V can undergo diffuse motions on microtubules [Zimmermann *et al.* 2011] and that myosin X mediates podosome positioning by linking actin to the microtubule network [McMichael *et al.* 2010].

In sharp contrast, there is little evidence that vimentin can be connected to the actin network through myosins. To our knowledge, the only reported direct bond between a myosin and intermediate filaments occurs in neurons through Myosin Va, which binds to neurofilaments [Rao *et al.* 2002]. For other intermediate filament proteins, rather than myosins, crosslinking proteins ensure the crosstalk with actin networks.

- **Kinesins and dynein transport vimentin.**

The assembly and maintenance of an extended vimentin network requires an intact microtubule network. The idea that microtubules may transport vimentin intermediate filaments *via* kinesin or dynein motors have been supported by several results. In fibroblasts, vimentin filamentous squiggles associate with conventional kinesin which is required for the assembly and maintenance of the vimentin network [Prahlaad *et al.* 1998]. Similarly, in Chinese Hamster Ovary (CHO) cells, ubiquitous kinesin heavy chain (but not dynein)

²The other known-to-date direct binding involves neurofilaments and microtubules and will not be described here.

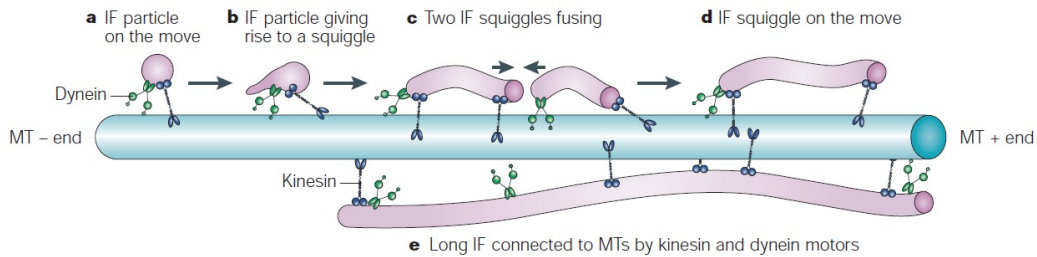


Figure 3.1: Role of microtubules in vimentin filament assembly and motility. From [Chang & Goldman 2004].

is involved in recruiting vimentin to focal adhesions [Bhattacharya *et al.* 2009]. This result, obtained by using Short Hairpin Ribonucleic Acids (shRNA) specifically targeting the dynein heavy chain or the ubiquitous kinesin heavy chain, suggests that plus-end-directed microtubule motor proteins facilitate this process. Moreover, the retrograde transport of vimentin was shown to depend on the minus-end-directed motor complex that consists of cytoplasmic dynein and dynactin [Helfand *et al.* 2002] [Helfand *et al.* 2004]. The association of microtubule-based motor proteins with mature intermediate filaments and intermediate filament precursors is required both for their correct assembly and their retrograde and anterograde movements, as depicted in figure 3.1 [Chang & Goldman 2004].

3.1.2 Crosstalk through crosslinking proteins

- **Plectin plays a key role in cytoskeletal crosstalk.**

Among cytoskeletal crosslinking proteins, plectin is, to our knowledge, the only one which has been reported to interact with the three cytoskeletal sub-systems. Plectin isoforms have a conserved C-terminus but differ in their N-terminus. Through its C-terminus, plectin is able to bind to several intermediate filament proteins, such as vimentin, keratin, desmin, *etc.* [Wiche & Winter 2011]. It is often categorized as an intermediate filament-associated protein. Regarding vimentin, plectin has been shown to have a dramatic influence on the networks of vimentin intermediate filaments in living cells. In polarized fibroblasts, the vimentin network forms a cage surrounding the nucleus which is linked to actin-based fibrillar adhesions through plectin (see figure 3.2.A). In plectin-deficient fibroblasts, the vimentin network spreads within the whole cell which loses its polarity (see figure 3.2.B). Plectin has also been shown to bind to actin filaments (both actin and myosin directly interact with plectin) and to microtubules, mostly through MAPs (*e.g.* MAP1/2, tau) [Castañón *et al.* 2013]. Therefore, plectin can link vimentin intermediate filaments with microtubules [Svitkina *et al.* 1996], vimentin intermediate filaments with actin filaments [Serres *et al.* 2020] [Osmanagic-Myers *et al.* 2015], but also actin filaments with microtubules [Goldmann 2018] (see figure 3.3).

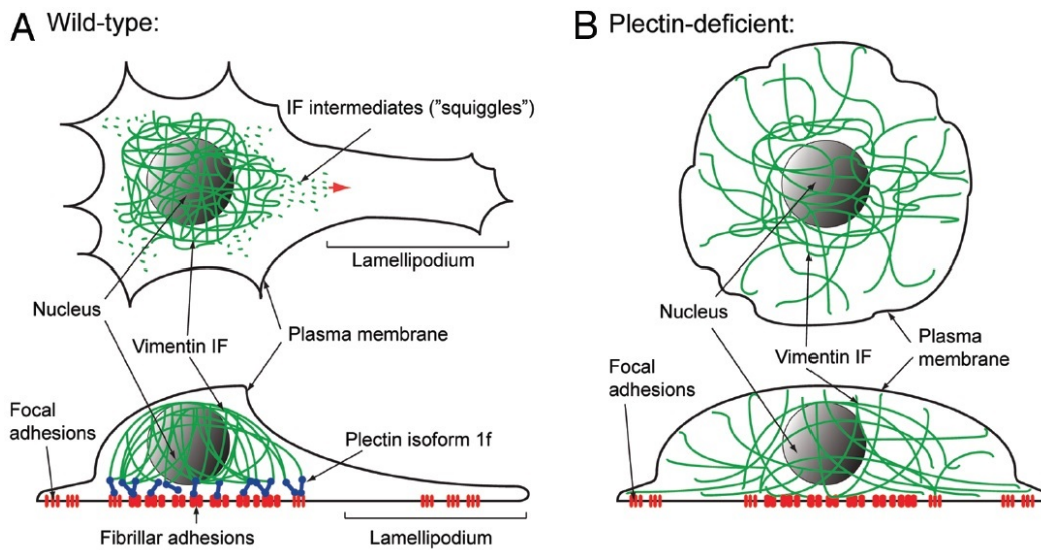


Figure 3.2: Influence of plectin on vimentin network organization in fibroblasts.

A: Schematic representation of a WT fibroblast. Plectin mediates cell polarity by anchoring the vimentin cage around the nucleus to fibrillar and focal adhesions. The squiggles going to the cell periphery attach to focal adhesions and can eventually link to the central vimentin cage. B: Schematic representation of a plectin-deficient fibroblast. Cell polarity is lost as the vimentin network is not restricted to the central part of the cell, preventing it from correctly encasing the nucleus. From [Wiche & Winter 2011].

Much more than a cytoskeletal crosslinking protein, plectin is involved in many cellular functions as it also interacts with numerous proteins present at the nuclear membrane (lamin B, nesprin), the plasma membrane (spectrin, dystrophin, *etc.*), the centrosome (BRCA2) and at cell junctions (desmoplakin, utrophin, integrin, *etc.*). Mutations in the plectin gene are thus implicated in a wide range of diseases, such as muscular dystrophy, neuropathy and skin blistering [Castañón *et al.* 2013] [Winter & Wiche 2013].

- **Many cytoskeletal crosslinkers connect actin filaments and microtubules.**

Microtubule Plus-end tracking proteins (+TIPs) refer to a heterogeneous group of proteins that specifically accumulate at (mostly growing) microtubule plus-ends. Microtubule +TIPs are involved in many cellular functions and interact with a lot of cellular structures: organelles, vesicles, cytoskeleton, *etc.* [Akhmanova & Steinmetz 2010]. Some of them have been shown to interact with actin filaments, such as MACF, CLASP, Adenomatous Polyposis Coli (APC), CLIP-170, Kar9, RhoGEF2, p140CAP, *etc.* [Akhmanova & Steinmetz 2010] [Huber *et al.* 2015]. Among them (*e.g.* MACF), we can mention the peculiar case of spectraplakins. They belong to the spectrin family, today considered as the fourth cytoskeletal subsystem. Because of their structure which includes a conserved amino acid sequence close to the N-terminus,

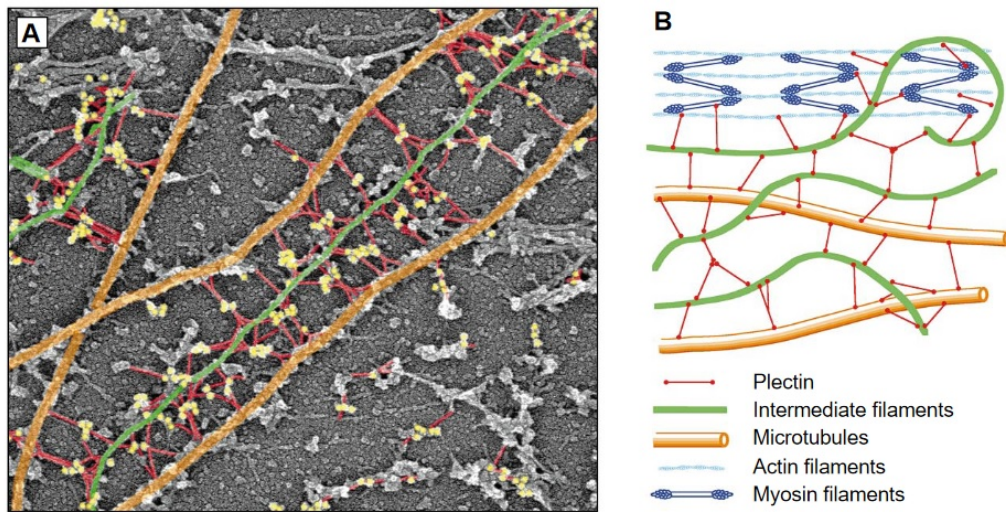


Figure 3.3: Plectin crosslinks vimentin, microtubule and actomyosin networks.

A: Electron microscopy image of the residual cytoskeleton of a rat embryo fibroblast after dissolution of actin filaments with gelsolin. Pseudocolored elements are microtubules (orange), vimentin intermediate filaments (green), plectin (red). Gold particles (yellow) also mark plectin. B: Schematic representation of the links between plectin and the cytoskeletal subsystems. From [Fuchs & Cleveland 1998].

spectraplakins can directly bind to actin filaments. Many of them link actin to other cytoskeletal filaments (sometimes another actin filament) and are therefore described as cytoskeletal crosslinking proteins, while also being part of the cytoskeleton [Zhang *et al.* 2017]. For instance, because of their ability to link microtubules to focal adhesions, spectraplakins are particularly important in the context of cell migration [Etienne-Manneville 2013].

While there are many proteins connecting microtubules and actin filaments, only a few proteins specifically link vimentin to the other two cytoskeletal subsystems. Fimbrin have been shown to crosslink vimentin intermediate filaments and actin filaments [Correia *et al.* 1999]. Microtubules are mostly connected to vimentin intermediate filaments through MAPs, like tau [Capote & Maccioni 1998] or MAP2 [Etienne-Manneville 2013]. A recent study showed that in endothelial cells, Rudhira/Breast Carcinoma Amplified Sequence 3 (BCAS3) binds both microtubules and vimentin intermediate filaments and bridges these cytoskeletal subcomponents [Joshi & Inamdar 2019]. The authors also demonstrated that this cytoskeletal protein stabilizes microtubules and enhances cytoskeletal crosstalk by regulating the association and dynamics of vimentin intermediate filaments and microtubules.

Figure 3.4 gives an overview of the cytoskeletal crosstalk and recapitulates some of the results mentioned in this section.

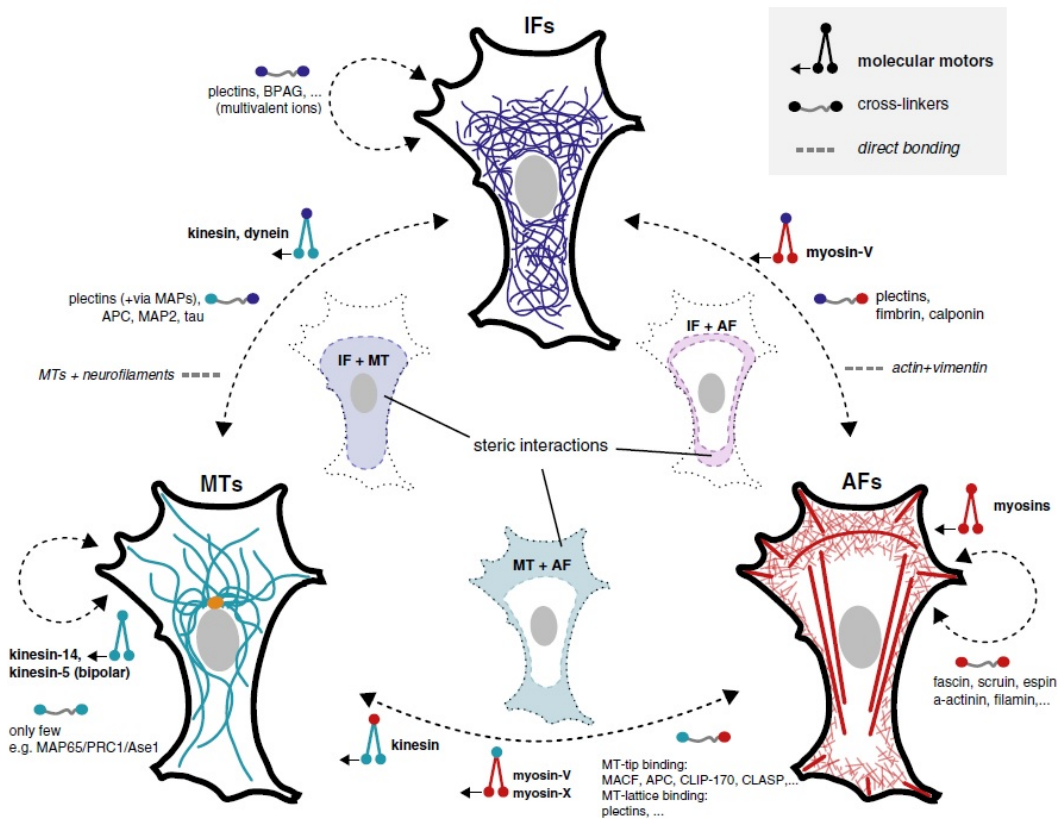


Figure 3.4: Physical interactions between the three cytoskeletal subsystems.

Note that plectin is involved in actin/microtubule, actin/intermediate filament and intermediate filament/microtubule crosstalks. Adapted from [Huber et al. 2015].

3.2 Impact of cytoskeletal crosstalk on network organization and cell mechanics

3.2.1 Synergistic organization of cytoskeletal networks

Considering the numerous physical links within the cytoskeleton presented above, the understanding of one given cytoskeletal subsystem needs to take into account the existence of the other two. For instance, the fact that vimentin particles and squiggles are transported along microtubules is reflected in the global organization of the vimentin intermediate filament network: in many cell lines, vimentin intermediate filaments and microtubules are often colocalized [Goldman 1971] [Prahlaad et al. 1998]. One of the first publications which studied the three cytoskeletal subsystems in living cells reported that BHK-21 cells (baby hamster kidney cells) treated with colchicine - a drug preventing microtubule elongation and which has a similar effect to that of nocodazole - exhibit a typical retraction of the intermediate filament network onto the nucleus [Goldman 1971]. The same effect was observed with the microinjection of antibodies against α -tubulin and β -tubulin:

the intermediate filament network was found to collapse into the perinuclear region [Klymkowsky 1981] [Blose *et al.* 1984].

Blose *et al.* hypothesized that the antibodies, due to their very high affinity for tubulin, drastically disrupted the interactions between microtubules and intermediate filaments. Interestingly, the collapse has been shown to be reversible as re-growing microtubules in cells previously treated with nocodazole induces the rapid realignment of vimentin intermediate filaments with stabilized microtubules [Gurland & Gundersen 1995]. In the same work, the authors establish that tyrosination, a microtubule PTM, plays an important role in the process of intermediate filament retraction. By specifically targeting detyrosinated and tyrosinated microtubules, Gurland & Gundersen demonstrate that detyrosinated microtubules are mostly involved in the vimentin network collapse, unlike tyrosinated microtubules. Conversely, vimentin intermediate filaments preferentially reform along detyrosinated microtubules. Deacetylated microtubules have also been shown to induce the collapse of the vimentin intermediate filament network: overexpression of the microtubule deacetylase HDAC6 is sufficient for the vimentin intermediate filaments to collapse in human fibroblasts. Inhibiting HDAC6 with tubacin also decreases the fraction of cells with collapsed vimentin [Rathje *et al.* 2014].

However, as stated in [Gurland & Gundersen 1995]: "Vimentin IFs were not stabilizing the Glu³ Microtubules (MTs) since collapse of the IF network to a perinuclear location, induced by microinjection of monoclonal anti-IF antibody, had no noticeable effect on the array of Glu MTs." Together, these data suggest that while the presence of an extended microtubule network is crucial for the organization of the vimentin network, the converse is not true. Yet, more recent studies have provided evidence that the presence of the vimentin network plays a role in the organization of the microtubule network. In micropatterned MEFs, the loss of vimentin leads to a reorganization of the microtubule network which becomes denser around the nucleus, whereas it has no effect on the actin network (see figure 3.5.A) [Shabbir *et al.* 2014]. In breast cancer cells, the distribution of microtubules and actin filaments was characterized by acquiring 3D images with a confocal microscope in control and vimentin knockdown stable clones [Liu *et al.* 2015]. Unlike Shabbir *et al.*, the authors found that the organization of the actin network was modified by the absence of vimentin: instead of forming regular stress fibers in the cytosol, actin filaments formed spikes next to the cell membrane and irregular stress fibers. Regarding microtubules, Liu *et al.* showed that they are found at the top and at the bottom of the cell in vimentin knockdown cells, whereas they are only positioned at the bottom of control cells (see figure 3.5.B).

More than just modifying the organization of the microtubule network, vimentin intermediate filaments are now thought to template microtubule growth due to their longer turnover [Gan *et al.* 2016]. Altogether, these results suggest that microtubules and vimentin intermediate filaments are involved in a positive feedback loop: while microtubules transport vimentin particles and squiggles and thus me-

³detyrosinated

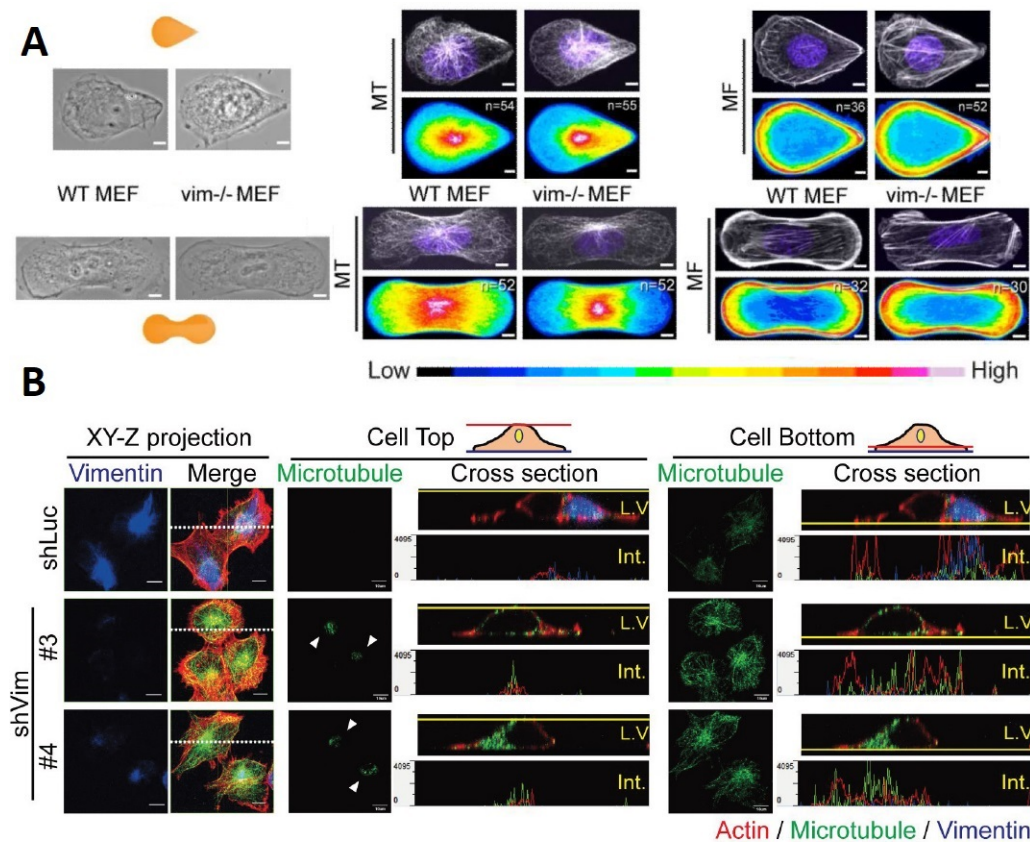


Figure 3.5: The absence of vimentin intermediate filaments disturbs the organization of the microtubule network.

*A: Immunofluorescence/phase contrast images of micropatterned wild-type and vimentin-null MEFs cells in which MTs, Actin Filaments (MFs) and nuclei (blue) were stained. Scale bar: 5 μ m. *n*: number of cells used to generate the heat map. The used color scale appears below, with dark/blue colors corresponding to the lowest probability of presence and pink/red to the highest one. The shapes (tear drop and dumbbell) of the corresponding micropatterns are shown in orange on the left images. Adapted from [Shabbir et al. 2014].*

B: Images of top and bottom sections in control (shLuc) and vimentin knockdown clones (shVim). Left panels: XY-Z projection images of vimentin and merged images of the three cytoskeletal subcomponents. The horizontal white dashed line indicates the lateral view section. Middle and left panels: microtubule staining, lateral view and section intensity profile at cell top (middle) and bottom (right). Arrows indicate microtubule staining at cell top. Red: actin, green: microtubule, blue: vimentin. Scale bars: 10 μ m. From [Liu et al. 2015].

diate the establishment and the maintenance of the vimentin network in cells, vimentin intermediate filaments, as they disassemble much slower than microtubules, exhibit a templating function for microtubules. These interactions are very important to preserve cell polarity, specially during migration events. Besides, the vimentin network has been recently shown to regulate the actin retrograde flow by reorienting actin-based forces [Costigliola et al. 2017], enhancing its key role in cell

migration.

3.2.2 Mechanical reinforcement mediated by cytoskeletal interactions

- **Mechanics of heterogeneous reconstituted networks.**

Among the cytoskeleton, actin filaments and (vimentin) intermediate filaments are known to be the main contributors to cell mechanics, and specially to cell stiffness [Mendez *et al.* 2014] [Huber *et al.* 2015]. Intracellular measurements allow to discriminate between cytoplasmic stiffness - mostly determined by vimentin intermediate filaments - and cortical stiffness - driven by the actin network [Guo *et al.* 2013].

The interactions between actin and vimentin intermediate filaments were first studied *in vitro*. By using networks of actin and vimentin mixed in different proportions, Esue *et al.* could compare the mechanical properties of vimentin gels, actin gels and mixed gels [Esue *et al.* 2006]. At a given total concentration, the frequency-dependent shear modulus in a mixed gel is significantly higher than those of both pure actin or pure vimentin gels. The authors also demonstrated that the tail domain of vimentin is crucial for direct interactions between these two different filaments (see figure 3.6.A). Indeed, mixed networks of actin and tailless vimentin intermediate filaments exhibit a lower shear stress modulus compared to the condition with full-length vimentin. This originates from much weaker inter-filament interactions inside the gel.

A similar study was conducted *in vitro* on reconstituted networks made of actin filaments and microtubules [Lin *et al.* 2011]. The results show that the storage modulus G' of an actin network is almost constant with the shear strain γ - like that of a solid - before reaching a critical shear strain where G' decreases while γ increases: pure actin gels strain-weaken. Interestingly, with the addition of microtubules, the first plateau-like region remains unchanged but the second region exhibit a typical strain-stiffening behaviour (see figure 3.6.B). Microtubules seem to be involved in the mechanical reinforcement at high strain, whilst playing an insignificant role at low strains. A recent work *in vitro* has confirmed that, depending on the microtubule fraction in mixed actin/microtubule gels, strain-softening and strain-stiffening can be measured [Ricketts *et al.* 2018]. A large fraction of microtubules is needed to substantially increase the measured force, supporting the fact that microtubules do not contribute much to cell stiffness in living cells.

Although a recent work has studied how vimentin intermediate filaments stabilize microtubules in mixed networks made of purified vimentin and tubulin [Schaedel *et al.* 2021], there is not, to our knowledge, any study on similar networks that focuses on the mechanical properties of these networks, by varying *e.g.* protein concentration, crosslinking, *etc.*

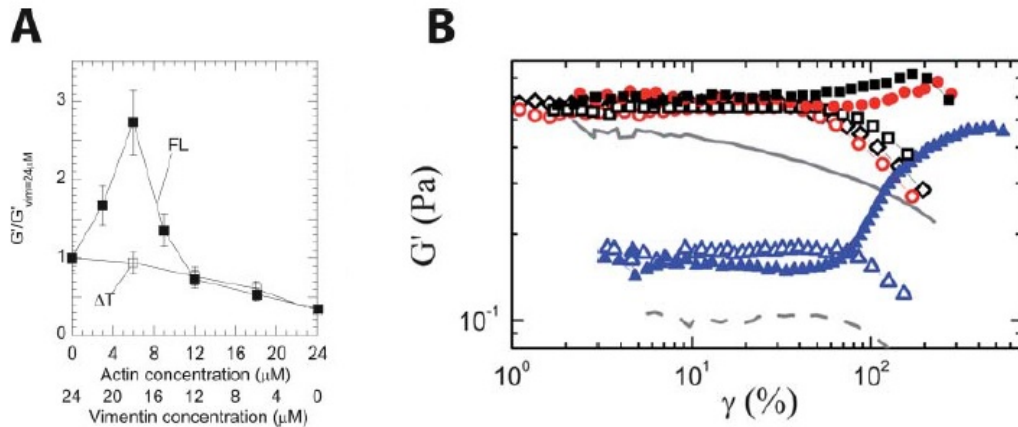


Figure 3.6: Heterogeneous reconstituted networks exhibit peculiar mechanical behaviours.

*A: Normalized shear storage modulus G' of actin networks mixed with full-length (FL, closed squares) or tailless (ΔT , open squares) vimentin plotted as a function of protein concentration. The absence of a peak in the storage modulus indicates that the tail domain of vimentin is essential for direct interactions between vimentin and actin filaments. From [Esue *et al.* 2006].*

*B: Storage modulus G' as a function of shear strain γ . Addition of microtubules in actin networks (solid symbols) at different concentrations and crosslink densities always leads to a strain-stiffening response of these networks. Corresponding networks without microtubules (open symbols) exhibit a typical strain-weakening behaviour, like microtubule networks alone (solid and dashed lines). From [Lin *et al.* 2011].*

- **In cells: regulations and compensations in a complex network.**

In living cells, we already mentioned that both actin and vimentin intermediate filaments protect microtubules against compressive forces (see figure 2.10). They act as an elastic background network that provides a mechanical reinforcement and decreases the buckling wavelength, enabling microtubules to bear increased compressive loads [Brangwynne *et al.* 2006]. The presence of the surrounding cytoskeleton and of crosslinking proteins is crucial in cell mechanics. For instance, plectin has been found to significantly influence the mechanical properties of living cells [Na *et al.* 2009]. As expected, plectin-deficient cells, despite being of similar shape and size, are less stiff than control cells and are not able to propagate forces at the whole-cell-scale, unlike control cells.

Recently, the pivotal role of vimentin in the context of cell migration and cell mechanics has been investigated [Li *et al.* 2019] [De Pascalis *et al.* 2018] [Sharma *et al.* 2017] [Gregor *et al.* 2013] [Hu *et al.* 2019]. These studies have shed light on its integration into the cytoskeleton, some of them leading to unexpected and surprising results. For instance, vimentin knockout human mesenchymal cells have been measured to be less deformable than control cells (see 3.7.A-B), which seems to contradict most of the results presented above [Sharma *et al.* 2017]. By using drugs to specifically disrupt microtubules (colchicine) and actin filaments (cytochalasin D), the authors showed that the

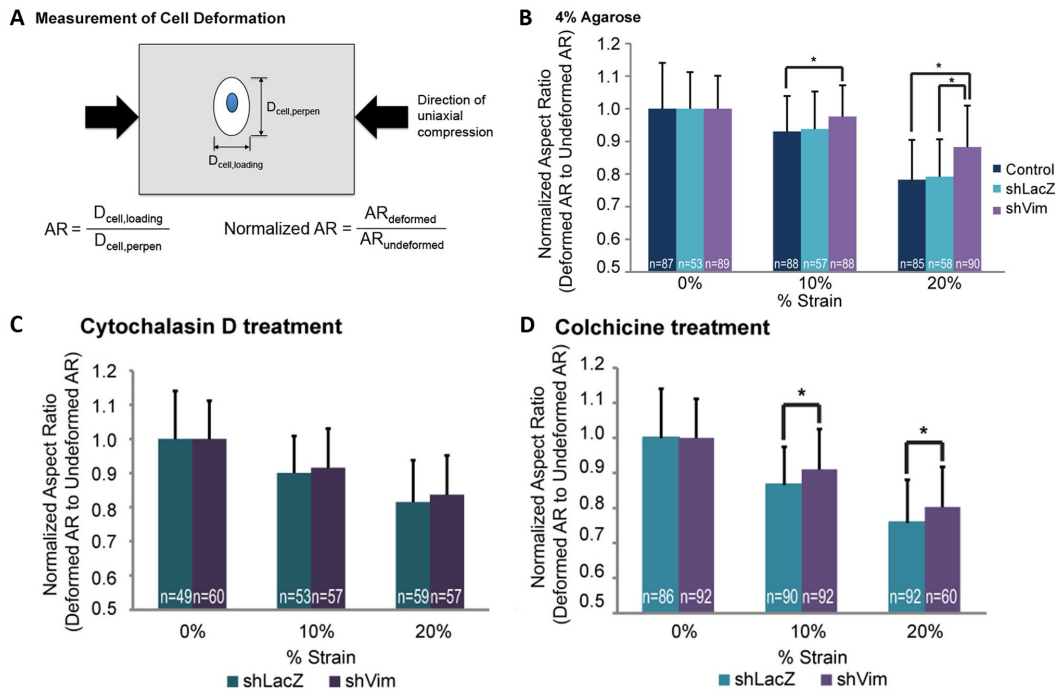


Figure 3.7: Vimentin-dependent cell deformability is compensated by actin filaments but not by microtubules.

A: Deformability of cells undergoing a uniaxial compression is calculated by measuring the major axis and the minor axis of the fitted ellipse. Deformation of untransfected cells, transfected control cells (*shLacZ*) and vimentin-deficient cells (*shVim*) at different strains without drugs (B), with cytochalasin D (C) and with colchicine (D). Asterisks represent statistically significant differences ($p < 0.05$). Adapted from [Sharma et al. 2017].

deformability of *shVim* cells remained higher than that of *shLacZ* (control) cells upon colchicine treatment (see figure 3.7.D). On the contrary, cytochalasin D treatment reduced the deformability of *shVim* cells, making it not significantly different from that of control cells (see figure 3.7.C). Altogether, these results suggest that this complex mechanical behaviour originates from compensatory mechanisms between actin filaments and vimentin intermediate filaments.

In the previous work, deformations were measured at the whole-cell-scale. At the intracellular scale, vimentin intermediate filaments have been shown to extend deformation fields under local loading [Hu et al. 2019]. Hu et al. demonstrate that vimentin intermediate filaments increase both stretchability and strength *in cellulo*. In addition, the effect of microtubules and actin filaments on the apparent vimentin stiffness has been characterized in living cells by tracking vimentin intermediate filaments [Smoler et al. 2020]. Using vinblastine to reduce the rate of microtubule polymerization and depolymerization events, the authors show that treating cells with vinblastine does not significantly affect the organization of the vimentin network. However, the

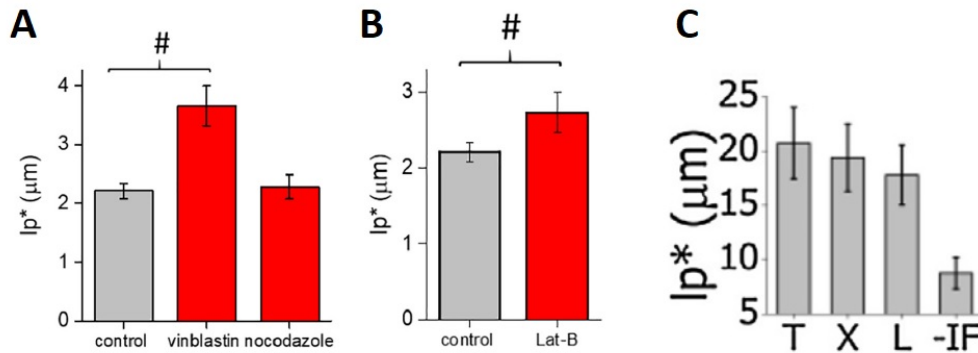


Figure 3.8: Effect of network disruptions on the persistence lengths of vimentin intermediate filaments and microtubules.

A&B: Apparent persistence lengths of vimentin intermediate filaments of cells treated with drugs disrupting the microtubule network (A) or the actin network (B). Hashes indicate significant differences in apparent persistence lengths ($p < 0.05$). Adapted from [Smoler *et al.* 2020]. *C:* Apparent persistence lengths of microtubules for cells transfected with enhanced Green Fluorescent Protein (eGFP) α -tubulin (T), eGFP-XTP cells (X), eGFP-XTP cells treated with latrunculin A to disrupt the actin network (L) and eGFP-XTP cells transfected with a dominant-negative construct of eGFP-vimentin that disrupts the vimentin intermediate filament network. Note that XTP is part of the MAPs. From [Pallavicini *et al.* 2014].

apparent persistence length of vimentin intermediate filaments is increased by 65% (see figure 3.8.A). Similarly, Smoler *et al.* use latrunculin B to depolymerize actin filaments. At high concentrations, actin depolymerization leads to the well-characterized collapse of the vimentin network but at low concentrations, the organization of the vimentin network is not affected even though the number of stress fibers and the cell spreading area are reduced. Surprisingly, they find that the apparent persistence length of vimentin is increased by 20% in latrunculin B-treated cells (see figure 3.8.B). Whilst the spreading area of the cells is reduced, increased compressive forces do not lead to a higher curvature of vimentin intermediate filaments due to a compaction of the vimentin network [Smoler *et al.* 2020]. Here again, this result shows that vimentin and actin networks exhibit compensatory mechanisms, perhaps through feedback loops reflected in cell mechanics. Besides, an earlier study by the same group reported that disruption of the vimentin network decreases microtubule persistence length (see figure 3.8.C).

Vimentin intermediate filaments have also been shown to be involved in mechanotransduction at focal adhesions: in vimentin-deficient fibroblasts and plectin-deficient fibroblasts, mechanosensing through focal adhesions is reduced [Gregor *et al.* 2013]. The actomyosin network can be an efficient mechanosensing structure because vimentin intermediate filaments store most of the energy coming from mechanical stresses. The authors also show that loss of vimentin perturbs the ability of the cell to migrate and protrude. This

point has been further investigated in astrocytes where it has been found that the vimentin network is crucial for collective directed migration [De Pascalis *et al.* 2018]. Altogether, the results suggest that vimentin intermediate filaments control traction forces by limiting them to the front of leader cells and are also involved in sustaining contacts between cells.

Aims of the PhD project

The mechanical properties of the cytoskeleton has been extensively studied *in vitro* but is still largely unexplored in living cells. In particular, few measurements and comparisons of the rheological properties of cytoskeletal filaments have been carried out *in cellulo*. If *in vitro* minimal systems have provided great insights on the mechanics of the cytoskeleton, experiments in living cells give the opportunity to highlight the importance of the coupling between the different cytoskeletal subcomponents in the context of cell mechanics. Before detailing the aims of the PhD project, we summarize here the most important elements - mentioned in the previous chapters - of the scientific context in which this thesis PhD work fits:

- the mechanical properties of the cytoskeleton are crucial for cell functions and mechanotransduction. For instance, intermediate filaments play a key role in nuclear mechanics and cell migration [Dupin & Etienne-Manneville 2011] [Etienne-Manneville 2018] [Keeling *et al.* 2017];
- while cytoplasmic intermediate filaments are stable long-lived structures that assemble in several steps [Hohmann & Dehghani 2019], microtubules are highly dynamic and exhibit frequent polymerization and depolymerization events, following a process called dynamic instability [Mauro *et al.* 2019]. They are decorated by numerous PTM, like K40 acetylation [Janke & Montagnac 2017] [Janke & Magiera 2020];
- to measure mechanical properties of single cytoskeletal filaments, passive (imaging the fluctuations of filaments to deduce their persistence length) or active (elongating filaments, bending filaments) approaches can be used [Felgner *et al.* 1996] [Felgner *et al.* 1997] [Guzmán *et al.* 2006] [Kreplak *et al.* 2008]. Historically, the first studies on the cytoskeleton were conducted on reconstituted gels and networks [Janmey *et al.* 1991] and macroscopic rheometers were used to perform the measurements [Esue *et al.* 2006] [Pujol *et al.* 2012];
- intermediate filaments have been the least studied cytoskeletal subsystem. Intermediate filaments are the most deformable structures of the cytoskeleton as they can withstand strains up to 100% [Janmey *et al.* 1991]. *In vitro*, they exhibit a strain-stiffening behaviour at high forces [Charrier & Janmey 2016] which depends on the loading-rate in a non-linear fashion [Block *et al.* 2017]. Vimentin intermediate filaments are sometimes seen as the safety belt of cells [Kreplak *et al.* 2005] [Qin *et al.* 2009] [Block *et al.* 2017];

- the mechanics of microtubules have been more investigated, essentially *in vitro*, either by studying single microtubules or by performing bulk rheology experiments on microtubule networks. Due to their anisotropic stiffness, microtubules can have very different responses according to the way their mechanical properties are measured [Schaap *et al.* 2006] [Hawkins *et al.* 2010]. Microtubules associate a high longitudinal stiffness and a high lateral deformability [Huber *et al.* 2013]. One of the most measured mechanical parameter in the literature is the flexural rigidity κ , and its values vary on 3 orders of magnitude, typically from 10^{-25} N m² to 10^{-22} N m² [Hawkins *et al.* 2010]. The effects of MAPs and taxol on microtubule flexural rigidity are still unclear and debated;
- the effects of repeated mechanical stress on microtubules [Schaedel *et al.* 2015] [Xu *et al.* 2017] and intermediate filaments [Kraxner *et al.* 2021] have been studied *in vitro*: softening of both filaments were measured under appropriate experimental conditions;
- in cells, different mechanical parameters have been measured: the persistence length l_p of microtubules was estimated by microtubule buckling [Pallavicini *et al.* 2017]. Two studies estimated the flexural rigidity of microtubule bundles following opposite hypothesis regarding the crosslinks within microtubule bundles [Baba 1972] [Battle *et al.* 2015]. A Fourier analysis of the shape of cytoskeletal led to persistence length measurements [Pallavicini *et al.* 2014] [Smoler *et al.* 2020];
- the cytoskeleton features many direct interactions between microtubules, actin filaments and intermediate filaments [Huber *et al.* 2015]. Microtubules and intermediate filaments colocalize [Prahlad *et al.* 1998] and kinesin and dynein transport vimentin along microtubules [Prahlad *et al.* 1998] [Chang & Goldman 2004]. Microtubules and vimentin intermediate filaments are crosslinked *via* a protein called plectin [Wiche & Winter 2011] [Winter & Wiche 2013]. While microtubules are required for the organization of the intermediate filament network [Gurland & Gundersen 1995] [Bloese *et al.* 1984], a depletion of vimentin, conversely, disturbs the microtubule network [Shabbir *et al.* 2014] [Liu *et al.* 2015]. Also, intermediate filaments appear as a stable scaffold for microtubule growth [Gan *et al.* 2016];
- the role of the intermediate filament network in cell mechanics at large deformations has been characterized: the dependence on the loading rate during cycles of loading and unloading depends on the interactions between the different cytoskeletal elements [Hu *et al.* 2019]. *In vitro*, vimentin intermediate filaments stabilize microtubules in mixed vimentin/tubulin networks [Schaedel *et al.* 2021]. In cells, vimentin knockout reduces cell deformability through cytoskeletal crosstalk [Sharma *et al.* 2017].

This PhD work aims at **quantifying the mechanical properties of vimentin intermediate filaments and microtubules in living cells**. The specific questions I have addressed are:

1. **What is the stiffness of vimentin intermediate filaments and of microtubules in living cells?**

The aim here is to deduce from optical tweezers-based intracellular rheological experiments a mechanical parameter that allows to quantitatively compare the mechanics of vimentin intermediate filaments and microtubules.

2. **What is the effect of repeated mechanical stress on vimentin intermediate filaments and microtubules in living cells?**

By performing sequences of deflections on a given cytoskeletal bundle, I have aimed at determining whether softening of vimentin bundles and microtubules is also observed in living cells, as suggested by the literature on *in vitro* reconstituted systems.

3. **How does the vimentin network impact on microtubule mechanics?**

I have used a vimentin-KO cell line to quantify the influence of vimentin intermediate filaments on the mechanical properties of microtubules undergoing single or sequential deflections.

4. **How does the microtubule network impact on vimentin bundle mechanics?**

By using drugs that specifically target microtubules (nocodazole to partially depolymerize microtubules, taxol to stabilize them, and tubacin to induce microtubule acetylation), I have measured the effects of stabilizing or destabilizing microtubules and the effects of PTM on vimentin mechanics, in particular when vimentin bundles undergo sequential deflections.

To our knowledge, it is the first time that these questions are addressed in living cells. As opposed to *in vitro* approaches, in which defined components are studied, we chose here to study the cell with all its complexity (variability, out-of-equilibrium activity, *etc.*). This novel approach aims at better understanding the mechanics of cytoskeletal filaments, their interactions, and the potential applications of these findings in mechanotransduction.

Materials and Methods

Contents

5.1	Cell culture	67
5.2	Immunofluorescence staining and fixed cell imaging	68
5.3	Live cell imaging of vimentin and tubulin <i>in cellulo</i>	68
5.4	Drugs targeting microtubules	68
5.5	ATP depletion	69
5.6	Optical tweezer-based microrheology	69
5.7	Data analysis: from the movies to the effective stiffness	72
5.8	Statistical tests	74

5.1 Cell culture

- **Cell lines**

Because it mainly expresses three intermediate filament proteins (nestin, GFAP and vimentin), we use a human malignant glioma cell line known as U-373 MG (Uppsala)¹. Gliomas - like each central nervous system tumour - have long been classified into four groups according to the pathologic evaluation of the tumour [Louis *et al.* 2016]. The U373 cell line is derived from an anaplastic astrocytoma, a grade III glioma [Westermarck *et al.* 1973]. This type of tumour is malignant and associated with a bad prognosis.

In collaboration with Juliana GEAY, former research engineer, and Emma VAN BODEGRAVEN, postdoctoral researcher in the lab of Sandrine ETIENNE-MANNEVILLE, we use a vimentin-KO cell line established by a Clustered Regularly Interspaced Short Palindromic Repeats (CRISPR)-Cas9 strategy from U373 cells.

- **Supplemented medium**

The U373 cell line is cultured in MEM, GlutaMAX™ with Earle's Salts (Gibco™-41090-028) supplemented with 10% of Fetal Calf Serum (FCS) (Eurobio-CVFFCS00-01) and with 1% of MEM Non-Essential Amino Acids Solution (100X) (Gibco™-11140-050).

¹For simplicity, we will refer to it as U373 in this manuscript.

Cells are standardly split at 1/10 each 4 or 5 days when the confluence is about 80%-90%.

5.2 Immunofluorescence staining and fixed cell imaging

To stain cytoskeletal subcomponents and nuclei, we seed cells on 18 mm-diameter coverslips in a 12-well plate. The protocol has four main steps that are described in appendix A. The antibodies listed in table 5.1 are used. Fixed cell imaging is performed with a spinning disk confocal microscope (objective 100X).

Antibody against	Species	Reference	Dilution
Vimentin	Rabbit	Santa Cruz Biotechnology sc-6260	1/100
α -tubulin	Rat	Bio-rad MCA77G YL1/2	1/500
Acetyl-tubulin	Mouse	Sigma-Aldrich T7451	1/10000
Rabbit/Mouse/Rat	Donkey	Jackson ImmunoResearch	1/400

Table 5.1: List of used antibodies.

5.3 Live cell imaging of vimentin and tubulin *in cellulo*

In U373 cells, we label both vimentin and/or tubulin by using two different strategies. While tubulin is stained with commercial probes² (SiR-tubulin or SPYTM655-tubulin), a GFP-vimentin plasmid is nucleofected to induced overexpression of GFP-vimentin in U373 cells by using the Basic NucleofectorTM Kit for Primary Mammalian Glial Cells provided by Lonza®. The corresponding protocols appear in appendix A.

5.4 Drugs targeting microtubules

Microtubules are targeted with specific drugs according to table 5.3. All drugs do not need to be washed out before imaging the cells.

Drug	Effect on microtubules	Incubation time	Concentration
Nocodazole	Partial depolymerization	20 min	0.5 μ M
Taxol	Stabilization	20 min	10 μ M
Tubacin	Increased acetylation	4 h	2 μ M

Table 5.2: Drugs targeting microtubules: experimental procedures

²I tried to label tubulin by nucleofecting a Green Fluorescent Protein (GFP)-tubulin construct, but the signals were much noisier than those obtained with the probes mentioned above.

5.5 ATP depletion

To deplete ATP in U373 cells, they were incubated at 37 °C with 5% CO₂ for 30 min in 2 mL of the solution prepared with the following compounds.

Condition	Chemical compound	Reference	Concentration
ATP depletion	2-Deoxy-D-glucose	Sigma-Aldrich D6134	10 mM
	Sodium azide	Sigma-Aldrich S2002	10 mM
	DPBS, Ca ²⁺ , Mg ²⁺	Gibco™-14190	Solvent
Control	D-glucose	VWR 101175P	5 mM
	DPBS, Ca ²⁺ , Mg ²⁺	Gibco™-14190	Solvent

Table 5.3: ATP depletion protocol

5.6 Optical tweezer-based microrheology

- **Description of the experimental setup.**

The setup I have used combines optical trapping and confocal imaging and was described in a previous publication of the team [Guet *et al.* 2014].

Imaging was performed with a Nikon® A1R confocal scanning head mounted on a Nikon® Eclipse Ti-E inverted microscope. Four lasers could be used, emitting at 405 nm, 488 nm, 561 nm and 640 nm. The corresponding output powers are respectively 360 mW, 150 mW, 480 mW and 500 mW. Image acquisition was made thanks to the software Nikon® NIS-Elements. The resonant mode of the confocal head was used at a frame rate between 1.28 fps and 1.93 fps. Resolution was 62.15 nm/px and the images are 512 px × 512 px.

An optical trap had previously been installed on the setup by focusing a 1063 nm Nd:YAG laser (IPG Photonics 2 W) through a 100X oil immersion objective (1.45 NA, apochromatic objective, Nikon®), as represented in figure 5.1. The typical laser power at the objective is 200 mW.

Optical tweezers consist in a highly focused laser beam. This laser beam exerts two forces on a micrometric particle: first, due the high number of photons, the micrometric particle is subject to radiation pressure. The force associated to this pressure is the *scattering force* and tends to repulse the micrometric particle away from the laser beam. Second, the waist³ of the laser beam has a minimal value that corresponds to the point where the electric field is the strongest. Hence, there is an important gradient of electric field and it can be shown that dielectric particles are strongly attracted towards this point through a force called *gradient force* [Killian *et al.* 2018]. In optical tweezers, particles are submitted to one attractive force and one repulsive force. If the expression of both forces will not be displayed here, it is important to men-

³The waist can be seen as the radius of the laser beam along the axis perpendicular to its propagation.

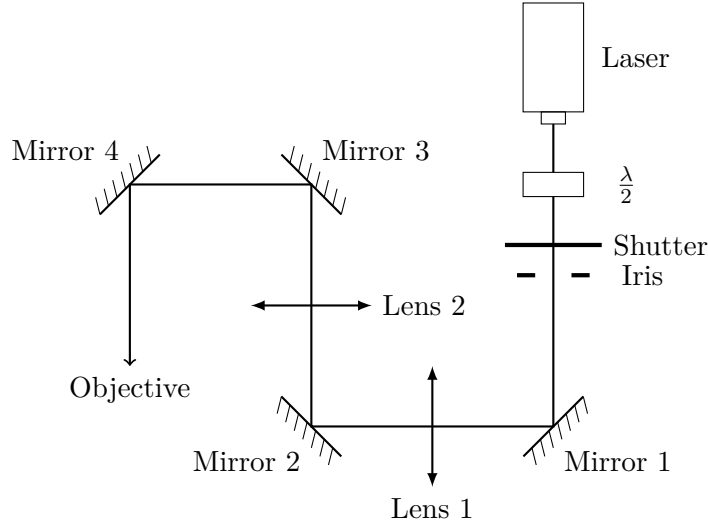


Figure 5.1: Schematic representation of the optical tweezers.

The optical trap set up in our laboratory was designed following an earlier method publication [Lee et al. 2007].

tion that, as long as the distance Δx between the particle and the trap center (where the waist is minimal) remains low, the resulting force \vec{F}_{trap} depends linearly on this distance:

$$\vec{F}_{\text{trap}} = -k_{\text{trap}} \Delta x \vec{u} \quad (5.1)$$

where k_{trap} is a constant called the trap stiffness dependant on the laser parameters and the bead size, Δx is the distance between the bead and the trap center and \vec{u} is the unit vector originating from the trap center and pointing towards the bead. In this regime, the bead is elastically linked to the center of the trap that represents its resting position, following Hooke's law (see figure 5.2).

- **Calibration of the optical tweezers.**

The laser used in our device emits in the infrared wave range ($\lambda_e = 1063 \text{ nm}$) and its power is adjustable and can be set between 0 W and 2 W. The minimal waist w_0 of the laser beam is between $2 \mu\text{m}$ and $3 \mu\text{m}$. Unless specified, we work at a constant laser power equal to 1 W. To be able to perform an accurate quantitative analysis of the recorded images, we previously calibrate the optical trap. The principle is as follows: in a dish filled with water, we trap a $2 \mu\text{m}$ fluorescent bead at a given laser power. By imposing a displacement of the stage at a constant speed U , the distance between the center of mass of the bead and the trap center increases and quickly reaches a steady-state value Δx_∞ . The bead is subjected to two forces: the attractive force of the optical trap \vec{F}_{trap} and a viscous drag force \vec{F}_{drag} exerted by the flowing fluid on the bead. A quick calculation of the Reynolds number gives $\mathcal{R}e = 2 \times 10^{-3} \ll 1$,

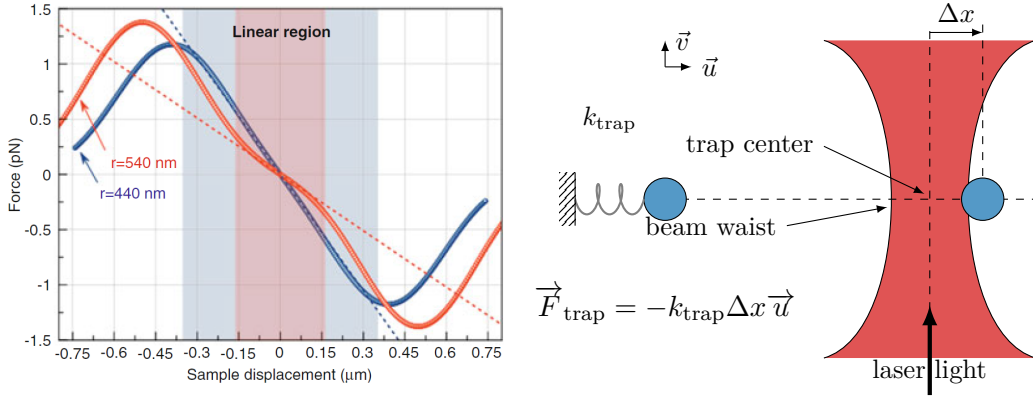


Figure 5.2: Optical tweezers: analogy with a hookean spring.

Left: Force-displacement curves for two sample sizes (dots) and linear fits (dashed lines). From [Farré et al. 2016]. Right: Schematic representation of the optical tweezers seen as an elastic spring.

which allows us to identify the expression of \vec{F}_{drag} to Stokes' drag force:

$$\vec{F}_{\text{drag}} = -6\pi\eta R \vec{v} \quad (5.2)$$

where η is the dynamic viscosity of water, $R = 1 \mu\text{m}$ the radius of the bead and \vec{v} is the velocity of the water relative to the bead. At steady state, the bead remaining at a constant distance to the trap, $\|\vec{v}\| = U$. Also at steady state, the principle of inertia states that forces exerted on the bead are such as $\vec{F}_{\text{trap}} + \vec{F}_{\text{drag}} = \vec{0}$. By using the expression of \vec{F}_{trap} given by equation 5.1, we have:

$$k_{\text{trap}}\Delta x_{\infty} = 6\pi\eta R U \quad (5.3)$$

We repeat the experiment by varying the speed of the stage between $100 \mu\text{m s}^{-1}$ and $4000 \mu\text{m s}^{-1}$ for powers ranging from 0.25 W to 1.5 W (see figure 5.3). Using this calibration method, we did not observe any significant difference between the X- and Y-directions, so that $k_{X,\text{trap}} \approx k_{Y,\text{trap}} \approx k_{\text{trap}}$. For most experiments presented in this manuscript, $k_{\text{trap}} = 240 \pm 40 \text{ pN } \mu\text{m}^{-1}$ for a power (of the optical trap) of 1.00 W. Also, the left panel of figure 5.3 shows that the hookean expression of F_{trap} corresponding to equation 5.1 is valid at least until $\Delta x = 0.5 \mu\text{m}$. Because we mostly study the small forces/small deformations domain in our experiments, we did not aim at precisely measuring the limits of the spatial domain in which this equation was valid.

- **Microrheology experiments.**

In all experiments, $2 \mu\text{m}$ -diameter fluorescent beads were introduced in the culture dish 48 hours prior to the microscopy experiment. These beads are internalized by endocytosis and then distributed within the cytoplasm, some of them being close to a fluorescent cytoskeletal bundle. In this case, such beads are selected to perform microrheology experiments (see figure 5.4.A).

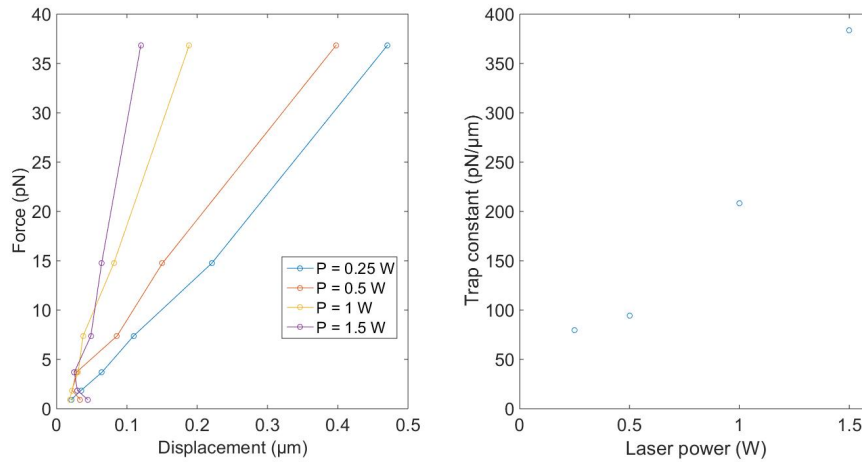


Figure 5.3: Calibration of the optical trap.

Left: Calibration curves for several power values of the laser of the optical trap. The force $6\pi\eta RU$ is represented as a function of the distance between the center of mass of the bead and the trap center at steady state Δx_∞ . *Right:* The spring constant of the optical trap k_{trap} is calculated for each power value by fitting linearly the curves of the left panel. This fit gives a spring constant per unit of power $k_{\text{trap,p}} = 250 \text{ pN } \mu\text{m}^{-1} \text{ W}^{-1}$.

Thanks to the optical tweezers, a bead is trapped and the sample is displaced in order to create a force - exerted by the cytoskeletal bundle - that tends to take the bead out of the trap. Sample displacements are controlled by a piezoelectric stage monitored by the software Nano-Route@3D (Mad City Labs). For most experiments, the stage displacement is set at $2.5 \mu\text{m}$ over an interval of 60s at a constant speed. To detach the internalized bead from potential linkers to the cytoskeleton or internal membrane, a step of typically $0.2 \mu\text{m}$ is applied to the bead by a short pulse of the trap laser prior to the experiment.

5.7 Data analysis: from the movies to the effective stiffness

The confocal microscopy images acquired contained several informations: by tracking the bead, the force exerted on the optical trap by the bead is calculated thanks to the calibration that was previously done. In parallel, the images of the cytoskeleton of interest (see figure 5.4.B) make it possible to quantify the deformation - called *deflection* - of the filament which the bead exerts a force on thanks to an analysis based on kymographs. Force and deflection are thus separately plotted as functions of time, to eventually give a force-deflection curve.

- **Tracking of the bead.**

This first step is performed using a MATLAB programme. After converting

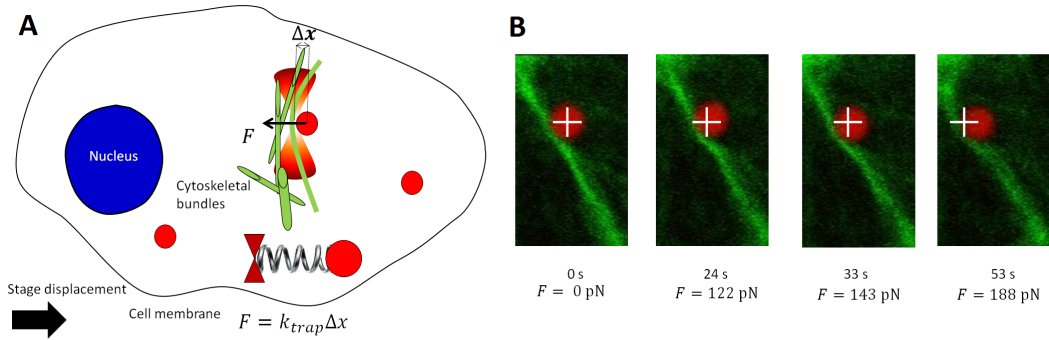


Figure 5.4: Scheme and images of an optical tweezer-based intracellular microrheology experiment.

A: After trapping a bead which was in contact with a cytoskeletal bundle of interest, the stage was displaced towards the right. The chosen bundle is progressively deflected and the force F exerted by the bead on the bundle (towards the left on the scheme) increases linearly with the distance between the center of mass of the bead and the center of the trap Δx following $F = k_{\text{trap}}\Delta x$ where k_{trap} is the trap stiffness. *B:* 4 images of a typical movie of the experiment are shown. GFP-vimentin appears in green and the bead appears in red. The white cross represents the center of the trap. Below each image, the value of the force F and of the time of the image after the beginning of the stage displacement are indicated.

the movie to AVI format and cropping it to have a $162 \text{ px} \times 162 \text{ px}$ square around the bead, a single-particle tracking programme is used to detect the center of the bead at subpixel resolution. This programme gives the evolution of x and y coordinates as a function of time. As the trap is immobile, and assuming that the bead is in the center of the trap at $t = 0$, we can adapt the expression of the force as followed:

$$F = \|\vec{F}_{\text{trap}}(t)\| = k_{\text{trap}}\sqrt{(x(t) - x(0))^2 + (y(t) - y(0))^2} \quad (5.4)$$

where the force and coordinates are expressed as a function of time. This equation gives the temporal evolution of the force exerted by the cellular micro-environment on the bead. As long as the bead remains in the vicinity of the trap, the force gradually increases with time. Yet, the computed force often exhibits a strong increase at a given point: this corresponds to the moment when the bead gets ejected from the trap because of the real shape of the force against sample displacement curve (see figure 5.2 as a reminder). When the bead is ejected from the trap, it is not linked anymore to the trap, thus leading to a null value: the force vs. time curve can only be plotted before the bead ejection. Typically, in most experiments, the bead ejects from the trap before reaching $F = 300 \text{ pN}$.

- **Measuring the deflection of cytoskeletal bundles.**

The stage displacement induces a cell movement that appears on the recorded images: an overall motion is added to the deflection of the probed filament. In

order to remove this global displacement, an ImageJ plugin called Template Matching is used. The steps listed in appendix A are followed under ImageJ and MATLAB. Finally, a movie in which the cell is immobile is created and a kymograph is created from a perpendicular line drawn where the deflection occurs.

- **Force/deflection curves and effective stiffness.**

After these steps, a MATLAB code created with the help of David PEREIRA, postdoctoral fellow in the team (2018-2020) was used (see appendix C). This code needs three input files to work: the table with the positions of the bead (.mat), the kymograph mentioned above and (optional) a reference kymograph that can be useful if there is a wide-range deformation inside the cell (this case is quite rare). The user chooses whether the reference kymograph is necessary and select a few points (typically 5) to roughly follow the deflection of the filament on the kymograph. The code then detects the maximal intensity in the neighbouring pixels and automatically infers the deflection of the filament. The programme plots deflection against time, force against time and eventually the force/deflection curve corresponding to the experiment, excluding all the points after ejection if necessary .

A linear fit of this curve is made in the regime of small forces using MATLAB Curve Fitting Toolbox. The slope of this linear fit is the effective stiffness k (see figure 5.5), which is expressed in $\text{pN } \mu\text{m}^{-1}$ and which links the force F and the deflection δ at small forces (linear regime):

$$F = k\delta \quad (5.5)$$

Note that due to the resolution of the confocal microscope which is used, subpixel deflections can not be detected with our analysis method: $\delta_{\text{lim}} = 0.062 \mu\text{m}$. As the bead often escapes from the trap before reaching $F = 300 \text{ pN}$, it is impossible to measure effective stiffnesses greater than typically $k_{\text{lim}} = \frac{F}{\delta_{\text{lim}}} \approx 5 \times 10^3 \text{ pN } \mu\text{m}^{-1}$.

5.8 Statistical tests

- **Non-paired data.**

To compare the effective stiffness values in two different biological conditions, statistical tests were chosen depending on the number of stiffness values N in each condition. These values are taken from at least three independent experiments.

If in both cases, $N \geq 30$, the equality of variances for the two conditions (homoscedasticity) was assessed with a Levene's test (with a level of significance $\alpha = 0.05$). If the null hypothesis can not be rejected, variances are considered as equal and a standard Student's t -test was used to compare the means in the two conditions. If the null hypothesis is rejected, then variances are different between the two conditions and a Welch's t -test was used to compare

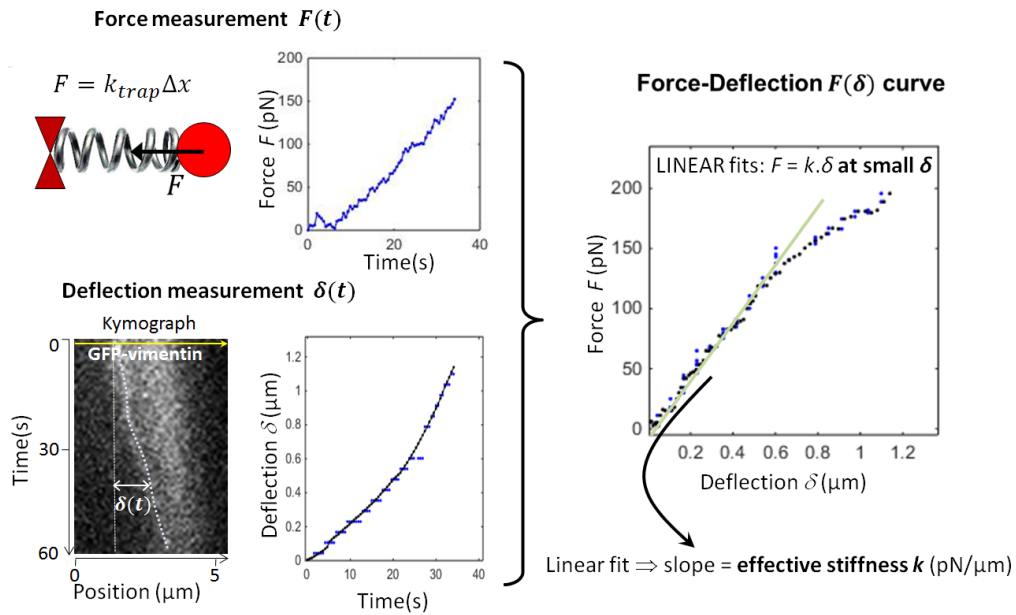


Figure 5.5: The effective stiffness is calculated from linear fits of force-deflection curves at small deformations.

The force exerted by the bead on the cytoskeletal bundle $F(t)$ is plotted as a function of time by analyzing the bead displacement (top left). Independently, the deflection of this bundle $\delta(t)$ is automatically detected by using kymographs (bottom left). Force-deflection curves $F(\delta)$ are finally plotted from the $F(t)$ and $\delta(t)$ curves, and the effective stiffness k corresponds to the slope of a linear fit of this curve at small forces such that $F(\delta) = k\delta$ (right).

the effective stiffness means.

Otherwise ($N < 30$), the normal distribution was checked with a Shapiro-Wilk test (with a level of significance $\alpha = 0.05$). If the null hypothesis can not be rejected, it is assumed that the data is normally distributed and the procedure described in the previous paragraph was followed to choose the final test. If the null hypothesis is rejected, the data is not normally distributed and a Mann-Whitney U test was used to compare the effective stiffness means.

- **Paired data.**

To compare the effective stiffness values before (first deflection) and after (second deflection), statistical tests were chosen depending on the number of stiffness values N in each condition. These values are taken from at least three independent experiments.

If in both cases, $N \geq 30$, the equality of variances for the two conditions (homoscedasticity) was assessed with a Levene's test (with a level of significance $\alpha = 0.05$). If the null hypothesis can not be rejected, variances are considered as equal and a paired Student's t -test was used to compare the paired effective stiffness values before and after. If the null hypothesis is rejected, then variances are different between the two conditions and a Wilcoxon signed-rank

test was used to compare the paired effective stiffness values.

Otherwise ($N < 30$), the normal distribution was checked with a Shapiro-Wilk test (with a level of significance $\alpha = 0.05$). If the null hypothesis can not be rejected, it is assumed that the data is normally distributed and the procedure described in the previous paragraph was followed to choose the final test. If the null hypothesis is rejected, the data is not normally distributed and a Wilcoxon signed-rank test was used to compare the effective stiffness values before and after.

Finally, paired data containing more than two time points (sequence of more than two deflections) were analyzed with the Friedman test - a nonparametric statistical test for matched data - to detect differences in repeated measurements of the effective stiffness. Post-hoc statistical tests to make comparisons between two time points were performed following a Conover's test with Benjamini-Hochberg's procedure.

Results and Discussion

Contents

6.1	Mechanics of vimentin bundles and microtubules	77
6.1.1	<i>In cellulo</i> , vimentin bundles are stiffer than microtubules . . .	77
6.1.2	Sequential deflections make vimentin bundles more rigid . . .	83
6.2	Mechanical coupling between microtubules and vimentin intermediate filaments	87
6.2.1	The vimentin network does not play a key role in the mechan- ical properties of microtubules	88
6.2.2	Modifying microtubule stability affects vimentin mechanical behaviour	90
6.3	Study of a post-translational modification: acetylation . . .	94
6.3.1	Acetylation leads to microtubule softening	96
6.3.2	Acetylated microtubules impact vimentin bundle mechanics .	99
6.4	Preliminary results: role of ATP in cytoskeletal mechanics	101

6.1 Mechanics of vimentin bundles and microtubules

In this section, the effective stiffness of vimentin bundles and microtubules is measured in living cells using an optical tweezers-based microrheology technique. How the bead micro-environment affects the measurements is discussed using high-resolution images. Similarly to some studies of vimentin bundles and microtubules carried out *in vitro*, the effect of repeated mechanical stress on the stiffness is also investigated with the aim of comparing my *in cellulo* experiments with published *in vitro* studies. Experiments probing the mechanical coupling within the cytoskeleton will be presented in the next sections.

6.1.1 *In cellulo*, vimentin bundles are stiffer than microtubules

In order to perform measurements on the cytoskeleton in living cells, a force - perpendicular to the bundle of filaments - is exerted by the trapped bead on a bundle. The stage is displaced at a constant velocity (typically $2.5 \mu\text{m min}^{-1}$), thus pushing the bead against and bending the bundle. By tracking the bead and analyzing the shape of the bundle, force-deflection curves are plotted (see chapter

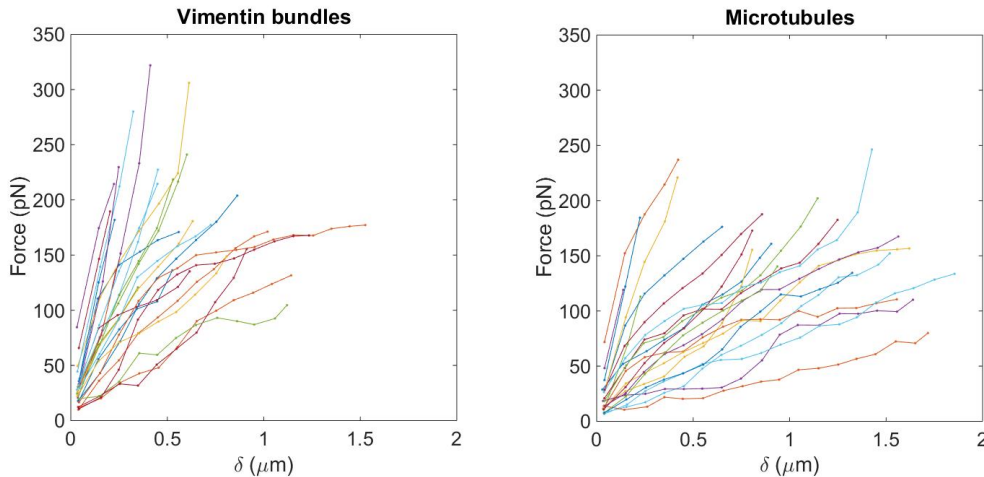


Figure 6.1: The force-deflection curves exhibit an important variability. The force-deflection curves of 28 vimentin bundles (A) and 22 microtubules (B) are plotted by using a moving average on 5 points. The shape of these curves, the initial slope, the maximal force and the maximal deflection vary a lot between experiments. The number of points for each curve depends on the time at which the bead is ejected from the trap.

5 for more details). As mentioned in chapter 5, if ejection from the trap occurs, such curves are drawn between the beginning of the experiment - corresponding to a zero force - and the ejection of the bead from the optical trap.

- **Comparison of microtubule and vimentin effective stiffness.**

Figure 6.1 represents the force-deflection curves of $N = 28$ vimentin bundles and of $N = 22$ microtubules on which I applied a mechanical stress. Because of the heterogeneous mechano-responses of the cytoskeletal bundles undergoing a deflection, the force-deflection curves exhibit different shapes: some are well fitted by a linear model or a power law model (see appendix C), others exhibit several regimes, that can also be fitted by linear models. For this type of curves, the slope of the linear fits is generally decreasing with the deflection (indicating a power law exponent slightly below 1, see appendix C). As these curves have been obtained in the same experimental conditions (cell line, laser power, stage displacement, type of cytoskeletal bundle tested), plotting an average force-deflection curve to compare it to another average curve obtained in a different condition could seem relevant. However, the number of points for each curve depends on the time of ejection of the bead from the optical trap: the sooner the bead was ejected, the lower the number of points. It is thus difficult to provide an average force-deflection curve without biasing it in favour of the softest bundles¹. Hence, it was necessary to find another way of extracting a mechanical parameter that would allow a

¹When the bead micro-environment is rather soft and deformable, the bead is not displaced far away from the center of the trap. In sharp contrast, when the bead micro-environment is very rigid, it is quickly displaced and eventually escapes from the optical trap.

comparison between different conditions. In order to do so, I have extracted the effective stiffness k that links the deflection δ to the force F exerted by the bead on the cytoskeletal bundle in the small forces/small deformations linear regime:

$$F = k\delta \quad (6.1)$$

Using this mechanical parameter, I can compare the properties of microtubules and vimentin bundles upon deflection *in cellulo*. The average effective stiffness of vimentin bundles ($N = 61$) is $342 \pm 30 \text{ pN } \mu\text{m}^{-1}$ while the average effective stiffness of microtubules ($N = 52$) is $195 \pm 21 \text{ pN } \mu\text{m}^{-1}$. The comparison of the means with a Student's t -test gives a p -value equal to $1,5 \times 10^{-4}$ (see figure 6.2).

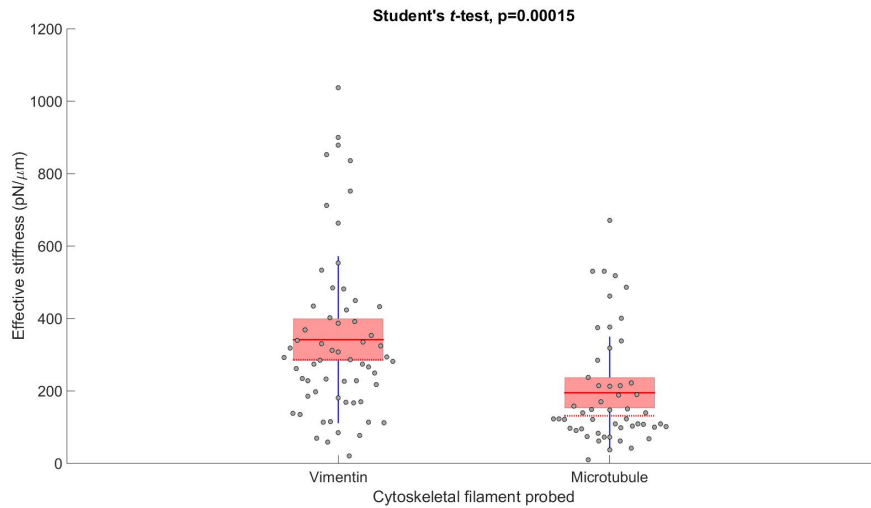


Figure 6.2: The effective stiffness of vimentin bundles is higher than that of microtubules. The average effective stiffness of $N = 61$ vimentin bundles is compared to that of $N = 52$ microtubules. One point corresponds to one cell in which a cytoskeletal fiber was mechanically probed. Points are laid over a 1.96 standard error mean (corresponding to 95% confidence interval, in pink) and the standard deviation is represented with a blue line. The solid red line represents the average value in each condition, whereas the median is highlighted as a dotted line.

- **From the effective stiffness to the flexural rigidity.**

In my optical tweezers-based intracellular microrheology experiments, microtubules are significantly softer than vimentin bundles at low forces. In order to compare the values I obtain to values found in the literature, it is necessary to know a geometric parameter and to make some more hypothesis. By looking at the images, we make the assumption that the probed cytoskeletal bundles can be compared to fixed-fixed beams. It is supposed to be exposed to point loading, and the bundle is deflected over a length L (the length between the

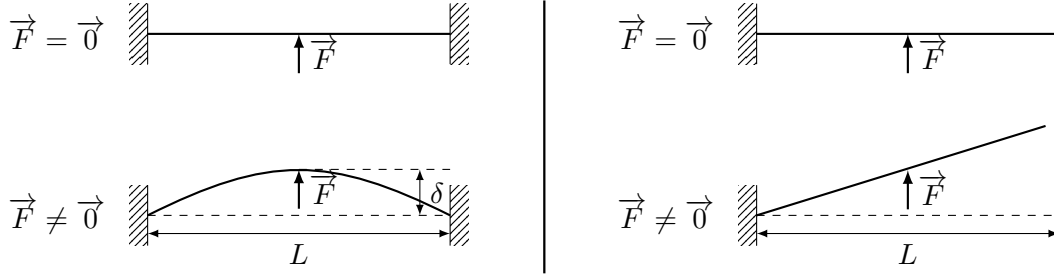


Figure 6.3: Cytoskeletal fibers are not deformed in the same way if they are fixed to one or to both ends.

Left: scheme of a fixed-fixed beam. Right: scheme of a cantilevered beam. These schemes define the mechanical parameters used in this section.

two fixed points, see figure 6.3) such as:

$$\delta = \frac{FL^3}{192\kappa} \quad (6.2)$$

This equation is valid in the linear elastic region, which corresponds to the domain of the curve fits, *i.e.* small forces and small deformations. Equation 6.1 gives:

$$\kappa = \frac{kL^3}{192} \quad (6.3)$$

The minimum value for the length L over which the bundle is deflected is the bead diameter : $L_{\min} = 2.0 \mu\text{m}$. The corresponding average flexural rigidity for vimentin bundles is $\kappa = 1.4 \times 10^{-23} \text{ N m}^2$. For microtubules, $\kappa = 8.1 \times 10^{-24} \text{ N m}^2$. This value is in the range of values that have been measured in several studies (from $\kappa = 10^{-25} \text{ N m}^2$ to $\kappa = 10^{-22} \text{ N m}^2$, see section 2.2.2). However, the key importance of the geometry of the cytoskeletal bundle (fixed-fixed vs. cantilevered, see figure 6.3) and of the length L makes it challenging to measure a precise value of flexural rigidity in each experiment. Hence, I have chosen to compare the average effective stiffness k between different conditions, rather than κ , in this PhD manuscript.

- **High-resolution imaging of microtubules and vimentin intermediate filaments.**

The significant difference in effective stiffness between microtubules and vimentin bundles suggests that microtubules and vimentin intermediate filaments, even if they are known to be in close proximity [Huber *et al.* 2015], do not always colocalize in the U373 cell line. By imaging $N = 21$ fixed cells (with endocytosed beads) with a spinning disk confocal microscope, I used line intensity profiles to determine if beads were systematically found next to a composite structure in which a microtubule and a vimentin bundle colocalized (see figure 6.4.A). The analysis from 29 beads shows that slightly less than half of the beads were found close to such a composite structure, others localized next to a single cytoskeletal element: either a microtubule (see figure

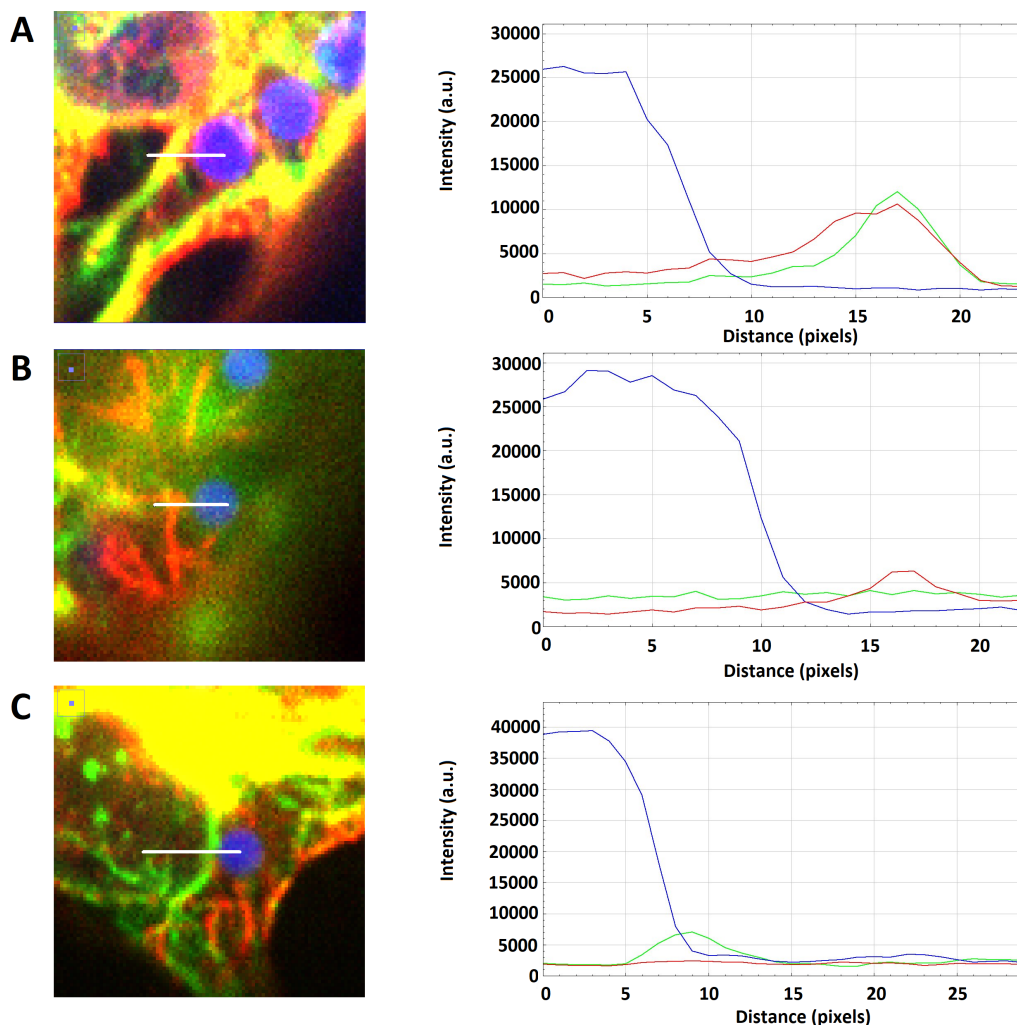


Figure 6.4: Beads can localize next to a single cytoskeletal subcomponent or next to a composite structure made of vimentin bundles and microtubules.

Left: spinning disk confocal microscopy images of a cell in which beads are colored in blue, vimentin in green and α -tubulin in red. The confocal slices shown correspond to the equatorial plane of the beads. The corresponding line profiles are plotted along the white line shown on the image, from right to left. Right: Line intensity profile of the corresponding image. The color code used matches the colors of the image. The peak in the red (respectively green) signal indicates that the selected bead is next to a microtubule (respectively a vimentin bundle). A: Bead next to a composite structure made of a microtubule and a vimentin bundle. B: Bead next to a microtubule. C: Bead next to a vimentin bundle.

6.4.B) or a vimentin bundle (see figure 6.4.C). Table 6.1 recapitulates how often these cases were found in the pool of fixed cells I analyzed. In section 6.2, the mechanical coupling within the cytoskeleton will be studied experimentally. In this context, it is important to mention at this stage that table 6.1 does not provide any information on the mechanical coupling. For instance, a

Bead micro-environment	Number of beads	Percentage
Microtubule alone	9	31%
Vimentin bundle alone	7	24%
Composite: microtubule & vimentin bundle	13	45%

Table 6.1: Nature of the bead micro-environment: quantification.

bead localized next to a vimentin bundle (without visible microtubule in the bead-microenvironment) can probe mechanical interactions further away, *e.g.* at crosslinking points of the cytoskeleton. Conversely, when a bead deflects a composite structure, microtubules and vimentin bundles can either exhibit an identical deflection as a function of time, or they can deform in a different way (see figure 6.5).

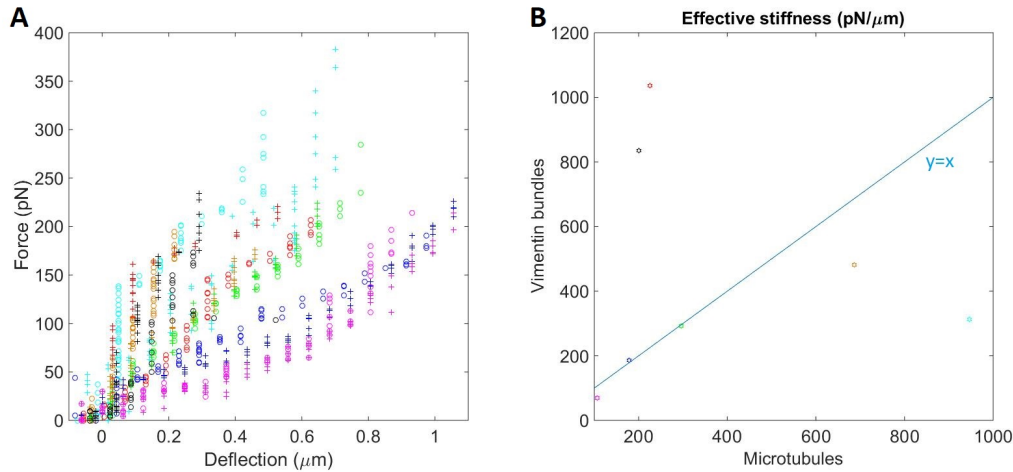


Figure 6.5: Simultaneous labelling of vimentin and microtubules shows that they can deform in a different way in composite structures.

A: Force-deflection curves of 7 composite structures in which vimentin bundles (crosses) and microtubules (circles) were labeled simultaneously. One colour correspond to one experiment. *B:* Effective stiffness of vimentin bundles as a function of effective stiffness of microtubules. The blue line represents the equality of effective stiffness values. The color code corresponds to that of panel A.

- **Discussion.**

The experiments I have performed show that microtubules are less rigid than vimentin intermediate filaments in the U373 cell line. This result needs to be discussed since, as reported in 2.1.1, microtubules are described as rigid biopolymers and vimentin intermediate filaments as flexible biopolymers. Vimentin bundles are stiffer than microtubules in my experiments, which seems to challenge this distinction. It is important to remember that my results have been obtained in a very specific configuration: cytoskeletal filaments are deformed perpendicular to their axis. Several studies report that microtubules

exhibit anisotropic stiffness *in vitro* (see 2.2.1). It is precisely in the configuration of my experiments that microtubules deform the most: microtubules have been compared to wood or bamboo, materials that associate a high longitudinal stiffness with a high lateral deformability [Hawkins *et al.* 2010]. This result also echoes to one of the first mechanical comparison of the cytoskeletal subcomponents *in vitro* [Janmey *et al.* 1991]. In this early work, microtubules deformed more than vimentin intermediate filaments for the same level of applied shear stress. Even if both the scale of the study (gels of cytoskeletal networks) and the type of applied stress (shear) differ from our experiments, it is worth mentioning that the comparison of stress/deformation curves can lead to results that apparently contradict mechanical parameters - such as the persistence length - and therefore strongly depend on the experimental procedure.

Finally, one can notice that the effective stiffness distributions of both microtubules and vimentin bundles are wide, reflecting an important variability in the mechanical measurements. Along with other biological parameters, this variability could relate to the variability of the localization of the bead in relation to the cytoskeletal subcomponents.

6.1.2 Sequential deflections make vimentin bundles more rigid

For all the measurements presented in the previous section, each bundle was probed only once: it is a single experiment on a given cytoskeletal element. As the literature reports a role of mechanical repeated stress on the mechanics of the cytoskeleton *in vitro* (see chapter 2), we have designed a protocol based on probing a given cytoskeletal bundle with the same bead several times. After a 1 min stage displacement, a resting time of 20 min was observed. This bead was trapped and the same displacement (same direction, same velocity) was applied to the stage. An additional cycle of 20 min-rest followed by a 1 min-displacement was also performed in some experiments.

- **Microtubule stiffness is not modified by repeated mechanical stress.**
The comparison between the first and the second deflection on the same microtubule does not highlight any clear trend on the evolution of the effective stiffness. Among the 17 deflected microtubules, 5 of them were softer during the second deflection while 12 were slightly stiffer (see figure 6.6.A). For 13 out of 17 probed microtubules, the effective stiffness ratio is between 0.5 and 2, which means that no dramatic change in effective stiffness is observed for the majority of experiments. By using a nonparametric paired statistical test, I show that the effective stiffness can not be considered to be different in the second experiment ($p > 0.05$, see figure 6.6.B).
- **Vimentin bundles systematically stiffen upon sequential deflections.**

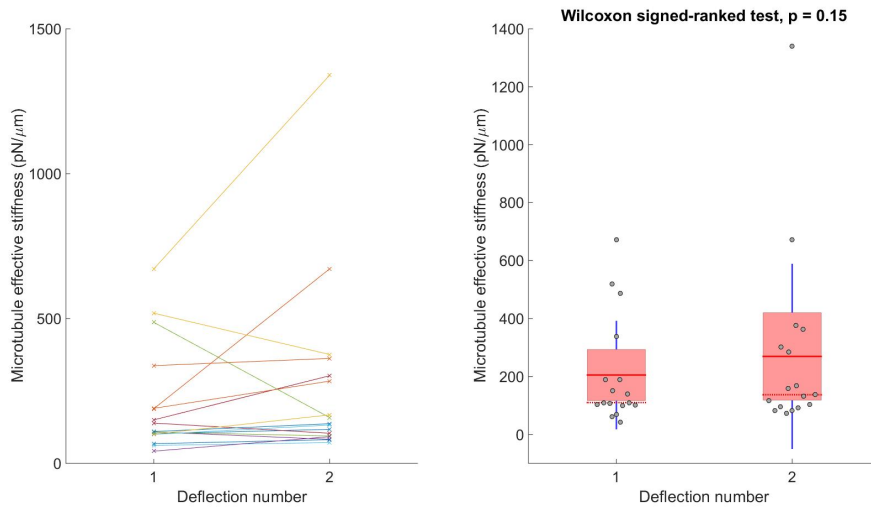


Figure 6.6: Microtubule effective stiffness does not change upon repeated mechanical stress. *A*: The effective stiffness of 17 microtubules is deduced from force-deflection curves. Lines link points that represent the same cell. Deflections number 1 and 2 are separated by a 20 min-long waiting time. *B*: Stiffness values are plotted as in figure 6.2. The effective stiffness is not statistically different between first and second experiments ($p = 0.15$).

– *Two successive deflections of vimentin bundles.*

In sharp contrast, vimentin intermediate filaments exhibit a clear stiffening upon sequential deflections. All tested vimentin bundles had an effective stiffness higher in the second experiment than in the first (see figure 6.7). The ratio of effective stiffness is between 1.32 and 15.82, with only 3 out of 13 probed vimentin bundles that show less than a 2-fold stiffening. Upon a sequence of two deflections, the average ratio of effective stiffness is 4.79. The effective stiffness of the second experiment is significantly higher than that of the first experiment. The same paired statistical test than for microtubules gives $p < 0.001$ (see figure 6.7). Interestingly, the initial pool of experiments contained 15 different cells but for two of them, the stiffening was so high that it was impossible to measure a deflection during the second experiment due to the resolution of the measurement of the deflection (see chapter 5). Here, I choose to remove these two points from the plots. Again, this situation has not occurred with microtubules, and the maximum effective stiffness I have measured ($k = 1340 \text{ pN } \mu\text{m}^{-1}$) for microtubules is much lower than the effective stiffness corresponding to the resolution limit ($k_{lim} \approx 5 \times 10^3 \text{ pN } \mu\text{m}^{-1}$, see chapter 5).

– *Three successive deflections of vimentin bundles.*

While microtubules do not stiffen upon a sequence of two deflections separated by 20 min, vimentin bundles show a clear increase in effective stiffness. We thus asked whether vimentin filaments could further stiffen

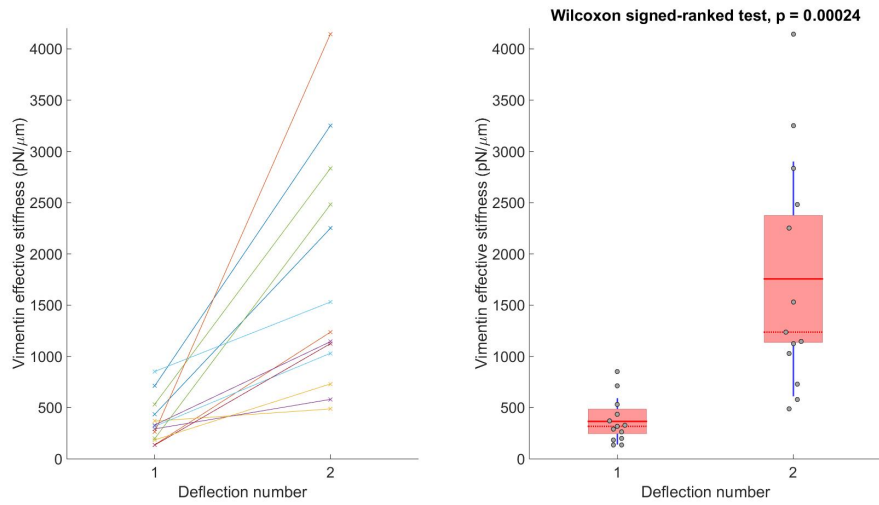


Figure 6.7: The effective stiffness of vimentin bundles increases upon repeated mechanical stress.

A: Effective stiffness of 13 vimentin bundles. The experimental procedure is identical to figure 6.6. B: Stiffness values are plotted as in figure 6.2. The effective stiffness is statistically different between first and second experiments ($p = 0.00024$).

upon an additional (third) deflection. Due to changes in cell morphology that can occur during imaging, performing more than two microrheology experiments on the same cytoskeletal subcomponent (and with the same bead) is challenging. Yet, I have been able to further investigate the mechanical behaviour of vimentin bundles under repeated mechanical stress in a distinct pool of experiments. Except for one vimentin bundle, the effective stiffness during the third experiment was higher than that during the second experiment, which was also higher than that of the first experiment (see figure 6.8.A). Between the first and the second experiment, 8 out of 13 vimentin bundles stiffen more than twice, with an average ratio of 2.49. In contrast, between the second and the third experiment, only one vimentin bundle exhibits more than a 2-fold stiffening. The average ratio of effective stiffness between the second and third experiment equals 1.35, suggesting that the stiffening effect saturates after the third deflection. A nonparametric statistical test for matched variables (Friedman test) was used to detect differences across multiple test attempts. It gives $p < 0.001$, supporting the fact that first, second and third experiments have significantly different effective stiffnesses (see figure 6.8.B).

Altogether, these results suggest that: 1) vimentin bundles keep on stiffening upon sequential deflections after the second experiment, 2) the most significant stiffening is observed between the first and the second deflection, and 3) some of the vimentin bundles probed in the experiments have reached a

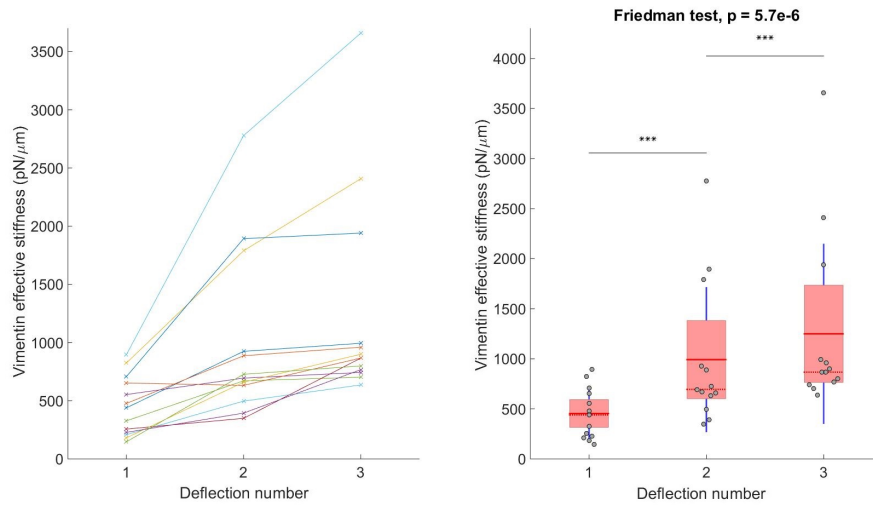


Figure 6.8: Increase in vimentin effective stiffness upon a sequence of three intracellular microrheology experiments.

A: Effective stiffness of 13 vimentin bundles. The experimental procedure is identical to previous figures. B: Stiffness values are plotted as in figure 6.2. The effective stiffness is statistically different between the three experiments. Post-hoc statistical tests are performed following a Conover's test with Benjamini-Hochberg's procedure: $p = 9.2 \times 10^{-8}$ between first and second deflections and $p = 1.7 \times 10^{-9}$ between the second and third deflections.

plateau in effective stiffness when they are deflected for the third time in a row, while others keep on stiffening.

- **Discussion.**

In vitro, microtubules have been shown to soften under repeated mechanical stress [Schaedel *et al.* 2015]. Similarly, cyclic loading decreases the stiffness of individual vimentin intermediate filaments [Forsting *et al.* 2019]. Here, I have shown that sequential deflections do not change microtubule effective stiffness while they make vimentin bundles stiffer. These experiments in living cells thus give different (if not opposite!) results to that obtained with experiments carried out *in vitro*. However, some crucial experimental differences need to be further discussed before any comparison with the literature.

First, the timing of the experiments is known to influence their outcome. *In vitro*, Schaedel *et al.* showed that a 100 s rest period was sufficient for microtubules to mechanically recover and therefore regain their initial persistence length (these results are presented in more details in 2.2.3). Only a rest period of lower order of magnitude (typically 10 s) allows to observe microtubule softening upon bending cycles [Schaedel *et al.* 2015]. This is probably due to the rapid turnover of microtubules. In our experiments for which the waiting time between two mechanical stimulations was higher than 1000 s, it is consistent not to observe any change in effective stiffness between the first and the second deflection. However, the slight changes in effective stiffness

that I measure could originate from microtubule turnover occurring during this rest period that could affect the probed microtubule *per se*, its (physical) links with the other cytoskeletal filaments or the surrounding cell environment. However, as far as vimentin is concerned, Forsting *et al.* showed that individual vimentin filaments soften during cyclic loading, regardless of the rest period (0 min to 60 min) [Forsting *et al.* 2019]. Intermediate filaments are known to be very stable structures with a long turnover (typically 1 h). It is likely that softening of vimentin filaments is observed because, unlike microtubules, the waiting time is not greater than the turnover. Consistently, in the experiments I have performed, the waiting time (20 min) is smaller than the physical turnover time. We can thus consider that the vimentin bundles probably experienced very little structural changes between the end of one intracellular microrheology experiment and the beginning of the next one. While it is not surprising that we measure a systematic trend in the evolution of effective stiffness upon sequential deflections, the fact that (individual) vimentin filaments soften during cyclic loading *in vitro* is much more intriguing. Another important aspect that has to be taken into account in our experiments in living cells is that we do not probe the mechanics of individual vimentin filaments. Intermediate filament associated proteins crosslink vimentin filaments to form bundles. We can hypothesize that the interactions within the bundle - *e.g.* lateral interactions between the individual vimentin filaments - can impact on vimentin bundle mechanics, which may explain why intermediate filament bundles stiffen in cells in my experiments, while individual intermediate filaments soften *in vitro*. Also, the studies that reported vimentin softening during cyclic loading were based on elongating filaments [Forsting *et al.* 2019], whereas intermediate filament bundles are bent perpendicular to their long axis in our experiments. The stiffening of vimentin filaments upon sequential deflections I observe might originate from these differences, and/or from vimentin bundles being connected to the rest of the cytoskeleton, other organelles, membranes, *etc.* in living cells.

6.2 Mechanical coupling between microtubules and vimentin intermediate filaments

I have next focused on how the vimentin and microtubule networks interact mechanically. Several recent studies addressed the question of the interactions between cytoskeletal elements in cells (see chapter 3). In this section, the aim is to quantify the impact of the vimentin network on microtubule mechanics by using vimentin-KO U373 cells. Conversely, the use of drugs targeting microtubules allows to characterize their influence on the mechanical properties of vimentin intermediate filament bundles, and especially their stiffening upon sequential deflections.

6.2.1 The vimentin network does not play a key role in the mechanical properties of microtubules

To achieve a better understanding of the results on microtubule mechanics, the contribution of the intermediate filaments was investigated. In collaboration with the team of Sandrine ETIENNE-MANNEVILLE, I have used U373 cells that were knocked-out for vimentin using CRISPR-Cas9. The goal was to: 1) compare the effective stiffness of deflected microtubules in vimentin-KO cells and in control cells, and 2) compare the effect of sequential deflections on microtubules in these two conditions.

- **Biological features of the probed cells.**

Western blot analysis performed by our collaborators shows that vimentin-KO cells not only show absence of vimentin filaments but also a strong decrease in GFAP, nestin and synemin levels (see figure 6.9) which leads to a complete disruption of the intermediate filament network. As far as vimentin is concerned, I have confirmed these results by performing immunostaining of both control and vimentin-KO cells (see figure 6.10).

- **Microtubule mechanics is not significantly affected by the loss of vimentin.**

To characterize the role of the vimentin network in microtubule mechanics, the experiments described in the previous section have been performed in vimentin-KO cells. I have shown that the absence of vimentin does not modify the effective stiffness of microtubules. The average value is $k = 168 \pm 26 \text{ pN } \mu\text{m}^{-1}$, whereas $k = 205 \pm 46 \text{ pN } \mu\text{m}^{-1}$ for control cells. The Mann-Whitney U test, a nonparametric statistical test, was used to evaluate the probability of the distribution of the effective stiffness being equal in the two cell lines and gives $p > 0.05$ (see figure 6.11). The effect of vimentin on the mechanics of microtubules undergoing sequential deflections has also been characterized. Among 13 deflected microtubules in cells where vimentin was knocked-out, 6 have a higher effective stiffness during the second experiment and 7 have a lower one. Like in control cells, a paired statistical test shows that the distributions of effective stiffness are equal ($p > 0.05$) in vimentin-KO cells (see figure 6.11).

- **Discussion.**

Our results suggest that the vimentin network does not significantly affect microtubule mechanics in living cells. However, when looking closely at the distribution of effective stiffness, it is worth mentioning that the effective stiffness in vimentin-KO cells has a lower standard deviation than in control cells, due to the absence of outliers (note that control cells have 3 outliers out of 17 cells). The mean value is closer to the median (see figure 6.11). This more narrowly spread distribution in the absence of vimentin intermediate filaments might indicate that high values of microtubule effective stiffness (in

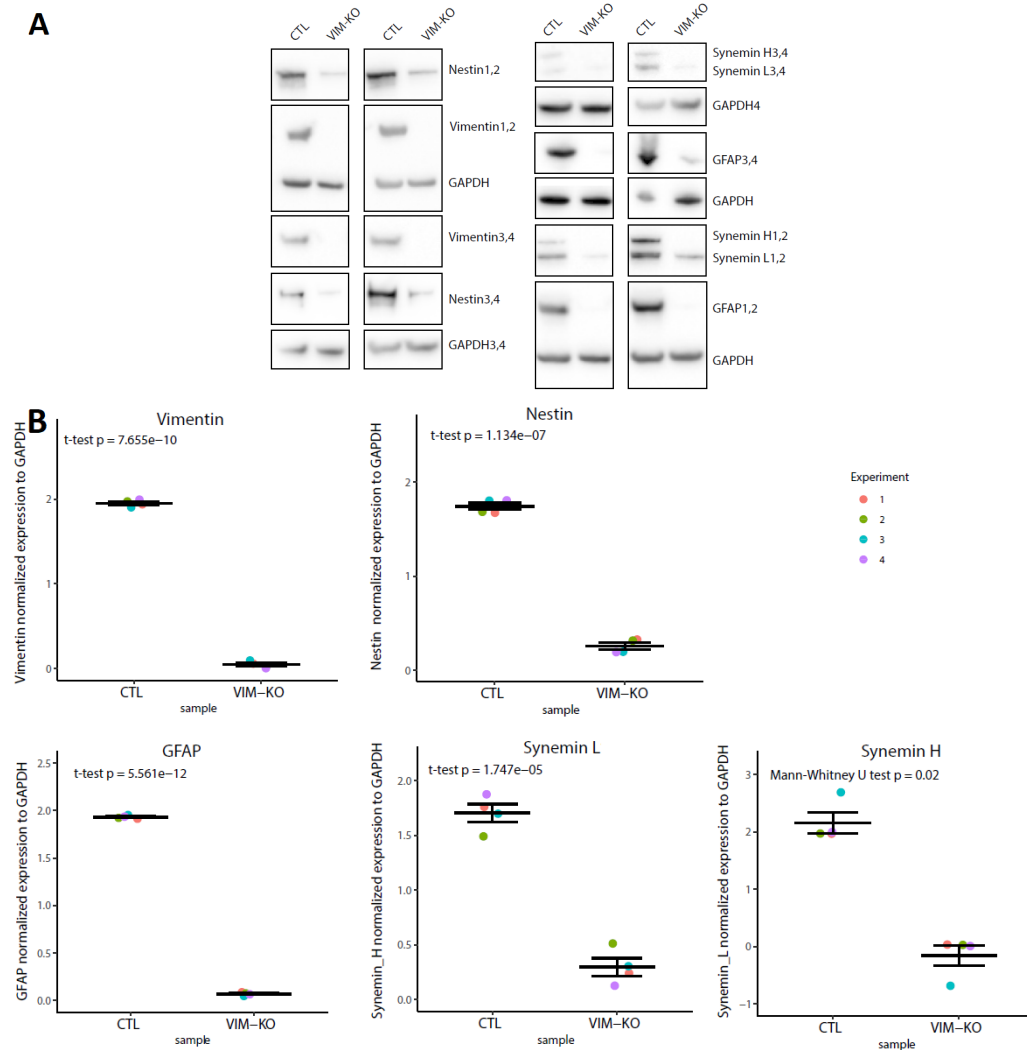


Figure 6.9: The expression of intermediate filament proteins is greatly reduced in vimentin-KO cells.

A: Western blots of vimentin, nestin, GFAP and synemin in vimentin-KO cells from 4 independent experiments (labeled 1 to 4). B: Quantifications of the intensity of corresponding intermediate filament proteins normalized by that of Glyceraldehyde-3-phosphate dehydrogenase (GAPDH). The quantifications were made from 4 independent experiments. For each intermediate filament protein, the decrease is statistically significant ($p < 0.05$). Courtesy of Emma VAN BODEGRAVEN.

control cells) correspond to the few probed microtubules which are strongly mechanically coupled to the surrounding vimentin network, which increases microtubule stiffness.

The fact that the behaviour of microtubules upon sequential deflections is unchanged is more expected. Whether vimentin is present or not, the data is similar to what has been previously measured *in vitro* [Schaedel *et al.* 2015].

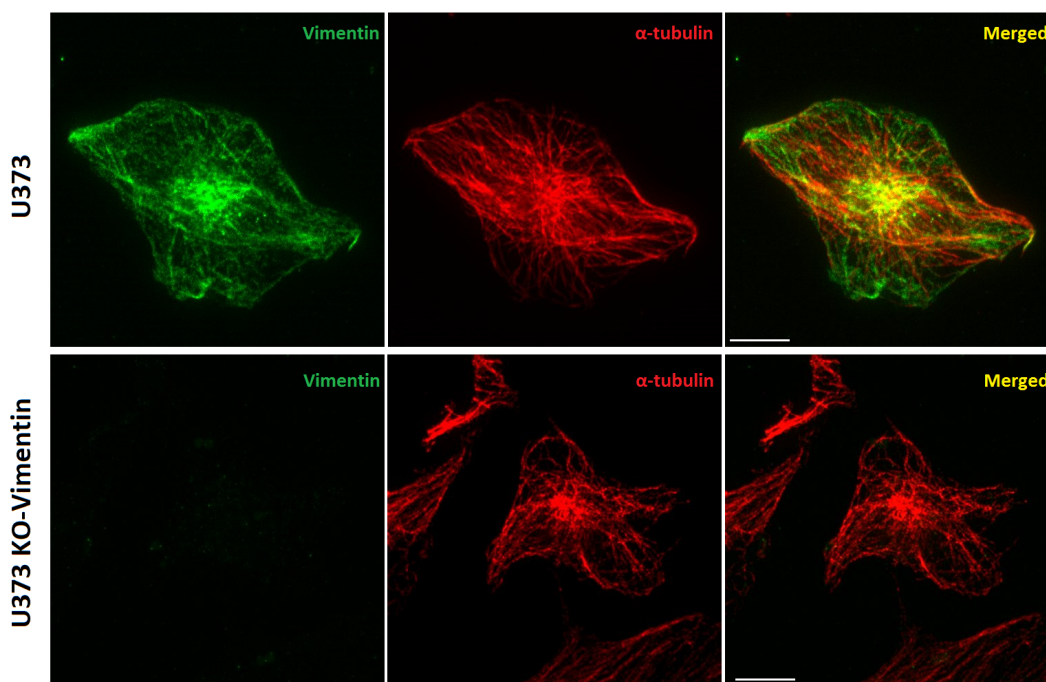


Figure 6.10: Immunofluorescence images of control and vimentin-KO U373 cells. *Spinning disk confocal microscopy images of vimentin (green) and α -tubulin (red) immunostaining of U373 cells. Top: Control cells. Bottom: Vimentin-KO cells. Scale bars: 10 μ m*

6.2.2 Modifying microtubule stability affects vimentin mechanical behaviour

After studying the impact of the vimentin network on microtubule mechanics *in cellulo*, I have investigated how, conversely, microtubules may be involved in the mechanical properties of vimentin bundles. Our approach relies on modulating the dynamic instability of microtubules to quantify whether this affects the effective stiffness of vimentin bundles. As vimentin stiffening upon sequential deflections has not been observed previously, especially *in vitro*, we also aim at identifying a potential role of microtubules in this process.

- **Performing measurements on vimentin while targeting microtubules.**

Due to the interactions between the vimentin and microtubule networks, inducing dramatic perturbations of the microtubule network, for instance by using high doses of nocodazole to depolymerize microtubules, is not an appropriate strategy. Indeed, without an extended microtubule network, the vimentin network is known to collapse into the perinuclear region (see section 3.2.1). In such a collapsed network, measuring force/deflection curves is not relevant as vimentin does not form long elongated bundles of filaments, but rather a very dense, thick and continuous layer around the nucleus. Instead, I used low doses of nocodazole to affect microtubule dynamics and partially depolymerize the microtubule network. This part of the work has been carried

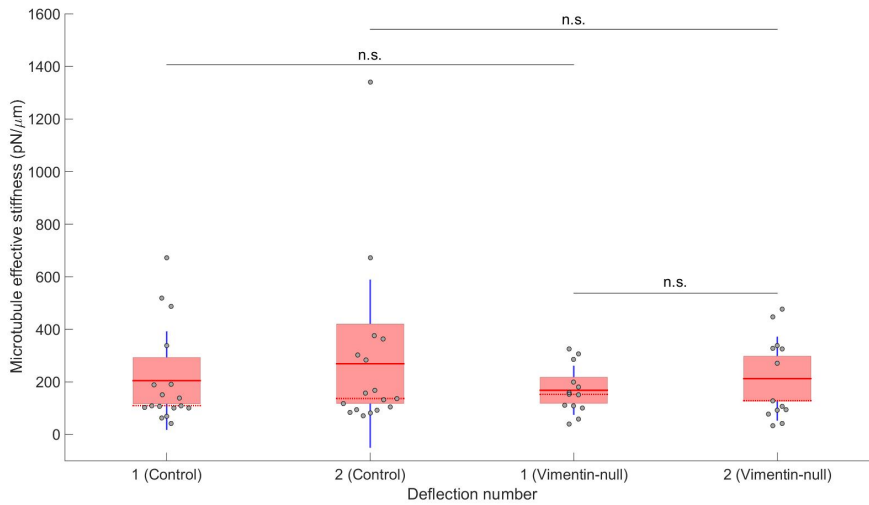


Figure 6.11: Knock-out of vimentin has no effect on microtubule mechanics.

The effective stiffness of microtubules was measured in 13 vimentin-KO cells and 17 control cells. The difference is non-significant (Mann-Whitney U test, $p = 0.74$). A sequence of two deflections was applied on microtubules in control cells ($N = 17$) and vimentin-KO cells ($N = 13$). The comparison of the distributions of the second deflection gives a non-significant difference (Mann-Whitney U test, $p = 0.71$). As for control cells, the distributions of first and second deflections in vimentin-KO cells are not statistically different (Wilcoxon signed-rank test, $p = 0.64$).

out with the help of Tanguy CHOCAT, a former Master student in the lab. Figure 6.12 shows that treatment with $0.5 \mu\text{M}$ nocodazole induces a partial depolymerization of the microtubule network, without the collapse of the vimentin network around the nucleus. Cells were also treated with $10 \mu\text{M}$ taxol to study the impact of a stabilized microtubule network on vimentin bundle mechanics (see figure 6.12).

- **Microtubule-targeting drugs do not dramatically change vimentin stiffness.**

To measure the effect of microtubule-targeting drugs on the effective stiffness of vimentin bundles, I incubated drugs for 20 min before intracellular microrheology experiments. In cells treated with $0.5 \mu\text{M}$ nocodazole, deflected vimentin bundles have a similar effective stiffness distribution compared to that in control cells treated with DMSO ($p > 0.05$, see figure 6.13). Partial depolymerization of microtubules using $0.5 \mu\text{M}$ nocodazole does not lead to any significant change in vimentin bundle effective stiffness. Regarding cells in which microtubules have been stabilized with $10 \mu\text{M}$ taxol, a weak increase of the effective stiffness of vimentin bundles is measured: $k = 494 \pm 76 \text{ pN } \mu\text{m}^{-1}$, compared to $k = 353 \pm 33 \text{ pN } \mu\text{m}^{-1}$ (see figure 6.13). The p -value is just over the limit of significance ($p = 0.061$). Overall, both treatments do not induce

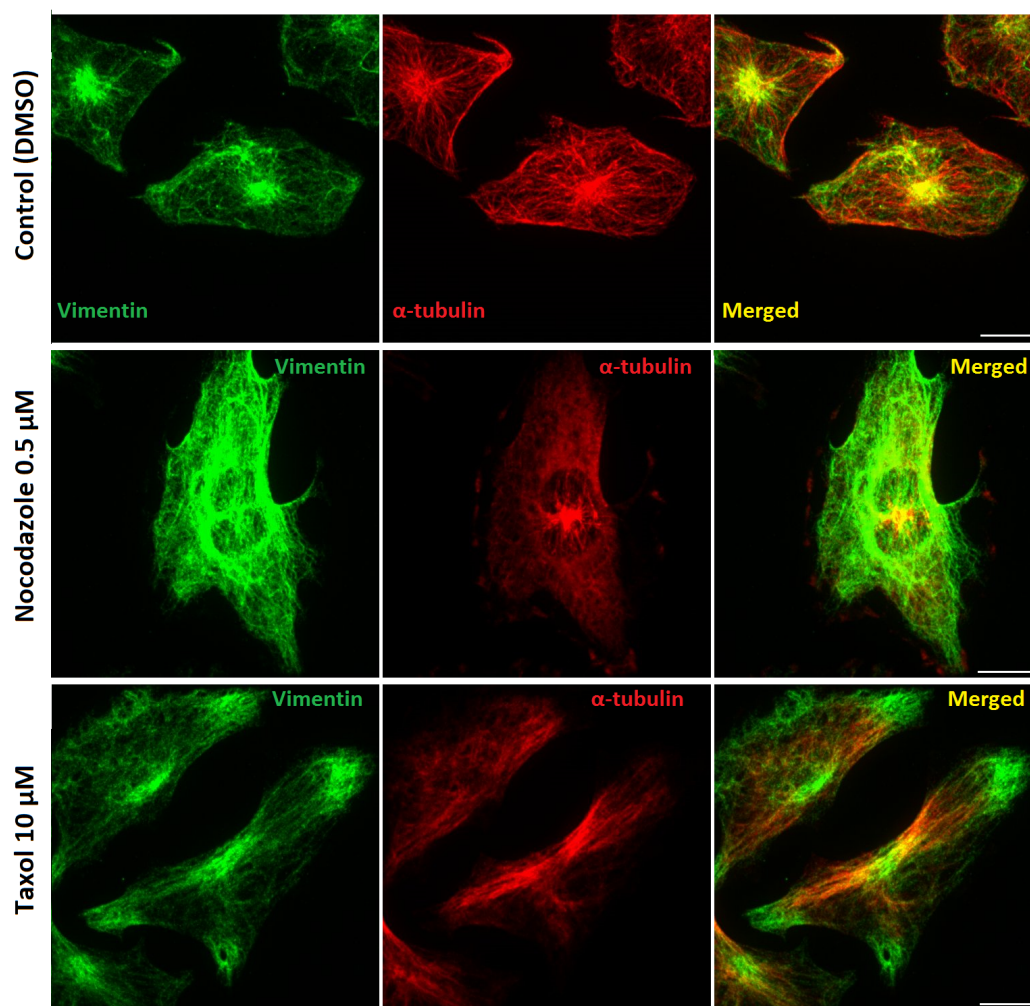


Figure 6.12: Immunofluorescence images of U373 cells treated with microtubule-targeting drugs. *Spinning disk confocal microscopy images of vimentin (green) and α -tubulin (red) immunostaining of U373 cells. Top row: Control cells treated with solvent (Dimethyl Sulfoxide (DMSO)). Middle row: Cells treated with 0.5 μ M nocodazole. Bottom row: Cells treated with 10 μ M taxol. Scale bars: 10 μ m*

major changes in the mechanical outcome of single deflections of vimentin bundles.

- **Partial depolymerization of microtubules greatly reduces vimentin bundle stiffening upon sequential deflections.**

In order to decipher the contribution of microtubules to the process of vimentin bundle stiffening upon sequential deflections, I have chosen to perform sequences of two deflections on vimentin bundles. Indeed, the sequences of three deflections performed in section 6.1.2 do not provide more information on the mechanical behaviour of vimentin bundles. I have followed the following protocol: immediately after the first deflection, a microtubule-targeting

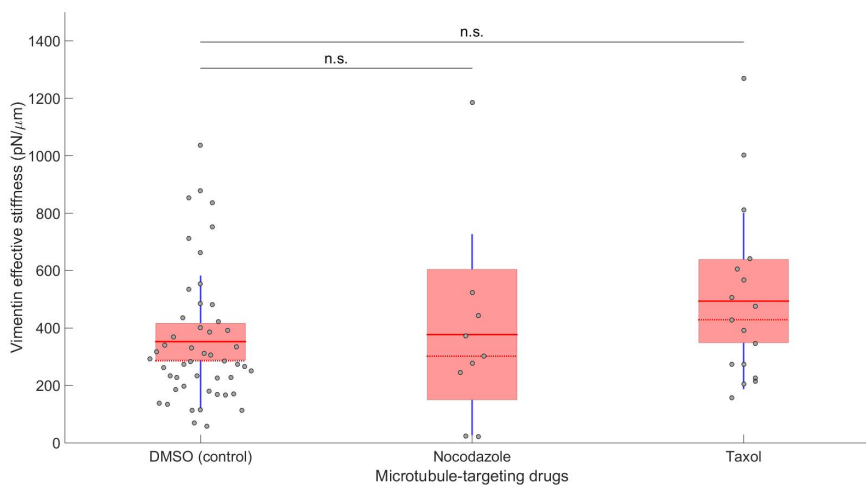


Figure 6.13: Microtubule-stabilizing drugs have no major effects on vimentin bundle effective stiffness.

The effective stiffness of vimentin bundles is measured in 9 cells treated with $0.5 \mu\text{M}$ nocodazole, 17 cells treated with $10 \mu\text{M}$ taxol and 49 control cells treated with **DMSO**. The difference between cells treated with nocodazole and control cells is non significant (Mann-Whitney U test, $p = 0.86$). The difference between cells treated with taxol and control cells is non significant but only slightly above the limit of significance (Mann-Whitney U test, $p = 0.061$).

drug ($0.5 \mu\text{M}$ nocodazole or $10 \mu\text{M}$ taxol) was added in the culture dish. The second deflection was performed 20 min after the first one. I have chosen this protocol rather than incubating cells with drugs before the first experiment in order to avoid any change in the effective stiffness of the first deflected vimentin bundles. I have checked that the distributions of stiffness values during the first deflection (*i.e.* before treatment with either **DMSO** as a control, nocodazole or taxol) are similar in the three conditions ($p > 0.05$ in both cases, see figure 6.14).

Taxol-treated cells are mechanically very similar to control cells (see figure 6.14). Like in control cells, each vimentin bundle has an effective stiffness which is higher during the second deflection. The effective stiffness distribution during the second deflection is significantly higher in taxol-treated cells compared to that during the first deflection ($p < 0.001$, like for control cells). The effective stiffness during the second deflection for taxol-treated cells is not significantly different to that of control cells ($p > 0.05$), suggesting that stabilizing microtubules does not affect the ability of vimentin bundles to stiffen upon a sequence of two deflections.

In contrast, the vimentin network of nocodazole-treated cells exhibits an interesting mechanical behaviour. The effective stiffness during the second deflection is significantly different from that of control cells ($p < 0.01$): $k = 670 \pm 135 \text{ pN } \mu\text{m}^{-1}$ versus $k = 1570 \pm 350 \text{ pN } \mu\text{m}^{-1}$ in control cells. In

nocodazole-treated cells, vimentin bundles still stiffen upon sequential deflections, but much less than in control cells (see figure 6.14). Partially depolymerizing microtubules thus prevents a strong increase of the effective stiffness during the second microrheology experiment on the same probed vimentin bundle, suggesting that microtubules are involved in vimentin stiffening upon repeated stress in living cells.

- **Discussion.**

While perturbing microtubule dynamics does not change the stiffness of vimentin bundles undergoing a single deflection, we show here that the increase in the effective stiffness of vimentin bundles upon sequential deflections originates from its mechanical coupling with another cytoskeleton: the microtubule network. This finding could explain why this effect has not been observed *in vitro*. This result raises the question of the mechanism that allows such a strengthening in presence of a non-disrupted microtubule network (and that, conversely, is impaired in its absence). One hypothesis could be that deflecting microtubules leads to a reinforcement of the vimentin bundle due to vimentin recruitment during the 20 min waiting time between the first and the second deflection. Microtubules could be required in this recruitment by transporting vimentin particles and squiggles, as described in chapter 3. Alternatively, vimentin bundles could experience structural changes during the first deflection and microtubules could play a role in their structural and mechanical recovery.

Besides, the off-target effects of the drugs I have used add to the difficulty of interpreting the results. As nocodazole is known to lead to increased contractility of the actin cytoskeleton, it is also possible that the reduced vimentin bundle stiffening results from a coupling between actin and vimentin. However, the beads used to deflect vimentin bundles are located into the perinuclear region and vimentin deformations are local (and far from the actin cortex). It thus seems rather unlikely that the actin network plays such a dramatic role in vimentin bundle stiffening. Also, the usual concentrations (and incubation time) at which nocodazole induces a strong increase in actin contractility are higher than in our experiments (typically 10 μM for 1 h to induce a complete depolymerization of the microtubule network).

To confirm that microtubules are involved in the mechanics of vimentin bundles undergoing repeated mechanical stress, we have examined the effect of a PTM on tubulin: acetylation.

6.3 Study of a post-translational modification: acetylation

Since destabilizing the microtubule network seems to impact our mechanical measurements, I have asked whether acetylation could impact intracellular mechanics.

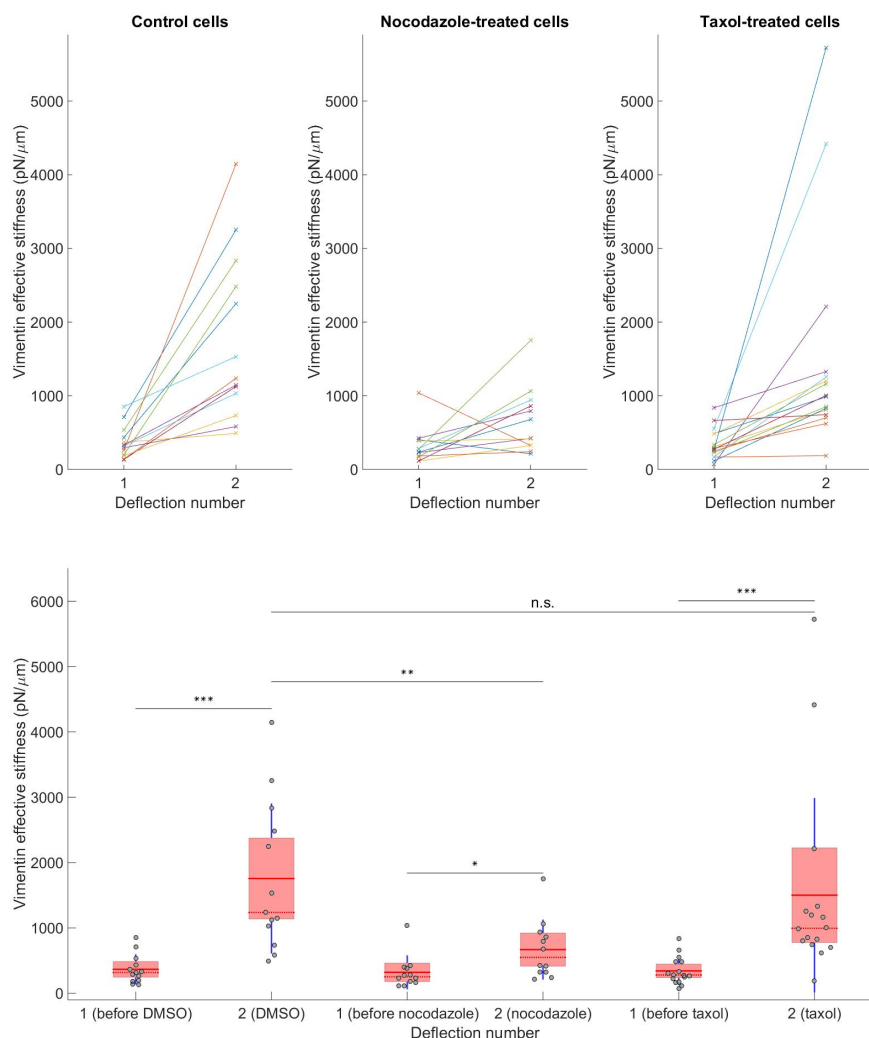


Figure 6.14: Destabilizing microtubules reduces vimentin bundle stiffening upon sequential deflections.

Top: Effective stiffness of 13 control cells, 12 cells treated with nocodazole and 16 cells treated with taxol between the first and the second deflections. Lines join effective stiffness values taken from the same vimentin bundle. Bottom: Distribution of effective stiffness values in each condition. The difference between the first and the second deflections is significant (Wilcoxon signed-rank test) for control cells ($p = 2.4 \times 10^{-4}$), nocodazole-treated cells ($p = 0.034$) and taxol-treated cells ($p = 3.1 \times 10^{-5}$). Statistical tests comparing the second deflection with control: $p = 0.0058$ for nocodazole (t-test with Welch's correction) and $p = 0.35$ for taxol (Mann-Whitney U test).

By using tubacin, I have induced increased acetylation of microtubules and measured the effective stiffness of both types of microtubules and vimentin intermediate filaments. The effect of acetylation on vimentin bundle stiffening upon sequential deflections was also measured and is discussed in this section.

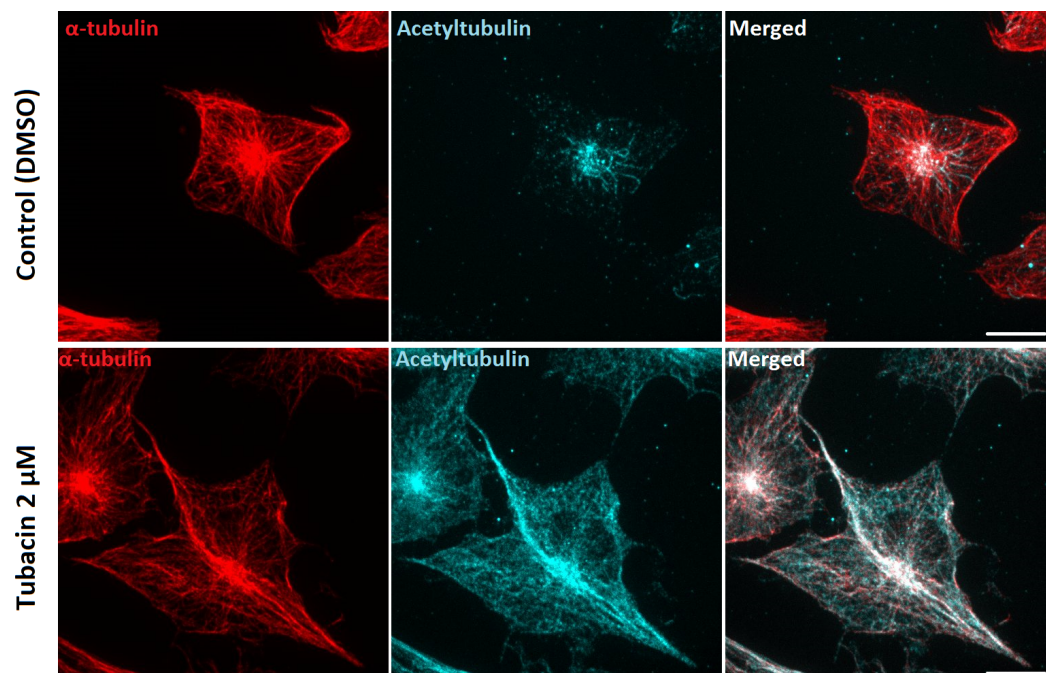


Figure 6.15: Immunofluorescence images of U373 cells treated with tubacin. *Spinning disk confocal microscopy images of α -tubulin (red) and acetyl-tubulin (cyan) immunostaining of U373 cells. Top: control cells treated with solvent (DMSO). Bottom: cells treated with 2 μ M tubacin for 4 h. Scale bars: 10 μ m.*

6.3.1 Acetylation leads to microtubule softening

- **The U373 cell line exhibits poorly acetylated microtubules.**

To modify the average K40 acetylation of microtubules, two options are available: either a downregulation of acetylation is performed (*e.g.* by silencing the gene coding for the acetyltransferase *ATAT1*), or acetylation can be up-regulated. Selecting the appropriate strategy depends on the basal acetylation level of the cell line in which experiments are carried out. U373 cells are known to have a low level of acetylation (Sandrine ETIENNE-MANNEVILLE personal communication). Accordingly, we chose to increase microtubule K40 acetylation using tubacin, a drug which inhibits the action of *HDAC6*, a deacetylase. Immunofluorescence experiments to confirm the increase in acetylation in tubacin-treated cells compared to control cells are shown in figure 6.15. In control cells, acetylated tubulin localizes mostly in the vicinity of the nucleus, either forming elongated structures - suggesting that corresponding microtubules are acetylated along their length -, or appearing as dots. In sharp contrast, tubacin-treated cells exhibit a microtubule network which is fully acetylated (see figure 6.15). In our experiments, microtubules are labeled with SiR-tubulin, a probe based on the microtubule binding drug docetaxel, an analogue to taxol. As microtubule acetylation and microtubule stabilization are linked [Janke & Montagnac 2017], it was also important to ensure that

SiR-tubulin did not induce a high increase of microtubule K40 acetylation, so that the action of tubacin became insignificant. To measure the effect of SiR-tubulin and tubacin, I performed immunofluorescence experiments in 4 conditions: control cells (treated with DMSO), cells treated with tubacin and DMSO, cells treated with SiR-tubulin and DMSO, cells treated with SiR-tubulin and tubacin. Figure 6.16 shows that SiR-tubulin induces a smaller increase in the K40 acetylation level as compared to tubacin, thus validating our experimental procedure.

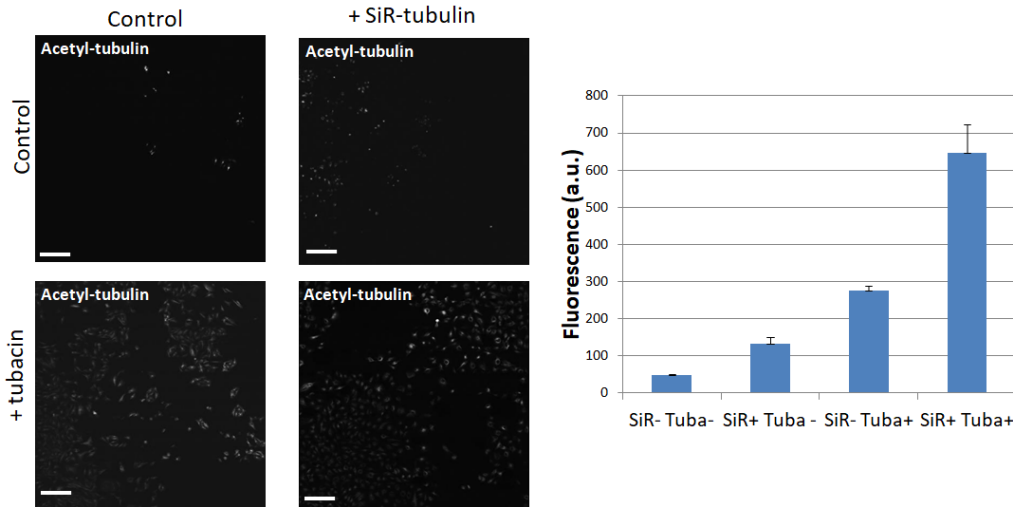


Figure 6.16: SiR-tubulin has a much weaker effect than tubacin on K40 acetylation. *Confocal microscopy images of acetyl-tubulin (white) immunostaining of U373 cells. Left: images were stitched in 4 conditions (with or without tubacin, with or without SiR-tubulin). Scale bars: 200 μm . Right: quantification of the average fluorescence per cell (SiR- Tuba-: control cells treated with DMSO, SiR+ Tuba-: cells treated with SiR-tubulin and DMSO, SiR- Tuba+: cells treated with tubacin and DMSO, SiR+ Tuba+: cells treated with tubacin and SiR-tubulin).*

- **Acetylation affects microtubule effective stiffness.**

After incubating U373 cells with tubacin for 4 h, I have performed intracellular microrheology experiments and compared the effective stiffness of microtubules in tubacin-treated cells and in control cells. The 27 deflected microtubules in tubacin-treated cells are significantly softer than the 31 deflected microtubules in cells treated with vehicle (DMSO) ($p < 0.05$, see figure 6.17.A). As tubacin is a chemical inhibitor of HDAC6, this result suggests that increased microtubule acetylation softens microtubules in living cells.

- **Discussion.**

Acetylated microtubules have been previously described to be softer than non-acetylated microtubules *in vitro* [Xu *et al.* 2017]. In this paper, Xu *et al.* measured the persistence length of microtubules made of enzymatically

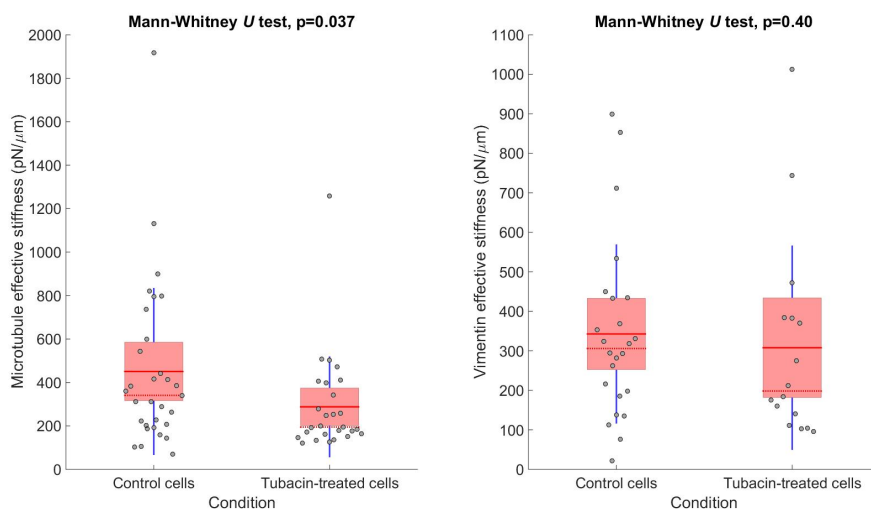


Figure 6.17: **K40** acetylation reduces microtubule effective stiffness but does not affect that of vimentin bundles.

A: The effective stiffness distribution of 27 microtubules of cells treated with tubacin is compared to that of 31 microtubules of cells treated with vehicle (DMSO). B: The effective stiffness distribution of 16 vimentin bundles of cells treated with tubacin is compared to that of 24 vimentin bundles of cells treated with vehicle (DMSO).

acetylated and deacetylated tubulin (see 2.2.3 for more details). With the microfluidic setup the authors used, microtubules were subjected to forces perpendicular to their axis, as in my experiments. Unlike other results in the literature, this *in vitro* experiment can be directly compared to our *in cellulo* experiments. In both cases, **K40** acetylation leads to decreasing the rigidity of microtubules. However, while a striking difference in persistence length was measured in this study ($p < 0.001$), with at least a 2-fold reduction [Xu *et al.* 2017], I only measure a 35% decrease in the average effective stiffness (see figure 6.17.A). Admittedly, the measured mechanical parameter is not the same, but the effective stiffness k is proportional to the persistence length l_p . Along with the possible contribution from the surrounding organelles and cytoskeleton, the difference probably comes from the fact that we probe microtubules into the perinuclear region. Indeed, in control cells, microtubules close to the nucleus are already (partially) acetylated. Tubacin-treatment increases this acetylation, but the most dramatic effect does not occur close to the nucleus. However, even without knowing the precise level of **K40** acetylation for each microtubule we measured, the number of deflections allows to statistically detect a difference which minors that observed *in vitro* and which would potentially be much more significant further away from the nucleus.

6.3.2 Acetylated microtubules impact vimentin bundle mechanics

- **In tubacin-treated cells, vimentin stiffening is reduced.**

After performing the same treatment with tubacin to increase microtubule acetylation, I have measured the effective stiffness of vimentin bundles in order to get more insight into the mechanical coupling between vimentin intermediate filaments and microtubules in living cells. I have compared the effective stiffness of 16 vimentin bundles in tubacin-treated cells with that of 24 vimentin bundles in control cells. The average stiffness of vimentin bundles in tubacin-treated cells was $k = 308 \pm 66 \text{ pN } \mu\text{m}^{-1}$ while that of control cells was $k = 343 \pm 47 \text{ pN } \mu\text{m}^{-1}$. The difference between the two distributions is not significant ($p > 0.05$, see figure 6.17.B), showing that increased microtubule acetylation does not change the effective stiffness of vimentin bundles. As for microtubule stability, the effect of microtubule acetylation on vimentin bundle stiffening upon sequential deflections was tested *in cellulo*. However, due to the incubation time of tubacin², the protocol has been slightly adapted: tubacin was not added just after the first deflection like nocodazole or taxol, but 4 h prior to it. Over 16 deflected vimentin bundles in tubacin-treated cells, 4 of them softened and 12 stiffened. In this condition, I have tested the difference between the first and the second effective stiffness using a paired statistical test and the p -value is just below the significance level ($p = 0.040$, see figure 6.18). Consistently, while there is no significant difference in the effective stiffness of the first deflection, there is a significant difference ($p < 0.001$) when I compare the effective stiffness of the second experiment in tubacin-treated cells ($k = 515 \pm 105 \text{ pN } \mu\text{m}^{-1}$) and in control cells ($k = 1167 \pm 222 \text{ pN } \mu\text{m}^{-1}$). We conclude that an increase K40 acetylation level induces a decrease in vimentin bundle stiffening upon sequential deflections.

- **Discussion.**

Similarly to a partial depolymeration of the microtubule network by low doses of nocodazole (see figure 6.14), an increase in microtubule K40 acetylation impairs the ability of vimentin bundles to stiffen when they are subjected to repeated bending assays. This finding provides further indication that microtubules and vimentin intermediate filaments are mechanically coupled in living cells. However, the fact that increased microtubule acetylation has a similar effect as microtubule depolymerization challenges the interpretation of the experiments. Indeed, acetylation is often correlated with stable and long-lived microtubules. Microtubules in tubacin-treated cells being significantly softer, they potentially do not provide enough strength for the vimentin network to stiffen as much as in control cells. This hypothesis must be tempered by the fact that vimentin bundles have similar effective stiffnesses in both conditions, so that the softer microtubules of tubacin-treated cells do

²An incubation time of 20 min would not be sufficient to see any increased acetylation between the first and the second deflection.

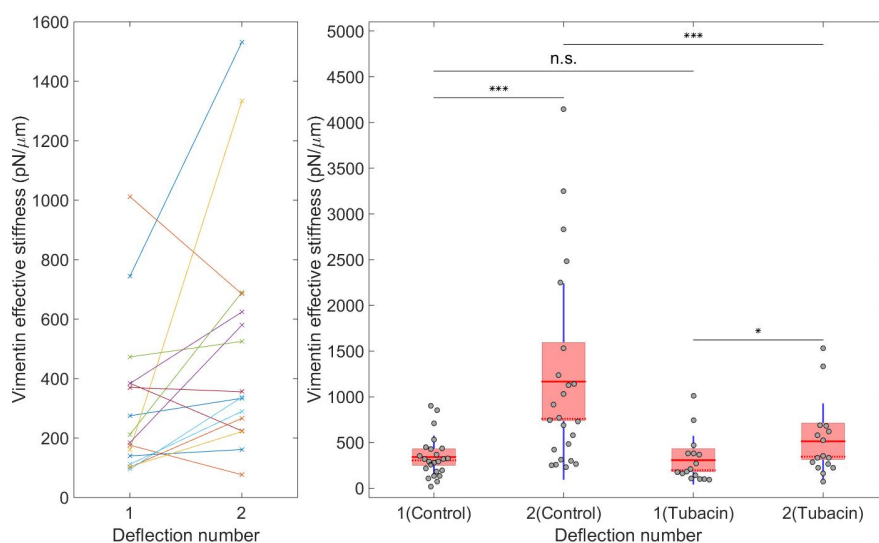


Figure 6.18: Microtubule acetylation reduces the stiffening of vimentin bundles upon sequential deflections.

A: Effective stiffness of 16 vimentin bundles. Lines joint paired points (from the same bundle). B: Effective stiffness of vimentin bundles undergoing sequential deflections in tubacin-treated cells and control cells (treated with DMSO). Control cells: distributions are significantly different: $p = 6.7 \times 10^{-6}$ (paired Student's t-test). Tubacin-treated cells: distributions are significantly different: $p = 0.040$ (Wilcoxon signed-rank test). There is no significant difference between the distributions of the first deflections in each condition: $p = 0.40$ (Mann-Whitney U test). The distributions of the second deflections are significantly different: $p = 0.00025$ (Mann-Whitney U test).

not seem to directly impact vimentin bundle stiffness, but only the stiffening of vimentin upon repeated stress. In agreement, partial microtubule depolymerization did not perturb the effective stiffness of vimentin bundles (figure 6.13), but decreased this stiffening upon repeated stress.

There is also a common feature between these two experiments: both nocodazole and tubacin treatments reduce the number of deacetylated microtubules compared to control cells. Another hypothesis could be that deacetylated microtubules are required for vimentin bundles to stiffen when they undergo a sequence of two deflections in living cells. Like in fibroblasts where deacetylated and acetylated microtubules have very different effects on the integrity of the vimentin network [Rathje *et al.* 2014], in my experiments, acetylated and deacetylated microtubules might be dissimilarly coupled to vimentin bundles, leading to different mechanical outcomes.

6.4 Preliminary results: role of ATP in cytoskeletal mechanics

To investigate further the potential mechanical links coupling microtubules and intermediate filaments, I have asked how cellular active processes modulate the mechanical properties of vimentin bundles in living cells.

- **Vimentin bundles are stiffer in ATP-depleted cells than in control cells.**

In order to check the efficiency of ATP depletion protocol in U373 cells, I nucleofected a GFP-RAB6³ plasmid to visualize the impact on intracellular transport. Figure 6.19.A shows the average intensity and the maximum intensity projection of a 1 min-movie in ATP-depleted cells and in control cells. In control cells, GFP-RAB6 proteins are transported along microtubules whereas in ATP-depleted cells, vesicular transport is inhibited, so that the average and maximum intensity are similar. Unlike in all other experiments presented in this manuscript, the laser power of the optical tweezers was set at 1.50 W.

In ATP-depleted cells, the average effective stiffness of vimentin bundles is $k = 2220 \pm 460 \text{ pN}\mu\text{m}^{-1}$ whereas in control cells I measured $k = 858 \pm 377 \text{ pN}\mu\text{m}^{-1}$. The difference between these two conditions is significant ($p < 0.01$, see figure 6.19.B) and shows stiffening upon ATP depletions.

- **Discussion.**

A recent study used mitochondrial fluctuations in mouse embryo cells to show that ATP depletion induces a decrease of the measured creep compliance [Xu *et al.* 2018]. Consistently, the same protocol was used in our group to show that ATP depletion leads to stiffening of the cytoplasm [Mandal *et al.* 2016]. Here, I find a similar trend, as depleting ATP leads to a 2.6-fold increase of the effective stiffness of vimentin bundles compared to control cells. This result suggests that some active processes (which can not occur in ATP-depleted cells) modulate the mechanical properties of the cytoskeleton, potentially by downregulating its stiffness. In order to better characterize the coupling which is at stake between microtubule and vimentin networks, it would also be interesting to measure the effect of depleting ATP on vimentin bundles undergoing sequential deflections.

³RAB6 is a GTPase involved in transport from the Golgi apparatus regulating (in particular) exocytosis. It is known to move along microtubules [Miserey-Lenkei *et al.* 2017].

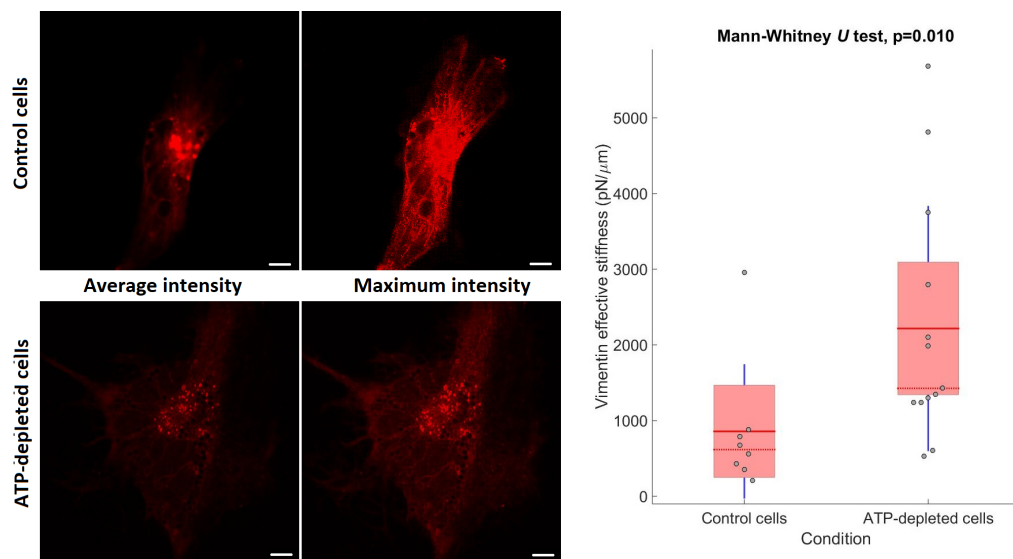


Figure 6.19: Inhibiting active cellular processes by **ATP** depletion increases the effective stiffness of vimentin bundles.

A: Live confocal microscopy images of U373 cells nucleofected with GFP-RAB6 of a 58 frames movie (total duration: 1 min). Top: Control cell. Bottom: ATP-depleted cell. Average intensity image (left), maximum intensity projection (right). Scale bars: 10 μ m. B: The effective stiffness of 8 vimentin bundles of control cells is compared to that of 13 vimentin bundles of ATP-depleted cells.

Conclusion and Perspectives

With this PhD work, I have given more insights into the mechanical properties of the cytoskeleton in living cells. In particular, the mechanics of vimentin intermediate filaments and microtubules under deflection has been characterized. By fitting force-deflection curves at small forces, I have shown that microtubules are significantly softer than vimentin bundles in living cells. Besides, microtubules and vimentin bundles do not respond in the same way to a sequence of deflections: while vimentin bundles systematically stiffen upon sequential deflections, microtubules do not exhibit the same mechanical behaviour, as their average effective stiffness remains unchanged.

I have investigated how microtubule and vimentin networks are mechanically coupled. The experiments highlight dissymmetric interactions occurring when bending filaments in living cells. The experiments in a vimentin-KO cell line show that the mechanical outcome regarding the microtubule network in vimentin-KO and in control cells is the same, whether single or sequential deflections are performed on microtubules. Although vimentin bundles are stiffer than microtubules, their absence does not modify microtubule stiffness. Conversely, I have used drugs to perturb or modify the microtubule network and see how this affects the mechanics of vimentin bundles. If stabilizing microtubules, partially depolymerizing them or increasing their K40 acetylation level does not change the stiffness of vimentin bundles, there is a dramatic effect on their response to sequential deflections. In nocodazole- and tubacin-treated cells, the ability of vimentin bundles to stiffen upon sequential deflections is highly reduced, whereas no effect is observed in taxol-treated cells. Taken together, these results indicate that microtubules are involved in the stiffening of vimentin bundles undergoing sequential deflections which has been measured in living cells. Even if microtubules and intermediate filaments are spatially separated, they may be linked *via* crosslinks. These crosslinks may have an effect on the stiffening under repeated stress only and not on the effective stiffness. In conclusion, the results of this work underline the importance of the coupling and interactions between cytoskeletal filaments in the context of cell mechanics. If the nature of these interactions remains unknown, vimentin bundles can however be shown as mechanosensitive structures that exhibit history-dependent mechano-responses in which microtubules are implicated.

Due to the novelty of the work, there are several perspectives to its findings which need to be discussed here. As I have used physical tools and analysis to answer biological questions, I divide the following into two corresponding paragraphs.

- **Physical perspectives**

In order to be able to compare the different experiments between them, I have fixed a number of physical parameters in all my experiments, such as the stage velocity used to push cytoskeletal bundles against the bead held in the optical tweezers, the power of the laser of the optical trap, the experiment time, or the concentration of the drugs. Also, I have systematized the analysis by studying the force-deflection curves in their linear regime at small forces. Here I discuss the relevance of modifying some aspects of the experimental protocol and analysis I have performed.

- The mechanical parameter I have used - the effective stiffness k - is calculated from linear fits at low forces. This parameter does not represent all the information contained in force-deflection curves. Especially, the evolution of force-deflection curves at higher forces has not been investigated in this PhD manuscript. It would thus be relevant to develop other ways of analyzing the curves. For instance, a power law analysis ($F = F_0 \left(\frac{\delta}{\delta_0}\right)^\alpha$) where F_0 is the prefactor, δ_0 a constant characteristic length and α is the exponent of the power law, which is a typical tool in rheology, could provide complementary mechanical information. I have performed such an analysis for part of the data (see appendix C) and we could not detect any difference in the values of the exponent α .
- As stated in chapter 6, in some cases (mostly when a sequence of deflections was performed and the cytoskeletal bundle became rigid) it was not possible to extract the effective stiffness k from the curves due to the resolution limit when measuring the deflection. Many studies, both *in vitro* and in living cells, highlight the key importance of the speed at which forces are applied (the so called pulling speed or loading rate). In the experiments I have carried out, it is likely that the effective stiffness depends on the stage velocity. Changing the loading rate probably allows to probe a wider range of mechanical behaviours, especially for the stiffest cytoskeletal filaments.
- One of the most important results of this PhD thesis is the mechanical behaviour of the cytoskeleton upon sequential deflections. The fact that the turnover of microtubules and vimentin filaments occurs at totally different time scales is an element that needs to be taken into account when attempting to build a mechanistic model from the results. The protocol of sequential deflections I have designed probably better suits the study of vimentin mechanics than that of microtubules. Specific experiments could thus be performed to study the effect of sequential

deflections on microtubule mechanics at shorter time scales. For instance, microtubules could be deflected for periods of 15 s separated by typically a 1 min-waiting time. However, as the duration of the movie is divided by 4, the precision of the extracted effective stiffness would certainly decrease in this experiment, as imaging at a higher frame rate would make confocal images noisier, and therefore the deflection more difficult to measure.

- All the intracellular rheological experiments I have carried out are based on bending cytoskeletal filaments. In the literature, *in vitro* mechanical measurements on cytoskeletal filaments were mostly performed by elongating filaments. Comparing the results of this PhD work to some of these studies can be challenging, as some phenomena may depend on the type of applied stress and the geometry of the experiment. It could therefore be worth designing an experimental protocol to try and stretch cytoskeletal filaments in living cells. For instance, beads could be treated in order to be physically coupled to a given cytoskeletal filament. If several beads bind the same filament, it could be stretched with a double optical trap. The limit of this approach lies in the bead microenvironment: the lysosomal membrane surrounding the bead does not allow a direct coupling between the bead and the cytoskeletal filament, and interferes with the mechanical measurement [Guet *et al.* 2014].

- **Biological perspectives**

- During this PhD thesis, I have used two cell lines: the U373 cell line, and a vimentin-KO U373 cell line. This raises the question of the generality of the conclusions I have drawn and whether they depend on the cell type. In particular, U373 cells are known for only expressing four intermediate filament proteins: vimentin, GFAP, nestin and synemin. It would be interesting to carry out experiments in cells that feature a more heterogeneous and complex intermediate filament network. For instance, would increasing microtubule acetylation lead to such a clear reduction of the stiffening effect of vimentin filaments in such cells?
- Another interesting question is whether the stiffening of intermediate filaments upon repeated stress observed here depends on the composition of intermediate filaments. I have obtained preliminary results using siRNA of GFAP, nestin, GFAP+nestin showing that the depletion of either nestin, or GFAP, or both does not affect significantly the effective stiffness of vimentin bundles. However, whether the stiffening upon sequential deflections is perturbed still has to be tested.
- Related to the above, the mechanical coupling between microtubules and other intermediate filament types could be of interest. In other cell lines, performing experiments on other well-characterized intermediate filaments, such as keratins or even nuclear lamins, and quantifying

their mechanical interactions with microtubules could allow to determine whether the mechanical coupling exhibited in this PhD work applies to all intermediate filaments.

- This work focuses on the mechanical coupling between microtubules and intermediate filaments. We have not looked at the role of actin filaments here. The rationale is that, in the location where the beads are found, *i.e.* the perinuclear region, polymerized actin is mostly absent, as opposed to microtubules and intermediate filaments. However, studying the role of the actin filaments in cytoskeletal coupling is obviously very important. By using drugs that specifically target the actin filaments such as latrunculin A, cytochalasin D or jasplakinolide, it would be possible, with our experimental setup, to study how disrupting the actin network impacts the mechanical properties of vimentin bundles and microtubules. Due to the perinuclear localization of the beads used for deflecting the cytoskeletal filaments and the mostly cortical localization of actin filaments, these experiments would potentially evaluate the contribution of longer-range interactions within the cell compared to the ones presented in this manuscript.
- While vimentin was fluorescently labeled with a GFP-vimentin construct, tubulin was stained with probes based on the microtubule binding drug docetaxel (SiR-tubulin or SPYTM655-tubulin). First, the effective stiffness values measured for microtubules (respectively vimentin bundles) correspond to microtubules (respectively vimentin bundles) stained with SiR-tubulin or SPYTM655-tubulin (respectively by overexpressing GFP-vimentin). Hence, k may be different from the non-labeled (respectively endogenous) cytoskeletal filament. Second, docetaxel (Taxotere) is known to bind the β -tubulin subunit and is analogous to taxol. For this reason, taxol and docetaxel compete in living cells. Therefore, I was not able to measure the effective stiffness of taxol-treated cells as microtubules staining by SiR-tubulin or SPYTM655-tubulin quickly disappeared after taxol addition. In order to measure the mechanics of microtubules in taxol-treated cells, resorting to a plasmid - *e.g.* a GFP-tubulin construct - might be relevant. However, direct comparison with the experiments carried out with docetaxel during this PhD is challenging because of the potential stabilizing effect of docetaxel.
- Preliminary results on ATP depletion are presented in this manuscript. The fact that depleting ATP leads to a stiffening of vimentin bundles raises the question of the active processes involved in the mechano-response of these bundles in living cells. Experiments on microtubule mechanics in ATP-depleted cells and studying the effect of ATP depletion on the response of cytoskeletal filaments to sequential deflections should shed light on the contribution of ATP-dependent processes in cytoskeletal mechanics.

- As a complement to the previous point, exploring the nature of the coupling between vimentin intermediate filaments and microtubules which is at stake in our work seems particularly crucial to understand the underlying molecular mechanisms. Several hypothesis could be tested by following a similar protocol than the one I have used in the experiments. First, the role of microtubule-based molecular motors such as dynein and kinesins can be investigated by using drugs that specifically target these motors, such as dynarrestin for dynein, or by specific depletion (siRNA, CRISPR-Cas9) of motor proteins. Second, proteins which crosslink microtubules, intermediate filaments and actins such as plectin or APC could be depleted by *e.g.* siRNA.

To conclude on the biological perspectives derived from this work, it is important to stress that this study was designed in the context of intracellular mechanotransduction [Mathieu & Manneville 2019]. If we have shown that vimentin bundles exhibit mechano-responses that depend on the previous stress they have undergone, how forces are transmitted from the cytoskeleton to intracellular organelles remains totally unclear. Different experimental strategies could be followed to monitor mechanotransduction events at a given intracellular organelle or at the nucleus, such as developing specific Förster Resonance Energy Transfer (FRET) sensors. These experiments should highlight the role of the cytoskeleton in transmitting external and internal mechanical inputs to several intracellular organelles (nucleus, Golgi apparatus, endoplasmic reticulum, mitochondria, *etc.*) and give more insights on the mechanical coupling, not only within the cytoskeleton, but with membranes, organelles or the nucleus.

Appendices

APPENDIX A

Protocols

A.1 Cell culture

- **Cell subculture**

The ideal confluence before splitting U373 cells is about 80% – 90%. Starting from a 75 cm²-flask (T75), the following protocol is used:

- aspirate the medium,
- wash with about 8 mL of Phosphate-buffered saline (PBS),
- aspirate the PBS,
- introduce 1 mL of Trypsin (Gibco™-25300-054) and place the flask in the incubator¹ for 5 min until the cells are completely detached,
- add 5 mL of supplemented medium to inhibit the effect of trypsin,
- according to the desired dilution, take the appropriate volume,
- introduce in a new flask with supplemented medium in order to have 12 mL in total,
- place in the incubator.

- **Freezing cells**

To prepare three 1 mL-cryogenic vials starting from a T75 close to confluence:

- put 3 mL of FCS and one empty 15 mL-conical centrifuge tube in ice,
- aspirate the medium,
- wash with about 8 mL of PBS and aspirate it,
- introduce 1 mL of Trypsin and place the flask in the incubator for 5 min until the cells are completely detached,
- add 5 mL of supplemented medium to inhibit the effect of trypsin, aspirate totally and insert in the centrifuge tube,
- centrifugate at 1200 rpm for 3 min at room temperature,
- aspirate the supernatant,
- resuspend the pellet in 3 mL of FCS with 5% of DMSO,
- dispense 1 mL into each cryogenic vial and immediately place them at –80 °C.

¹Cells are always incubated at 37 °C with 5% CO₂.

- **Thawing cells**

- bring the cryogenic vial to room temperature by rotating it in hands,
- add 1 mL of supplemented medium, aspirate and introduce in a 15 mL-conical centrifuge tube,
- centrifugate at 1200 rpm for 3 min at room temperature,
- aspirate the supernatant,
- resuspend the pellet in 4 mL of supplemented medium,
- introduce 8 mL of supplemented medium in a T75 flask and add the content of the tube,
- place in the incubator.

To remove any cell debris, the medium can be changed the day after the cells are thawed.

A.2 Immunofluorescence staining

- **Fixation**

- aspirate the medium in each well,
- introduce 1 mL of pure Methanol (chilled at -20°C) in each well,
- incubate the plate at -20°C for 3 min,
- wash three times with PBS.

- **Permeabilization**

- introduce 1 mL of PBS Buffer 1X with 0.2% of bovin serum albumin (BSA) and 0.05% of saponin in each well,
- incubate the plate at room temperature for 25 min in the dark,
- wash three times with PBS.

- **Immunostaining**

- prepare the primary antibody solution by mixing all desired antibodies at the good dilution (see 5.1) with PBS with 2% BSA,
- drop 25 μL of this solution on Parafilm® for each coverslip and put them on the drops,
- incubate coverslips at room temperature for 1 h in a humidified chamber in the dark,
- wash three times with PBS,
- prepare the secondary antibody solution by mixing all desired antibodies at 1/400 with PBS with 2% BSA,

- drop 25 μL of this solution on Parafilm® for each coverslip and put them on the drops,
- incubate coverslips at room temperature for 1 h in a humidified chamber in the dark,
- wash three times with PBS,
- optional: drop 25 μL of a solution of diluted Thermo Scientific™ Hoechst 33342 (1/500) on Parafilm® for each coverslip and put them on the drops,
- incubate coverslips at room temperature for 15 min in a humidified chamber in the dark,
- wash three times with PBS and once with water.

- **Mounting**

- wash once with Ethanol
- drop 17 μL of Mowiol® 4-88 on microscope slides and mount coverslips on them,
- optional: seal coverslips with nail polish,
- dry at room temperature in the dark for at least 2 h,
- store in the dark at 4 °C.

A.3 Live cell imaging of vimentin and tubulin *in cellulo*

- **Nucleofection of GFP-vimentin**

- starting from a T75 flask, perform the first five steps of the "Cell sub-culture" protocol (see A.1),
- introduce 2×10^6 cells (per nucleofection) in a centrifuge tube,
- centrifugate at 1200 rpm for 3 min at room temperature,
- aspirate the supernatant,
- in the centrifuge tube, introduce 100 μL of the supplemented Nucleofector™ Solution for Primary Mammalian Glial Cells, 3 μg of GFP-vimentin DNA and quickly resuspend the cell pellet
- introduce immediately in an aluminium cuvette and close it with its lid,
- insert the cuvette in the Nucleofector™ and select the T-020 program,
- take the cuvette out of the holder and immediately add 500 μL of supplemented medium,
- aspirate the sample with a single use pipette and introduce it in a new centrifuge tube previously filled with 7.5 mL of supplemented medium,
- introduce typically 2 mL per FluoroDish™ or MatTek dish,
- place in the incubator,

- six hours later: change the medium to eliminate cell debris,
- optional: add fluorospheres if required,
- place in the incubator.

Cells are ready to be imaged 48 hours after nucleofection, adding HEPES (Gibco™-15630-056) at 20 mM just before performing microscopy experiments.

- **Tubulin probes**

To label tubulin, probes based on the microtubule binding drug Docetaxel are used: SiR-tubulin and SPY™655-tubulin. The protocol for both probes is identical:

- introduce the probe at 500 nM (dilution by 2000),
- optional: in case of using SiR-tubulin, add Verapamil at 10 μ M,
- place in the incubator for 4 h.

Probes do not have to be removed before microscopy experiments.

A.4 Post-treatment of images before creating kymographs

The steps listed below are followed under ImageJ and MATLAB:

- open the raw movie and split channels,
- in one of the channels, select a rectangular zone² and click "Template Matching" and then "Align Slices in Stack". Launch the procedure after checking that "show align coordinates in result tables?" is ticked,
- save result tables as CSV and all the channels as TIF,
- under MATLAB, use the "recal.m" routine (see appendix B) to apply the same transformations to all the other channels,
- under ImageJ, open the new channel corresponding to the cytoskeleton of interest, draw a line from the bead towards the deflected filament, perpendicular to it, and click "Multi Kymograph". Choose a linewidth equal to 3 px,
- save the created kymograph as TIF.

²Pixel values inside this rectangle have to be heterogeneous: it is the *template* the plugin will search for in each frame to align the frames. In particular, it is crucial not to select a motif that can exit from the recorded field in other frames.

MATLAB codes

```
1 M(:,:,1)=imread('F:\Nathan\210113\15W\ATPdepletion\Ctrl\c4b.tif',1);
2 clear ans
3
4 for k=1:size(resultsc4,1)
5     dy=resultsc4(k,1);
6     dx=resultsc4(k,2);
7     xmin=1;
8     xmax=512;
9     ymin=1;
10    ymax=512;
11    nxmin=1;
12    nxmax=512;
13    nymin=1;
14    nymax=512;
15    imread('F:\Nathan\210113\15W\ATPdepletion\Ctrl\c4b.tif',k+1);
16
17        if dx<0
18            nxmax=nxmax+dx;
19            xmin=xmin-dx;
20        elseif dx>0
21            xmax=xmax-dx;
22            nxmin=nxmin+dx;
23        end
24        if dy<0
25            nymax=nymax+dy;
26            ymin=ymin-dy;
27        elseif dy>0
28            ymax=ymax-dy;
29            nymin=nymin+dy;
30        end
31
32    M(:,:,k+1)=zeros(512);
33    M(nxmin:nxmax,nymin:nymax,k+1)=ans(xmin:xmax,ymin:ymax);
34    clear dx
35    clear dy
36    clear xmin
37    clear xmax
38    clear ymin
39    clear ymax
40    clear nxmin
41    clear nxmax
42    clear nymin
43    clear nymax
44    clear ans
```

```

45     disp(k)
46 end
47 clear k
48
49 imwrite(M(:,:,1),'F:\Nathan\210113\15W\ATPdepletion\Ctrl\c4outputb.
      tif');
50 for j=1:size(resultsc4,1)
51 imwrite(M(:,:,j+1),'F:\Nathan\210113\15W\ATPdepletion\Ctrl\c4outputb.
      tif','WriteMode','append');
52 end
53 clear j

```

Listing B.1: The code recal.m is used to have immobile cells before plotting the kymograph required to determine the filament deflection.

```

1 %% analyse kymographe
2
3 % Copyright David Pereira 2018
4 %
5 %   Trois fichiers sont necessaires pour l'utilisation de ce code:
6 %       - le kymographe de la partie deflechie (.tif) (recale
7 %       de preference)
8 %       - le kymographe d'une zone de reference (.tif)
9 %       le fichier DOIT avoir le meme nom que le
10 %       kymographe
11 %       de la partie deflechie avec a la fin '_ref' ex
12 %       :
13 %       'kymo_ref.tif'
14 %       - les positions de la bille XY (fichier .mat et non .
15 %       txt)
16 %       le fichier peut avoir n'importe quel nom (ex:
17 %       'niqn.mat')
18 %
19 % a l'ouverture de la fenetre de recuperation des fichiers il faut
20 % selecitonner le kymographe de la partie deflechie (ex: 'kymo.tif
21 % ') et le
22 % fichier des positions de la bille (peut importe l'ordre de
23 % selection)
24 %
25 % Lorsque la fenetre avec une image s'ouvre il faut selectionner a
26 % l'aide du
27 % pointeur la zone a analyser. Plusieurs lignes successives peuvent
28 % etre
29 % tracees faire attention a ne pas tracer des lignes droites trop
30 % courtes. Faire egalement attention a ne pas cliquer trop pres des
31 % bords
32 % horizontaux de l'image.
33 %
34 % ! Attention ! mettre le bon pas de temps (ligne 74)
35 % ! Attention ! mettre le la bonne conversion pixel => microm (
36 % ligne 72)

```

```
29 %
30 %
31 % Copyright David Pereira 2018
32
33 clear
34 close all
35
36 cd 'G:\Nathan\200618\Tubacine'
37 % cd '\\zserver\umr144\equipe_goud\n_lardier\180302'
38 % cd 'C:\Users\Camilla\Desktop\analyse\routine\FI\Alice\GFP Vim +
    siLuc'
39
40
41 [FileName,PathName] = uigetfile('*. *','All Files (*.*)','MultiSelect'
    ,'on');
42
43 pattern_tif='.tif';
44 pattern_mat='.mat';
45 trouve_tif=strfind(FileName,pattern_tif);
46 trouve_mat=strfind(FileName,pattern_mat);
47 tt_1=isempty(trouve_tif{1});
48 tt_2=isempty(trouve_tif{2});
49 cd(PathName)
50
51
52 choix_ref=choix_image;
53 % Pour Nathan
54 currentfolder=pwd;
55 mkdir([PathName FileName{1}(1:trouve_mat{1}-1)]);
56
57 while choix_ref==0
58
59     choix_ref=choix_image;
60
61 end
62
63 %%%%%% test pour l'ouverture des fichiers %%%
64 if tt_1==1 || tt_2==0
65     load(FileName{1});
66     kymo_recal=imread(FileName{2});
67     kymo_recal_ref=imread([FileName{2}(1:trouve_tif{2}-1) '_ref.tif'
68     ]);
69 else
70     load(FileName{2});
71     kymo_recal=imread(FileName{1});
72     kymo_recal_ref=imread([FileName{1}(1:trouve_tif{1}-1) '_ref.tif'
73     ]);
74 end
75 %%%%%%
76 %%% donnees provenant du fichier (.mat) GUI_v10 (position de la
    bille) %%
77 coordX=[results.TrackingData.X];
```

```

78 coordY=[results.TrackingData.Y];
79 newcoordX=coordX-coordX(1);
80 newcoordY=coordY-coordY(1);
81 %%%
82
83 %%% mettre la taille du pixel en micromon %%%
84 pixel_micron=0.0621; %conversion 1 pixel => X.XXX micromon
85 %%% mettre le pas de temps en seconde %%%
86 pas=0.517
87 %pas=0.78;
88 %quand moyennage oublie :
89 % pas=0.12925;
90 % FI : 0.517 (Alice); 0.13 0.07 (Yasmine) %Nucleus : 0.26 % en
    seconde
91 %%% constante de raideur du piege %%%
92 kk=240;
93 %% calcul distance parcourue par la bille %%
94 distance=sqrt(newcoordX.^2+newcoordY.^2)*pixel_micron;
95 %%% Force de rappel du piege %%%
96 Force=kk*distance;
97 %%% Temps converti en seconde %%%
98 temps=0:pas:pas*(size(kymo_recal,1)-1);
99 %%% Temps sur lequel les graphes sont affiches %%
100 % [val,limit]=max(deflected); voir ligne 321
101
102
103 %%%
104 %%% Gaussian blur %%%
105 % uncomment if needed
106 HH = fspecial('gaussian',200,2);
107 kymo_recal=imfilter(kymo_recal,HH,'replicate');
108 kymo_recal_ref=imfilter(kymo_recal_ref,HH,'replicate');
109 %%%
110
111 %%% mesure de l'epaisseur de la ligne %%%
112
113 hh(11)=figure(11);
114 % subplot(121)
115 % hold on
116 imshow(kymo_recal,[])
117 ylabel('time (frame)')
118 xlabel('deflection (pixel)')
119 title('Fibre thickness measurement')
120
121 [xi,yi]=getline(hh(11));
122 subplot(122)
123 c=improfile(kymo_recal,xi,yi);
124 [val,indice]=max(c);
125 % taille=(1-indice)*pixel_micron:pixel_micron:(indice-1)*pixel_micron
    ;
126 taille=1:size(c);
127 taille=(taille-indice)*pixel_micron;
128 plot(taille,c,'r.-');
129 [pks,locs,w,p] = findpeaks(c,'WidthReference','halfprom');

```

```

130 diametre=max(w)*pixel_micron;
131 % hold on
132 % line([0,0,0],[0.7*min(val) 100 1.2*max(val)],'Color','black','
      LineStyle','--','LineWidth',1)
133 ylabel('pixel intensity')
134 xlabel('fibre thickness')
135 epaisseur=sprintf('2R = %0.2f microm \n',diametre);
136 title(epaisseur)
137 axis square
138 box on
139
140 subplot(121)
141 % hold on
142 imshow(kymo_recal,[])
143 hold on
144 line(xi,yi,'Color','red','LineStyle','-','LineWidth',3)
145 ylabel('time (frame)')
146 xlabel('deflection (pixel)')
147 title('deflected')
148
149
150
151
152
153 %%%%%%%%%
154
155 hh(1)=figure(1);
156 subplot(121)
157 imshow(kymo_recal,[])
158 ylabel('time (frame)')
159 xlabel('deflection (pixel)')
160 title('deflected')
161
162 [xi,yi]=getline(hh(1));
163
164 %%%%%%%%%
165 %%%%%%%%% calcul des pentes et des distances des segments %%%%
166
167 for dd=1:length(xi)-1
168
169 pente(dd)=(yi(length(xi)-dd+1)-yi(length(xi)-dd))/(xi(length(xi)-dd
      +1)-xi(length(xi)-dd));
170 distanceY(dd)=yi(length(xi)-dd+1)-yi(length(xi)-dd);
171
172 end
173
174 %%%%%%%%%
175
176 yi(1)=1;
177 yi(end)=size(kymo_recal,1);
178 pente=fliplr(pente);
179
180 %%%%%%%%%%%%%%%
181 %%%% calcul des positions en X associer aux segments %%%

```

```

182
183 for nn=1:size(pente,2)
184
185     bb=yi(nn)-pente(nn)*round(xi(nn));
186
187     for yyy=floor(yi(nn)):floor(yi(nn+1))
188
189         posX(yyy)=round((yyy-bb)/pente(nn));
190
191     end
192
193 end
194
195
196 %%%% calcul des max autour des segments %%%%
197
198 tolerance=3; % +/- largeur (en pixel) de la recherche du max autour
199           de posX
200
201 for ii=1:size(kymo_recal,1)
202
203     [pks,locs]=max(double(kymo_recal(ii,posX(ii)-tolerance:posX(ii)+
204           tolerance)));
205
206     pos_kymo_recal(:,ii)=locs+posX(ii)-(tolerance+1);
207
208     %%%%%%%%%%%%%%
209
210 subplot(121)
211 hold on
212 plot(posX,1:size(posX,2),'b.')
213 hold on
214 plot(pos_kymo_recal,1:size(pos_kymo_recal,2),'r.')
215 hold off
216 ylabel('time (frame)')
217 xlabel('deflection (pixel)')
218 title('deflected')
219
220
221 %%% Repetition sequence precedente pour image reference %%
222
223 if choix_ref==1
224
225     subplot(122)
226     imshow(kymo_recal_ref,[])
227     ylabel('time (frame)')
228     xlabel('deflection (pixel)')
229     title('reference')
230
231     clear xi yi pente
232
233 [xi,yi]=getline(hh(1));

```

```

234
235
236 for dd=1:length(xi)-1
237
238 pente(dd)=(yi(length(xi)-dd+1)-yi(length(xi)-dd))/(xi(length(xi)-dd
      +1)-xi(length(xi)-dd));
239 distanceY(dd)=yi(length(xi)-dd+1)-yi(length(xi)-dd);
240
241 end
242
243 yi(1)=1;
244 yi(end)=size(kymo_recal,1);
245 pente=fliplr(pente);
246
247 for nn=1:size(pente,2)
248
249     bb=yi(nn)-pente(nn)*round(xi(nn));
250
251     for yyy=floor(yi(nn)):floor(yi(nn+1))
252
253         posX(yyy)=round((yyy-bb)/pente(nn));
254
255     end
256
257 end
258
259
260 for ii=1:size(kymo_recal_ref,1)
261     %         floor((max(xi))+jj/pente)-10:floor((max(xi))+jj/pente)+10)
262 [pks,locs_ref]=max(double(kymo_recal_ref(ii,posX(ii)-tolerance:posX(
      ii)+tolerance)));
263
264 pos_kymo_recal_ref(:,ii)=locs_ref+posX(ii)-(tolerance+1);
265 end
266
267
268 subplot(122)
269 hold on
270 plot(posX,1:size(posX,2),'b. ')
271 hold on
272 plot(pos_kymo_recal_ref,1:size(kymo_recal_ref,1),'r. ')
273 hold off
274 ylabel('time (frame)')
275 xlabel('deflection (pixel)')
276 title('reference')
277
278 else
279
280     disp('no ref')
281
282 end
283
284 %%% Fin de Repetition sequence precedente pour image reference %%
285

```

```

286
287
288 %%%%%%%%%%%%%%%%%%%%%%%%%%%%%%%%%%%%%%%%%%%%%%%%%%%%%%%%%%%%%%%
289 %% analyse des donnees (Force, deflexion, deplacement) %%
290
291
292 deflected=pos_kymo_recal-mean(pos_kymo_recal(1:10));
293 if choix_ref==1
294 reference=pos_kymo_recal_ref-mean(pos_kymo_recal_ref(1:10));
295 else
296     reference=deflected*0;
297     pos_kymo_recal_ref=pos_kymo_recal*0;
298 end
299
300
301
302
303 hh(2)=figure(2);
304 subplot(131);
305 imshow(kymo_recal,[]);
306 ylabel('time (frame)')
307 xlabel('deflection (pixel)')
308 title('deflected fibre')
309 hold on
310 plot(pos_kymo_recal,1:size(temps,2),'b.')
311 subplot(132);
312 imshow(kymo_recal_ref,[]);
313 hold on
314 plot(pos_kymo_recal_ref,1:size(temps,2),'r.')
315 ylabel('time (frame)')
316 xlabel('deflection (microm)')
317 title('reference fibre')
318
319 subplot(133)
320 plot(temps,deflected*pixel_micron,'b.-')
321 hold on
322 plot(temps,reference*pixel_micron,'r.-')
323 hold on
324 plot(temps,(deflected-reference-mean(deflected(1:10)-reference(1:10))
    )*pixel_micron,'k.-')
325 axis square
326 xlabel('time (s)')
327 ylabel('deflection (microm)')
328 legend('deflected','reference','substracted','Location','northwest')
329
330
331
332
333
334 hh(4)=figure(4);
335 subplot(221)
336 plot(temps,newcoordX*pixel_micron,'b.')
337 axis square
338 ylabel('X displacement (microm)')

```

```

339 xlabel('time (s)')
340 subplot(222)
341 plot(temps,coordX*pixel_micron,'b.')
342 axis square
343 ylabel('X displacement (microm)')
344 xlabel('time (s)')
345 subplot(223)
346 plot(temps,newcoordY*pixel_micron,'b.')
347 axis square
348 ylabel('Y displacement (microm)')
349 xlabel('time (s)')
350 subplot(224)
351 plot(temps,coordY*pixel_micron,'b.')
352 axis square
353 ylabel('Y displacement (microm)')
354 xlabel('time (s)')
355
356 figure(5);
357 plot(temps,distance,'b.');
```

358 axis square

359 ylabel('distance travelled by the bead (euclidian) (microm)')

360 xlabel('time (s)')

361

362

363

364 %%%%%%%%% moyenne glissante %%%%%%%%%

365 aa=20;

366 deflected2=(deflected-reference-mean(deflected(1:10)-reference(1:10))

)*pixel_micron;

367 % movingAverage = conv(deflected2, ones(aa,1)/aa, 'same');

368 movingAverage = smooth(deflected2,20);

369 %%%%%%%%%%

370 [val,limit]=max(abs(movingAverage));

371

372 hh(6)=figure(6);

373 subplot(231)

374 plot(deflected2,Force,'b.');

375 hold on

376 plot(movingAverage(1:end-10),Force(1:end-10),'k.')

377 axis square

378 xlabel('deflection \delta (microm)')

379 ylabel('Force (pN)')

380 title('Force vs Deflection')

381 XMIN=min(movingAverage)*1.2;

382 XMAX=max(movingAverage)*1.2;

383 YMIN=-5;

384 YMAX=max(Force)*1.2;

385 axis([XMIN XMAX YMIN YMAX])

386 box on

387

388 subplot(232)

389 plot(temps,deflected2,'b.')

390 hold on

391 plot(temps(1:end-10),movingAverage(1:end-10),'k.-')

```

392 axis square
393 xlabel('time (s)')
394 ylabel('deflection \delta (microm)')
395 title('Deflection vs Time')
396 XMIN=-0.5;
397 XMAX=max(temps)*1.2;
398 YMIN=min(deflected2)*1.2;
399 YMAX=max(deflected2)*1.2;
400 axis([XMIN XMAX YMIN YMAX])
401 box on
402
403 subplot(233)
404 plot(temps,Force,'b.-');
405 hold on
406 axis square
407 xlabel('time (s)')
408 ylabel('Force (pN)')
409 title('Force vs Time')
410 box on
411
412
413
414 subplot(234)
415 plot(deflected2(1:limit),Force(1:limit),'b. ');
416 hold on
417 plot(movingAverage(1:limit),Force(1:limit),'k. ')
418 axis square
419 xlabel('deflection \delta (microm)')
420 ylabel('Force (pN)')
421 % legend('aligned')
422 title('Force vs Deflection')
423 XMIN=min(movingAverage(1:limit))*1.2;
424 XMAX=max(movingAverage(1:limit))*1.2;
425 YMIN=-5;
426 YMAX=max(Force(1:limit))*1.2;
427 axis([XMIN XMAX YMIN YMAX])
428 box on
429
430 subplot(235)
431 plot(temps(1:limit),deflected2(1:limit),'b. ')
432 hold on
433 plot(temps(1:limit),movingAverage(1:limit),'k.-')
434 axis square
435 xlabel('time (s)')
436 ylabel('deflection \delta (microm)')
437 title('Deflection vs Time')
438 XMIN=-0.5;
439 XMAX=max(temps(1:limit))*1.2;
440 YMIN=min(deflected2(1:limit))*1.2;
441 YMAX=max(deflected2(1:limit))*1.2;
442 axis([XMIN XMAX YMIN YMAX])
443 box on
444
445 subplot(236)

```

```

446 plot(temps(1:limit),Force(1:limit),'b.-');
447 hold on
448 axis square
449 xlabel('time (s)')
450 ylabel('Force (pN)')
451 title('Force vs Time')
452 box on
453
454 hh(7)=figure(7);
455 plot(deflected2(1:limit)/(diametre/2),Force(1:limit),'b. ');
456 hold on
457 movingAverage = conv(deflected2/(diametre/2), ones(aa,1)/aa, 'same');
458 plot(movingAverage(1:limit-10),Force(1:limit-10),'k. ');
459 axis square
460 xlabel('\delta/R')
461 ylabel('Force (pN)')
462 title('Force vs Deflection Nondimensionalized')
463 XMIN=min(movingAverage)*1.2;
464 XMAX=max(movingAverage)*1.2;
465 YMIN=-5;
466 YMAX=max(Force(1:limit))*1.2;
467 axis([XMIN XMAX YMIN YMAX])
468 box on
469
470 % Sauvegarde standard
471 if choix_ref==1
472     saveas(hh(1),[PathName 'image_ligne_deflection.fig']);
473     saveas(hh(2),[PathName 'image_graphe_deflection.fig']);
474     saveas(hh(4),[PathName 'deplacement_bille_xy.fig']);
475     saveas(hh(6),[PathName 'force_deflection.fig']);
476     saveas(hh(7),[PathName 'force_deflection_adim.fig']);
477     saveas(hh(11),[PathName 'fibre_thickness.fig']);
478     save([PathName 'data_analysed'],'deflected','reference','Force','
deflected2','temps','distance','movingAverage','limit','diametre',
'kk','pixel_micron','pas')
479 else
480     saveas(hh(1),[PathName 'image_ligne_deflection_withoutRef.fig']);
481     saveas(hh(2),[PathName 'image_graphe_deflection_withoutRef.fig']);
482     ;
483     saveas(hh(4),[PathName 'deplacement_bille_xy_withoutRef.fig']);
484     saveas(hh(6),[PathName 'force_deflection_withoutRef.fig']);
485     saveas(hh(7),[PathName 'force_deflection_adim_withoutRef.fig']);
486     saveas(hh(11),[PathName 'fibre_thickness_withoutRef.fig']);
487     save([PathName 'data_analysed_withoutRef'],'deflected','reference
','Force','deflected2','temps','distance','movingAverage','limit',
'diametre','kk','pixel_micron','pas')
488 end

```

Listing B.2: This code written by David PEREIRA is used to plot force-deflection curves.

Power law analysis

In the fields of rheology and mechanics of materials, power law analysis are frequently used to analyze the behaviour of a given solid or fluid. As mentioned earlier, the force-deflection curves were systematically analyzed by fitting them at small deformations. The advantage of such a technique is that comparisons between the different conditions are easy to perform. Yet, these fits do not take into account the variability of mechanical behaviours that cytoskeletal bundles exhibit at higher forces. Here, we postulate a simple power law equation to fit the whole force-deflection curves without selecting a particular regime:

$$F = F_0 \left(\frac{\delta}{\delta_0} \right)^\alpha \quad (\text{C.1})$$

where α is the exponent, F_0 is a prefactor that has the dimension of a force and $\delta_0 = 1 \mu\text{m}$. If $\alpha > 1$, the bundle is strain-stiffening and if $\alpha < 1$, the bundle is strain-softening.

I carried out a power law analysis for all the experiments presented in section 6.2.2. The corresponding plots for α and F_0 can be found in figure C.1.

Conditions	p -value (F_0)	Statistical test
Sequential deflections DMSO	4.9×10^{-4}	Wilcoxon signed-rank
Sequential deflections nocodazole	0.021	Wilcoxon signed-rank
Sequential deflections taxol	6.1×10^{-4}	Wilcoxon signed-rank
Second deflection nocodazole vs. DMSO	0.0070	Mann-Whitney U

Table C.1: List of p -values that are below the level of significance for the prefactor F_0 . All the p -values calculated that do not appear in this table are above the level of significance ($\alpha = 0.05$).

In conclusion, the power law analysis I performed on the results shown in 6.2.2 does not allow to see significant differences when the exponent α of the power law fit is compared between different conditions. That could imply that there is no global strain-stiffening (or strain-softening) induced by any treatment or by repeated mechanical stress.

The only statistical differences I measured (see table C.1) are obtained when comparing the prefactor F_0 which is proportional to k if the exponent α is close to 1. Consistently, these differences are identical to that obtained with comparing the effective stiffness k (see section 6.2).

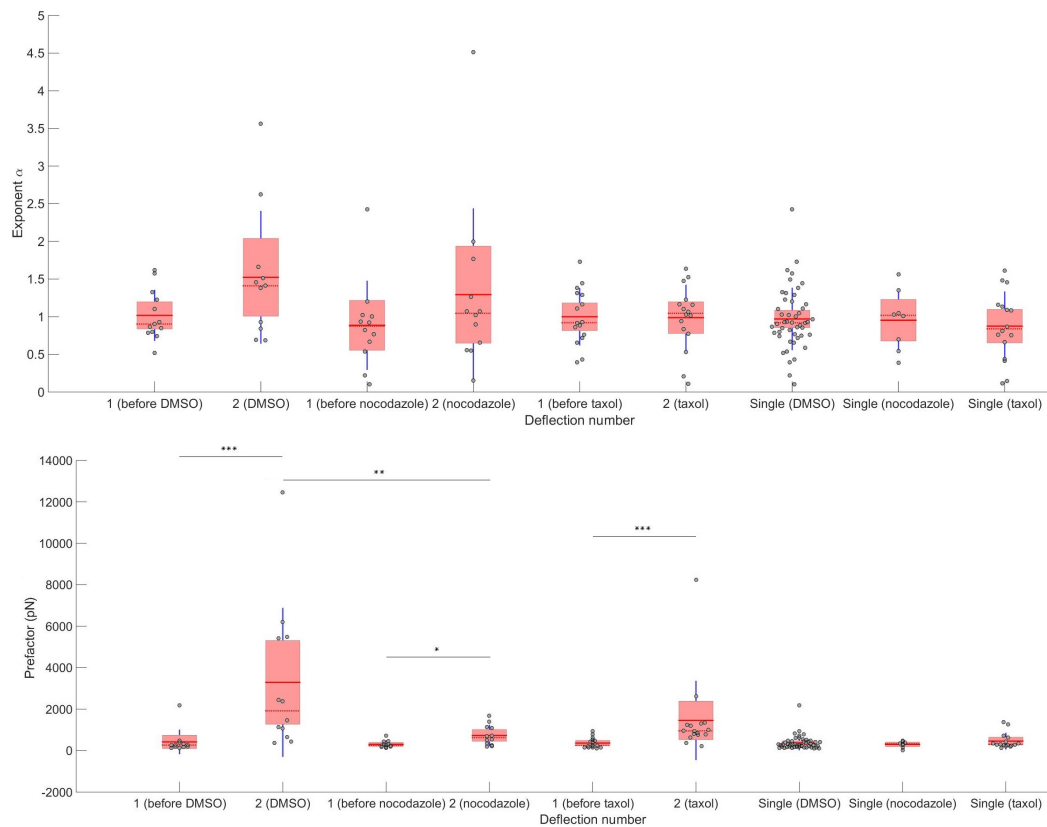


Figure C.1: Power law analysis of the force-deflection curves of vimentin bundles in DMSO-, nocodazole- and taxol-treated cells.

Top: exponent α (dimensionless) for each condition. Statistical tests were used to perform all the comparisons that appear in section 6.2.2. All p -values are greater than 0.05. Bottom: prefactor F_0 expressed in pN for each condition. Statistical tests were used to perform the comparisons as in section 6.2.2. p -values that are not greater than 0.05 appear in table C.1.

Bibliography

- [Ackbarow & Buehler 2007] Theodor Ackbarow and Markus J. Buehler. **Supere-
lasticity, energy dissipation and strain hardening of vimentin
coiled-coil intermediate filaments: atomistic and continuum stud-
ies.** *Journal of Materials Science*, vol. 42, no. 21, pages 8771–8787, jul 2007.
(Cited on pages 38 and 40.)
- [Ackbarow *et al.* 2007] T. Ackbarow, X. Chen, S. Keten and M. J. Buehler. **Hierar-
chies, multiple energy barriers, and robustness govern the fracture
mechanics of α -helical and β -sheet protein domains.** *Proceedings of
the National Academy of Sciences*, vol. 104, no. 42, pages 16410–16415, oct
2007. (Cited on page 38.)
- [Ahmed *et al.* 2018] Wylie W. Ahmed, Étienne Fodor, Maria Almonacid, Matthias
Bussonnier, Marie-Hélène Verlhac, Nir Gov, Paolo Visco, Frédéric van Wij-
land and Timo Betz. **Active Mechanics Reveal Molecular-Scale Force
Kinetics in Living Oocytes.** *Biophysical Journal*, vol. 114, no. 7, pages
1667–1679, apr 2018. (Cited on page 43.)
- [Akhmanova & Steinmetz 2010] Anna Akhmanova and Michel O. Steinmetz. **Mi-
crotubule +TIPs at a glance.** *Journal of cell science*, vol. 123, pages
3415–3419, October 2010. (Cited on page 52.)
- [Alibert *et al.* 2021] Charlotte Alibert, David Pereira, Nathan Lardier, Sandrine
Etienne-Manneville, Bruno Goud, Atef Asnacios and Jean-Baptiste Man-
neville. **Multiscale rheology of glioma cells.** *Biomaterials*, vol. 275,
page 120903, aug 2021. (Cited on page 31.)
- [Ashkin 1970] A. Ashkin. **Acceleration and Trapping of Particles by Radia-
tion Pressure.** *Physical Review Letters*, vol. 24, no. 4, pages 156–159, jan
1970. (Cited on page 31.)
- [Baba 1972] S. A. Baba. **Flexural rigidity and elastic constant of cilia.** *The
Journal of experimental biology*, vol. 56, pages 459–467, April 1972. (Cited
on pages 42 and 64.)
- [Battle *et al.* 2015] Christopher Battle, Carolyn M. Ott, Dylan T. Burnette, Jen-
nifer Lippincott-Schwartz and Christoph F. Schmidt. **Intracellular and
extracellular forces drive primary cilia movement.** *Proceedings of the
National Academy of Sciences*, vol. 112, no. 5, pages 1410–1415, jan 2015.
(Cited on pages 42 and 64.)
- [Bhattacharya *et al.* 2009] Ramona Bhattacharya, Annette M. Gonzalez, Phillip J.
Debiase, Humberto E. Trejo, Robert D. Goldman, Frederick W. Flitney and

- Jonathan C. R. Jones. **Recruitment of vimentin to the cell surface by beta3 integrin and plectin mediates adhesion strength.** *Journal of cell science*, vol. 122, pages 1390–1400, May 2009. (Cited on page 51.)
- [Block *et al.* 2015] Johanna Block, Viktor Schroeder, Paul Pawelzyk, Norbert Wilenbacher and Sarah Köster. **Physical properties of cytoplasmic intermediate filaments.** *Biochimica et Biophysica Acta (BBA) - Molecular Cell Research*, vol. 1853, no. 11, pages 3053–3064, nov 2015. (Cited on page 7.)
- [Block *et al.* 2017] Johanna Block, Hannes Witt, Andrea Candelli, Erwin J. G. Peterman, Gijs J. L. Wuite, Andreas Janshoff and Sarah Köster. **Nonlinear Loading-Rate-Dependent Force Response of Individual Vimentin Intermediate Filaments to Applied Strain.** *Physical Review Letters*, vol. 118, no. 4, page 048101, jan 2017. (Cited on pages 28, 39, 40, 47 and 63.)
- [Blöse *et al.* 1984] S H Blöse, D I Meltzer and J R Feramisco. **10-nm filaments are induced to collapse in living cells microinjected with monoclonal and polyclonal antibodies against tubulin.** *Journal of Cell Biology*, vol. 98, no. 3, pages 847–858, mar 1984. (Cited on pages 55 and 64.)
- [Bollinger *et al.* 2020] Jonathan A. Bollinger, Zachary I. Imam, Mark J. Stevens and George D. Bachand. **Tubulin islands containing slowly hydrolyzable GTP analogs regulate the mechanism and kinetics of microtubule depolymerization.** *Scientific reports*, vol. 10, page 13661, August 2020. (Cited on page 18.)
- [Bonakdar *et al.* 2012] Navid Bonakdar, Justyna Luczak, Lena Lautscham, Maja Czonstke, Thorsten M. Koch, Astrid Mainka, Tajana Jungbauer, Wolfgang H. Goldmann, Rolf Schröder and Ben Fabry. **Biomechanical characterization of a desminopathy in primary human myoblasts.** *Biochemical and biophysical research communications*, vol. 419, pages 703–707, March 2012. (Cited on page 45.)
- [Bousquet *et al.* 2001] Olivier Bousquet, Linglei Ma, Soichiro Yamada, Changhong Gu, Toshihiro Idei, Kenzo Takahashi, Denis Wirtz and Pierre A. Coulombe. **The nonhelical tail domain of keratin 14 promotes filament bundling and enhances the mechanical properties of keratin intermediate filaments in vitro.** *Journal of Cell Biology*, vol. 155, no. 5, pages 747–754, nov 2001. (Cited on page 30.)
- [Brangwynne *et al.* 2006] Clifford P. Brangwynne, Frederick C. MacKintosh, Sanjay Kumar, Nicholas A. Geisse, Jennifer Talbot, L. Mahadevan, Kevin K. Parker, Donald E. Ingber and David A. Weitz. **Microtubules can bear enhanced compressive loads in living cells because of lateral reinforcement.** *Journal of Cell Biology*, vol. 173, no. 5, pages 733–741, jun 2006. (Cited on pages 41, 42 and 58.)

- [Brochard-Wyart *et al.* 2019] Françoise Brochard-Wyart, Pierre Nassoy and Pierre-Henri Puech. **Essentials of Soft Matter Science**. *Taylor & Francis Inc*, aug 2019. (Cited on pages 24, 25 and 26.)
- [Brown *et al.* 2001] Martin J. Brown, John A. Hallam, Emma Colucci-Guyon and Stephen Shaw. **Rigidity of Circulating Lymphocytes Is Primarily Conferred by Vimentin Intermediate Filaments**. *The Journal of Immunology*, vol. 166, no. 11, pages 6640–6646, jun 2001. (Cited on page 45.)
- [Capote & Maccioni 1998] C. Capote and R. B. Maccioni. **The association of tau-like proteins with vimentin filaments in cultured cells**. *Experimental cell research*, vol. 239, pages 202–213, March 1998. (Cited on page 53.)
- [Cassimeris *et al.* 2001] L. Cassimeris, D. Gard, P. T. Tran and H. P. Erickson. **XMAP215 is a long thin molecule that does not increase microtubule stiffness**. *Journal of cell science*, vol. 114, pages 3025–3033, August 2001. (Cited on page 34.)
- [Castañón *et al.* 2013] Maria J. Castañón, Gernot Walko, Lilli Winter and Gerhard Wiche. **Plectin-intermediate filament partnership in skin, skeletal muscle, and peripheral nerve**. *Histochemistry and cell biology*, vol. 140, pages 33–53, July 2013. (Cited on pages 51 and 52.)
- [Chang & Goldman 2004] Lynne Chang and Robert D. Goldman. **Intermediate filaments mediate cytoskeletal crosstalk**. *Nature reviews. Molecular cell biology*, vol. 5, pages 601–613, August 2004. (Cited on pages 51 and 64.)
- [Chang *et al.* 2009] Lynne Chang, Kari Barlan, Ying-Hao Chou, Boris Grin, Margot Lakonishok, Anna S. Serpinskaya, Dale K. Shumaker, Harald Herrmann, Vladimir I. Gelfand and Robert D. Goldman. **The dynamic properties of intermediate filaments during organelle transport**. *Journal of cell science*, vol. 122, pages 2914–2923, August 2009. (Cited on page 15.)
- [Charrier & Janmey 2016] Elisabeth E. Charrier and Paul A. Janmey. **Mechanical Properties of Intermediate Filament Proteins**. In *Methods in Enzymology*, pages 35–57. Elsevier, 2016. (Cited on pages 37, 44, 45 and 63.)
- [Charrier *et al.* 2016] Elisabeth E. Charrier, Atef Asnacios, Rachel Milloud, Richard De Mets, Martial Balland, Florence Delort, Olivier Cardoso, Patrick Vicart, Sabrina Batonnet-Pichon and Sylvie Hénon. **Desmin Mutation in the C-Terminal Domain Impairs Traction Force Generation in Myoblasts**. *Biophysical Journal*, vol. 110, no. 2, pages 470–480, jan 2016. (Cited on page 45.)
- [Charrier *et al.* 2018] Elisabeth E. Charrier, Lorraine Montel, Atef Asnacios, Florence Delort, Patrick Vicart, François Gallet, Sabrina Batonnet-Pichon and

- Sylvie Hénon. **The desmin network is a determinant of the cytoplasmic stiffness of myoblasts.** *Biology of the Cell*, vol. 110, no. 4, pages 77–90, feb 2018. (Cited on pages 31, 32, 45 and 46.)
- [Chung *et al.* 2013] Byung-Min Chung, Jeremy D Rotty and Pierre A Coulombe. **Networking galore: intermediate filaments and cell migration.** *Current Opinion in Cell Biology*, vol. 25, no. 5, pages 600–612, oct 2013. (Cited on page 11.)
- [Cooper 2000] Geoffrey Cooper. **The cell : a molecular approach.** *ASM Press Sinauer Associates*, Washington, D.C. Sunderland, Mass, 2000. (Cited on page 11.)
- [Correia *et al.* 1999] I. Correia, D. Chu, Y. H. Chou, R. D. Goldman and P. Matsudaira. **Integrating the actin and vimentin cytoskeletons. Adhesion-dependent formation of fimbrin-vimentin complexes in macrophages.** *The Journal of cell biology*, vol. 146, pages 831–842, August 1999. (Cited on page 53.)
- [Costigliola *et al.* 2017] Nancy Costigliola, Liya Ding, Christoph J. Burckhardt, Sangyoon J. Han, Edgar Gutierrez, Andressa Mota, Alex Groisman, Timothy J. Mitchison and Gaudenz Danuser. **Vimentin fibers orient traction stress.** *Proceedings of the National Academy of Sciences*, vol. 114, no. 20, pages 5195–5200, may 2017. (Cited on page 56.)
- [De Brabander *et al.* 1976] M. J. De Brabander, R. M. Van de Veire, F. E. Aerts, M. Borgers and P. A. Janssen. **The effects of methyl (5-(2-thienylcarbonyl)-1H-benzimidazol-2-yl) carbamate, (R 17934; NSC 238159), a new synthetic antitumoral drug interfering with microtubules, on mammalian cells cultured in vitro.** *Cancer research*, vol. 36, pages 905–916, March 1976. (Cited on page 19.)
- [De Pascalis *et al.* 2018] Chiara De Pascalis, Carlos Pérez-González, Shailaja Seetharaman, Batiste Boëda, Benoit Vianay, Mithila Burute, Cécile Leduc, Nicolas Borghi, Xavier Trepot and Sandrine Etienne-Manneville. **Intermediate filaments control collective migration by restricting traction forces and sustaining cell–cell contacts.** *Journal of Cell Biology*, vol. 217, no. 9, pages 3031–3044, jul 2018. (Cited on pages 58 and 61.)
- [Desai & Mitchison 1997] Arshad Desai and Timothy J. Mitchison. **Microtubule polymerization dynamics.** *Annual Review of Cell and Developmental Biology*, vol. 13, no. 1, pages 83–117, nov 1997. (Cited on pages 3 and 17.)
- [Desprat *et al.* 2006] N. Desprat, A. Guiroy and A. Asnacios. **Microplates-based rheometer for a single living cell.** *Review of Scientific Instruments*, vol. 77, no. 5, page 055111, may 2006. (Cited on page 31.)

- [Dimitrov *et al.* 2008] A. Dimitrov, M. Quesnoit, S. Moutel, I. Cantaloube, C. Pous and F. Perez. **Detection of GTP-Tubulin Conformation in Vivo Reveals a Role for GTP Remnants in Microtubule Rescues.** *Science*, vol. 322, no. 5906, pages 1353–1356, nov 2008. (Cited on page 18.)
- [Dittmer & Misteli 2011] Travis A Dittmer and Tom Misteli. **The lamin protein family.** *Genome Biology*, vol. 12, no. 5, page 222, 2011. (Cited on page 14.)
- [Dráber *et al.* 2012] Pavel Dráber, Vadym Sulimenko and Eduarda Dráberová. **Cytoskeleton in Mast Cell Signaling.** *Frontiers in Immunology*, vol. 3, 2012. (Cited on page 18.)
- [Duarte *et al.* 2019] Sofia Duarte, Álvaro Viedma-Poyatos, Elena Navarro-Carrasco, Alma E. Martínez, María A. Pajares and Dolores Pérez-Sala. **Vimentin filaments interact with the actin cortex in mitosis allowing normal cell division.** *Nature Communications*, vol. 10, no. 1, sep 2019. (Cited on page 50.)
- [Dupin & Etienne-Manneville 2011] Isabelle Dupin and Sandrine Etienne-Manneville. **Nuclear positioning: mechanisms and functions.** *The international journal of biochemistry & cell biology*, vol. 43, pages 1698–1707, December 2011. (Cited on pages 7 and 63.)
- [Dye *et al.* 1993] R. B. Dye, S. P. Fink and R. C. Williams. **Taxol-induced flexibility of microtubules and its reversal by MAP-2 and Tau.** *The Journal of biological chemistry*, vol. 268, pages 6847–6850, April 1993. (Cited on page 34.)
- [Eckes *et al.* 1998] B. Eckes, D. Dogic, E. Colucci-Guyon, N. Wang, A. Maniotis, D. Ingber, A. Merckling, F. Langa, M. Aumailley, A. Delouvé, V. Kotliansky, C. Babinet and T. Krieg. **Impaired mechanical stability, migration and contractile capacity in vimentin-deficient fibroblasts.** *Journal of cell science*, vol. 111 (Pt 13), pages 1897–1907, July 1998. (Cited on page 44.)
- [Ehrlicher *et al.* 2015] Allen J. Ehrlicher, Ramaswamy Krishnan, Ming Guo, Cécile M. Bidan, David A. Weitz and Martin R. Pollak. **Alpha-actinin binding kinetics modulate cellular dynamics and force generation.** *Proceedings of the National Academy of Sciences*, vol. 112, no. 21, pages 6619–6624, apr 2015. (Cited on page 31.)
- [Eshun-Wilson *et al.* 2019] Lisa Eshun-Wilson, Rui Zhang, Didier Portran, Maxence V. Nachury, Daniel B. Toso, Thomas Löhr, Michele Vendruscolo, Massimiliano Bonomi, James S. Fraser and Eva Nogales. **Effects of α -tubulin acetylation on microtubule structure and stability.** *Proceedings of the National Academy of Sciences*, vol. 116, no. 21, pages 10366–10371, may 2019. (Cited on page 36.)

- [Esue *et al.* 2006] Osigwe Esue, Ashley A. Carson, Yiider Tseng and Denis Wirtz. **A Direct Interaction between Actin and Vimentin Filaments Mediated by the Tail Domain of Vimentin.** *Journal of Biological Chemistry*, vol. 281, no. 41, pages 30393–30399, oct 2006. (Cited on pages 30, 49, 57, 58 and 63.)
- [Etienne-Manneville 2013] Sandrine Etienne-Manneville. **Microtubules in cell migration.** *Annual review of cell and developmental biology*, vol. 29, pages 471–499, 2013. (Cited on page 53.)
- [Etienne-Manneville 2018] Sandrine Etienne-Manneville. **Cytoplasmic Intermediate Filaments in Cell Biology.** *Annual Review of Cell and Developmental Biology*, vol. 34, no. 1, pages 1–28, oct 2018. (Cited on pages 8 and 63.)
- [Farré *et al.* 2016] Arnau Farré, Ferran Marsà and Mario Montes-Usategui. **Beyond the Hookean Spring Model: Direct Measurement of Optical Forces Through Light Momentum Changes.** In *Optical Tweezers*, pages 41–76. Springer New York, nov 2016. (Cited on page 71.)
- [Felgner *et al.* 1996] H. Felgner, R. Frank and M. Schliwa. **Flexural rigidity of microtubules measured with the use of optical tweezers.** *Journal of cell science*, vol. 109 (Pt 2), pages 509–516, February 1996. (Cited on pages 27, 34 and 63.)
- [Felgner *et al.* 1997] H. Felgner, R. Frank, J. Biernat, E. M. Mandelkow, E. Mandelkow, B. Ludin, A. Matus and M. Schliwa. **Domains of neuronal microtubule-associated proteins and flexural rigidity of microtubules.** *The Journal of cell biology*, vol. 138, pages 1067–1075, September 1997. (Cited on pages 27, 33 and 63.)
- [Forsting *et al.* 2019] Johanna Forsting, Julia Kraxner, Hannes Witt, Andreas Janshoff and Sarah Köster. **Vimentin Intermediate Filaments Undergo Irreversible Conformational Changes during Cyclic Loading.** *Nano Letters*, vol. 19, no. 10, pages 7349–7356, sep 2019. (Cited on pages 40, 41, 86 and 87.)
- [Fuchs & Cleveland 1998] E. Fuchs and D. W. Cleveland. **A structural scaffolding of intermediate filaments in health and disease.** *Science (New York, N.Y.)*, vol. 279, pages 514–519, January 1998. (Cited on page 53.)
- [Fudge *et al.* 2003] Douglas S. Fudge, Kenn H. Gardner, V. Trevor Forsyth, Christian Riekel and John M. Gosline. **The Mechanical Properties of Hydrated Intermediate Filaments: Insights from Hagfish Slime Threads.** *Biophysical Journal*, vol. 85, no. 3, pages 2015–2027, sep 2003. (Cited on page 40.)

- [Gan *et al.* 2016] Zhuo Gan, Liya Ding, Christoph J. Burckhardt, Jason Lowery, Assaf Zaritsky, Karlyndsay Sitterley, Andressa Mota, Nancy Costigliola, Colby G. Starker, Daniel F. Voytas, Jessica Tytell, Robert D. Goldman and Gaudenz Danuser. **Vimentin Intermediate Filaments Template Microtubule Networks to Enhance Persistence in Cell Polarity and Directed Migration.** *Cell Systems*, vol. 3, no. 3, pages 252–263.e8, sep 2016. (Cited on pages 55 and 64.)
- [Gao & Sztul 2001] Y. Gao and E. Sztul. **A novel interaction of the Golgi complex with the vimentin intermediate filament cytoskeleton.** *The Journal of cell biology*, vol. 152, pages 877–894, March 2001. (Cited on page 15.)
- [Gardner *et al.* 2013] Melissa K Gardner, Marija Zanic and Jonathon Howard. **Microtubule catastrophe and rescue.** *Current Opinion in Cell Biology*, vol. 25, no. 1, pages 14–22, feb 2013. (Cited on page 18.)
- [Gittes *et al.* 1993] F Gittes, B Mickey, J Nettleton and J Howard. **Flexural rigidity of microtubules and actin filaments measured from thermal fluctuations in shape.** *Journal of Cell Biology*, vol. 120, no. 4, pages 923–934, feb 1993. (Cited on pages 26 and 32.)
- [Gladilin *et al.* 2014] Evgeny Gladilin, Paula Gonzalez and Roland Eils. **Dissecting the contribution of actin and vimentin intermediate filaments to mechanical phenotype of suspended cells using high-throughput deformability measurements and computational modeling.** *Journal of Biomechanics*, vol. 47, no. 11, pages 2598–2605, aug 2014. (Cited on page 45.)
- [Goldman 1971] Robert D. Goldman. **The role of three cytoplasmic fibers in BHK-21 cell motility.** *Journal of Cell Biology*, vol. 51, no. 3, pages 752–762, dec 1971. (Cited on page 54.)
- [Goldmann 2018] Wolfgang H. Goldmann. **Intermediate filaments and cellular mechanics.** *Cell biology international*, vol. 42, pages 132–138, February 2018. (Cited on page 51.)
- [Gregor *et al.* 2013] Martin Gregor, Selma Osmanagic-Myers, Gerald Burgstaller, Michael Wolfram, Irmgard Fischer, Gernot Walko, Guenter P. Resch, Almut Jörgl, Harald Herrmann and Gerhard Wiche. **Mechanosensing through focal adhesion-anchored intermediate filaments.** *The FASEB Journal*, vol. 28, no. 2, pages 715–729, dec 2013. (Cited on pages 58 and 60.)
- [Guét *et al.* 2014] David Guét, Kalpana Mandal, Mathieu Pinot, Jessica Hoffmann, Yara Abidine, Walter Sigaut, Sabine Bardin, Kristine Schauer, Bruno Goud and Jean-Baptiste Manneville. **Mechanical Role of Actin Dynamics in the Rheology of the Golgi Complex and in Golgi-Associated**

- Trafficking Events.** *Current Biology*, vol. 24, no. 15, pages 1700–1711, aug 2014. (Cited on pages 32, 69 and 105.)
- [Guo *et al.* 2013] Ming Guo, Allen J. Ehrlicher, Saleemulla Mahammad, Hilary Fabich, Mikkel H. Jensen, Jeffrey R. Moore, Jeffrey J. Fredberg, Robert D. Goldman and David A. Weitz. **The Role of Vimentin Intermediate Filaments in Cortical and Cytoplasmic Mechanics.** *Biophysical Journal*, vol. 105, no. 7, pages 1562–1568, oct 2013. (Cited on pages 31, 32, 45, 46 and 57.)
- [Gurland & Gundersen 1995] G Gurland and G G Gundersen. **Stable, detyrosinated microtubules function to localize vimentin intermediate filaments in fibroblasts.** *Journal of Cell Biology*, vol. 131, no. 5, pages 1275–1290, dec 1995. (Cited on pages 55 and 64.)
- [Guzmán *et al.* 2006] C. Guzmán, S. Jeney, L. Kreplak, S. Kasas, A.J. Kulik, U. Aebi and L. Forró. **Exploring the Mechanical Properties of Single Vimentin Intermediate Filaments by Atomic Force Microscopy.** *Journal of Molecular Biology*, vol. 360, no. 3, pages 623–630, jul 2006. (Cited on pages 27, 38 and 63.)
- [Hanukogle *et al.* 1983] Israel Hanukogle, Naoko Tanese and Elaine Fuchs. **Complementary DNA sequence of a human cytoplasmic actin.** *Journal of Molecular Biology*, vol. 163, no. 4, pages 673–678, feb 1983. (Cited on page 2.)
- [Haudenschild *et al.* 2011] Dominik R. Haudenschild, Jianfen Chen, Nina Pang, Nikolai Steklov, Shawn P. Grogan, Martin K. Lotz and Darryl D. D’Lima. **Vimentin contributes to changes in chondrocyte stiffness in osteoarthritis.** *Journal of Orthopaedic Research*, vol. 29, no. 1, pages 20–25, january 2011. (Cited on page 45.)
- [Hawkins *et al.* 2010] Taviare Hawkins, Matthew Mirigian, M. Selcuk Yasar and Jennifer L. Ross. **Mechanics of microtubules.** *Journal of Biomechanics*, vol. 43, no. 1, pages 23–30, jan 2010. (Cited on pages 33, 64 and 83.)
- [Hawkins *et al.* 2013] Taviare L. Hawkins, David Sept, Binyam Mogessie, Anne Straube and Jennifer L. Ross. **Mechanical Properties of Doubly Stabilized Microtubule Filaments.** *Biophysical Journal*, vol. 104, no. 7, pages 1517–1528, apr 2013. (Cited on page 34.)
- [Helfand *et al.* 2002] Brian T. Helfand, Atsushi Mikami, Richard B. Vallee and Robert D. Goldman. **A requirement for cytoplasmic dynein and dynactin in intermediate filament network assembly and organization.** *Journal of Cell Biology*, vol. 157, no. 5, pages 795–806, may 2002. (Cited on page 51.)

- [Helfand *et al.* 2004] Brian T. Helfand, Lynne Chang and Robert D. Goldman. **Intermediate filaments are dynamic and motile elements of cellular architecture.** *Journal of cell science*, vol. 117, pages 133–141, January 2004. (Cited on page 51.)
- [Herpers *et al.* 1986] M. J. Herpers, F. C. Ramaekers, J. Aldeweireldt, O. Moesker and J. Slooff. **Co-expression of glial fibrillary acidic protein- and vimentin-type intermediate filaments in human astrocytomas.** *Acta neuropathologica*, vol. 70, pages 333–339, 1986. (Cited on page 16.)
- [Herrmann & Aebi 2016] Harald Herrmann and Ueli Aebi. **Intermediate Filaments: Structure and Assembly.** *Cold Spring Harbor Perspectives in Biology*, vol. 8, no. 11, page a018242, nov 2016. (Cited on page 12.)
- [Herrmann *et al.* 2007] Harald Herrmann, Harald Bär, Laurent Kreplak, Sergei V. Strelkov and Ueli Aebi. **Intermediate filaments: from cell architecture to nanomechanics.** *Nature Reviews Molecular Cell Biology*, vol. 8, no. 7, pages 562–573, jul 2007. (Cited on page 12.)
- [Hohmann & Dehghani 2019] Hohmann and Dehghani. **The Cytoskeleton—A Complex Interacting Meshwork.** *Cells*, vol. 8, no. 4, page 362, apr 2019. (Cited on pages 14 and 63.)
- [Hosu *et al.* 2007] Basarab G Hosu, Mingzhai Sun, Françoise Marga, Michel Grandbois and Gabor Forgacs. **Eukaryotic membrane tethers revisited using magnetic tweezers.** *Physical Biology*, vol. 4, no. 2, pages 67–78, apr 2007. (Cited on page 32.)
- [Hu *et al.* 2019] Jiliang Hu, Yiwei Li, Yukun Hao, Tianqi Zheng, Satish K. Gupta, German Alberto Parada, Huayin Wu, Shaoting Lin, Shida Wang, Xuanhe Zhao, Robert D. Goldman, Shengqiang Cai and Ming Guo. **High stretchability, strength, and toughness of living cells enabled by hyperelastic vimentin intermediate filaments.** *Proceedings of the National Academy of Sciences*, vol. 116, no. 35, pages 17175–17180, aug 2019. (Cited on pages 32, 46, 48, 58, 59 and 64.)
- [Huang *et al.* 1999] Jian-Dong Huang, Scott T. Brady, Bruce W. Richards, David Stenoien, James H. Resau, Neal G. Copeland and Nancy A. Jenkins. **Direct interaction of microtubule- and actin-based transport motors.** *Nature*, vol. 397, no. 6716, pages 267–270, jan 1999. (Cited on page 50.)
- [Hubbert *et al.* 2002] Charlotte Hubbert, Amaris Guardiola, Rong Shao, Yoshiharu Kawaguchi, Akihiro Ito, Andrew Nixon, Minoru Yoshida, Xiao-Fan Wang and Tso-Pang Yao. **HDAC6 is a microtubule-associated deacetylase.** *Nature*, vol. 417, no. 6887, pages 455–458, may 2002. (Cited on page 20.)
- [Huber *et al.* 2013] F. Huber, J. Schnauß, S. Rönicke, P. Rauch, K. Müller, C. Fütterer and J. Käs. **Emergent complexity of the cytoskeleton: from**

- single filaments to tissue.** *Advances in Physics*, vol. 62, no. 1, pages 1–112, feb 2013. (Cited on pages 33 and 64.)
- [Huber *et al.* 2015] Florian Huber, Adeline Boire, Magdalena Preciado López and Gijsje H Koenderink. **Cytoskeletal crosstalk: when three different personalities team up.** *Current Opinion in Cell Biology*, vol. 32, pages 39–47, feb 2015. (Cited on pages 52, 54, 57, 64 and 80.)
- [Janke & Bulinski 2011] Carsten Janke and Jeannette Chloë Bulinski. **Post-translational regulation of the microtubule cytoskeleton: mechanisms and functions.** *Nature Reviews Molecular Cell Biology*, vol. 12, no. 12, pages 773–786, nov 2011. (Cited on page 19.)
- [Janke & Magiera 2020] Carsten Janke and Maria M. Magiera. **The tubulin code and its role in controlling microtubule properties and functions.** *Nature Reviews Molecular Cell Biology*, vol. 21, no. 6, pages 307–326, feb 2020. (Cited on pages 19 and 63.)
- [Janke & Montagnac 2017] Carsten Janke and Guillaume Montagnac. **Causes and Consequences of Microtubule Acetylation.** *Current Biology*, vol. 27, no. 23, pages R1287–R1292, dec 2017. (Cited on pages 20, 21, 63 and 96.)
- [Janmey *et al.* 1991] P A Janmey, U Euteneuer, P Traub and M Schliwa. **Viscoelastic properties of vimentin compared with other filamentous biopolymer networks.** *Journal of Cell Biology*, vol. 113, no. 1, pages 155–160, apr 1991. (Cited on pages 30, 36, 37, 63 and 83.)
- [Janmey *et al.* 2006] Paul A. Janmey, Margaret E. McCormick, Sebastian Ramensee, Jennifer L. Leight, Penelope C. Georges and Fred C. MacKintosh. **Negative normal stress in semiflexible biopolymer gels.** *Nature Materials*, vol. 6, no. 1, pages 48–51, dec 2006. (Cited on page 30.)
- [Janson & Dogterom 2004] Marcel E. Janson and Marileen Dogterom. **A Bending Mode Analysis for Growing Microtubules: Evidence for a Velocity-Dependent Rigidity.** *Biophysical Journal*, vol. 87, no. 4, pages 2723–2736, oct 2004. (Cited on page 33.)
- [Jordan & Wilson 2004] Mary Ann Jordan and Leslie Wilson. **Microtubules as a target for anticancer drugs.** *Nature Reviews Cancer*, vol. 4, no. 4, pages 253–265, apr 2004. (Cited on page 19.)
- [Joshi & Inamdar 2019] Divyesh Joshi and Maneesha S. Inamdar. **Rudhira/B-CAS3 couples microtubules and intermediate filaments to promote cell migration for angiogenic remodeling.** *Molecular Biology of the Cell*, vol. 30, no. 12, pages 1437–1450, jun 2019. (Cited on page 53.)

- [Keeling *et al.* 2017] Michael C. Keeling, Luis R. Flores, Asad H. Dodhy, Elizabeth R. Murray and N uria Gavara. **Actomyosin and vimentin cytoskeletal networks regulate nuclear shape, mechanics and chromatin organization.** *Scientific Reports*, vol. 7, no. 1, jul 2017. (Cited on pages 7 and 63.)
- [Kikumoto *et al.* 2006] Mahito Kikumoto, Masashi Kurachi, Valer Tosa and Hideo Tashiro. **Flexural Rigidity of Individual Microtubules Measured by a Buckling Force with Optical Traps.** *Biophysical Journal*, vol. 90, no. 5, pages 1687–1696, mar 2006. (Cited on pages 26 and 34.)
- [Killian *et al.* 2018] Jessica L. Killian, Fan Ye and Michelle D. Wang. **Optical Tweezers: A Force to Be Reckoned With.** *Cell*, vol. 175, no. 6, pages 1445–1448, nov 2018. (Cited on page 69.)
- [Klymkowsky 1981] Michael W. Klymkowsky. **Intermediate filaments in 3T3 cells collapse after intracellular injection of a monoclonal anti-intermediate filament antibody.** *Nature*, vol. 291, no. 5812, pages 249–251, may 1981. (Cited on page 55.)
- [Kollman *et al.* 2011] Justin M. Kollman, Andreas Merdes, Lionel Mourey and David A. Agard. **Microtubule nucleation by γ -tubulin complexes.** *Nature Reviews Molecular Cell Biology*, vol. 12, no. 11, pages 709–721, oct 2011. (Cited on pages 17 and 18.)
- [Kraxner *et al.* 2021] Julia Kraxner, Charlotta Lorenz, Julia Menzel, Iwan Parfentev, Ivan Silbern, Manuela Denz, Henning Urlaub, Blanche Schwappach and Sarah K oster. **Post-translational modifications soften vimentin intermediate filaments.** *Nanoscale*, vol. 13, no. 1, pages 380–387, 2021. (Cited on pages 40 and 64.)
- [Kreplak *et al.* 2001] L. Kreplak, J. Doucet and F. Briki. **Unraveling double stranded α -helical coiled coils: An x-ray diffraction study on hard α -keratin fibers.** *Biopolymers*, vol. 58, no. 5, pages 526–533, 2001. (Cited on page 38.)
- [Kreplak *et al.* 2005] L. Kreplak, H. B ar, J.F. Leterrier, H. Herrmann and U. Aebi. **Exploring the Mechanical Behavior of Single Intermediate Filaments.** *Journal of Molecular Biology*, vol. 354, no. 3, pages 569–577, dec 2005. (Cited on pages 37 and 63.)
- [Kreplak *et al.* 2008] Laurent Kreplak, Harald Herrmann and Ueli Aebi. **Tensile Properties of Single Desmin Intermediate Filaments.** *Biophysical Journal*, vol. 94, no. 7, pages 2790–2799, apr 2008. (Cited on pages 27, 28 and 63.)

- [Kurachi *et al.* 1995] Masashi Kurachi, Masayuki Hoshi and Hideo Tashiro. **Buckling of a single microtubule by optical trapping forces: Direct measurement of microtubule rigidity.** *Cell Motility and the Cytoskeleton*, vol. 30, no. 3, pages 221–228, 1995. (Cited on pages 26, 33 and 34.)
- [Kuznetsova *et al.* 2007] Tatyana G. Kuznetsova, Maria N. Starodubtseva, Nicolai I. Yegorenkov, Sergey A. Chizhik and Renat I. Zhdanov. **Atomic force microscopy probing of cell elasticity.** *Micron*, vol. 38, no. 8, pages 824–833, dec 2007. (Cited on page 30.)
- [Köster *et al.* 2015] Sarah Köster, David A Weitz, Robert D Goldman, Ueli Aebi and Harald Herrmann. **Intermediate filament mechanics in vitro and in the cell: from coiled coils to filaments, fibers and networks.** *Current Opinion in Cell Biology*, vol. 32, pages 82–91, feb 2015. (Cited on page 38.)
- [Langford 1995] G. M. Langford. **Actin- and microtubule-dependent organelle motors: interrelationships between the two motility systems.** *Current opinion in cell biology*, vol. 7, pages 82–88, February 1995. (Cited on page 50.)
- [Leduc & Etienne-Manneville 2015] Cécile Leduc and Sandrine Etienne-Manneville. **Intermediate filaments in cell migration and invasion: the unusual suspects.** *Current Opinion in Cell Biology*, vol. 32, pages 102–112, feb 2015. (Cited on page 11.)
- [Leduc & Etienne-Manneville 2017] Cécile Leduc and Sandrine Etienne-Manneville. **Regulation of microtubule-associated motors drives intermediate filament network polarization.** *Journal of Cell Biology*, vol. 216, no. 6, pages 1689–1703, apr 2017. (Cited on page 16.)
- [Lee *et al.* 2007] Woei Ming Lee, Peter J Reece, Robert F Marchington, Nikolaus K Metzger and Kishan Dholakia. **Construction and calibration of an optical trap on a fluorescence optical microscope.** *Nature Protocols*, vol. 2, no. 12, pages 3226–3238, dec 2007. (Cited on page 70.)
- [Leterrier & Eyer 1987] J F Leterrier and J Eyer. **Properties of highly viscous gels formed by neurofilaments in vitro. A possible consequence of a specific inter-filament cross-bridging.** *Biochemical Journal*, vol. 245, no. 1, pages 93–101, jul 1987. (Cited on pages 29 and 36.)
- [Leterrier *et al.* 1996] J.F. Leterrier, J. Käs, J. Hartwig, R. Vegners and P.A. Janmey. **Mechanical Effects of Neurofilament Cross-bridges. Modulation by Phosphorylation, Lipids, and Interactions with F-Actin.** *Journal of Biological Chemistry*, vol. 271, no. 26, pages 15687–15694, jun 1996. (Cited on pages 30 and 36.)

- [L'Hernault & Rosenbaum 1985] Steven W. L'Hernault and Joel L. Rosenbaum. **Chlamydomonas α -tubulin is posttranslationally modified by acetylation on the ϵ -amino group of a lysine.** *Biochemistry*, vol. 24, no. 2, pages 473–478, jan 1985. (Cited on page 20.)
- [Li *et al.* 2019] Jian Li, Yun Zou, Zhifang Li and Yaming Jiu. **Joining actions: crosstalk between intermediate filaments and actin orchestrates cellular physical dynamics and signaling.** *Science China Life Sciences*, vol. 62, no. 10, pages 1368–1374, may 2019. (Cited on page 58.)
- [Liem 2013] R.K.H. Liem. **Neuronal Intermediate Filaments.** In William J. Lennarz and M. Daniel Lane, editors, *Encyclopedia of Biological Chemistry (Second Edition)*, pages 233–237. Academic Press, Waltham, 2013. (Cited on page 10.)
- [Lin *et al.* 2010a] Yi-Chia Lin, Chase P. Broedersz, Amy C. Rowat, Tatjana Wedig, Harald Herrmann, Frederick C. MacKintosh and David A. Weitz. **Divalent Cations Crosslink Vimentin Intermediate Filament Tail Domains to Regulate Network Mechanics.** *Journal of Molecular Biology*, vol. 399, no. 4, pages 637–644, jun 2010. (Cited on page 30.)
- [Lin *et al.* 2010b] Yi-Chia Lin, Norman Y. Yao, Chase P. Broedersz, Harald Herrmann, Fred C. MacKintosh and David A. Weitz. **Origins of Elasticity in Intermediate Filament Networks.** *Physical Review Letters*, vol. 104, no. 5, page 058101, feb 2010. (Cited on pages 30 and 36.)
- [Lin *et al.* 2011] Yi-Chia Lin, Gijsje H. Koenderink, Frederick C. MacKintosh and David A. Weitz. **Control of non-linear elasticity in F-actin networks with microtubules.** *Soft Matter*, vol. 7, no. 3, pages 902–906, 2011. (Cited on pages 57 and 58.)
- [Liu *et al.* 2015] Ching-Yi Liu, Hsi-Hui Lin, Ming-Jer Tang and Yang-Kao Wang. **Vimentin contributes to epithelial-mesenchymal transition cancer cell mechanics by mediating cytoskeletal organization and focal adhesion maturation.** *Oncotarget*, vol. 6, pages 15966–15983, June 2015. (Cited on pages 14, 55, 56 and 64.)
- [Lopez *et al.* 2016] Carlos G. Lopez, Oliva Saldanha, Klaus Huber and Sarah Köster. **Lateral association and elongation of vimentin intermediate filament proteins: A time-resolved light-scattering study.** *Proceedings of the National Academy of Sciences*, vol. 113, no. 40, pages 11152–11157, sep 2016. (Cited on page 12.)
- [Louis *et al.* 2016] David N. Louis, Arie Perry, Guido Reifenberger, Andreas von Deimling, Dominique Figarella-Branger, Webster K. Cavenee, Hiroko Ohgaki, Otmar D. Wiestler, Paul Kleihues and David W. Ellison. **The 2016 World Health Organization Classification of Tumors of the**

- Central Nervous System: a summary.** *Acta Neuropathologica*, vol. 131, no. 6, pages 803–820, may 2016. (Cited on page 67.)
- [Lowery *et al.* 2015] Jason Lowery, Edward R. Kuczmarski, Harald Herrmann and Robert D. Goldman. **Intermediate Filaments Play a Pivotal Role in Regulating Cell Architecture and Function.** *Journal of Biological Chemistry*, vol. 290, no. 28, pages 17145–17153, jul 2015. (Cited on page 15.)
- [Ludueña & Banerjee 2008] Richard F. Ludueña and Asok Banerjee. **The Iso-types of Tubulin.** In *The Role of Microtubules in Cell Biology, Neurobiology, and Oncology*, pages 123–175. Humana Press, 2008. (Cited on page 19.)
- [Mandal *et al.* 2016] Kalpana Mandal, Atef Asnacios, Bruno Goud and Jean-Baptiste Manneville. **Mapping intracellular mechanics on micropatterned substrates.** *Proceedings of the National Academy of Sciences*, vol. 113, no. 46, pages E7159–E7168, oct 2016. (Cited on pages 31, 32, 43 and 101.)
- [Mathieu & Manneville 2019] Samuel Mathieu and Jean-Baptiste Manneville. **Intracellular mechanics: connecting rheology and mechanotransduction.** *Current Opinion in Cell Biology*, vol. 56, pages 34–44, 2019. Cell Architecture. (Cited on page 107.)
- [Mattila & Lappalainen 2008] Pieta K. Mattila and Pekka Lappalainen. **Filopodia: molecular architecture and cellular functions.** *Nature Reviews Molecular Cell Biology*, vol. 9, no. 6, pages 446–454, may 2008. (Cited on page 6.)
- [Mauro *et al.* 2019] Ava J. Mauro, Erin M. Jonasson and Holly V. Goodson. **Relationship between dynamic instability of individual microtubules and flux of subunits into and out of polymer.** *Cytoskeleton*, vol. 76, no. 11-12, pages 495–516, sep 2019. (Cited on pages 18 and 63.)
- [McMichael *et al.* 2010] Brooke K. McMichael, Richard E. Cheney and Beth S. Lee. **Myosin X Regulates Sealing Zone Patterning in Osteoclasts through Linkage of Podosomes and Microtubules.** *Journal of Biological Chemistry*, vol. 285, no. 13, pages 9506–9515, mar 2010. (Cited on page 50.)
- [Mendez *et al.* 2010] Melissa G. Mendez, Shin-Ichiro Kojima and Robert D. Goldman. **Vimentin induces changes in cell shape, motility, and adhesion during the epithelial to mesenchymal transition.** *The FASEB Journal*, vol. 24, no. 6, pages 1838–1851, jan 2010. (Cited on page 14.)
- [Mendez *et al.* 2014] M.G. Mendez, D. Restle and P.A. Janmey. **Vimentin Enhances Cell Elastic Behavior and Protects against Compressive Stress.** *Biophysical Journal*, vol. 107, no. 2, pages 314–323, jul 2014. (Cited on page 57.)

- [Mickey & Howard 1995] B Mickey and J Howard. **Rigidity of microtubules is increased by stabilizing agents.** *Journal of Cell Biology*, vol. 130, no. 4, pages 909–917, aug 1995. (Cited on pages 33 and 34.)
- [Miserey-Lenkei *et al.* 2017] Stéphanie Miserey-Lenkei, Hugo Bousquet, Olena Pylpenko, Sabine Bardin, Ariane Dimitrov, Gaëlle Bressanelli, Raja Bonifay, Vincent Fraissier, Catherine Guillou, Cécile Bougeret, Anne Houdusse, Arnaud Echard and Bruno Goud. **Coupling fission and exit of RAB6 vesicles at Golgi hotspots through kinesin-myosin interactions.** *Nature Communications*, vol. 8, no. 1, nov 2017. (Cited on page 101.)
- [Mitchison & Kirschner 1984] Tim Mitchison and Marc Kirschner. **Dynamic instability of microtubule growth.** *Nature*, vol. 312, no. 5991, pages 237–242, nov 1984. (Cited on page 17.)
- [Miyake *et al.* 2016] Yasuyuki Miyake, Jeremy J Keusch, Longlong Wang, Makoto Saito, Daniel Hess, Xiaoning Wang, Bruce J Melancon, Paul Helquist, Heinz Gut and Patrick Matthias. **Structural insights into HDAC6 tubulin deacetylation and its selective inhibition.** *Nature Chemical Biology*, vol. 12, no. 9, pages 748–754, jul 2016. (Cited on page 20.)
- [Mizushi-Masugano *et al.* 1983] J Mizushi-Masugano, T Maeda and T Miki-Noumura. **Flexural rigidity of singlet microtubules estimated from statistical analysis of their contour lengths and end-to-end distances.** *Biochimica et Biophysica Acta (BBA) - General Subjects*, vol. 755, no. 2, pages 257–262, jan 1983. (Cited on page 33.)
- [Mofrad 2009] Mohammad R.K. Mofrad. **Rheology of the Cytoskeleton.** *Annual Review of Fluid Mechanics*, vol. 41, no. 1, pages 433–453, jan 2009. (Cited on page 4.)
- [Mücke *et al.* 2004] N. Mücke, L. Kreplak, R. Kirmse, T. Wedig, H. Herrmann, U. Aebi and J. Langowski. **Assessing the Flexibility of Intermediate Filaments by Atomic Force Microscopy.** *Journal of Molecular Biology*, vol. 335, no. 5, pages 1241–1250, jan 2004. (Cited on page 38.)
- [Na *et al.* 2009] Sungsoo Na, Farhan Chowdhury, Bernard Tay, Mingxing Ouyang, Martin Gregor, Yingxiao Wang, Gerhard Wiche and Ning Wang. **Plectin contributes to mechanical properties of living cells.** *American Journal of Physiology-Cell Physiology*, vol. 296, no. 4, pages C868–C877, apr 2009. (Cited on page 58.)
- [Nekrasova *et al.* 2011] Oxana E. Nekrasova, Melissa G. Mendez, Ivan S. Chernouvanenko, Pyotr A. Tyurin-Kuzmin, Edward R. Kuczmarski, Vladimir I. Gelfand, Robert D. Goldman and Alexander A. Minin. **Vimentin intermediate filaments modulate the motility of mitochondria.** *Molecular*

- Biology of the Cell*, vol. 22, no. 13, pages 2282–2289, jul 2011. (Cited on page 15.)
- [Neuman *et al.* 2007] K.C. Neuman, T. Lionnet and J.-F. Allemand. **Single-Molecule Micromanipulation Techniques**. *Annual Review of Materials Research*, vol. 37, no. 1, pages 33–67, aug 2007. (Cited on page 32.)
- [North *et al.* 2003] Brian J North, Brett L Marshall, Margie T Borra, John M Denu and Eric Verdin. **The Human Sir2 Ortholog, SIRT2, Is an NAD-Dependent Tubulin Deacetylase**. *Molecular Cell*, vol. 11, no. 2, pages 437–444, feb 2003. (Cited on page 20.)
- [Nussenzveig 2017] H. Moysés Nussenzveig. **Cell membrane biophysics with optical tweezers**. *European Biophysics Journal*, vol. 47, no. 5, pages 499–514, nov 2017. (Cited on page 32.)
- [Nöding *et al.* 2014] Bernd Nöding, Harald Herrmann and Sarah Köster. **Direct Observation of Subunit Exchange along Mature Vimentin Intermediate Filaments**. *Biophysical Journal*, vol. 107, no. 12, pages 2923–2931, dec 2014. (Cited on page 38.)
- [Omary *et al.* 2004] M. Bishr Omary, Pierre A. Coulombe and W.H. Irwin McLean. **Intermediate Filament Proteins and Their Associated Diseases**. *New England Journal of Medicine*, vol. 351, no. 20, pages 2087–2100, nov 2004. (Cited on pages 7 and 10.)
- [Omary *et al.* 2009] M. Bishr Omary, Nam-On Ku, Pavel Strnad and Shinichiro Hanada. **Toward unraveling the complexity of simple epithelial keratins in human disease**. *Journal of Clinical Investigation*, vol. 119, no. 7, pages 1794–1805, jul 2009. (Cited on page 7.)
- [Osada *et al.* 2016] Yoshihito Osada, Ryuzo Kawamura and Ken-Ichi Sano. **Hydrogels of Cytoskeletal Proteins**. *Springer International Publishing*, 2016. (Cited on page 30.)
- [Osmanagic-Myers *et al.* 2015] Selma Osmanagic-Myers, Stefanie Rus, Michael Wolfram, Daniela Brunner, Wolfgang H. Goldmann, Navid Bonakdar, Irmgard Fischer, Siegfried Reipert, Aurora Zuzuarregui, Gernot Walko and Gerhard Wiche. **Plectin reinforces vascular integrity by mediating crosstalk between the vimentin and the actin networks**. *Journal of cell science*, vol. 128, pages 4138–4150, November 2015. (Cited on page 51.)
- [Ott *et al.* 1993] A. Ott, M. Magnasco, A. Simon and A. Libchaber. **Measurement of the persistence length of polymerized actin using fluorescence microscopy**. *Physical Review E*, vol. 48, no. 3, pages R1642–R1645, sep 1993. (Cited on page 26.)

- [Palazzo *et al.* 2003] Alexander Palazzo, Brian Ackerman and Gregg G. Gundersen. **Tubulin acetylation and cell motility.** *Nature*, vol. 421, no. 6920, pages 230–230, jan 2003. (Cited on page 44.)
- [Pallavicini *et al.* 2014] Carla Pallavicini, Valeria Levi, Diana E. Wetzler, Juan F. Angiolini, Lorena Benseñor, Marcelo A. Despósito and Luciana Bruno. **Lateral Motion and Bending of Microtubules Studied with a New Single-Filament Tracking Routine in Living Cells.** *Biophysical Journal*, vol. 106, no. 12, pages 2625–2635, jun 2014. (Cited on pages 42, 60 and 64.)
- [Pallavicini *et al.* 2017] Carla Pallavicini, Alejandro Monastera, Nicolás González Bardeci, Diana Wetzler, Valeria Levi and Luciana Bruno. **Characterization of microtubule buckling in living cells.** *European Biophysics Journal*, vol. 46, no. 6, pages 581–594, apr 2017. (Cited on pages 41 and 64.)
- [Pampaloni *et al.* 2006] Francesco Pampaloni, Gianluca Lattanzi, Alexandr Jonáš, Thomas Surrey, Erwin Frey and Ernst-Ludwig Florin. **Thermal fluctuations of grafted microtubules provide evidence of a length-dependent persistence length.** *Proceedings of the National Academy of Sciences of the United States of America*, vol. 103, pages 10248–10253, July 2006. (Cited on pages 26 and 33.)
- [Patteson *et al.* 2019] Alison E. Patteson, Katarzyna Pogoda, Fitzroy J. Byfield, Kalpana Mandal, Zofia Ostrowska-Podhorodecka, Elisabeth E. Charrier, Peter A. Galie, Piotr Deptuła, Robert Bucki, Christopher A. McCulloch and Paul A. Janmey. **Loss of Vimentin Enhances Cell Motility through Small Confining Spaces.** *Small*, vol. 15, no. 50, page 1903180, nov 2019. (Cited on page 45.)
- [Pawelzyk *et al.* 2014] Paul Pawelzyk, Norbert Mücke, Harald Herrmann and Norbert Willenbacher. **Attractive Interactions among Intermediate Filaments Determine Network Mechanics In Vitro.** *PLoS ONE*, vol. 9, no. 4, page e93194, apr 2014. (Cited on page 37.)
- [Pollard & Cooper 2009] Thomas D. Pollard and John A. Cooper. **Actin, a central player in cell shape and movement.** *Science (New York, N.Y.)*, vol. 326, pages 1208–1212, November 2009. (Cited on page 6.)
- [Pollard & Goldman 2018] Thomas D. Pollard and Robert D. Goldman. **Overview of the Cytoskeleton from an Evolutionary Perspective.** *Cold Spring Harbor Perspectives in Biology*, vol. 10, no. 7, page a030288, jul 2018. (Cited on page 2.)
- [Portran *et al.* 2013] D. Portran, M. Zoccoler, J. Gaillard, V. Stoppin-Mellet, E. Neumann, I. Arnal, J. L. Martiel and M. Vantard. **MAP65/Ase1 promote microtubule flexibility.** *Molecular biology of the cell*, vol. 24, pages 1964–1973, June 2013. (Cited on page 34.)

- [Portran *et al.* 2017] Didier Portran, Laura Schaedel, Zhenjie Xu, Manuel Théry and Maxence V. Nachury. **Tubulin acetylation protects long-lived microtubules against mechanical ageing.** *Nature Cell Biology*, vol. 19, no. 4, pages 391–398, feb 2017. (Cited on page 36.)
- [Prahlad *et al.* 1998] Veena Prahlad, Miri Yoon, Robert D. Moir, Ronald D. Vale and Robert D. Goldman. **Rapid Movements of Vimentin on Microtubule Tracks: Kinesin-dependent Assembly of Intermediate Filament Networks.** *Journal of Cell Biology*, vol. 143, no. 1, pages 159–170, oct 1998. (Cited on pages 50, 54 and 64.)
- [Pujol *et al.* 2012] T. Pujol, O. du Roure, M. Fermigier and J. Heuvingh. **Impact of branching on the elasticity of actin networks.** *Proceedings of the National Academy of Sciences*, vol. 109, no. 26, pages 10364–10369, jun 2012. (Cited on pages 30 and 63.)
- [Qin *et al.* 2009] Zhao Qin, Laurent Kreplak and Markus J Buehler. **Nanomechanical properties of vimentin intermediate filament dimers.** *Nanotechnology*, vol. 20, no. 42, page 425101, sep 2009. (Cited on pages 11, 38, 39 and 63.)
- [Ramms *et al.* 2013] L. Ramms, G. Fabris, R. Windoffer, N. Schwarz, R. Springer, C. Zhou, J. Lazar, S. Stiefel, N. Hersch, U. Schnakenberg, T. M. Magin, R. E. Leube, R. Merkel and B. Hoffmann. **Keratins as the main component for the mechanical integrity of keratinocytes.** *Proceedings of the National Academy of Sciences*, vol. 110, no. 46, pages 18513–18518, oct 2013. (Cited on page 7.)
- [Rao *et al.* 2002] Mala V. Rao, Linda J. Engle, Panaiyur S. Mohan, Aidong Yuan, Dike Qiu, Anne Cataldo, Linda Hassinger, Stephen Jacobsen, Virginia M-Y. Lee, Athena Andreadis, Jean-Pierre Julien, Paul C. Bridgman and Ralph A. Nixon. **Myosin Va binding to neurofilaments is essential for correct myosin Va distribution and transport and neurofilament density.** *Journal of Cell Biology*, vol. 159, no. 2, pages 279–290, oct 2002. (Cited on page 50.)
- [Rathje *et al.* 2014] L.-S. Z. Rathje, N. Nordgren, T. Pettersson, D. Ronnlund, J. Widengren, P. Aspenstrom and A. K. B. Gad. **Oncogenes induce a vimentin filament collapse mediated by HDAC6 that is linked to cell stiffness.** *Proceedings of the National Academy of Sciences*, vol. 111, no. 4, pages 1515–1520, jan 2014. (Cited on pages 55 and 100.)
- [Ricketts *et al.* 2018] Shea N. Ricketts, Jennifer L. Ross and Rae M. Robertson-Anderson. **Co-Entangled Actin-Microtubule Composites Exhibit Tunable Stiffness and Power-Law Stress Relaxation.** *Biophysical Journal*, vol. 115, no. 6, pages 1055–1067, sep 2018. (Cited on page 57.)

- [Ridley 2003] A. J. Ridley. **Cell Migration: Integrating Signals from Front to Back**. *Science*, vol. 302, no. 5651, pages 1704–1709, dec 2003. (Cited on page 5.)
- [Robert *et al.* 2012] Damien Robert, Kelly Aubertin, Jean-Claude Bacri and Claire Wilhelm. **Magnetic nanomanipulations inside living cells compared with passive tracking of nanoprobe to get consensus for intracellular mechanics**. *Physical Review E*, vol. 85, no. 1, page 011905, jan 2012. (Cited on page 31.)
- [Satelli & Li 2011] Arun Satelli and Shulin Li. **Vimentin in cancer and its potential as a molecular target for cancer therapy**. *Cellular and Molecular Life Sciences*, vol. 68, no. 18, pages 3033–3046, jun 2011. (Cited on page 15.)
- [Schaap *et al.* 2006] Iwan A.T. Schaap, Carolina Carrasco, Pedro J. de Pablo, Frederick C. MacKintosh and Christoph F. Schmidt. **Elastic Response, Buckling, and Instability of Microtubules under Radial Indentation**. *Biophysical Journal*, vol. 91, no. 4, pages 1521–1531, aug 2006. (Cited on pages 33, 44 and 64.)
- [Schaedel *et al.* 2015] Laura Schaedel, Karin John, Jérémie Gaillard, Maxence V. Nachury, Laurent Blanchoin and Manuel Théry. **Microtubules self-repair in response to mechanical stress**. *Nature materials*, vol. 14, no. 11, pages 1156–1163, November 2015. (Cited on pages 34, 35, 64, 86 and 89.)
- [Schaedel *et al.* 2021] Laura Schaedel, Charlotta Lorenz, Anna V. Schepers, Stefan Klumpp and Sarah Köster. **Vimentin Intermediate Filaments Stabilize Dynamic Microtubules by Direct Interactions**. *BioRxiv*, February 2021. (Cited on pages 57 and 64.)
- [Schopferer *et al.* 2009] Michael Schopferer, Harald Bär, Bernhard Hochstein, Sarika Sharma, Norbert Mücke, Harald Herrmann and Norbert Willenbacher. **Desmin and Vimentin Intermediate Filament Networks: Their Viscoelastic Properties Investigated by Mechanical Rheometry**. *Journal of Molecular Biology*, vol. 388, no. 1, pages 133–143, apr 2009. (Cited on pages 30 and 37.)
- [Schulze & Kirschner 1986] E Schulze and M Kirschner. **Microtubule dynamics in interphase cells**. *The Journal of Cell Biology*, vol. 102, no. 3, pages 1020–1031, mar 1986. (Cited on page 17.)
- [Sept & MacKintosh 2010] David Sept and Fred C. MacKintosh. **Microtubule elasticity: connecting all-atom simulations with continuum mechanics**. *Physical review letters*, vol. 104, page 018101, January 2010. (Cited on page 34.)

- [Serres *et al.* 2020] Murielle P. Serres, Matthias Samwer, Binh An Truong Quang, Geneviève Lavoie, Upamali Perera, Dirk Görlich, Guillaume Charras, Mark Petronczki, Philippe P. Roux and Ewa K. Paluch. **F-Actin Interactome Reveals Vimentin as a Key Regulator of Actin Organization and Cell Mechanics in Mitosis.** *Developmental Cell*, vol. 52, no. 2, pages 210–222.e7, jan 2020. (Cited on page 51.)
- [Shabbir *et al.* 2014] Shagufta H. Shabbir, Megan M. Cleland, Robert D. Goldman and Milan Mrksich. **Geometric control of vimentin intermediate filaments.** *Biomaterials*, vol. 35, no. 5, pages 1359–1366, feb 2014. (Cited on pages 55, 56 and 64.)
- [Sharma *et al.* 2017] Poonam Sharma, Zachary T. Bolten, Diane R. Wagner and Adam H. Hsieh. **Deformability of Human Mesenchymal Stem Cells Is Dependent on Vimentin Intermediate Filaments.** *Annals of Biomedical Engineering*, vol. 45, no. 5, pages 1365–1374, jan 2017. (Cited on pages 58, 59 and 64.)
- [Shida *et al.* 2010] T. Shida, J. G. Cueva, Z. Xu, M. B. Goodman and M. V. Nachury. **The major α -tubulin K40 acetyltransferase α TAT1 promotes rapid ciliogenesis and efficient mechanosensation.** *Proceedings of the National Academy of Sciences*, vol. 107, no. 50, pages 21517–21522, nov 2010. (Cited on page 20.)
- [Siegrist & Doe 2007] S. E. Siegrist and C. Q. Doe. **Microtubule-induced cortical cell polarity.** *Genes & Development*, vol. 21, no. 5, pages 483–496, mar 2007. (Cited on page 9.)
- [Smoler *et al.* 2020] Mariano Smoler, Giovanna Coceano, Ilaria Testa, Luciana Bruno and Valeria Levi. **Apparent stiffness of vimentin intermediate filaments in living cells and its relation with other cytoskeletal polymers.** *Biochimica et Biophysica Acta (BBA) - Molecular Cell Research*, vol. 1867, no. 8, page 118726, aug 2020. (Cited on pages 43, 59, 60 and 64.)
- [Snell *et al.* 2004] William J Snell, Junmin Pan and Qian Wang. **Cilia and Flagella Revealed.** *Cell*, vol. 117, no. 6, pages 693–697, jun 2004. (Cited on page 42.)
- [Straight & Field 2000] Aaron F. Straight and Christine M. Field. **Microtubules, membranes and cytokinesis.** *Current Biology*, vol. 10, no. 20, pages R760–R770, oct 2000. (Cited on page 9.)
- [Straub 1942] Ferenc Brunó Straub. **Actin.** *Studies from the Institute of Medical Chemistry University of Szeged*, vol. II, pages 3–15, 1942. (Cited on page 5.)
- [Sui & Downing 2010] Haixin Sui and Kenneth H. Downing. **Structural Basis of Interprotofilament Interaction and Lateral Deformation of Micro-**

- tubules.** *Structure*, vol. 18, no. 8, pages 1022–1031, aug 2010. (Cited on page 33.)
- [Svitkina *et al.* 1996] T. M. Svitkina, A. B. Verkhovsky and G. G. Borisy. **Plectin sidearms mediate interaction of intermediate filaments with microtubules and other components of the cytoskeleton.** *The Journal of cell biology*, vol. 135, pages 991–1007, November 1996. (Cited on page 51.)
- [Szeverenyi *et al.* 2008] Ildiko Szeverenyi, Andrew J. Cassidy, Cheuk Wang Chung, Bennett T. K. Lee, John E. A. Common, Stephen C. Ogg, Huijia Chen, Shu Yin Sim, Walter L. P. Goh, Kee Woei Ng, John A. Simpson, Li Lian Chee, Goi Hui Eng, Bin Li, Declan P. Lunny, Danny Chuon, Aparna Venkatesh, Kian Hoe Khoo, W. H. Irwin McLean, Yun Ping Lim and E. Birgitte Lane. **The Human Intermediate Filament Database: comprehensive information on a gene family involved in many human diseases.** *Human mutation*, vol. 29, pages 351–360, March 2008. (Cited on page 3.)
- [Tang *et al.* 2001] Jay Tang, Josef Käs, Jagesh Shah and Paul Janmey. **Counterion-induced actin ring formation.** *European Biophysics Journal*, vol. 30, no. 7, pages 477–484, dec 2001. (Cited on page 36.)
- [Terriac *et al.* 2019] Emmanuel Terriac, Susanne Schütz and Franziska Lautenschläger. **Vimentin Intermediate Filament Rings Deform the Nucleus During the First Steps of Adhesion.** *Frontiers in Cell and Developmental Biology*, vol. 7, jun 2019. (Cited on page 15.)
- [Toivola *et al.* 2005] Diana M. Toivola, Guo-Zhong Tao, Aida Habtezion, Jian Liao and M. Bishr Omary. **Cellular integrity plus: organelle-related and protein-targeting functions of intermediate filaments.** *Trends in Cell Biology*, vol. 15, no. 11, pages 608–617, nov 2005. (Cited on page 7.)
- [Tseng *et al.* 2011] Qingzong Tseng, Irene Wang, Eve Duchemin-Pelletier, Ammar Azioune, Nicolas Carpi, Jie Gao, Odile Filhol, Matthieu Piel, Manuel Théry and Martial Balland. **A new micropatterning method of soft substrates reveals that different tumorigenic signals can promote or reduce cell contraction levels.** *Lab on a chip*, vol. 11, pages 2231–2240, July 2011. (Cited on page 31.)
- [Vahabikashi *et al.* 2019] Amir Vahabikashi, Chan Young Park, Kristin Perkumas, Zhiguo Zhang, Emily K. Deurloo, Huayin Wu, David A. Weitz, W. Daniel Stamer, Robert D. Goldman, Jeffrey J. Fredberg and Mark Johnson. **Probe Sensitivity to Cortical versus Intracellular Cytoskeletal Network Stiffness.** *Biophysical Journal*, vol. 116, no. 3, pages 518–529, feb 2019. (Cited on page 30.)

- [Valdman *et al.* 2012] David Valdman, Paul J. Atzberger, Dezhi Yu, Steve Kuei and Megan T. Valentine. **Spectral Analysis Methods for the Robust Measurement of the Flexural Rigidity of Biopolymers.** *Biophysical Journal*, vol. 102, no. 5, pages 1144–1153, mar 2012. (Cited on page 26.)
- [Vale *et al.* 1985] R Vale, T Reese and M Sheetz. **Identification of a novel force-generating protein, kinesin, involved in microtubule-based motility.** *Cell*, vol. 42, no. 1, pages 39–50, aug 1985. (Cited on page 9.)
- [Vale *et al.* 1994] R. D. Vale, C. M. Coppin, F. Malik, F. J. Kull and R. A. Milligan. **Tubulin GTP hydrolysis influences the structure, mechanical properties, and kinesin-driven transport of microtubules.** *The Journal of biological chemistry*, vol. 269, pages 23769–23775, September 1994. (Cited on page 34.)
- [VanBuren *et al.* 2005] Vincent VanBuren, Lynne Cassimeris and David J. Odde. **Mechanochemical model of microtubule structure and self-assembly kinetics.** *Biophysical journal*, vol. 89, pages 2911–2926, November 2005. (Cited on page 34.)
- [Vasquez *et al.* 1997] R J Vasquez, B Howell, A M Yvon, P Wadsworth and L Cassimeris. **Nanomolar concentrations of nocodazole alter microtubule dynamic instability in vivo and in vitro.** *Molecular Biology of the Cell*, vol. 8, no. 6, pages 973–985, jun 1997. (Cited on page 19.)
- [Venier *et al.* 1994] P. Venier, A. C. Maggs, M. F. Carlier and D. Pantaloni. **Analysis of microtubule rigidity using hydrodynamic flow and thermal fluctuations.** *The Journal of biological chemistry*, vol. 269, pages 13353–13360, May 1994. (Cited on pages 27 and 34.)
- [Wagner *et al.* 2007] Oliver I. Wagner, Sebastian Rammensee, Neha Korde, Qi Wen, Jean-Francois Leterrier and Paul A. Janmey. **Softness, strength and self-repair in intermediate filament networks.** *Experimental Cell Research*, vol. 313, no. 10, pages 2228–2235, jun 2007. (Cited on pages 30 and 36.)
- [Walker *et al.* 1988] R A Walker, E T O'Brien, N K Pryer, M F Soboeiro, W A Voter, H P Erickson and E D Salmon. **Dynamic instability of individual microtubules analyzed by video light microscopy: rate constants and transition frequencies.** *Journal of Cell Biology*, vol. 107, no. 4, pages 1437–1448, oct 1988. (Cited on page 18.)
- [Wang & Stamenović 2000] Ning Wang and Dimitrije Stamenović. **Contribution of intermediate filaments to cell stiffness, stiffening, and growth.** *American Journal of Physiology-Cell Physiology*, vol. 279, no. 1, pages C188–C194, jul 2000. (Cited on page 44.)

- [Wang *et al.* 1984] E. Wang, J. G. Cairncross and R. K. Liem. **Identification of glial filament protein and vimentin in the same intermediate filament system in human glioma cells.** *Proceedings of the National Academy of Sciences*, vol. 81, no. 7, pages 2102–2106, apr 1984. (Cited on page 16.)
- [Westermarck *et al.* 1973] B. Westermarck, J. Pontén and R. Hugosson. **Determinants for the establishment of permanent tissue culture lines from human gliomas.** *Acta Pathologica Microbiologica Scandinavica Section A Pathology*, vol. 81A, no. 6, pages 791–805, December 1973. (Cited on page 67.)
- [Wiche & Winter 2011] Gerhard Wiche and Lilli Winter. **Plectin isoforms as organizers of intermediate filament cytoarchitecture.** *BioArchitecture*, vol. 1, no. 1, pages 14–20, jan 2011. (Cited on pages 51, 52 and 64.)
- [Winter & Wiche 2013] Lilli Winter and Gerhard Wiche. **The many faces of plectin and plectinopathies: pathology and mechanisms.** *Acta neuropathologica*, vol. 125, pages 77–93, January 2013. (Cited on pages 52 and 64.)
- [Wu *et al.* 2018] Pei-Hsun Wu, Dikla Raz-Ben Aroush, Atef Asnacios, Wei-Chiang Chen, Maxim E. Dokukin, Bryant L. Doss, Pauline Durand-Smet, Andrew Ekpenyong, Jochen Guck, Nataliia V. Guz, Paul A. Janmey, Jerry S. H. Lee, Nicole M. Moore, Albrecht Ott, Yeh-Chuin Poh, Robert Ros, Mathias Sander, Igor Sokolov, Jack R. Staunton, Ning Wang, Graeme Whyte and Denis Wirtz. **A comparison of methods to assess cell mechanical properties.** *Nature Methods*, vol. 15, no. 7, pages 491–498, jun 2018. (Cited on page 32.)
- [Xu *et al.* 2017] Zhenjie Xu, Laura Schaedel, Didier Portran, Andrea Aguilar, Jérémie Gaillard, M. Peter Marinkovich, Manuel Théry and Maxence V. Nachury. **Microtubules acquire resistance from mechanical breakage through intralumenal acetylation.** *Science*, vol. 356, no. 6335, pages 328–332, apr 2017. (Cited on pages 20, 34, 43, 44, 64, 97 and 98.)
- [Xu *et al.* 2018] Wenlong Xu, Elaheh Alizadeh and Ashok Prasad. **Force Spectrum Microscopy Using Mitochondrial Fluctuations of Control and ATP-Depleted Cells.** *Biophysical Journal*, vol. 114, no. 12, pages 2933–2944, jun 2018. (Cited on page 101.)
- [Xue *et al.* 2013] John Z. Xue, Eileen M. Woo, Lisa Postow, Brian T. Chait and Hironori Funabiki. **Chromatin-Bound Xenopus Dppa2 Shapes the Nucleus by Locally Inhibiting Microtubule Assembly.** *Developmental Cell*, vol. 27, no. 1, pages 47–59, oct 2013. (Cited on page 9.)

- [Yamada *et al.* 2003] Soichiro Yamada, Denis Wirtz and Pierre A. Coulombe. **The mechanical properties of simple epithelial keratins 8 and 18: discriminating between interfacial and bulk elasticities.** *Journal of Structural Biology*, vol. 143, no. 1, pages 45–55, jul 2003. (Cited on page 30.)
- [Zhang & Liu 2008] Hu Zhang and Kuo-Kang Liu. **Optical tweezers for single cells.** *Journal of The Royal Society Interface*, vol. 5, no. 24, pages 671–690, apr 2008. (Cited on page 31.)
- [Zhang *et al.* 2014] Jian Zhang, Wei-Hui Guo and Yu-Li Wang. **Microtubules stabilize cell polarity by localizing rear signals.** *Proceedings of the National Academy of Sciences*, vol. 111, no. 46, pages 16383–16388, nov 2014. (Cited on page 9.)
- [Zhang *et al.* 2017] Jamie Zhang, Jiping Yue and Xiaoyang Wu. **Spectraplakins family proteins – cytoskeletal crosslinkers with versatile roles.** *Journal of Cell Science*, vol. 130, no. 15, pages 2447–2457, jul 2017. (Cited on page 53.)
- [Zhao *et al.* 2018] Jiaxin Zhao, Liqiu Zhang, Xingli Dong, Lu Liu, Linman Huo and Huirong Chen. **High Expression of Vimentin is Associated With Progression and a Poor Outcome in Glioblastoma.** *Applied Immunohistochemistry & Molecular Morphology*, vol. 26, no. 5, pages 337–344, may 2018. (Cited on page 15.)
- [Zimmermann *et al.* 2011] Dennis Zimmermann, Basma Abdel Motaal, Lena Voith von Voithenberg, Manfred Schliwa and Zeynep Ökten. **Diffusion of Myosin V on Microtubules: A Fine-Tuned Interaction for Which E-Hooks Are Dispensable.** *PLoS ONE*, vol. 6, no. 9, page e25473, sep 2011. (Cited on page 50.)

RÉSUMÉ

Bien que largement étudiée *in vitro*, la mécanique du cytosquelette reste encore peu explorée dans les cellules vivantes. Nous utilisons une technique de micromanipulation intracellulaire basée sur des pinces optiques pour appliquer des forces directement sur les filaments du cytosquelette afin de sonder la mécanique des microtubules et des filaments intermédiaires et de nous intéresser à leur interaction mécanique. En mesurant simultanément la force appliquée aux filaments et leur déflexion, c'est-à-dire la déformation des filaments perpendiculairement à leur axe longitudinal, en fonction du temps, nous pouvons déduire les courbes force-déflexion des filaments et caractériser la rigidité des filaments intermédiaires de vimentine et des microtubules. Par un ajustement linéaire des courbes force-déflexion dans le régime des faibles forces, nous montrons que les microtubules ont une rigidité effective plus faible que la vimentine lors de la déflexion.

Nous appliquons ensuite des forces deux fois sur le même faisceau de cytosquelette pour montrer que les filaments de vimentine, mais pas les microtubules, se rigidifient d'un facteur supérieur à trois lors de déflexions répétées. Nous caractérisons plus en détail le couplage mécanique entre les filaments de vimentine et les microtubules en utilisant des agents déstabilisateurs et stabilisateurs des microtubules et en augmentant l'acétylation des microtubules. De façon intéressante, nous constatons que ces modifications n'affectent pas la rigidité effective des filaments de vimentine alors que la déstabilisation ou l'acétylation des microtubules réduit significativement la rigidité des filaments de vimentine lors de déflexions répétées. Dans l'ensemble, ces résultats suggèrent que les microtubules favorisent la rigidification des faisceaux de vimentine lors de contraintes mécaniques répétées.

En revanche, dans les cellules où la vimentine est inactivée, les propriétés mécaniques des microtubules sont inchangées. Nos résultats soulignent l'importance des interactions entre les microtubules et les filaments intermédiaires dans la mécanique cellulaire et suggèrent que les filaments intermédiaires de vimentine sont des structures mécano-sensibles qui présentent des réponses dépendantes des contraintes mécaniques passées.

MOTS CLÉS

Mécanique cellulaire ; micro-rhéologie ; pinces optiques ; cytosquelette ; vimentine ; microtubules

ABSTRACT

Although extensively studied *in vitro*, the mechanics of the cytoskeleton is still largely unexplored in living cells. We use an intracellular optical tweezers-based micromanipulation technique to apply forces directly on cytoskeletal filaments in order to probe microtubules and intermediate filament mechanics and focus on how they interact mechanically. Measuring simultaneously the force applied to the filaments and their deflection, i.e. the deformation of the filaments perpendicular to their axis, as a function of time, allows us to deduce the force-deflection curves of the filaments and to characterize the rigidity of vimentin intermediate filaments and microtubules. By fitting the force-deflection curves at small forces, we show that microtubules have a lower effective stiffness than vimentin upon deflection.

We then apply forces twice on the same cytoskeletal bundle to show that vimentin filaments, but not microtubules, stiffen more than three times upon repeated deflections. We further characterize the mechanical coupling between vimentin filaments and microtubules by using microtubule destabilizing and stabilizing drugs and by increasing microtubule acetylation. Interestingly, we find that these modifications do not affect the effective stiffness of vimentin filaments while destabilizing or acetylating microtubules significantly reduces vimentin filament stiffening upon repeated deflection. Altogether, these results suggest that microtubules promote stiffening of vimentin bundles under repeated mechanical stress.

In sharp contrast, in cells knockout for vimentin, the mechanical properties of microtubules are unchanged. Our findings highlight the importance of the interactions between microtubules and intermediate filaments in cell mechanics and suggest that vimentin intermediate filaments are mechanosensitive structures which exhibit history-dependent mechano-responses.

KEYWORDS

Cell mechanics; microrheology; optical tweezers; cytoskeleton; vimentin; microtubules